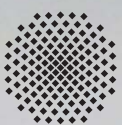
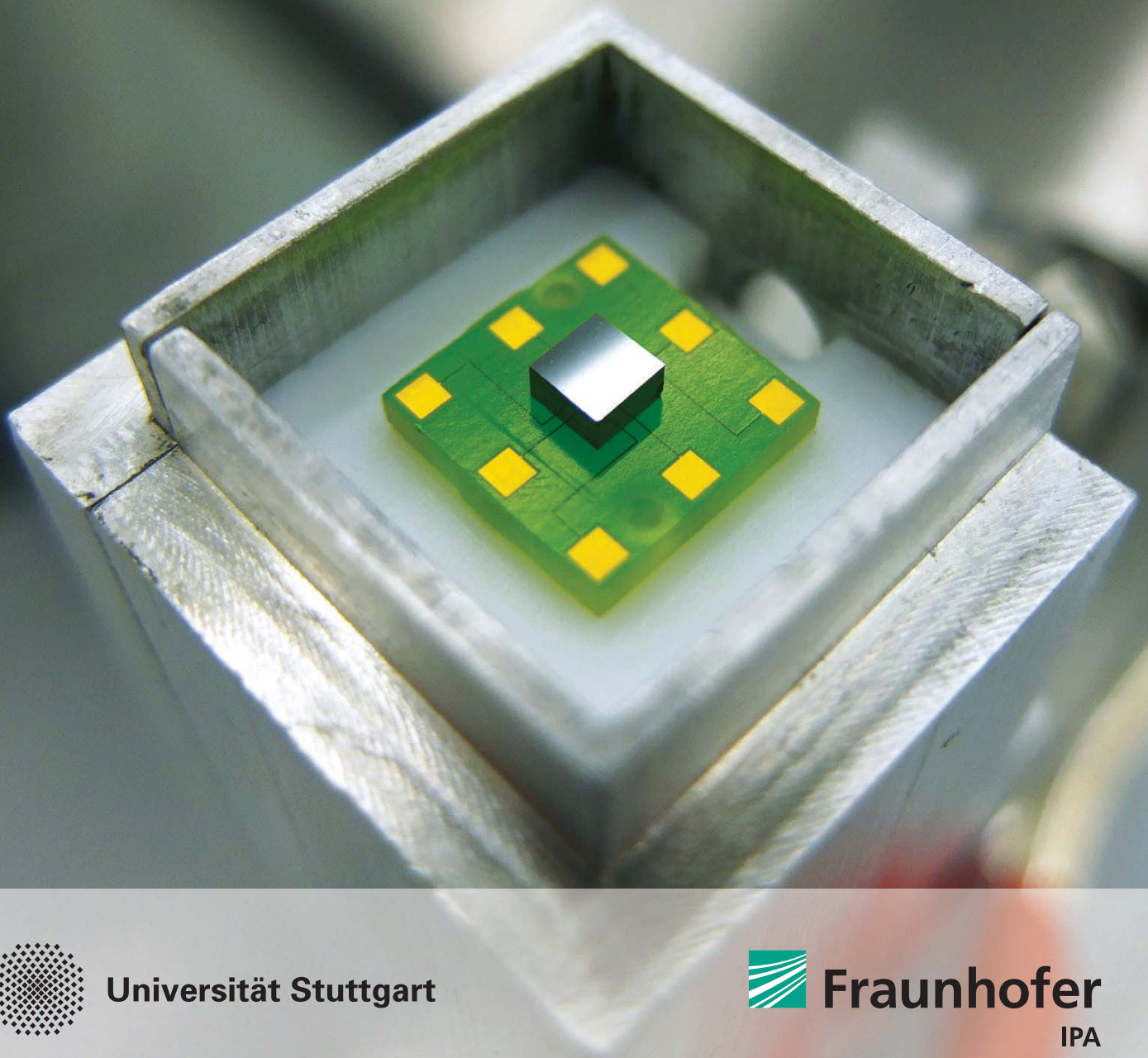


STUTTGARTER BEITRÄGE ZUR PRODUKTIONSFORSCHUNG

RAPHAEL ADAMIETZ

A Method for the Assembly of Microelectronic Packages using Microwave Curing



Universität Stuttgart



Fraunhofer
IPA

Herausgeber:

Univ.-Prof. Dr.-Ing. Thomas Bauernhansl

Univ.-Prof. Dr.-Ing. Dr. h.c. mult. Alexander Verl

Univ.-Prof. a. D. Dr.-Ing. Prof. E.h. Dr.-Ing. E.h. Dr. h.c. mult. Engelbert Westkämper

Raphael Adamietz

**A Method for the Assembly of Microelectronic
Packages using Microwave Curing**

Kontaktadresse:

Fraunhofer-Institut für Produktionstechnik und Automatisierung IPA, Stuttgart
Nobelstraße 12, 70569 Stuttgart
Telefon 0711 970-00, Telefax 0711 970-1399
info@ipa.fraunhofer.de, www.ipa.fraunhofer.de

STUTTGARTER BEITRÄGE ZUR PRODUKTIONSFORSCHUNG**Herausgeber:**

Univ.-Prof. Dr.-Ing. Thomas Bauernhansl
Univ.-Prof. Dr.-Ing. Dr. h.c. mult. Alexander Verl
Univ.-Prof. a. D. Dr.-Ing. Prof. E.h. Dr.-Ing. E.h. Dr. h.c. mult. Engelbert Westkämper

Fraunhofer-Institut für Produktionstechnik und Automatisierung IPA, Stuttgart
Institut für Industrielle Fertigung und Fabrikbetrieb (IFF) der Universität Stuttgart
Institut für Steuerungstechnik der Werkzeugmaschinen und Fertigungseinrichtungen (ISW)
der Universität Stuttgart

Titelbild: © Raphael Adamietz

Bibliografische Information der Deutschen Nationalbibliothek

Die Deutsche Nationalbibliothek verzeichnet diese Publikation in der Deutschen Nationalbibliografie; detaillierte bibliografische Daten sind im Internet über www.dnb.de abrufbar.

ISSN: 2195-2892

ISBN (Print): 978-3-8396-1333-7

D 93

Zugl.: Stuttgart, Univ., Diss., 2017

Druck: Mediendienstleistungen des Fraunhofer-Informationszentrum Raum und Bau IRB, Stuttgart
Für den Druck des Buches wurde chlor- und säurefreies Papier verwendet.

© by **FRAUNHOFER VERLAG**, 2018

Fraunhofer-Informationszentrum Raum und Bau IRB
Postfach 800469, 70504 Stuttgart
Nobelstraße 12, 70569 Stuttgart
Telefon 0711 970-2500
Telefax 0711 970-2508
E-Mail verlag@fraunhofer.de
URL <http://verlag.fraunhofer.de>

Alle Rechte vorbehalten

Dieses Werk ist einschließlich aller seiner Teile urheberrechtlich geschützt. Jede Verwertung, die über die engen Grenzen des Urheberrechtsgesetzes hinausgeht, ist ohne schriftliche Zustimmung des Verlages unzulässig und strafbar. Dies gilt insbesondere für Vervielfältigungen, Übersetzungen, Mikroverfilmungen sowie die Speicherung in elektronischen Systemen.

Die Wiedergabe von Warenbezeichnungen und Handelsnamen in diesem Buch berechtigt nicht zu der Annahme, dass solche Bezeichnungen im Sinne der Warenzeichen- und Markenschutz-Gesetzgebung als frei zu betrachten wären und deshalb von jedermann benutzt werden dürften. Soweit in diesem Werk direkt oder indirekt auf Gesetze, Vorschriften oder Richtlinien (z.B. DIN, VDI) Bezug genommen oder aus ihnen zitiert worden ist, kann der Verlag keine Gewähr für Richtigkeit, Vollständigkeit oder Aktualität übernehmen.

GELEITWORT DER HERAUSGEBER

Produktionswissenschaftliche Forschungsfragen entstehen in der Regel im Anwendungszusammenhang, die Produktionsforschung ist also weitgehend erfahrungsbasiert. Der wissenschaftliche Anspruch der „Stuttgarter Beiträge zur Produktionsforschung“ liegt unter anderem darin, Dissertation für Dissertation ein übergreifendes ganzheitliches Theoriegebäude der Produktion zu erstellen.

Die Herausgeber dieser Dissertations-Reihe leiten gemeinsam das Fraunhofer-Institut für Produktionstechnik und Automatisierung IPA und jeweils ein Institut der Fakultät für Konstruktions-, Produktions- und Fahrzeugtechnik an der Universität Stuttgart.

Die von ihnen betreuten Dissertationen sind der marktorientierten Nachhaltigkeit verpflichtet, ihr Ansatz ist systemisch und interdisziplinär. Die Autoren bearbeiten anspruchsvolle Forschungsfragen im Spannungsfeld zwischen theoretischen Grundlagen und industrieller Anwendung.

Die „Stuttgarter Beiträge zur Produktionsforschung“ ersetzt die Reihen „IPA-IAO Forschung und Praxis“ (Hrsg. H.J. Warnecke / H.-J. Bullinger / E. Westkämper / D. Spath) bzw. ISW Forschung und Praxis (Hrsg. G. Stute / G. Pritschow / A. Verl). In den vergangenen Jahrzehnten sind darin über 800 Dissertationen erschienen.

Der Strukturwandel in den Industrien unseres Landes muss auch in der Forschung in einen globalen Zusammenhang gestellt werden. Der reine Fokus auf Erkenntnisgewinn ist zu eindimensional. Die „Stuttgarter Beiträge zur Produktionsforschung“ zielen also darauf ab, mittelfristig Lösungen für den Markt anzubieten. Daher konzentrieren sich die Stuttgarter produktionstechnischen Institute auf das Thema ganzheitliche Produktion in den Kernindustrien Deutschlands. Die leitende Forschungsfrage der Arbeiten ist: Wie können wir nachhaltig mit einem hohen Wertschöpfungsanteil in Deutschland für einen globalen Markt produzieren?

Wir wünschen den Autoren, dass ihre „Stuttgarter Beiträge zur Produktionsforschung“ in der breiten Fachwelt als substanziell wahrgenommen werden und so die Produktionsforschung weltweit voranbringen.

Alexander Verl

Thomas Bauernhansl

Engelbert Westkämper

A Method for the Assembly of Microelectronic Packages using Microwave Curing

Von der Fakultät Konstruktions-, Produktions- und Fahrzeugtechnik der
Universität Stuttgart zur Erlangung der Würde eines Doktor-Ingenieurs (Dr.-Ing.)
genehmigte Abhandlung

Vorgelegt von

Dipl.-Ing. Raphael Adamietz
aus Wetzlar

Hauptberichter: Prof. Dr.-Ing. Dr. h. c. mult. Alexander Verl

Mitberichter: Prof. Marc Desmulliez, PhD

Tag der mündlichen Prüfung: 13.12.2017

Institut für Steuerungstechnik der Werkzeugmaschinen und Fertigungseinrichtungen
der Universität Stuttgart

2018

Danksagung

Die vorliegende Arbeit entstand während meiner Tätigkeit als wissenschaftlicher Mitarbeiter und Projektleiter in der Abteilung Reinst- und Mikroproduktion am Fraunhofer IPA in Stuttgart. Sie wurde teilweise im Rahmen des von der EU im 7. Rahmenprogramm finanzierten Projekts FAMOBS unter dem Kennzeichen FP7-SME-2007-218350 gefördert.

Herrn Prof. Dr.-Ing. Dr. h.c. mult. Alexander Verl danke ich für die wissenschaftliche Betreuung und Förderung dieser Arbeit und die Übernahme des Hauptberichts. Mein weiterer Dank gilt Herrn Prof. Marc Desmulliez für die wertvollen Diskussionen, die Durchsicht der Arbeit und die Übernahme des Mitberichts. Dr.-Ing. Udo Gommel und Dr.-Ing. Markus Rochowicz möchte ich für die mir entgegengebrachte, umfassende Unterstützung während der Promotionserstellung meinen Dank aussprechen. Bei Frau Heide Kreuzburg möchte ich mich für die Organisation des Promotionsprozesses bedanken.

Meinen Kolleginnen und Kollegen aus der Abteilung Reinst- und Mikroproduktion danke ich für die stets gute und sehr angenehme Zusammenarbeit während der Anfertigung der Dissertation und darüber hinaus. Meinem Vorgesetzten Herrn Dirk Schlenker bin ich dankbar für die ständige Unterstützung und das bereitwillige Entgegenkommen in den verschiedensten Belangen des Arbeitsalltages. Mein besonderer Dank gilt meinen Kollegen Dr.-Ing. Nabih Othman, Dr.-Ing. Tim Giesen, Matthias Burgard, Tobias Iseringhausen, Uwe Mai, Roman Stuhlberg und Marcel Daumüller für die vielfältige Unterstützung und Motivation. Dr. Tim Tilford sage ich Dank für die vielen Anregungen und die Durchsicht des Manuskripts. Bei Dr. Sumanth Pavuluri und Johannes Rupp möchte ich mich für die Unterstützung beim Aufbau des Systems und bei Dr. Thomas Schreier-Alt und Jens Warmuth für die Unterstützung bei der Versuchsdurchführung bedanken.

Meinen Eltern danke ich für die Förderung, Motivation und Unterstützung, die Sie mir während des Studiums und während meiner Promotion entgegengebracht haben. Von ganzem Herzen möchte ich mich bei meiner Frau Gudrun bedanken, die mir sehr viel Unterstützung entgegengebracht und stets enormen Rückhalt gegeben hat.

Stuttgart, im Juni 2017

Raphael Adamietz

List of Contents

1	Introduction.....	1
1.1	Problem statement	1
1.2	Aim and structure of this work	2
2	Initial Situation	4
2.1	Terminology	4
2.1.1	Electronic packaging	4
2.1.2	Micro assembly	5
2.1.3	Surface-mount technology	5
2.2	Trends in electronic packaging	6
2.2.1	Miniaturization and functional integration	6
2.2.2	3D integration	7
2.2.3	Microsystem packaging	9
2.2.4	Mass to individual low-volume production	10
2.3	Technologies for advanced packaging.....	12
2.3.1	Flip chip	12
2.3.2	Equipment.....	13
3	Analysis and Derivation of Requirements	15
3.1	Surface-mount devices.....	15
3.1.1	Chip-to-package interconnection	15
3.1.2	Chip attachment	16
3.2	Flip-chip assembly	17
3.2.1	Die.....	17
3.2.2	Substrate	17
3.3	Assembly processes	19
3.3.1	Flip-chip assembly process	19
3.3.2	Contacting.....	20
3.3.3	Placement.....	20
3.3.4	Underfill.....	21
3.3.5	Encapsulant.....	22
3.3.6	Electrically conductive adhesive	23
3.3.7	Curing	24
3.3.8	Temperature-sensitive components	32
3.3.9	Selective heating	33
3.3.10	Reliability	35
3.3.11	Process analysis	36
3.4	Conclusions on requirement analysis	38

4	State of the Art	40
4.1	Review of curing methods.....	40
4.1.1	Convection heating.....	40
4.1.2	Infrared heating.....	42
4.1.3	Ultraviolet light curing.....	43
4.1.4	Microwave heating.....	44
4.1.5	Indirect electrical heating.....	46
4.1.6	Laser heating.....	47
4.1.7	Further curing methods.....	47
4.2	Assembly equipment.....	48
4.2.1	Manual assembly machines.....	48
4.2.2	Semi-automatic assembly machines.....	49
4.2.3	SMT placement machines.....	49
4.2.4	Automated die-bonding machines.....	50
4.2.5	Dispensing equipment.....	50
4.3	Assessment of the state of the art technologies.....	51
4.4	Conclusions on state-of-the-art technology.....	54
5	Conception of a Potential Solution	56
5.1	Assessment and selection of curing method.....	56
5.2	Conception of heating system.....	58
5.2.1	Microwave source.....	58
5.2.2	Microwave applicator.....	60
5.2.3	Open-ended microwave applicator.....	63
5.3	Control concept.....	64
5.3.1	Frequency control.....	65
5.3.2	Temperature control.....	69
5.4	Heating control.....	74
5.4.1	Constant frequency.....	74
5.4.2	Linear sweep.....	75
5.4.3	Frequency hopping.....	76
5.4.4	Control system.....	77
5.4.5	Temperature sensor.....	80
5.4.6	Curing system concept overview and discussion.....	81
5.5	Concept of an assembly machine with microwave curing system.....	82
5.5.1	Machine requirements.....	83
5.5.2	Product analysis.....	83
5.5.3	Assembly process.....	84
5.5.4	Dispensing.....	86
5.5.5	Pick and place.....	87

5.5.6	Process analysis	88
5.5.7	Sensor assessment and selection.....	89
5.5.8	Absolute positioning strategy	91
5.5.9	Process chain	93
5.5.10	Machine concept	96
5.5.11	Integration of the microwave curing equipment.....	97
5.5.12	Machine concept overview and discussion.....	98
6	Design and Set-up of Prototype System.....	100
6.1	Integrable microwave curing system	100
6.1.1	Solid-state power amplifier.....	100
6.1.2	RF power measurement	100
6.1.3	Integration of temperature sensor	103
6.1.4	Control software	108
6.1.5	Human machine interface	111
6.1.6	Integrated microwave system set-up.....	115
6.2	Design of process components	116
6.2.1	Dispensing system	116
6.2.2	Gripping system.....	117
6.2.3	Vision system.....	118
6.2.4	Distance measurement sensor.....	119
6.2.5	Workpiece holder.....	120
6.3	Surface-mount assembly machine with integrated microwave curing system ..	121
6.3.1	Mechanical design	121
6.3.2	Chip fixture	123
6.4	Control system for integrated machine.....	124
6.4.1	Control system architecture	124
6.4.2	Process control software	126
6.4.3	Vision software.....	128
6.5	System integration	129
6.6	Conclusion	131
7	Validation of the Proposed Solution Approach	136
7.1	Curing system capabilities.....	136
7.1.1	Frequency control	136
7.1.2	Temperature control.....	139
7.1.3	Curing tests	140
7.1.4	Selective heating	143
7.1.5	Arcing and sparking.....	148
7.2	Flip-chip bonding.....	149
7.2.1	Assembly	149

7.2.2	Process	150
7.2.3	Die bonding	151
7.2.4	Underfill.....	152
7.2.5	Encapsulation.....	153
7.2.6	Functional testing.....	153
7.3	Performance and effort comparison of microwave and reference heating methods.....	154
7.3.1	Serial processing.....	155
7.3.2	Batch processing.....	156
7.3.3	Conclusions.....	158
7.4	Reliability tests	158
7.4.1	Production of test samples	159
7.4.2	Temperature cycling test.....	160
7.4.3	Highly accelerated stress test.....	164
7.4.4	Overview of reliability tests	166
7.5	Stress measurement	167
7.5.1	Stress-measurement chips.....	167
7.5.2	Preparation of samples for stress-measurement tests	169
7.5.3	Results	169
7.6	Assessment of results.....	173
7.7	Progress beyond the state of the art	175
8	Summary and Outlook.....	179
8.1	Summary.....	179
8.2	Outlook.....	182
	Appendix.....	184
I.	Flip-chip-on-board process.....	184
II.	Primary–Secondary analysis.....	185
III.	Flip-chip assembly process.....	186
IV.	Extended reliability test results.....	189
	Bibliography	190

List of Figures

Figure 1 – Structure of this work	3
Figure 2 – Electronic packaging hierarchy (Lau et al. 2003).....	4
Figure 3 – Trends in the semiconductor industry (IRDS 2016).....	7
Figure 4 – 3D packaging and package on package technologies (Wolter 2012).....	8
Figure 5 – 2015–2021 MEMS market forecast in US\$Billion (Yole 2016).....	9
Figure 6 – 3D IC market overview (Beica 2015).....	11
Figure 7 – Flip-chip assembly.....	12
Figure 8 – Sample electronic packaging line (ASE Group 2016).....	13
Figure 9 – Representative flip-chip process.....	13
Figure 10 – Representative flip-chip assembly process.....	19
Figure 11 – Encapsulation methods	23
Figure 12 – Flip chip with ECAs	23
Figure 13 – Generalized TTT cure diagram (Urbaniak et al. 2007)	25
Figure 14 – Transitions in a DSC curve (Thomas 2005)	26
Figure 15 – Curing behaviour of a polymer adhesive.....	27
Figure 16 – Processing diagram for polymer adhesives (Hsiung et al. 1997)	28
Figure 17 – Peak temperatures and cycle duration of pastes applied in electronic packaging	29
Figure 18 – Generic temperature profile.....	31
Figure 19 – Temperature-sensitive components	32
Figure 20 – Target definition for selective heating.....	34
Figure 21 – Primary–secondary analysis of the flip-chip assembly process	37
Figure 22 – Convection ovens (Hivision 2017; Heller 2017).....	41
Figure 23 – Infrared and ultraviolet spotlights (Jenton 2016; Lambda 2016)	44
Figure 24 – Microwave curing devices (Lambda Technologies 2007; Sinclair 2009)...	46
Figure 25 – Manual assembly machine (left) and rework station (right) (Finetech 2016; Martin 2016).....	48
Figure 26 – Semi-automated assembly machine (left), SMT placement machine (centre), and automated die-bonding machine (right) (AMICRA 2016; Tresky 2016; Wikipedia 2016).....	50
Figure 27 – Schematic of the open-ended microwave applicator	63
Figure 28 – Incident and reflected microwave power of an open-ended applicator	65
Figure 29 – Tracking of resonant frequency	68
Figure 30 – Energy balance of the open-ended applicator.....	71

Figure 31 – Cure experiment with Hysol EO1080 with maximum ramp rate $R_{a,3} = 2.5 \text{ }^\circ\text{C/s}$	72
Figure 32 – Cure experiment with Hysol EO1080 and adjusted ramp rates.....	73
Figure 33 – Constant frequency control.....	75
Figure 34 – Linear sweep.....	76
Figure 35 – Frequency hopping	77
Figure 36 – Absolute assembly strategy	91
Figure 37 – Absolute assembly strategy with intermediate microwave curing steps. Process steps are described in anticlockwise direction.	95
Figure 38 – Selection of kinematic configurations	96
Figure 39 – Overview of microwave components and their insertion losses (IL) (Rupp 2011)	101
Figure 40 – Concepts for pyrometer integration.....	105
Figure 41 – Open-ended microwave applicator with integrated pyrometer	106
Figure 42 – Design of modified open-ended microwave applicator.....	106
Figure 43 – Correction of pyrometer-measured temperature values	108
Figure 44 – PLC program state machine	109
Figure 45 – Cure profile structure.....	109
Figure 46 – Curing process program structure	110
Figure 47 – HMI class diagram	112
Figure 48 – HMI information flow	113
Figure 49 – Cure profile management and temperature control set-up	114
Figure 50 – Frequency set-up	114
Figure 51 – Visualization of the curing process	115
Figure 52 – Curing system overview	116
Figure 53 – Time–pressure dispensing system design.....	117
Figure 54 – Gripper system design	118
Figure 55 – Vision system design.....	119
Figure 56 – Displacement sensor.....	120
Figure 57 – Package and chip magazines and process position.....	121
Figure 58 – Machine design overview	122
Figure 59 – CAD model of the process tools.....	123
Figure 60 – CAD model of fixture for single chip.....	123
Figure 61 – 3D-printed fixture for a single chip	124
Figure 62 – Control system architecture	125
Figure 63 – Process control software architecture	126

Figure 64 – Process control software screenshot	127
Figure 65 – Pose determination of a semiconductor die	128
Figure 66 – Vision software state machine	129
Figure 67 – Integrated machine	130
Figure 68 – Realized process tools	131
Figure 69 – Derivation of tests from requirements	134
Figure 70 – Frequency auto-tuning algorithm	137
Figure 71 – Frequency hopping	138
Figure 72 – Linear frequency sweep.....	138
Figure 73 – Specimen for heating tests	139
Figure 74 – Curing of encapsulant Hysol EO1080	139
Figure 75 – Heating of silicon with reflow profile	140
Figure 76 – Test set-ups for curing tests	141
Figure 77 – Experimental set-up for selective heating.....	145
Figure 78 – Thermal image of silicon die and 8 LEDs on FR4 circuit board.....	145
Figure 79 – Temperature profile in tested specimen.....	146
Figure 80 – LEDs after three reflow cycles	147
Figure 81 – Arcing and sparking induced by 1000 V signal	148
Figure 82 – Circuit board, bare die and open QFN observed with high-speed camera during microwave heating.....	149
Figure 83 – LM358 die (left) and PCB (right).....	150
Figure 84 – Flip-chip test assembly process with test board	151
Figure 85 – Destroyed assembly (left) and flipped LM358 die on PCB (right)	152
Figure 86 – Underfill on assembly before (left) and after (right) cure	153
Figure 87 – Encapsulant on assembly before (left) and after (right) cure	153
Figure 88 – Process durations of convection and microwave heating for single- piece processing	155
Figure 89 – Throughput for different batch sizes for microwave and convection heating	158
Figure 90 – Encapsulation of open QFN package	159
Figure 91 – Thermal cycling profile	161
Figure 92 – Failures during the temperature cycling test.....	162
Figure 93 – Cracks on failed package – Microwave Profile 1, defect after 150 cycles.....	162
Figure 94 – Cracks on failed package – Microwave Profile 2, defect after 350 cycles.....	163

Figure 95 – Vaporized connection on failed package – Profile 3, defect after 150 cycles.....	163
Figure 96 – Cumulative failures against number of cycles.....	164
Figure 97 – Failures during HAST test.....	165
Figure 98 – Cumulative failures against number of cycles after HAST.....	166
Figure 99 – Equivalent stress (left) and SD of Microwave Profile 1 (right)	170
Figure 100 – Equivalent stress (left) and SD of Microwave Profile 2 (right)	170
Figure 101 – Equivalent stress (left) and SD of Microwave Profile 3 (right)	171
Figure 102 – Equivalent stress (left) and SD of conventional cure profile (right)	171
Figure 103 – Overview of measured stresses	172

List of Tables

Table 1 – Derived maximum values for cure profile parameters.....	32
Table 2 – List of requirements	39
Table 3 – Process integration in microelectronics assembly equipment.....	53
Table 4 – Heating and curing integration in microelectronics assembly equipment	54
Table 5 – Cycle duration with different curing methods (Garard et al. 2002; Berga et al. 2011).....	56
Table 6 – Assessment of relevant curing methods.....	57
Table 7 – Assessment of microwave amplifiers	60
Table 8 – Assessment of microwave applicators	62
Table 9 – Representative durations of frequency sweeps	67
Table 10 – Resonant frequencies of unloaded open-ended microwave applicator	67
Table 11 – Assessment of control systems	79
Table 12 – Assessment of temperature measurement methods	80
Table 13 – Curing system concept overview	82
Table 14 – Assessment and selection of dispensing systems (Othman 2005; Wiedenhöfer 2009)	87
Table 15 – Requirements of the main processes.....	89
Table 16 – Distance measurement principles (μ Epsilon 2016; Häusler et al. 1999; Blais 2003; Hocken et al. 2011).....	90
Table 17 – Machine concept overview	99
Table 18 – Curing system implementation overview	132
Table 19 – Machine implementation overview.....	133
Table 20 – Cure profiles (MW: microwave, Convection: convection heating).....	142
Table 21 – DSC measurements.....	143
Table 22 – Functionality of flip-chip samples	154
Table 23 – Assumed process durations for convection and microwave heating	155
Table 24 – Process durations for serial processing	156
Table 25 – Process durations for batch processing	157
Table 26 – Produced samples for reliability tests	160
Table 27 – Overview of reliability test results.....	167
Table 28 – Produced samples for stress-measurement tests	169
Table 29 – Assessment of fulfilment of requirements	174
Table 30 – Progress beyond state of the art regarding curing system.....	176
Table 31 – Progress beyond state of the art regarding the proposed machine.....	177
Table 32 – Progress beyond state of the art regarding experimental validation	178

Abbreviations

The following abbreviations are used in this thesis.

ACA	Anisotropic conductive adhesive
ASIC	Application-specific integrated circuit
BGA	Ball grid array
COB	Chip-on-board
CMOS	Complementary metal–oxide–semiconductor
CSP	Chip scale package
CTE	Coefficient of thermal expansion
DC	Direct current
DoC	Degree of cure
DoF	Degree of freedom
DSC	Differential scanning calorimetry
ECA	Electrically conductive adhesive
FR4	Flame-retardant 4. Grade designation assigned to printed circuit boards
GigE	Gigabit Ethernet
GigE Vision	Gigabit Ethernet Vision (Protocol)
GUI	Graphical user interface
HAST	Highly accelerated stress test
HMI	Human machine interface
IC	Integrated circuit
ICA	Isotropic conductive adhesive
IEC	International Electrotechnical Commission
IEEE	Institute of Electrical and Electronics Engineers
IO	Input/output
IPC	Industrial personal computer
IPC [®]	Institute for Printed Circuits
JEDEC	JEDEC solid-state technology association

LCD	Liquid crystal display
LED	Light-emitting diode
LGA	Land grid array
MEMS	Microelectromechanical systems
MPP	Maximum power point tracking
MW	Microwave
nMOS	n-type metal–oxide–semiconductor
OLED	Organic light-emitting diode
PC	Personal computer
PCB	Printed circuit board
PLC	Programmable logic controller
pMOS	p-type metal–oxide–semiconductor
PTFE	Polytetrafluoroethylene (“Teflon [®] ”)
PWM	Pulse width modulation
QFN	Quad flat pack with no leads
RADAR	Radio detection and ranging
RTOS	Real-time operating system
RF	Radio frequency
SCARA	Selective Compliance Assembly Robot Arm
SD	Standard deviation
Si-MOSFET	Silicon metal oxide semiconductor field-effect transistor
SiP	System in package
SMA	Subminiature version A connector
SMD	Surface-mount device
SMT	Surface-mount technology
SoC	System on chip
SPI	Serial peripheral interface
SSPA	Solid-state power amplifiers
TCP	Transmission control protocol

TCP/IP	Transmission control protocol/internet protocol
TM	Transverse magnetic mode
TSV	Through-silicon via
TTT	Time–temperature–transformation
TWT	Travelling wave tube
USB	Universal serial bus
UV	Ultraviolet
VDI	Verein Deutscher Ingenieure

1 Introduction

The electronics and MEMS packaging industries are following the trend of continuous miniaturization combined with concurrent functional integration. The impact of this trend is an increasing number of components and their functions integrated into a single package. The importance of advanced packaging solutions such as system on chip (SoC) and system in package (SiP) is continuously increasing. In order to reach higher packaging densities, multi-chip and three-dimensional packaging solutions are increasingly pursued by companies and research laboratories (Yole 2016; Ghaffarian et al. 2014; IRDS 2016).

Advanced packaging technologies, such as SoC and SiP, are, at present, applied predominantly in high-volume applications. Due to their high cost, these technologies are reserved for a small number of large enterprises. To render advanced packaging attractive for applications with lower volumes, and for prototyping purposes, more efficient processes for the assembly of electronic and MEMS packages are required, with associated reductions in investment costs (Beica 2015; Frost & Sullivan 2017).

Fresh challenges appear as the components, and their interfaces, become ever-smaller and evermore complex. As a result, the number of interconnects and the requirements for positioning precision continue to increase. At the same time, the reliability of electronic assemblies must comply with increasingly demanding standards, while the production costs must be steadily controlled and minimized (Ghaffarian et al. 2014; Pizzagalli et al. 2014; IRDS 2016).

Continuous development and improvement of the applied manufacturing processes is therefore required. These improvements include optimization of performance, quality and cost, but also the robustness of the applied processes (Kada 2015; Mahajan et al. 2017).

1.1 Problem statement

The application of adhesives for electronic and MEMS packaging applications provides a high degree of flexibility (Zhang 2011). Adhesives can be dispensed according to application-specific protocols and do not require masks or other expensive tooling (Lu et al. 2009). Dispensing systems are therefore particularly suitable for production in lower volumes and fields of application where a high degree of flexibility is needed (Tummala et al. 1997; Blackwell 2002).

A significant drawback of adhesive bonding is the duration of the curing processes. A typical assembly process of an electronic package (e.g. a flip-chip process) requires numerous heating cycles to cure the adhesive and encapsulant materials (Harper 2004). These heating cycles typically take between several minutes and several hours and represent a clear bottleneck in the production of microelectronic assemblies (Morris et al. 2009).

Numerous approaches for the reduction of curing cycle times exist. Microwave heating, in particular, has a high potential for dramatically increasing the curing rates of the adhesives applied in electronic packaging (Wei et al. 2000; Tilford et al. 2008d).

The bonding process in electronics packaging is typically implemented by a number of separate stations (Lee et al. 2012), where each station carries out one part of the process chain. While this approach is efficient for a batch production, a number of drawbacks become apparent for production at lower volumes (Lau 2010; Lee et al. 2012; Lotter 2013).

- Space is required for each of the stations, typically in a cleanroom.
- Investment in multiple, dedicated machines is required.
- Multiple machines need to be operated and maintained.
- The total efficiency of the process chain is significantly impaired by a number of manual handling steps.

In order to benefit from the full potential that adhesives provide in electronic packaging, particularly in advanced packaging solutions, these aforementioned drawbacks need to be addressed. A novel method for the assembly of electronic packages and MEMS is required, one that improves the overall performance and efficiency of the assembly process.

1.2 Aim and structure of this work

The aim of this work is to develop a novel method for the assembly of electronic packages and MEMS, specifically designed to improve the performance and efficiency of the assembly process for low- to medium-volume applications.

First, the initial situation is described and the problem is narrowed from electronic packaging in general down to the assembly process (Chapter 2). Next, the boundary conditions for the assembly process are analysed and a set of requirements is derived (Chapter 3). Then, based on the requirements, a review is made to determine whether the existing state-of-the-art technologies can meet these requirements (Chapter 4). A novel solution is then conceptually designed, with its different subdomains (Chapter 5).

Based on this concept, the prototype system is developed, realized and described in detail (Chapter 6). The proposed method is then experimentally validated in Chapter 7 before a summary and future outlook is provided in Chapter 8.

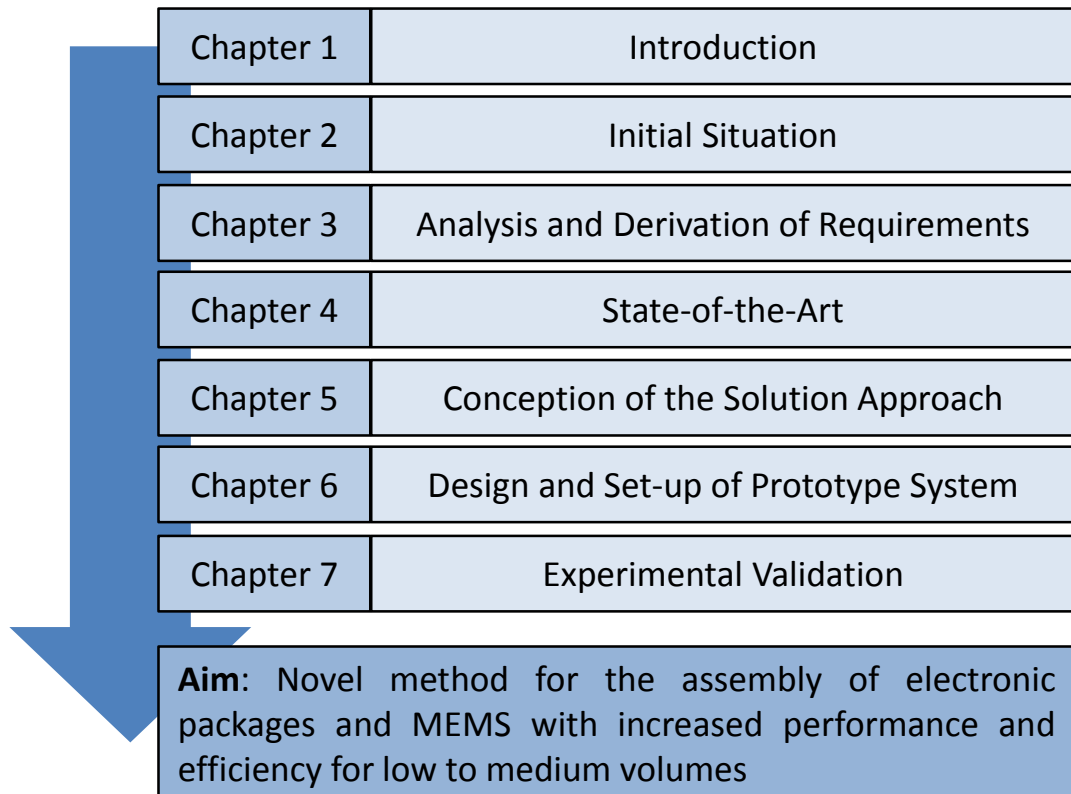


Figure 1 – Structure of this work

2 Initial Situation

2.1 Terminology

2.1.1 Electronic packaging

Electronic packaging provides housing and interconnection of integrated circuits to form electronic systems. The functions that electronic packaging must provide are manifold, principally comprising the physical support and protection of the electrical circuitry, the dissipation of heat, the distribution of electrical signals and the distribution of electrical power. Furthermore, the electronic packaging must be appropriately manufacturable and serviceable (Tummala et al. 1997; Harper 2004).

The issues central to electronic packaging assemblies and their manufacturing are the optimization of package and interconnection reliability, performance, cost and the yield. Besides the manufacturing of the packages themselves, extensive activities in the physical optimization of the packages are carried out. This comprises mechanical, thermal and electrical analysis and optimization of designs, material analysis and development, as well as a multitude of different testing protocols and design guidelines (Blackwell 2002; Ulrich et al. 2006; Liu 2012).

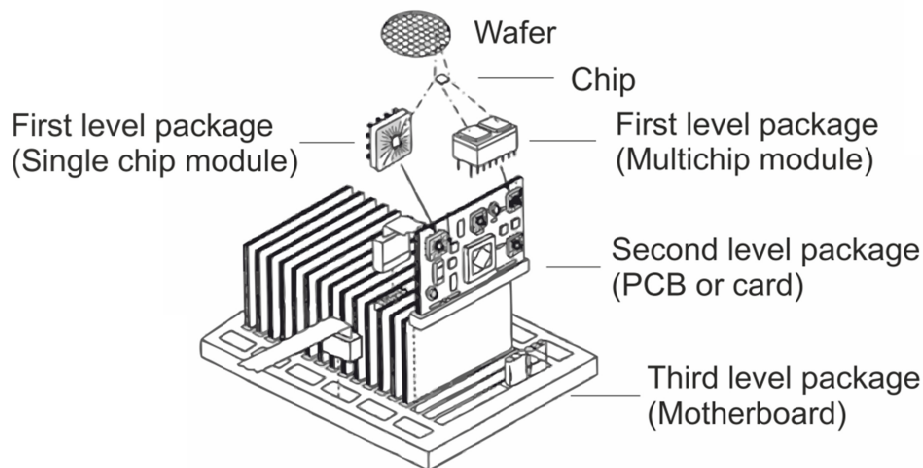


Figure 2 – Electronic packaging hierarchy (Lau et al. 2003)

The discipline of electronic packaging extends over several levels, as shown in Figure 2. The electronic packaging begins with the wafer, which is then built up to either single chip or multi-chip modules. These modules are then mounted on to second-level packages, which are typically PCBs or cards. Second-level packages can then be

integrated into superordinate assemblies, which are often referred to as motherboards (Blackwell 2002; Lau et al. 2003).

2.1.2 Micro assembly

According to VDI Guideline 2860 (VDI 2860), assembly is a subfunction of manufacturing. The starting point of assembly is parts, which are manufactured in different locations with different manufacturing processes. The task of assembly is to create a product based on these parts that is of higher complexity with a defined function in a set time frame. Sub-operations of assembly processes include joining, handling, inspection, adjustment and special operations (VDI 2860).

Micro assembly differs from conventional assembly in the dimensions of the handled parts and the requirements regarding the precision of the assembly process. Greitmann proposes a classification and specifies part dimensions of less than 2 mm with assembly accuracy of less than 25 μm for micro-precision assembly (Greitmann 1998). Van Brussel *et al.* refer to part dimensions of less than 1 mm (van Brussel et al. 2000). Popa and Stephanou define micro assembly as having part dimensions of less than 1 mm and assembly accuracy of less than 25 μm (Popa et al. 2004). They additionally propose the term meso assembly, situated between micro and macro assembly, which roughly corresponds to the classification by Greitmann (Popa et al. 2004).

2.1.3 Surface-mount technology

Surface-mount technology (SMT) is a method for the production of electronic circuits. The technology is based on a standardized component design of surface-mount devices (Prasad 2013). It provides similar dimensions or pitches thereof, that are independent of the function of the component (Prasad 2013). The attachment, using solder or conductive adhesive, typically also provides the electrical interconnect between the component and the circuit board (Lotter 2013).

The introduction of SMT led to significantly increased packaging densities and allowed a higher degree of automation in the assembly process, with less parasitic inductance and capacitance. Additionally, the cost and size of electronic assemblies were drastically reduced. The main drawbacks of SMT are poor manual solderability (compared to through-hole technology) and complicated rework and reliability issues due to mechanical and thermal stresses (Tummala et al. 1997; Blackwell 2002).

2.2 Trends in electronic packaging

2.2.1 Miniaturization and functional integration

In recent decades, an ongoing trend towards miniaturization with concurrent functional integration has been observed (Hesselbach et al. 2002; Raatz et al. 2012). This trend has affected different domains and fields of application, such as optics, medical technology, biotechnology, communication technology and aerospace technology (Dohda et al. 2004). As all these branches use electronic components extensively, there is a permanent drive to create smaller electronics with increased functionality.

The approach taken to achieve smaller, more-integrated electronic components has changed dramatically over the past few decades (Szendiuch 2011). Previously, integrated circuit (IC) design was performed separately from the package design. The IC was designed first and then a suitable (standard) package was selected (Szendiuch 2011). As the degree of integration increased and miniaturization progressed, the requirements evolved. The number of interconnects on a package increased dramatically, alongside the performance requirements. This led to the development of individual packages for complex ICs. This complexity also led to a concurrent design of IC and package. The packages became more complex and more diversified towards their application (Karnezos 2004; Miettinen et al. 2004; Lim 2005).

In the early years of ICs, development was mainly characterized by a reduction in feature sizes on the IC itself. A doubling of the functions per chip could be achieved every two years, as predicted by Moore, mainly through the miniaturization of structures on silicon. When the doubling of functions per chip could not be kept up by structuring methods, alternative ways were sought to keep up with the predictions (Peercy 2000; IRDS 2016). Consequently, novel advanced packaging methods were introduced. Figure 3 shows an overview of these ongoing trends.

Microprocessors, memories and different logic devices can be produced with CMOS technologies. To achieve higher packaging densities, these functions can be combined on one die. This approach is generally referred to as system on chip (SoC). An alternative is the combination of several chips and other electrical components with different functions into one package. This approach is referred to as system in package (SiP). A combination of both approaches is also possible, which is called heterogeneous integration (Wolter 2012).

The main driver for SoC solutions is to overcome limitations imposed by the baseline of CMOS processes and to achieve higher packaging densities at the board level. This can

be achieved if the functionality of several separate packages can be combined into a single one (Wolter 2012; IRDS 2016).

Another trend is the diversification of functionality in a semiconductor package, which is typical of SiP. ICs are applied to a broad spectrum of different domains and potential applications are virtually endless. Functionality for communication, signal acquisition, power management, sensors and actuators as well as biological or chemical functions are thereby integrated into a single package. MEMS may also be integrated into SiP. This can be regarded as an addition to Moore's law, as not just the computing capacity is increased, but also additional functions are squeezed into the volume of a semiconductor package (Wolter 2012; IRDS 2016).

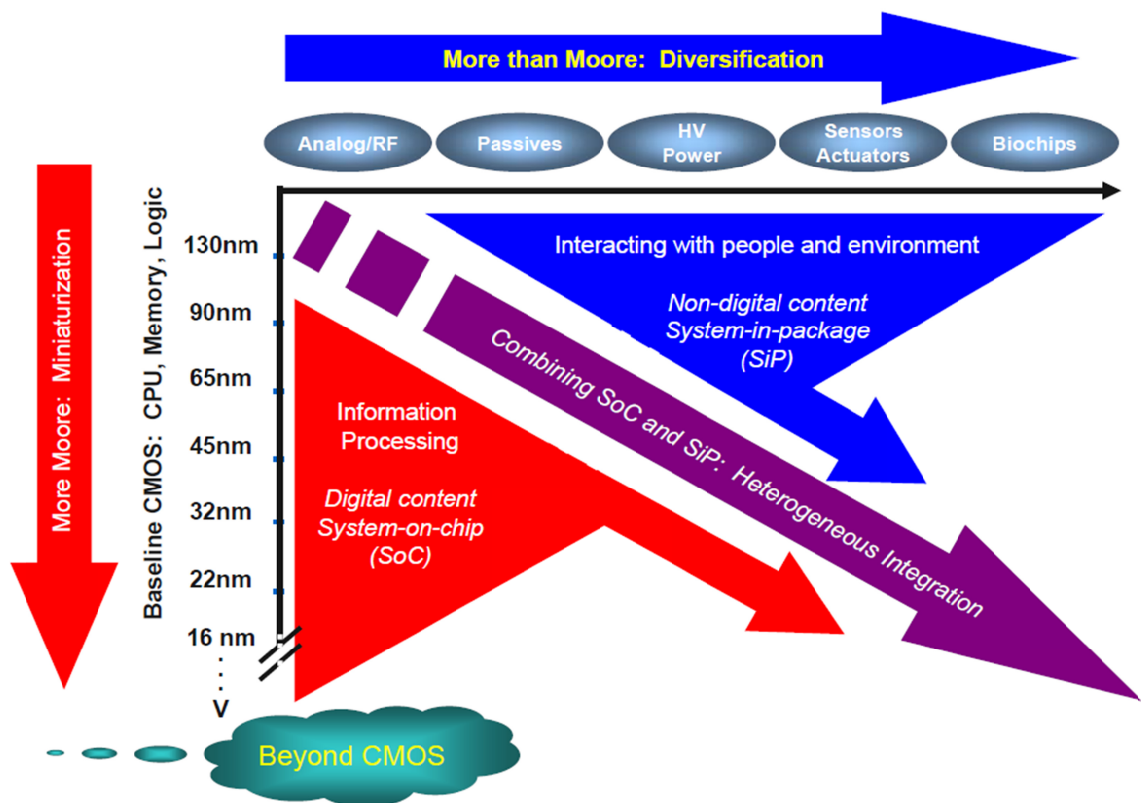


Figure 3 – Trends in the semiconductor industry (IRDS 2016)

2.2.2 3D integration

Packaging technologies are typically based on two-dimensional architectures. In order to further increase packaging densities, three-dimensional packaging technologies were introduced.

Three-dimensional architectures are a new way of increasing the performance of electronic systems. They can be defined as any technology that stacks semiconductor

elements on top of each other and utilizes vertical interconnects between the elements (Beyne 2006; Xie et al. 2010; Wolter 2012).

By application of 3D integration technologies, the size of electronic systems can be significantly reduced and higher volumetric packaging densities can be achieved. In a 3D assembly, the interconnects are potentially much shorter than in a 2D configuration, allowing for a higher operating speed and lower power consumption. This eventually enables the development of microelectronic systems that are smaller, require less power and provide a higher performance in comparison to conventional microelectronic packaging technologies (Beyne 2006).

According to Wolter, numerous technologies for 3D integration are in use to build up electronic systems with higher functionality per unit volume, reduced total package volume, lower electrical parasitics of interconnects, higher density of interchip interconnects and lower high-volume production costs (Wolter 2012). There are several 3D packaging technologies in use: package on package technologies; 3D packaging; and wafer-level 3D integration. Schematic illustrations of the three different packaging concepts are shown in Figure 4 (Beica et al. 2014).

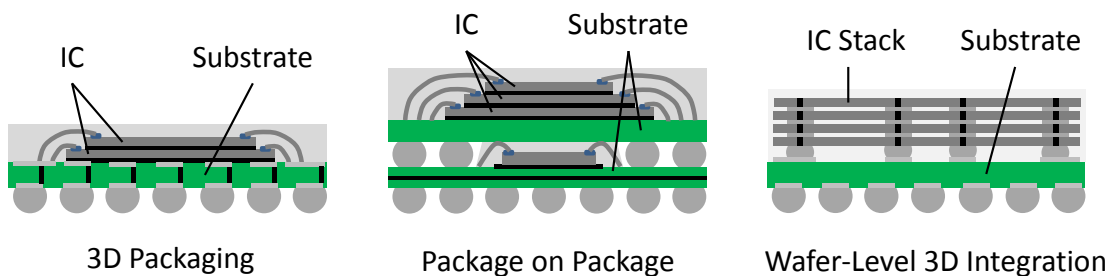


Figure 4 – 3D packaging and package on package technologies (Wolter 2012)

Package on package technologies (Figure 4 left) make use of specially designed packages, typically ball grid arrays (BGAs), which are mounted on top of each other. These stacks are then mounted on a printed circuit board (Dreiza et al. 2007).

3D packaging is a package-level method of 3D integration (Figure 4 centre). Bare dies are stacked and interconnected using wire bonding and flip-chip connections within a single package (Szendiuch 2011). Package-level integration is used for the integration of different types of dies into one package, i.e. heterogeneous integration.

3D integration at the wafer level (Figure 4 right) is done by aligning and subsequently bonding two or more wafers. These stacks are then singulated into 3D ICs. The vertical interconnection is realized by through-silicon vias. Wafer-to-wafer integration is primarily used for homogeneous integration, e.g. for memory die stacks.

2.2.3 Microsystem packaging

According to Fatikow and Rembold, MEMS integrate very small (down to nanometre scale) mechanical, electronic, optical and other components on a substrate to construct functional devices. These devices are used as intelligent sensors, actuators and controllers for medical, automotive, household and many other purposes (Fatikow et al. 2013).

Gad-el-Hak defines MEMS as devices that have a characteristic length of less than 1 mm but more than 1 μm , that combine electrical and mechanical components and are fabricated using integrated circuit batch processing technologies (Gad-el-Hak 2001).

MEMS are also referred to as micro-engineering in the UK, microsystems, mainly in Europe, or micro-machines, typically in Japan.

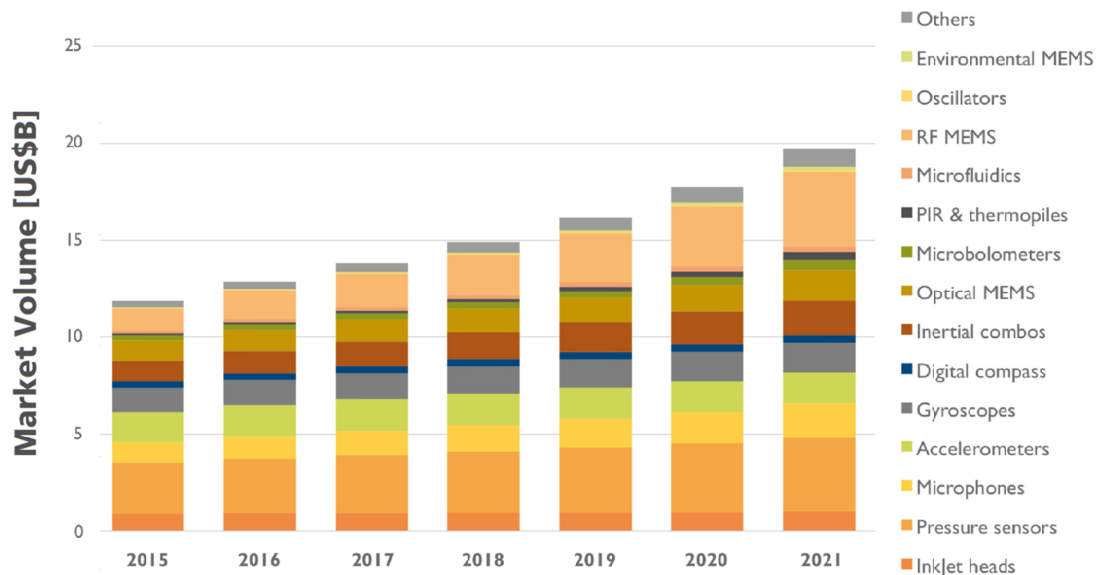


Figure 5 – 2015–2021 MEMS market forecast in US\$Billion (Yole 2016)

The MEMS market shows continuous growth, which is expected to continue in the upcoming years (Yole 2016). Figure 5 shows a forecast of the MEMS market volume for the period between 2015 and 2021. The annual growth rate of the market volume in the period from 2015 to 2021 is expected to be about 8.9% (Yole 2016). The number of units shipped in the same period is estimated to increase by 13% yearly (Yole 2016). The MEMS market has become increasingly diversified (Mounier 2012); while, for example, the automobile and consumer electronics industries are already applying a large number of MEMS, these systems are also increasingly available for niche markets such as analytical systems or special medical applications. High-volume applications are thereby opening up new technical possibilities for products with lower volumes.

The packaging of MEMS shall, as for the packaging of microelectronics, provide mechanical support, protection from the environment and an electrical connection to other system components. As MEMS attach additional functionality to electrical functions, additional requirements are imposed on the packaging of the micro system. For example, a MEMS chip may need to have fluidic connections, or to have open cavities for sensors or actuators to exert their functions. These additional requirements are subsequently imposed onto the packaging processes.

The microscopic structures on MEMS comprise different moving or non-moving features, which are susceptible to external influences. MEMS are therefore sensitive to shock, vibration and temperature. The stresses induced by external influences quickly lead to microscopic damage, which in turn leads to an impaired function or to total malfunction of the component. The microscopic dimensions of the structures increase the susceptibility to damage dramatically. In turn, potentially detrimental influences imposed onto MEMS must be controlled, reduced or ideally eliminated during the handling and joining of the component (Cohn et al. 1998; Bajenescu et al. 2012; Huang et al. 2012; Hu et al. 2014).

2.2.4 Mass to individual low-volume production

Currently, the advanced packaging market is dominated by computer and consumer electronics applications (Figure 6). These are high-volume applications, as the products are manufactured in numbers of millions of pieces per year. More specialized applications, which are produced in significantly lower volumes, include automotive and medical applications (Beica 2015).

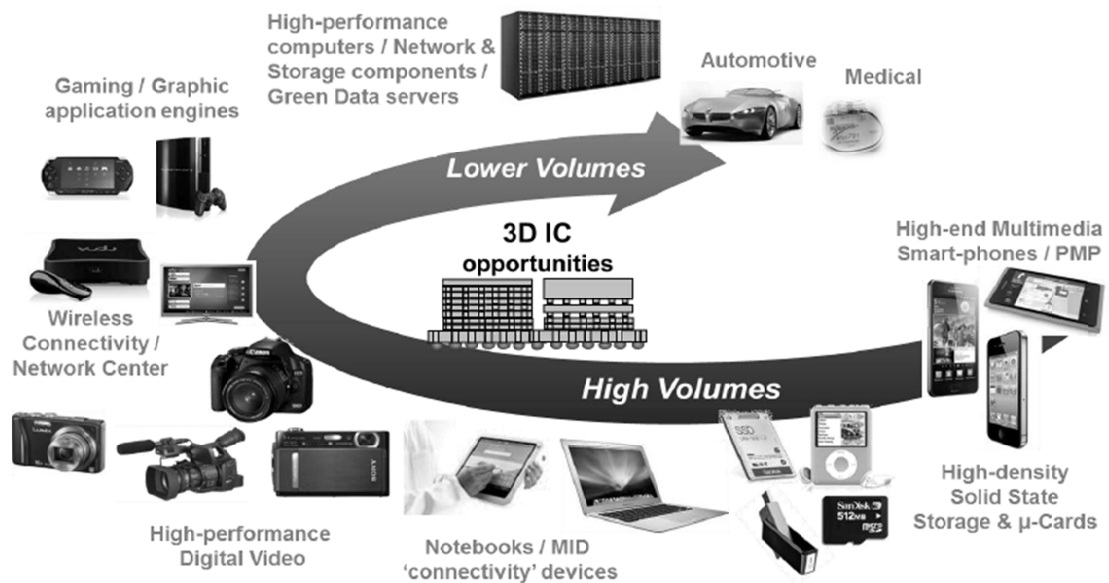


Figure 6 – 3D IC market overview (Beica 2015)

Beside the markets for bespoke high-volume products, there is a large potential for products with low to medium volumes, which is currently barely tapped. Production in low to medium volumes uses the existing mass-production equipment, which is currently not possible in a cost-efficient way. (Dickerhof et al. 2013; Scholz et al. 2016).

Consequently, novel and more efficient manufacturing methods for the development, prototyping and production of electronic packages and MEMS are required. These must not necessarily provide higher throughputs, but rather enable the reliable, cheap and efficient processing of a single component (Adamietz et al. 2010; Woegerer et al. 2014; Scholz et al. 2016).

Solutions with an improved performance of the packaging and assembly processes for lower volumes must be provided. An important component of this is the processes, which need to become more efficient for low-volume applications. Equipment is also needed that provides a higher performance for low-volume production. In consequence, a higher utilization of equipment, with lower effort to perform the processes, is required.

Additionally, the investment cost for assembly equipment is to be reduced. Through the reduction of investment cost, lower depreciation costs are achieved and the assembly of electronic packages and MEMS can be provided at a cheaper price.

Correspondingly, potential areas for the economization of electronics packaging equipment regarding investment cost and process efficiency for lower volumes need to be identified. Technical solutions are required in order to exploit this potential.

2.3 Technologies for advanced packaging

2.3.1 Flip chip

Wire bonding requires the interconnects to be placed in the area around the die. This limits the packaging density significantly as a considerable area around the die is used for the interconnects. Additionally, the wire density is limited and the necessary minimum spacing between wires must be respected.

Flip chip is based on the idea of using the whole area under the chip – not just around the chip. To achieve this, the active side of the die is “flipped” to have a direct path between the substrate, a PCB or a package. Compared to wire bonding, the electrical path between die and substrate is reduced significantly and a much higher number of interconnects per unit area can be realized.

The flip-chip mode of die attach is a combined way of realizing an electrical and a mechanical interconnection between a semiconductor die and a carrier substrate (Ulrich et al. 2006). In principle, this involves connecting metallic contacts on the die to a corresponding set of pads on the substrate using an array of solder balls (also called solder bumps, or simply, bumps) or dots of electrically conductive adhesive (ECA). The chip is placed face down on a carrier that has a corresponding set of metallized pads. Heat is then applied, causing the solder to reflow onto the substrate pads or the ECA to cure. A schematic illustration of a flip-chip assembly is shown in Figure 7.

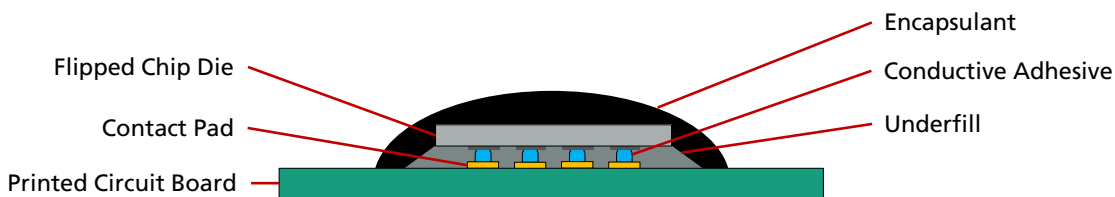


Figure 7 – Flip-chip assembly

Compared with wire bonding, flip-chip assemblies require substantially less space. Additionally, flip chip has lower interconnect dimensions, which gives them better electrical performance, reproducible electrical connection characteristics and less

electrical parasitics. This makes flip chip the preferred interconnect method for advanced packaging assemblies.

2.3.2 Equipment

The machinery used for electronic packaging processes consists typically of separate, dedicated stations. Each of the stations carries out a single process step. Die bonding, contacting and the dispensing of underfill and encapsulant have separate, specialized stations, designed for batch processing. An example of a high-volume electronic packaging line is shown in Figure 8. Whole wafers are usually the starting point for packaging processes.



Figure 8 – Sample electronic packaging line (ASE Group 2016)

A representative, simplified flip-chip assembly process chain is shown in Figure 9. The dispensing and pick-and-place processes can either be performed in one or two separate machines. A total of three adhesive compounds are applied during the process. Each of the materials is typically cured by a thermal curing process. These heating cycles are typically performed in ovens separate from the assembly equipment.

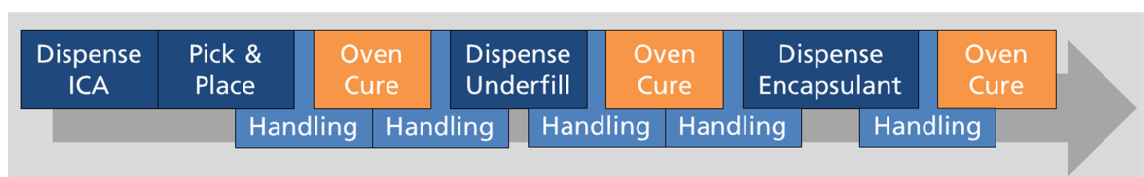


Figure 9 – Representative flip-chip process

While the dispensing and pick-and-place processes have process times in the order of seconds, the curing of polymer adhesives applied in electronic packaging can take between several minutes and several hours. This difference in process duration prevents the in-line implementation of microelectronic assembly processes, such as the process shown in Figure 9. As a consequence, the performance of the overall assembly process

is significantly impaired. A calculation for the example of a flip-chip-on-board process is presented in Appendix I.

This problem is typically circumvented by the massive parallelization and curing of large batches. However, these possibilities are only available if the produced volumes are high and a processing of large batches is possible.

For production scenarios with lower volumes and a higher flexibility, parallelization and large batches are not necessarily possible. In these cases, the throughput is massively impaired by the curing processes.

Curing processes are the main bottleneck of the flip-chip assembly process and often prevent the production from being implemented as an in-line process. More efficient assembly processes with higher performance are required; they must address the bottleneck of curing cycle times.

The next step to realize the research aim is to analyse the domain of electronic packaging and to derive detailed requirements to address the identified shortcomings.

3 Analysis and Derivation of Requirements

3.1 Surface-mount devices

According to Harper, there are four fundamental packaging technologies: moulded plastic technology; pressed ceramic (glass-sealed refractory) technology; co-fired laminated ceramic technology; and laminated plastic technology (Harper 2004).

Moulded plastic technology uses a lead frame – the support paddle – to mount the chip. The lead frame also provides the electrical fan-out path from the fingers to the outside leads. In post-moulded plastic technology, thermosetting epoxy resin is moulded around the lead frame chip sub-assembly after the chip has been wire bonded to the lead frame. In pre-moulded plastic technology, the epoxy resin is moulded around the lead frame before the chip is mounted (Parker et al. 1979; Blackwell 2002; Harper 2004).

Pressed ceramic technology packages are used mainly for economically encapsulating ICs requiring hermetic sealing. Glass is an effective material for achieving a hermetic seal for high-reliability applications. Typically, a lead frame carrying the chip is packaged using a ceramic base and a ceramic cap (Ghosal et al. 2001; Harper 2004; Bechtold 2009).

Co-fired laminated ceramic technology is the most reliable packaging technology available. Several ceramic sheets are sintered together in order to obtain a monolithic sintered body. The chip is then mounted onto this body. Wires are then bonded, before the chip is encapsulated and sealed (Gongora-Rubio et al. 2001; Imanaka 2005).

In laminated plastic technology, bare chips are mounted directly onto an organic substrate. After wire bonding, the chip is encapsulated and code-marked. If applicable, the package is then mounted onto the superior-level circuit board (Harper 2004; Bechtold 2009).

3.1.1 Chip-to-package interconnection

There are four chip-to-package interconnection options in use today (Blackwell 2002; Harper 2004): wire bond; flip chip; beam lead; and tape automated bonding.

For wire-bonded packages, the chip interconnection process generally consists of two steps. In the first step, the back of the chip is mechanically attached to an appropriate mounting surface, for example, the lead-frame paddle or the die-attach area of a

laminated ceramic or plastic substrate. This attachment sometimes enables electrical connections to be made to the backside of the chip. Three types of chip attachments are in use today: metal alloy bonding (AuSi eutectic, AuSn eutectic, and soft solders); organic adhesives (epoxies and polyimides); and inorganic adhesives (silver-filled glasses). In the second step, the bond pads on the circuit side of the chip are electrically interconnected to the package by wire bonding (Blackwell 2002; Harper 2004; Harman 2010).

The other interconnection options generally are done as one-step processes, where mechanical and electrical connections are provided by the same feature. The most popular interconnection process in general use is thermosonic ball-wedge bonding, a wire-bonding process (Blackwell 2002; Harper 2004).

3.1.2 Chip attachment

A comprehensive description of chip attachment has been provided by Harper (Harper 2004).

The major options for a die-attach process include metal alloys, organic adhesives (epoxies), and inorganic adhesives (silver-filled glasses). The eutectic die-attach process for ceramic packages is essentially contamination-free, has excellent shear strength, has high thermal conductivity across interfaces, and assures low moisture in package cavities. The major disadvantages are that the preforms are difficult to handle for high-speed automation when compared to epoxy die attach. Additionally, due to the high process temperatures, the assembly is exposed to significant thermal stresses, which in turn may affect the package reliability.

The organic die-attach process uses an epoxy, which may be electrically and thermally conductive or non-conductive. The epoxy has an advantage of being less expensive, more flexible, easy to automate, and it can be cured at low temperatures, which minimizes thermal stresses in large chips. As a result, epoxy chip-bond adhesives are preferred for attaching large chips in both ceramic and plastic packages.

Silver-filled die-attach epoxy adhesives use silver fillers, typically flakes, to make the epoxy between the chip and the substrate electrically conductive. They are also thermally conductive, providing a good thermal path between the chip and the rest of the package.

The epoxy die-attach process can be highly automated and accurate, since the epoxy can be applied at very high rates to the die-attach area by transfer printing, epoxy writing, or syringe dispensing. The chip can also be placed with high-speed pick-and-place tools.

Accurate chip placement affects automatic wire bonding by yielding greater consistency of wire lengths and improved looping characteristics. In addition, accurate chip placement also enhances the pattern-recognition performance and efficiency of the wire bonder.

In general, epoxy chip bonds are as good as or better than their metal counterparts, except in the most demanding applications where high temperatures, high current through the chip bond, and critical thermal performance are required.

3.2 Flip-chip assembly

As depicted in Figure 7, in flip-chip assembly a die is mounted on a substrate. In the following two subsections, typical properties of dies and substrates are discussed.

3.2.1 Die

Semiconductor components and silicon-based MEMS are typically produced by a series of deposition, patterning and etching processes, before the individual dies are separated (Menz et al. 2008). If necessary, the wafer is ground to a certain thickness before the individual dies are singulated either by sawing or laser cutting. Depending on the assembly method, solder bumps may be applied before die preparation (DeHaven et al. 1994).

The dimensions of a single die typically range between several hundred micrometres and several millimetres. A die has a number of contact pads, which represent its electrical interface. Very simple dies, such as diodes, may have just two contact pads while complex dies, like processors, often have several hundred contacts, which are arranged according to a pre-defined pitch. Typical pitches for modern chips range between 35 μm and 90 μm (ASE Group 2012). The contact pads have dimensions ranging between roughly 30 μm and 75 μm (ASE Group 2012).

3.2.2 Substrate

The substrate provides the necessary conductive paths in order to mount the die and to operate it accordingly. Typical substrates for flip-chip assembly are circuit boards or packages.

The assembly on a circuit board is referred to as chip-on-board (COB). This method allows the realization of higher packaging densities on the board (Lau 1994). Direct attachment without a package has electrical and thermal advantages, as well as economic benefits for high production volumes (Lau 1994).

There are numerous packages in different variants and designs that apply flip-chip assembly, such as ball grid arrays or pin grid arrays. There are also complex packages with numerous dies such as system on chip packages that apply flip-chip bonding. The packages provide a protective function, but also facilitate the handling and assembly of integrated circuits and MEMS (Blackwell 2002).

The substrate must provide the contact pad arrangement analogue to the applied die. The size, construction and uniformity of the contact pads are key to forming consistent, reliable and reworkable interconnections, with the required electrical and mechanical properties (DeHaven et al. 1994). The substrate must – like all components of the assembly – withstand the thermal processes during the assembly and, of course, during operation of the assembly (Tummala et al. 1997).

Electrical circuits around the board need to be designed and manufactured according to several design rules. These include limits for the width of electrical circuits, minimum distances between conductors and electrical properties of the materials. Comprehensive guidelines for the design and realization of reliable electronic packages can be found in the literature (Blackwell 2002; Harper 2004; Ulrich et al. 2006; ASE Group 2012).

3.3 Assembly processes

3.3.1 Flip-chip assembly process

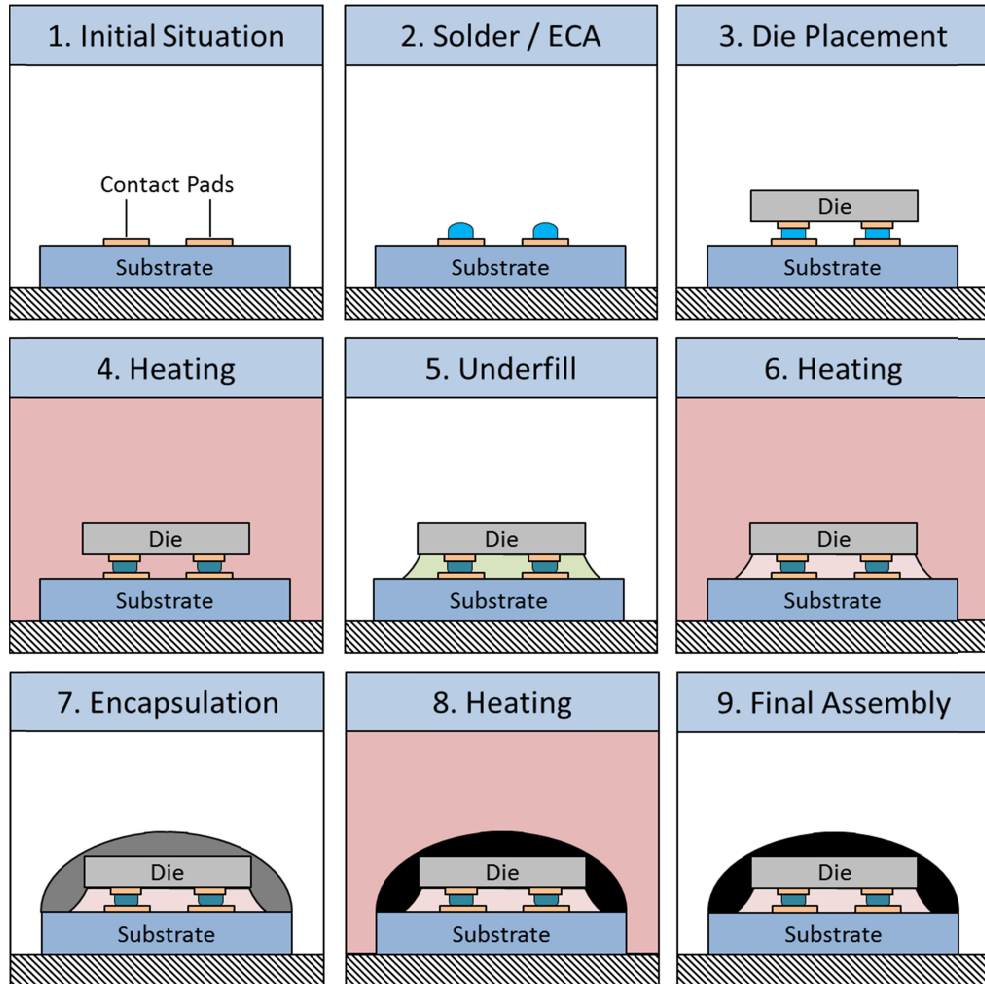


Figure 10 – Representative flip-chip assembly process

The steps of a representative flip-chip assembly process are shown in Figure 10. A package or a printed circuit board is the substrate (1). Next, a portion of solder or electrically conductive adhesive (ECA) is applied on either the substrate (bumping) or the die (not depicted) (2). The die is then placed face down onto the substrate, aligning the corresponding contacts with each other (3). The assembly is heated to melt the solder or to cure the adhesive (4). In the next step, a portion of underfill is applied between the die and the substrate (5). The material is subsequently cured (6) before encapsulant is applied over the assembly (7), which is also cured (8). After the encapsulation, the flip-chip assembly is complete (9).

3.3.2 Contacting

The contacts in flip-chip assemblies combine two separate functions: an electrical contact between the die and substrate is established; and a mechanical junction between the die and substrate is provided.

The electrical interconnection needs to fulfil several requirements. It needs to provide the specified electrical properties reliably and in a reproducible manner, and in needs to reduce possible parasitic effects. The resistance of the contacts must, therefore, be minimized. Loop inductance effects are also to be reduced. Both are significantly influenced by the dimensions and the material properties of the interconnection (Tummala et al. 1997). The probability of short circuits, and electromagnetic radiation effects needs to be minimized as well (DeHaven et al. 1994). These effects are mainly influenced by the distances between the interconnections, which are to be maximized. In addition, capacitances may exhibit unwanted effects and should therefore be minimized (Tummala et al. 1997).

The interconnection also performs the function of mechanically connecting the die with the substrate. This mechanical connection needs to provide the required strength to withstand different stresses induced by temperatures, forces, pressure, vibration and shock (Powell et al. 1993; Tummala et al. 1997; Blackwell 2002). It needs to withstand these influences during assembly and during the operation of the functional assembly.

The die, the mechanical junction and the substrate materials have different thermal expansion coefficients. Therefore, when the assembly is heated up, the unbalanced expansion of the materials leads to stresses within the assembly (Powell et al. 1993). These effects are to be reduced by choice of appropriate materials with balanced thermal coefficients and by adjusting the dimensions and materials of the junction so that it can withstand the thermal stresses.

To summarize, a contacting method providing reliable electrical and mechanical interconnection between die and substrate is required. Potential detrimental effects are to be reduced or, if possible, eliminated intrinsically by the method.

3.3.3 Placement

In the placement process, the die is picked up from a supply position and placed onto the substrate. The placement is performed in a way that accurately places all contact pads on the die over their counterparts on the substrate.

The required placement accuracy mainly depends on the size of the bond pads, the distance between each bond pad (i.e. the pitch) and the interconnection method applied.

The smaller the dimensions of the relevant structures, the higher the requirements on the placement system.

A guideline stated by Blackwell says that a deviation of $\frac{1}{4}$ of the bond pad diameter, paired with a maximum rotation of the die of 1° , is acceptable (Blackwell 2002). Thus, for a bond pad with a diameter of $80\ \mu\text{m}$, a deviation of $20\ \mu\text{m}$ would be acceptable. However, this relates specifically to solder processes, which show, for large pad sizes, self-alignment characteristics of the die when the solder is melted (DeHaven et al. 1994). For methods which do not exploit self-alignment effects, the requirements on placement accuracy increase significantly (Folmar 2000). However, the exact accuracy requirements have to be set individually for each application, taking the dimensions and joining method into account. Eventually a trade-off between the precision (and thereby quality), the throughput, and economic aspects must be found for each individual case (Negrea 2011).

3.3.4 Underfill

The combined electrical and mechanical connection using the die contacts provides a much smaller contact area compared to conventional die-attach processes; the resilience of the mechanical connection is, therefore, significantly lower (Lau et al. 1997). The reduced contact area also leads to thermal management problems, as the heat flow capacity is significantly lower through the contact pads (Lau 1996).

In order to improve the mechanical stability and to increase the heat flow capacity, a supporting material is typically applied between substrate and die. The material is generally referred to as underfill. Underfill materials are typically two phase composites, consisting of a thermoset polymer and some filling materials (Qu et al. 1998). While the thermosetting polymer establishes an adhesive bond, the filling materials are used to reduce the thermal expansion coefficient (CTE) of the underfill material and to improve the material flow (Gilleo 1998; Blackwell 2002). The thermal expansion of the underfill should be as close as possible to the thermal expansion characteristics of the solder or conductive adhesive joint (Gilleo 1998).

By application of underfill, the long-term reliability of flip-chip assemblies can be shown to be significantly improved, for both solder bumps (Palaniappan et al. 1999) and isotropically conductive adhesive bumps (Rösner et al. 1996). When using anisotropically conductive adhesives, the material provides electrical contact as well as sufficient mechanical stability (Liu et al. 1999).

There are several requirements imposed on the material and on the application process (Gopalakrishnan et al. 1998). The underfill material must be sufficiently viscous and

hydrophilic so as to fully fill the volume between chip and substrate. Voids would impair the reliability of the chip and must therefore be avoided. The dispensed volume is crucial in order to obtain a reliable assembly and must therefore be determined to form an ideal fillet. Excessive or deficient fillets lead to a decrease in reliability (Huang 1996). The properties of the filler particles, particularly their dimensions, have a strong influence on the flow characteristics and must therefore be taken into account. The CTE of the underfill should be close to that of the contact material.

3.3.5 Encapsulant

Adverse environments, contaminants, handling processes, storage, and assembly processes may have detrimental effects on the function of the semiconductor assembly. Encapsulants are used to protect the assembly with its fragile surfaces and features. The encapsulation processes must be tailored to the specific configuration and so the material properties must be chosen to provide a viscosity that is matched to the application. Voids are to be obviated, as these might affect the reliability. The material properties, such as elastic modulus, thermal properties, and electrical (insulating) properties are to be taken into account when an encapsulation material is selected (Tummala et al. 1997; Blackwell 2002; Harper 2004).

There are two typical ways to apply encapsulants: transfer moulding and dispensing methods. In the transfer moulding process, a preform of a resin material is preheated and then pressed under application of heat into a form. The resin melts and surrounds the semiconductor assemblies in the form. When the resin cools down and solidifies, the semiconductor assemblies are encapsulated (Harper 2004).

There are three typical dispensing methods: glob top; dam and fill; and cavity fill. Illustrations of the three methods are shown in Figure 11. Glob-top dispensing is a comparably simple process, in which a glob of encapsulant is dispensed on the chip and its interconnections. The material then flows over and around the device. The dam-and-fill method is performed by first dispensing a defining dam around the assembly. The cavity inside the dam is then filled with encapsulant material. This method is typically used where the height of the encapsulation is critical. For the cavity method, the assembly is performed within a pre-manufactured cavity, which is filled with a portion of encapsulant. This method is often used for pre-produced packages, particularly BGA packages (Tummala et al. 1997; Blackwell 2002; Harper 2004).

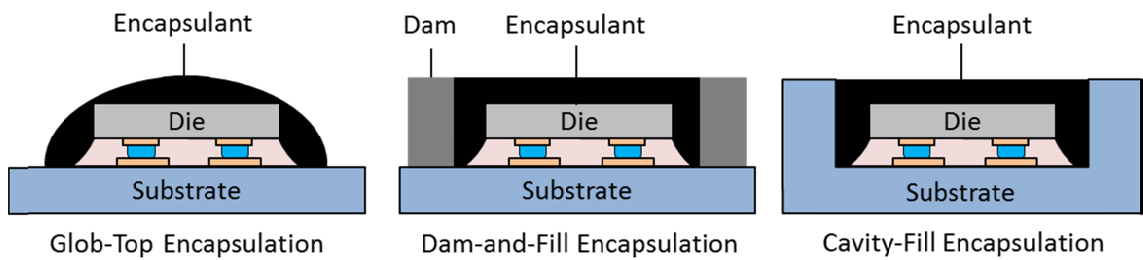


Figure 11 – Encapsulation methods

3.3.6 Electrically conductive adhesive

Electrically conductive adhesives (ECAs) are used for the bonding of surface-mount devices and for the realization of electrical interconnections, particularly in fine-pitch flip-chip applications (Jagt 1998). The materials are composite materials, consisting of a thermosetting polymer material and conductive particles. The contact between the conductive particles provides electrical conductivity, while the polymer resin provides favourable processing attributes and mechanical robustness (Ye et al. 1999; Yasuda et al. 2003b; Yasuda et al. 2003a; Gomatam et al. 2008). ECAs are widely applied in different applications in electronic packaging comprising die attach and electrical interconnections (Gomatam et al. 2008; Lu et al. 2009).

ECAs can be classified into isotropic and anisotropic materials. Figures of flip-chip assemblies with both types of ECAs are shown in Figure 12.



Figure 12 – Flip chip with ECAs

Isotropic conductive adhesives (ICA) provide uniform conductivity in all spatial directions (Gomatam et al. 2008). A very typical combination is a mixture of silver flakes and powder in polymer adhesive, usually epoxy (Morris 2011), although nickel, copper and gold are also used as filling materials. The adhesive conductivity depends on the ratio of metallic filler to polymer. The conductivity increases only slightly when the metal content is increased, but rises dramatically when the so-called ‘percolation threshold’ is reached (Li et al. 1997). This rise occurs when a continuous electrical path

is established by the filler particles (Liu et al. 1998; Morris 2011). Due to this conducting mechanism provided by distributed metallic content, the specific conductivity is generally lower than that of a solid metal conductor (Kim et al. 1993). The presence of the polymer material affects the contact resistance as it partially isolates the particles from the contact area (Liu et al. 1998). However, by application of pressure onto the joint before curing, the contact resistance can be significantly decreased (Li et al. 1997). Typical applications for ICAs are die attach, solder replacement for the attachment of surface-mount device (SMD) components, flip-chip interconnections, the filling of vias on PCB boards and through-silicon-via applications (Harper 2004; Gomatam et al. 2008; Morris 2011).

Anisotropic conductive adhesives (ACAs) are also polymer materials filled with metallic particles. However, the ratio of the filler content to polymer material ranges only between 5% and 10% (Morris et al. 2007). The filling content is therefore below the percolation threshold and the material is not electrically conductive. To achieve a local electrical conduction in a flip-chip assembly, a film of ACA is applied onto a substrate, covering the bond pads. Next, the die is positioned over the bond pads and pressed against the substrate. In this way, conducting particles are trapped in an increased concentration between the bond pads of the substrate and the die, providing a local electrical interconnection. The rest of the ACA remains non-conductive. In this state, heat is applied, using, for example, a thermode, in order to cure the adhesive. The key to obtaining a good electrical contact is achieving sufficient deformation of the particles in the joint (without damaging any of the components) (Fu et al. 2000). In this way, good electrical and mechanical performance can be achieved. In flip-chip assemblies, ACA joints can achieve comparable electrical properties to solder joints, especially for fine-pitch applications. In addition, the assembly process becomes simpler, as ACA enables the combined functions of electrical contact material and underfill. ACAs are typically used for the assembly of LCD screens and for fine-pitch flip-chip assemblies (Kristiansen et al. 1998; Liu et al. 1998; Liu et al. 1999).

3.3.7 Curing

The curing of thermosetting polymers is a complex process involving the interaction of chemical kinetics and changing physical properties (Enns et al. 1983). During the curing process, two main phenomena can be observed: gelation; and vitrification (Enns et al. 1983; Karkanis et al. 2000). While gelation corresponds to the incipient formation of a network of cross-linked polymer molecules, vitrification is the transformation from a liquid or rubbery state into a glassy state as a result of increased molecular weight (Enns et al. 1983). The relationship between time, temperature and material transformation is

often described using a time–temperature–transformation diagram (Simon et al. 1994; Urbaniak et al. 2007).

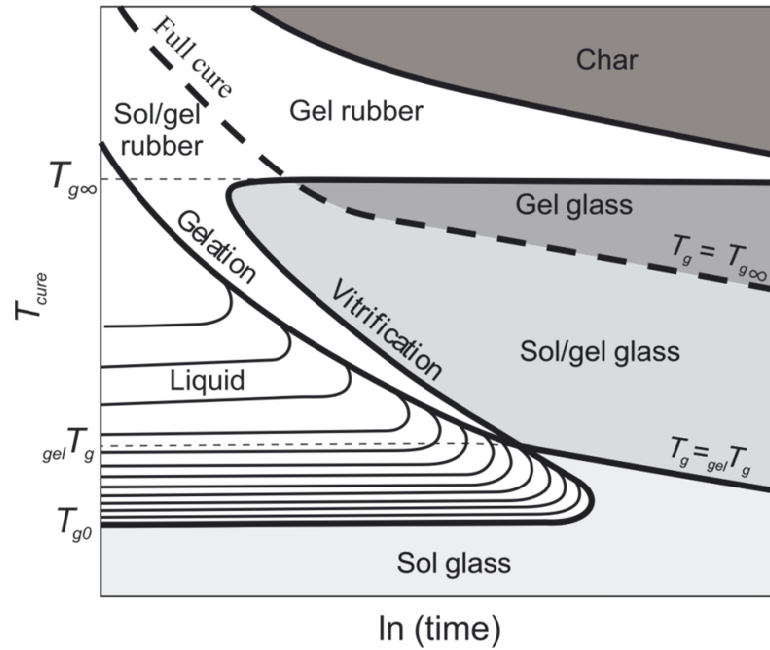


Figure 13 – Generalized TTT cure diagram (Urbaniak et al. 2007)

A generalized isothermal time–temperature–transformation (TTT) cure diagram for a thermosetting system is shown in Figure 13. The phenomena of gelation and vitrification control practically all properties of a thermosetting material, including rheology, reaction rate, density, dimensional stability, and internal stresses; these can be exploited during cure to optimize the processing and final material properties (Simon et al. 1994). Practically all properties can be controlled within a certain process window by a profile of temperature over time.

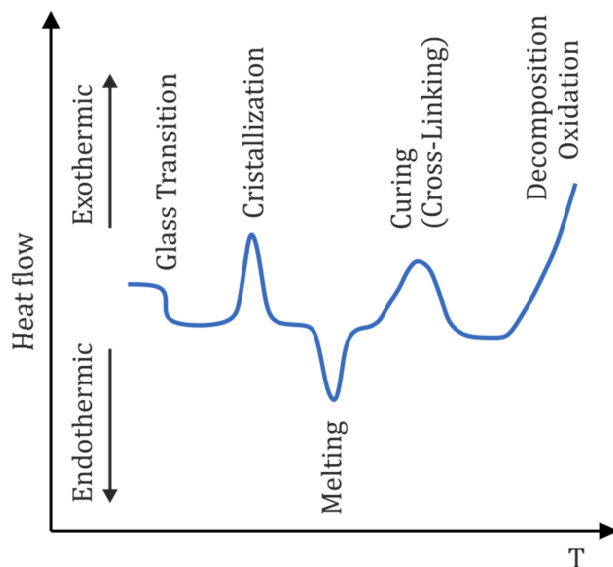


Figure 14 – Transitions in a DSC curve (Thomas 2005)

The numerous involved processes also have an impact onto the heat flow of the polymer. The heat flow can be measured by differential scanning calorimetry (DSC). A representative DSC curve of an epoxy polymer is shown in Figure 14. At the glass transition temperature T_g , the heat capacity of the polymer increases and the polymer is therefore able to store more heat (Gibbs et al. 1958). Polymers may also partially, or completely, crystallize within a curing cycle (Ozawa 1971). During the crystallization process, heat is dissipated, as it is an exothermic reaction (Ozawa 1971). Melting, however, requires additional energy to realize the phase change and is therefore an endothermic reaction. A phase change of the heated material or one of its compounds might lead to an increased heat flow (Blundell 1987). Cross-linking processes in polymers, as they happen, for example, in epoxy compounds, are exothermic reactions (Gabbott 2008). Therefore, heat is dissipated during curing of epoxies. If heated further, the polymer will dissipate further heat during the exothermic processes of oxidation and decomposition (Gabbott 2008).

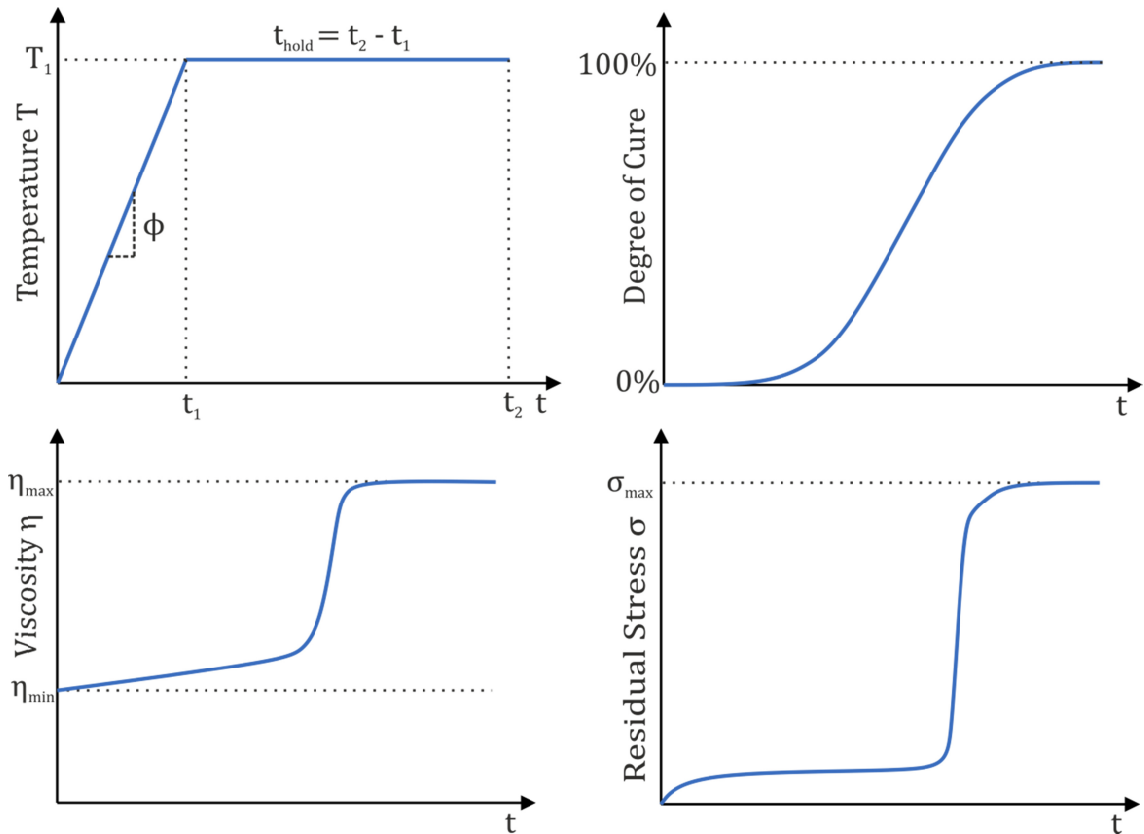


Figure 15 – Curing behaviour of a polymer adhesive

Figure 15 shows a qualitative overview of different variables during the cure of a polymer adhesive. These curves have been derived from data found in the literature (Enns et al. 1983; Loos et al. 1983; Tilford et al. 2008c; Morris et al. 2009).

The polymer material is exposed to a defined temperature profile comprising the heating, with ramp rate Φ , until the set point of temperature T_1 is reached. This temperature is held for time period $t_{hold} = t_2 - t_1$. This is a typical cure schedule for epoxy adhesives. Further possible temperature specifications include a pre-cure thermal soak or defined cooling of the polymer after cure.

Heating of the polymer expedites its curing process. The curing reaction starts at a very low rate, corresponding to the low temperature. The curing rate increases with temperature. When the majority of the polymer is cured, the degree of cure asymptotically approaches a full cure of 100% (Tilford et al. 2008c; Morris et al. 2009; Tilford et al. 2011).

When the temperature is ramped up, the viscosity η of the polymer increases slightly. With progressing solidification, its viscosity increases rapidly before approximating the maximum viscosity η_{max} (Hsiung et al. 1997).

With solidification of the material, stress in the polymer material can be observed. Before solidification, these are primarily thermally induced. When the cross-linking processes expedite gelation and vitrification processes, residual stresses in the material build up rapidly before they asymptotically approximate the maximum stress σ_{max} . High residual stresses affect the reliability of the adhesive joint and also of the whole assembly. Consequently, the residual stresses are to be minimized (Tilford et al. 2008c; Tilford et al. 2011).

Not depicted, but still relevant to the process is the mass loss. An epoxy compound may lose between 5% and 25% of its mass during a cure cycle (Loos et al. 1983).

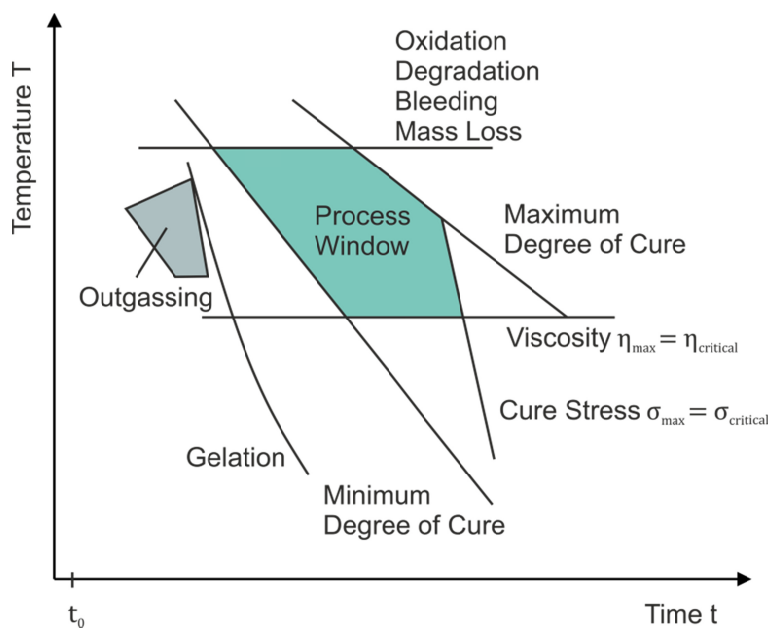


Figure 16 – Processing diagram for polymer adhesives (Hsiung et al. 1997)

To illustrate the different process variables and to aid finding appropriate process windows, Hsiung and Pearson propose a processing diagram (Hsiung et al. 1997). As shown in Figure 16, it allows the determination of applicable time–temperature profiles relative to a starting time t_0 for a certain polymer material. The actual process window is mainly defined by minimum and maximum degree of cure, viscosity, residual stress in the adhesive bond, and degradation effects including mass loss (Hsiung et al. 1997; Taweplengsangsuksue et al. 2000). Further requirements, such as temperature restrictions from bonded components, may further reduce the possible process windows. Based on the restrictions imposed by the different process variables and the resulting possible process window, applicable temperature profiles may be derived.

An overview of the peak temperatures and the duration of curing cycles for a number of typical electronic packaging materials is shown in Figure 17. Four classes of materials have been considered: ICAs; underfill materials; encapsulant materials; and Pb-free reflow solder materials. Recommended cure cycles for a total of 39 materials have been compiled. A point in the graph shows the peak temperatures and the total length of the cure cycle. The points of different material classes are marked in different colours.

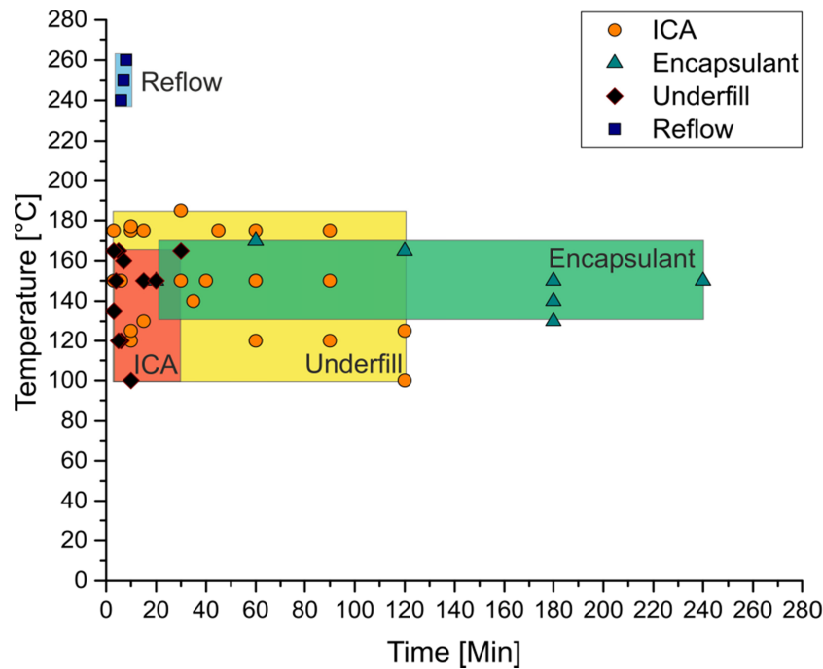


Figure 17 – Peak temperatures and cycle duration of pastes applied in electronic packaging¹

The considered ICAs are cured at temperatures between 100 and 165 °C. The duration of the curing cycles range between 3 and 30 minutes. A typical reflow curing profile requires between 5 and 8 minutes at a temperature of 240–260 °C. ICAs can, therefore, compete with reflow solder in terms of process duration and have significant advantages regarding the temperature load. Underfill material curing duration ranges from 3 minutes to 2 hours at temperatures of 100–185 °C. Encapsulant materials are cured at temperatures of 130–165 °C and require between 20 minutes and 4 hours to cure.

Precision dispensing and pick-and-place processes can be realized in the order of seconds, while curing processes require between a few minutes and several hours. Dispensing and pick-and-place processes are serial processes, while curing is typically a batch process. The low throughput for curing processes is often circumvented by

¹ Henkel Electronic Packaging Materials

performing a significant number of serial assembly operations before curing the processed parts all together in a batch. In all cases, there is a significant mismatch between the cycle times of assembly and curing operations, which affects the effectiveness of the assembly machines. Any reduction in curing cycle times would have a positive effect on the productivity and the cost-effectiveness of the whole process (Dong et al. 2009).

Pizzagalli *et al.* describe the cost-effective realization of 3D packaging for lower volumes as one of the main challenges in the electronics industry (Pizzagalli et al. 2014). In this context, one of the key challenges is the development of highly integrated machinery with significantly increased throughput at lower volumes (Pizzagalli et al. 2014). This would significantly reduce the fabrication cost, rendering 3D technologies more attractive to the industry (Chen et al. 2010; Beica et al. 2014).

As curing processes represent the main bottleneck in the process chain, a reduction of curing cycle times is identified as a key goal. A typical and standardized process in the backend of electronic packaging processes is the reflow process. The duration of reflow processes is, on average, significantly lower than typical adhesive curing processes – particularly regarding underfill and encapsulant curing processes. If the duration of curing processes can be reduced to the duration of reflow processes, then they no longer represent a bottleneck. Therefore, a working hypothesis is to reduce curing cycle times down to the duration of typical reflow processes according to J-STD-020E (JEDEC 2015). Reflow processes for lead-free solder, according to J-STD-020E, have an average duration of approximately 420 s (JEDEC 2015). Based on this target, a requirement can be described:

Requirement 1 – Reduction of curing cycle times down to the duration of reflow processes according to J-STD-020E.

Curing of thermosetting polymer adhesives is a complex process that affects a number of important aspects of processing and the resultant material properties. To ensure that the adhesive provides the desired properties, the processing is to be performed within a material- and application-specific process window. The process must, therefore, be performed according to a defined time–temperature profile, comprising ramp rate for curing and, optionally, hold times for pre-cure thermal soak, as well as hold times at specific temperatures for curing. While heating up the material, the heat flux is affected by exothermic and endothermic reactions. To compensate for these disturbances, control of the temperature is required.

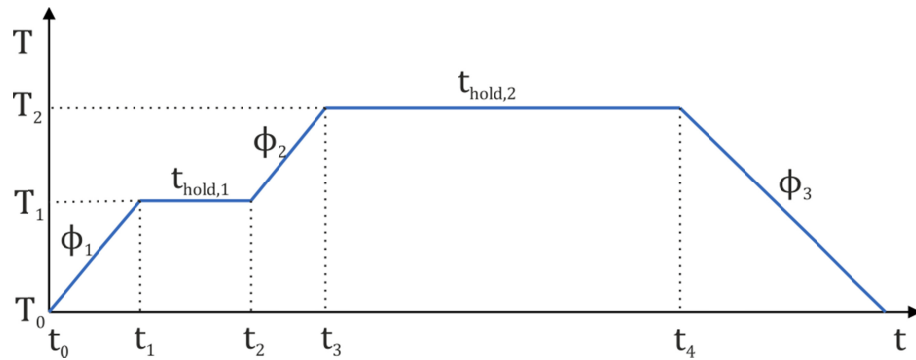


Figure 18 – Generic temperature profile

Recommended temperature profiles are usually provided together with the material. Figure 18 shows a generic temperature profile, which describes the set points for temperature over a given time, consisting of temperature ramps and hold periods. During a ramp period, the temperature is changed with a defined, and usually constant, ramp rate ϕ . The ramp rate can either describe a rise (heating) or a decrease (cooling) of the temperature within a defined time period. Within a hold period, a set temperature remains constant for a specific period t_{hold} (Loos et al. 1983; Morris et al. 2009).

Temperature profile specifications vary in their complexity. In many cases, just a single hold period at a defined temperature is described, without definition of ramp rates, (e.g. 150 °C for 2 h). For some materials, additional ramp rates for heating (ϕ_1 , ϕ_2) and cooling (ϕ_3) are defined. Materials applied for more complex packages may require a pre-cure thermal soak period ($t_{hold,1}$) in order to pre-heat the assembly at a lower temperature (T_1) below the actual curing temperature (T_2) in order to reduce temperature gradients and the associated undesired effects of uneven cure or residual stresses within the assembly. During processing, the temperature is to be controlled within defined limits, which are here described by ΔT .

Cure schedules are very much specific to the composition of the material used and are, therefore, usually provided by the material manufacturer; there are no standard profiles. To determine the requirements imposed for temperature control, the catalogues of three major providers of adhesives and pastes for electronic packaging have been analysed and the extreme values for ramp rates and hold times have been extracted (Henkel 2011; EPO-TEK 2013; Masterbond 2015). Some of the materials studied are designed to be used in reflow solder processes, which have the highest requirements for ramp rates and cooling among the considered specifications (JEDEC 2015). The tolerated deviation ΔT from the set temperature directly measured on the part is typically ± 5 °C (Rosu et al.

2003; Zhang et al. 2009; Wang et al. 2010). The derived parameters from the analysis are compiled in Table 1.

Table 1 – Derived maximum values for cure profile parameters

Φ_{min}	Φ_{max}	$t_{hold,min}$	$t_{hold,max}$	T_{max}	ΔT_{max}
$-6 \frac{^{\circ}C}{s}$	$3 \frac{^{\circ}C}{s}$	3 s	24 h	260 °C	$\pm 5 \text{ }^{\circ}C$

Based on the discussion of cure profiles and the derived process parameters from Table 1, a requirement can be formulated:

Requirement 2 – Controlled heating of the polymer adhesive according to a defined temperature profile within an industrially relevant range of process parameters.

3.3.8 Temperature-sensitive components

There are numerous temperature-sensitive devices used in electronic assemblies. Figure 19 shows an overview of temperature-sensitive device families as compiled by Pymiento *et al.* (Pymiento et al. 2008).

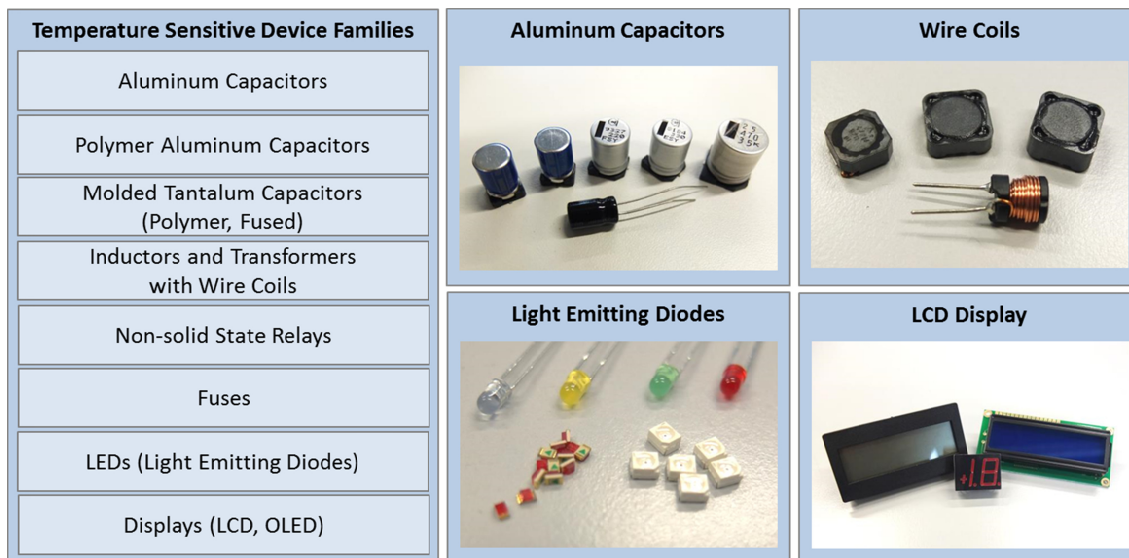


Figure 19 – Temperature-sensitive components

Overheating such sensitive devices during the assembly process, particularly during the soldering and curing processes, can result in serious reliability issues (Eveloy et al.

2005; Pymeto et al. 2008). The components may suffer from immediate or accelerated mechanical damage, such as popcorning, delamination or cracking (Eveloy et al. 2005). Also, the function of the component may be affected partly or completely. For example, LEDs are very temperature sensitive and may suffer from optical property degradation when exposed to heat (Eveloy et al. 2005).

In practice, temperature-sensitive components are assembled in a separate step at lower temperatures. The assembly of these components is often performed manually, which affects yield and the product quality.

Temperature-sensitive components can, in principle, be spared by not exposing them to detrimental temperatures; this can be achieved by cure profiles with sufficiently low peak temperatures or by selective heating of the area of interest. As only few materials can be cured at lower temperatures, and then often with significant drawbacks, selective heating should be further pursued.

3.3.9 Selective heating

A flip-chip-on-board assembly is typically performed separately and after conventional SMT processes, due to the increased accuracy requirements. In this case, the assembly is often exposed to a heating profile for the SMT assembly, and then to several further heating profiles for the flip-chip assembly. Each heating process induces thermal stresses and accelerates the ageing of the assembly and its components. Therefore, to prevent the whole assembly, and specifically process-sensitive components, from thermal damage, the thermal load on the assembly must be reduced.

One approach to thermal load reduction is selective heating. This refers to local and confined application of heat to a defined volume. The relevant volumes are heated to their processing temperatures, while the surrounding volume is spared.

Selective heating methods based on laser and infrared processing can effectively reduce the thermal load during assembly. This has been demonstrated for electronic packaging applications (Moon et al. 2004b; Anguiano et al. 2011; Felix et al. 2012; Ogochukwu 2014).

Within Section 3.3.7, a maximum temperature of 260 °C was derived (see Table 1). This temperature is detrimental for the previously described temperature-sensitive components, and for the assembly in general. Selective heating is therefore indicated as a potential solution.

When selective heating is applied, the heated component itself must be heated according to the previously defined temperature profile, as stated in Requirement 1 and

Requirement 2. The surrounding components, however, must be spared from the peak temperature.

Typically, there is a clearance between the components on a board or in a package. This clearance is defined during the design process with consideration to the component courtyard area, thermal management, and assembly requirements. In a package, the design must also consider tolerances and the subsequent processes, such as underfill or encapsulation. The clearance ranges are typically between 0.5 mm and 2.5 mm (Tummala et al. 1997; Blackwell 2002; IPC 7351; Beyne 2006).

If selective heating is applied, then the temperature decreases continuously with increasing distance from the heated volume. In this case, where flip-chip processes including complex packages and flip chip on board are considered, a significant temperature reduction within typical clearance distances must be achievable. Otherwise the packaging density would be impaired.

A worst-case assumption of the peak temperature in the studied case is a maximum temperature $T_{max} = 260\text{ }^{\circ}\text{C}$. Within the clearance area, this temperature should be reduced to an acceptable temperature for sensitive devices. A temperature of $150\text{ }^{\circ}\text{C}$ is generally deemed as acceptable for most temperature-sensitive devices (Tummala et al. 1997; Tong 2011).

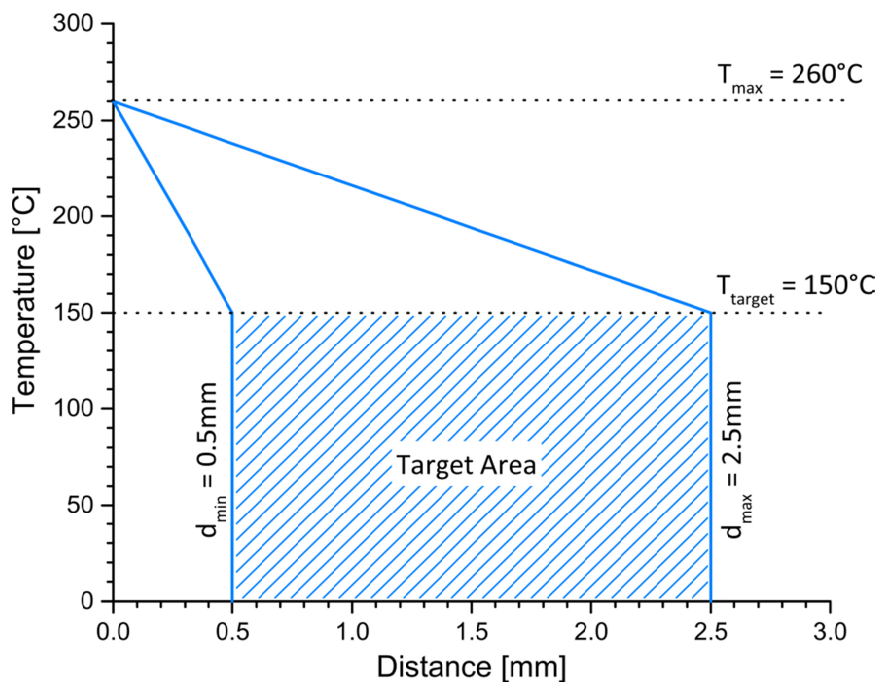


Figure 20 – Target definition for selective heating

The definition of temperature–distance target for selective heating is illustrated in Figure 20. T_{target} is the target temperature. Minimum and maximum distances from the edge of the processed component are described by d_{min} and d_{max} , respectively. Based on this target definition, a requirement can be described:

Requirement 3 – Selective heating with reduction to target temperature within clearance area.

3.3.10 Reliability

A product can be very sophisticated regarding its design and manufacturing, but becomes useless if it fails to provide the designed performance during its expected lifetime (Hsu 2006). Reliability can also be described as the probability that a piece of equipment operating under specified conditions shall perform satisfactorily for a given period of time. Especially for electronic packages or MEMS, reliability is a critical requirement. The failure of a single electronic package or MEMS may cause the failure of the whole assembly. The failure of an electronic package can be basically rooted to three basic failure modes: an electrical short; an electrical open; or an intermittent failure that includes an unacceptable change in a given parameter (Singh et al. 2012). These failures are triggered or provoked by stress of different kinds, which can occur in isolation or in combination.

In electronic equipment, the most prominent stresses are temperature, voltage, vibration, and temperature rise due to current (Singh et al. 2012). These stresses affect all components of the package, comprising the die, the interconnections and the substrate. Additionally, unforeseen events such as thermal or mechanical shock may lead to an immediate failure of the component or may reduce its lifetime significantly.

The design and manufacturing processes of a microelectronic component must therefore also include reliability considerations. To obtain a higher reliability, more development effort is necessary. A trade-off between time, cost and quality (reliability) needs to be found. The key to (and also the art of) a cost-effective product is to set the reliability requirements adequately for the application.

Temperature cycling tests are conducted to determine the ability of components and solder interconnects to withstand mechanical stresses induced by alternating high- and low-temperature extremes (JEDEC 2015). Permanent changes in electrical and/or physical characteristics can result from these mechanical stresses (JEDEC 2015). Among the many environmental accelerated testing methodologies for assessing reliability of electronic systems, thermal cycling is the most commonly used test for the characterization of devices as well as interconnections (Ghaffarian 2000).

A common and widely used standard for temperature cycling tests is JEDEC JESD22-A104 (JEDEC 2015). However, a variety of further standards for temperature cycling exist. Test specifications are often adapted for a specific field of application. For example, IPC[®] and IEC offer a number of standards for commercial components (IEC-60749-25, IPC-9701). Specific standards, with significantly higher requirements, are available for military applications (Mil-STD-883), as well as standards for space applications (e.g. NASA-STD-8739.3, IEC J-12). Temperature cycling tests are usually carried out using temperature cycle chambers, which allow temperature control according to the set profiles, including ramp rates.

The impact of a novel manufacturing technology on the reliability of the product, or specifically the package in this case, is an important factor for industry acceptance. Therefore, packages manufactured with the novel method must provide at least the same reliability as established technologies. Based on these findings, a further requirement can be derived:

Requirement 4 – Packages manufactured with the novel process must provide at least the same reliability as conventional technologies.

3.3.11 Process analysis

Key challenges of equipment manufacturers for advanced packaging lie in the reduction of costs and improvement of the process efficiency (Beica et al. 2014). Pizzagalli *et al.* identified the assembly processes and related equipment as important subjects for optimization (Pizzagalli et al. 2014).

A characteristic of economic assembly is the avoidance of any unnecessary movement of assembly parts, of persons and of the used appliances (Lotter et al. 2006). The concept of primary–secondary analysis is a simple and effective method to assess the economic effectiveness of an assembly system and to reveal potentials for optimization and rationalization (Lotter 1982; Lotter 1985; Lotter et al. 2006; Lotter 2013).

Primary processes are all expenditures of time, energy, information, and parts for the completion of the assembly, which add value during the assembly process (Lotter 2013). Secondary processes, on the other hand, are all necessary expenditures of time, energy and information, which occur due to the chosen assembly principle and do not cause an added value to the product (Lotter 2013).

A graphic interpretation of primary and secondary effort is possible by drawing the efforts as vectors (Lotter 2013). The portions of primary and secondary effort are

inserted into a coordinate system, which allows eventual determination of the effort in the form of a vector.

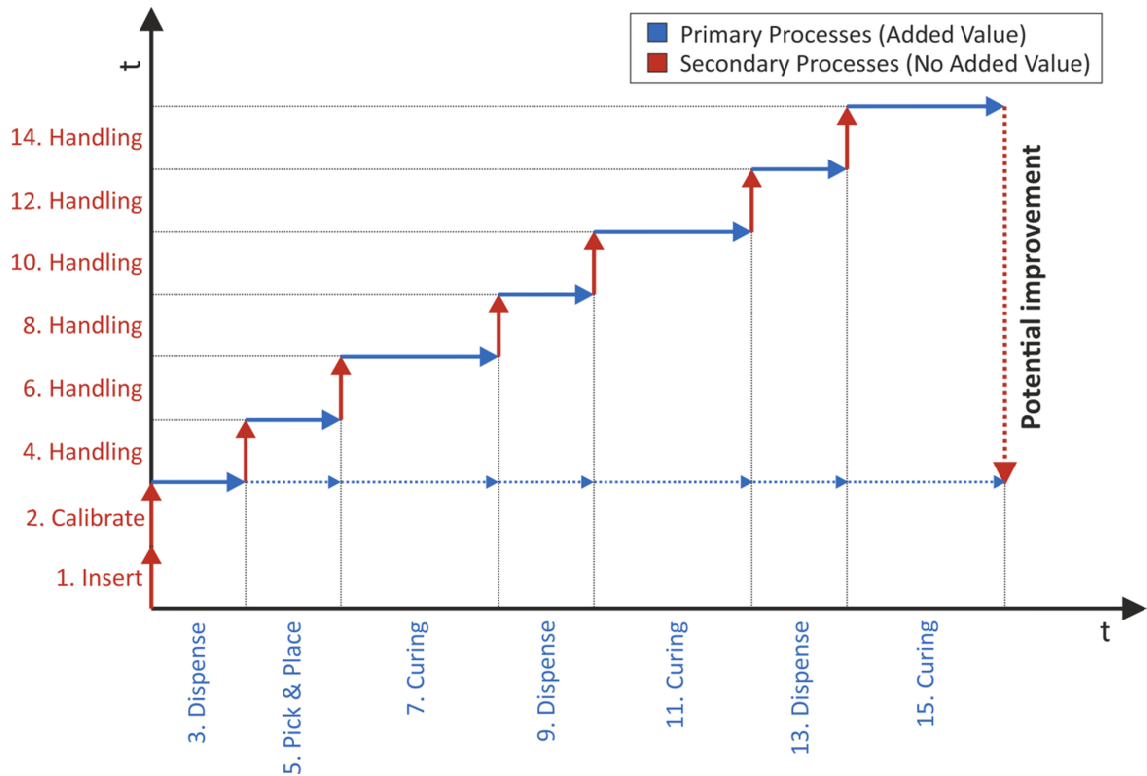


Figure 21 – Primary–secondary analysis of the flip-chip assembly process

Figure 21 shows a primary–secondary analysis of a representative flip-chip assembly process with conductive adhesive. The durations of each activity are not true to scale. In particular, the duration of the handling processes has been assumed as equal for all cases. Nonetheless, the chart provides a qualitative overview of the ratio between primary and secondary processes to help identify possible improvement potential.

A typical assembly process in electronics packaging is performed by providing a dedicated machine for each subprocess. These can be freely arranged, e.g. in a laboratory, or linked by a conveying system. In any case, the assembly has to be transferred to and removed from each station. These handling processes are secondary processes as no value is added to the product. The value-adding processes are assumed to be perfectly efficient, and the impact of handling processes on the assembly duration is the main subject of review.

As can be seen in Figure 21, handling processes between each machine (process) are required. Each handling operation reduces the overall process efficiency. If, theoretically, the intermediate handling processes could be completely eliminated, then the overall process efficiency would be substantially increased, as indicated by the red

pointed arrow. This corresponds to an integration of all processes into a single machine. With the assumptions made in this case, the efficiency would only be impaired by the insertion to the machine, calibration processes and the extraction from the machine. The overall process efficiency would be substantially improved if all processes were integrated into one single machine (and the efficiency of the value-adding processes is not decreased).

Three different materials are dispensed during the flip-chip assembly process. Each of the materials is cured, typically in a thermal process. In most cases, the assembly is transferred into a convection oven where it is exposed to a defined temperature profile. This means that during the flip-chip assembly process, three handling steps into similar or identical equipment are necessary. The integration of a curing device could therefore serve for three processes within the process chain and significantly reduce the handling effort. In this way, the overall efficiency of the process chain could be improved.

A further requirement can therefore be derived:

Requirement 5 – Integration of all process components into a single machine – particularly the curing equipment – in order to minimize the product-handling effort between the individual processes.

3.4 Conclusions on requirement analysis

Analysis of the aforementioned research problem has been performed. The field of electronic packaging in general has been analysed, with an emphasis on surface-mount devices. The underlying assembly processes were then explored in detail, focussing on the materials and their curing behaviour. In the course of the analysis, relevant requirements that are central to the research problem have been derived.

These requirements are additionally compiled and presented in Table 2.

Table 2 – List of requirements

Requirement	Description
1	Reduction of curing cycle times down to the duration of reflow processes according to J-STD-020E
2	Controlled heating of the polymer adhesive according to a defined temperature profile within an industrially relevant range of process parameters
3	Selective heating with reduction to target temperature within clearance area
4	Packages manufactured with the novel process must provide at least the same reliability as conventional technologies
5	Integration of all process components into a single machine – particularly the curing equipment – in order to minimize the product-handling effort between the individual processes

4 State of the Art

4.1 Review of curing methods

While convection heating is the most-used method to expedite and perform adhesive curing processes, alternative methods exist and offer distinct advantages. The different curing methods and equipment thereof are described in this section.

4.1.1 Convection heating

In applied convection heating, the polymer material is surrounded by a gas within an oven. This gas is heated to a set temperature and typically circulated within the oven. Heat energy is transferred into the bulk of polymer material through thermal conduction. The rate of energy absorption is typically described by Newton's law of cooling given by Equation (1) (O'Sullivan 1990):

$$\frac{1}{A} \cdot \frac{dQ}{dt} = h(T - T_a) \quad (1)$$

where

- A heat transfer surface area [m^2];
- Q thermal energy [J];
- h heat transfer coefficient [$\frac{\text{W}}{\text{m}^2\text{K}}$];
- T temperature of the object [K];
- T_a temperature of the fluid surrounding the body [K].

The rate of energy absorption is therefore proportional to the temperature difference between the bulk of the polymer material and the temperature of the surrounding fluid. Thus, the temperature curve of the heated material tends asymptotically towards the oven temperature.

The hot gas does not penetrate into the polymer. Therefore, the surface of the material is heated primarily, while the bulk of the material is heated gradually by conduction. The curing process of thermosetting polymer materials typically takes between several minutes and several hours, depending on the material.

Nearly all classes of polymer materials are available in a thermosetting form. Therefore, for practically all applications using polymer adhesives and encapsulants, the curing can be realized using convection ovens.

Due to its simplicity, its proven reliability, and wide range of possible applications, convection heating is the most-used heating process for polymer curing.



Figure 22 – Convection ovens (Hivision 2017; Heller 2017)

Two types of oven are prevalent in industrial environments: batch ovens; and in-line convection ovens. Examples of such ovens are shown in Figure 22, where batch ovens are shown on the left, and a reflow oven, as an example of an in-line oven, is presented on the right.

Batch ovens allow the processing of one batch at a time. State-of-the-art ovens feature a temperature controller, which allows the programming of defined temperature profiles. The control is normally based on the temperature of the heated gas. Some ovens additionally provide active cooling, which additionally improves the control performance of the oven. In batch ovens one batch may be processed at a time. Typical footprints of batch oven systems range from 0.25 m² to 1 m². An oven with a footprint of 0.5 m² can carry approximately 100 parts, with dimensions of 10 × 10 mm per shelf.

In-line convection ovens are equipped with a conveyor system, which transfers the product through the oven from a start to an end point. During the transfer through the oven, the product is exposed to a defined temperature profile, which is achieved by different temperature zones. This enables the oven to process several parts in parallel. Continuous convection ovens for mass-production purposes are often several metres long.

4.1.2 Infrared heating

Infrared radiation is a form of electromagnetic energy, which is transmitted in wave form, with wavelengths of between 0.78 μm and 1 mm, lying between visible light and microwaves (Tipler et al. 2007). Such radiation is provided by an infrared heater or heat lamp whose body, with a higher temperature, transfers energy to a body with a lower temperature through electromagnetic radiation (Deshmukh 2005). The wavelength at which a maximum of radiation occurs, also called the peak wavelength, is determined by the temperature of the heater (Tipler et al. 2007). This relationship is described by basic laws for black-body radiation (Sakai et al. 1994; Tipler et al. 2007).

When the infrared radiation hits the surface of the polymer material, a part of it is absorbed by the molecules on the surface and is transformed into heat (Serway et al. 2013). The rest of the polymer volume is then heated by convection from the surface to the inside of the material. The penetration depth is strongly dependent on the combination of wavelength and material. According to Kirchhoff's law (Tipler et al. 2007), the sum of the transmittance t , absorptance a and reflectance r is 1, irrespective of wavelength λ as indicated in Equation (2).

$$a(\lambda) + t(\lambda) + r(\lambda) = 1 \quad (2)$$

Therefore, the penetration depth can be significantly influenced by choosing an appropriate combination of infrared wavelength and thermosetting polymer material, characterized by a high transmittance relative to absorptance and reflectance.

The infrared light can be focussed by masks or optics to enable selective heating. However, infrared heating is not suitable to directly heat a covered material. For example, infrared heating is not suitable to heat the conductive adhesive under the die in flip-chip bonding.

Although strongly dependent on the applied material and the infrared wavelength spectrum, in many cases the curing of thermosetting polymer materials can be realized significantly faster than with a convection oven.

Infrared ovens are, as with their convection counterparts, available as batch ovens and in-line ovens. Additionally, spot-heating devices are available. These devices allow the selective heating of a defined area. The devices are relatively small and light, and can be integrated into existing machines.

If temperature control is implemented, then the temperature is usually measured directly on the surface of the product. This allows heating according to defined temperature profiles.

4.1.3 Ultraviolet light curing

Ultraviolet (UV) radiation is also a form of electromagnetic energy, which is transmitted in a wave form (Tipler et al. 2007). The wavelength is classified above X-rays and below visible light, with a spectrum lying between 100 nm and 400 nm (Tipler et al. 2007).

For industrial purposes, ultraviolet light is typically generated by special gas UV lamps, UV LEDs, UV lasers or Excimer flash lamps. The ultraviolet light is used to cure special UV-setting polymer materials. These materials contain resin and photosensitive components.

When exposed to UV light, a polymerization process is initiated and the adhesive is cured. This process may just require a single flash or irradiation for up to several minutes. The materials are typically transparent or white. They are often used in microelectronics packaging for the encapsulation of optical components, such as LEDs, and for dental applications.

UV light curing is a chemical cross-linking process and not a thermosetting process; adhesive bonds or encapsulations can therefore be realized without significant heat. As a photosensitive component is required, UV curing is a selective process. The process is fast, especially compared to convection ovens. The equipment is small and can be easily integrated.

The availability of materials is, however, quite limited, with mostly acrylate-based materials for optical purposes available, along with a number of encapsulant materials. However, there are only a few UV-curable conductive adhesives available. This significantly limits the application for electronics packaging. Furthermore, the polymer needs to be optically accessible for the UV light to initiate the curing. Thus, the application for flip-chip bonding would be severely restricted.

Ultraviolet light curing is not to be mistaken with photonic curing (also: photonic sintering). In photonic curing, a high-energy flash of UV light is emitted onto an ink containing silver nanoparticles. Due to the special properties of the silver nanoparticles, the ink is rapidly sintered without thermally stressing the substrate material.

UV-curing equipment is available for the irradiation of larger areas and for spot lighting. While gas-discharge lamps are used for the irradiation of larger areas, smaller

spots are typically irradiated by LED lamps. An often-used approach in the assembly of micro-optical systems is the preliminary fixing of UV adhesive by high-energy UV flashes. Afterwards, the adhesive is fully cured using a large, high-energy lamp.



Infrared Spotlight



Small area UV-curing device

Figure 23 – Infrared and ultraviolet spotlights (Jenton 2016; Lambda 2016)

4.1.4 Microwave heating

Microwave (MW) radiation is a form of electromagnetic energy, transmitted in wave form (Tipler et al. 2007). The wavelength is classified as above infrared, with a spectrum between 1 mm and 1 m (Tipler et al. 2007), which corresponds to frequencies between 300 MHz and 300 GHz.

Microwave radiation is used for communication (e.g. IEEE 812.15.1 ‘Bluetooth’, IEEE 802.11 ‘Wi-Fi’), navigation and RADAR. Another important application is microwave heating, as widely used in kitchen appliances. Most microwave ovens operate at or close to a frequency of 2.45 GHz, causing dielectric heating primarily by absorption of the energy in water (Metaxas et al. 1983).

Microwave heating of polymers is a primarily volumetric heating process in which strong dipole groups couple to the microwave field (Meredith 1998). The conversion of electric fields into heat is proportional to the frequency, the dielectric loss, and the electric field strength (Deshmukh 2005). The heating rate is strongly influenced by the dielectric losses in the heated material. By the selection of an appropriate material, or by adding materials with a high dielectric loss, selective heating can be achieved.

Furthermore, the electromagnetic fields can be focussed onto a defined region by the use of antennas, waveguide or within a closed cavity. For example, in microelectronics

packaging, the power can be focussed onto a certain region of a PCB in order to cure a polymer material while sparing the rest of the board from the heat stress.

The electromagnetic fields penetrate a 'lossy' non-conductive material typically several millimetres and exert dielectric heating throughout the volume of the material. Therefore, in contrast to other thermal curing mechanisms, the polymer material is heated from the inside, and the dependence on thermal conduction inside the material is significantly reduced. This heating mode is also referred to as volumetric heating.

Polymers cured by microwave heating typically cure significantly faster than conventionally cured polymers (Davis et al. 2002; Tilford et al. 2007). This can be attributed to the volumetric cure and the increased heating efficiency compared to convection heating processes.

Microwave heating has been applied for curing of practically all types of polymers used in microelectronics packaging and has been extensively reported in the literature. Microwave heating has been shown to cure ECAs (Hubbard et al. 2010; Hubbard et al. 2011), underfill materials (Mead et al. 2003; Diop et al. 2015) and encapsulant materials (Wei et al. 2000; Hubbard et al. 2006) successfully.

A microwave batch curing system specifically for microelectronic packaging applications has been developed and is already industrially applied (Bible et al. 1992; Wei et al. 2000) (Figure 24 left). In order to prevent the assembly from damage by arcing and sparking, and to achieve a more uniform heating pattern, the microwave source continuously sweeps through a frequency band (Bible et al. 1992). The system has been applied for several wafer-level packaging applications, such as curing of polyimide coatings (Famsworth et al. 2001; Hubbard et al. 2004), polymer dielectric materials (Tanikella et al. 2002; Tanikella et al. 2006; Davis et al. 2007; Davis et al. 2008b; Raeis-Zadeh et al. 2012), lead-free soldering (Moon et al. 2004b; Moon et al. 2004a), underfill materials (Mead et al. 2003; Diop et al. 2015) and glob-top encapsulants (Wei et al. 2000). Due to the electromagnetic fields, temperature sensor signals may be disturbed and so measurement close to or on the substrate is not implemented. To overcome the interference problems, an acoustic temperature sensor has been proposed (Davis et al. 2002; Davis et al. 2008a; Davis et al. 2008b).

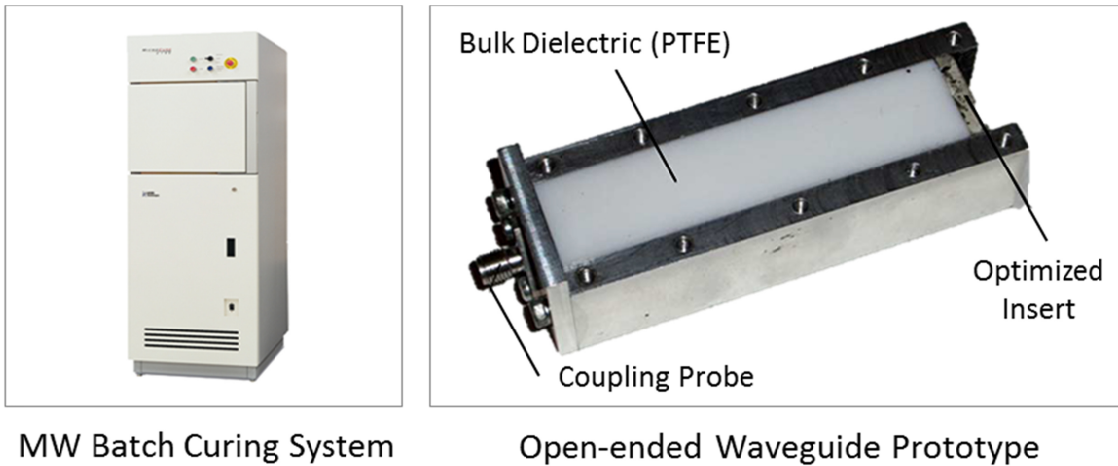


Figure 24 – Microwave curing devices (Lambda Technologies 2007; Sinclair 2009)

An approach to the thermal processing of individual components has been proposed by Sinclair *et al.* (Sinclair et al. 2008b) involving a microwave curing system based on an open-ended waveguide (Figure 24 right). The waveguide system also provides a variable-frequency microwave capability (Sinclair et al. 2008a). The system has been shown to cure different polymer materials in electronics packaging applications (Sinclair et al. 2008b; Sinclair et al. 2008d). In this work, no temperature control mechanism was implemented. Additionally, only very basic tests on electronic components have been conducted so far. Therefore, no statement on the applicability for different electronics packaging applications can currently be made. Furthermore, no investigations into potentially detrimental effects such as arcing or sparking have been performed. There is also no information on the reliability of microelectronic assemblies that have been processed with the open-ended applicator.

4.1.5 Indirect electrical heating

Indirect electrical heating makes use of the effect that electrically conductive materials dissipate a portion of the conducted energy in the form of heat. This easily controllable source of heat is used in large-scale industrial as well as domestic heating (Deshmukh 2005).

An object can be heated indirectly by exposing it to an electrically heated object. This effect is used in microelectronics assembly for hot plates or heated stamps. Hot plates are used to heat up assemblies to a base temperature below the actual temperature required to perform the desired melting or curing process. For example, if a solder melting temperature of 300 °C is required, then the hot plate might be heated up to 220 °C. The remaining temperature difference is then typically delivered by a spot-

heating device, such as an infrared spot heater or a focussed hot airstream (Tummala et al. 1997; Harper 2004).

Another common application of indirect heating is heated stamps. These are used to heat up the die and thereby indirectly heat the solder underneath it during die bonding or flip-chip assembly operations. Also, packages with solder attachment, such as land grid arrays (LGA) or ball grid arrays (BGA) are assembled this way (Tummala et al. 1997; Harper 2004; Ulrich et al. 2006).

While indirect heating is applicable for solder processes, the application for adhesive processes is considerably restricted. As the temperature distribution within the material is typically non-uniform, a reliable curing process without considerable internal stresses is hard to achieve. Additionally, the imbalance between the time required for an assembly operation and the curing process is a significant drawback.

4.1.6 Laser heating

Laser sources provide a beam of coherent, monochromic light. By focussing these beams using optics, energy densities sufficient for material heating, ablation or cutting processes can be achieved (Tipler et al. 2007).

Lasers can be used as selective heating devices. The lasers typically have a wavelength in the infrared spectrum. Typical sources for laser heating are CO₂ lasers or diode lasers. Such lasers may be used for selective melting of solders or for die-attach applications. Diode lasers are already available as optional features in die-bonding machines (Smolka et al. 2004; Seelert et al. 2012; Chryssolouris 2013; Ogochukwu 2014).

Lasers require, like UV-curing devices, an optical path to deliver their energy optimally (Smolka et al. 2004; Ogochukwu 2014). They can therefore be effectively used for optically accessible solder joints. The application for the joining of dies and packages is considerably more complex and requires auxiliary tools, but has been demonstrated (Teutsch et al. 2004). Laser curing of adhesives has mostly been performed on light-curing adhesives, but also pre-cure of underfills has been presented (Teutsch et al. 2004). The performance of full curing cycles of thermosetting polymers has yet to be demonstrated.

4.1.7 Further curing methods

Induction heating can be used for rapid curing of adhesives, but requires ferromagnetic components inside the adhesive to obtain a significant heating rate. Such adhesives are currently not commercially available.

Electron beam curing can be used to cure certain adhesives nearly instantly. This has been tested in high-pressure lamination. The equipment is complex, requires a vacuum to operate, and nearly no adhesives, especially for microelectronics packaging, are commercially available (Kinstle 1990).

4.2 Assembly equipment

4.2.1 Manual assembly machines

Manual assembly work stations are typically used for the assembly and rework of BGAs and CSPs, including flip-chip assemblies in low volumes (Jacob 2002). The operator performs the assembly processes by manipulating a highly accurate kinematic configuration and is supported by a vision system which allows an observation of the substrate and the bottom of the chip at the same time (Jacob 2002; Finetech 2016).

Particularly in rework stations, the substrate is placed on a hot plate, which heats up the assembly to a soak temperature. To perform solder and curing processes, the area of interest is additionally heated by a spot heat source, typically an infrared source.

While solder reflow or curing of ECAs is sometimes performed within the assembly station, underfill and encapsulant curing processes are almost always performed in an external (convection) oven.

As achievable production volumes are very low, manual assembly machines are preferred for R&D applications, rework of assemblies, and flexible low-volume production.

Examples of a manual assembly machine and a rework station are shown in Figure 25.

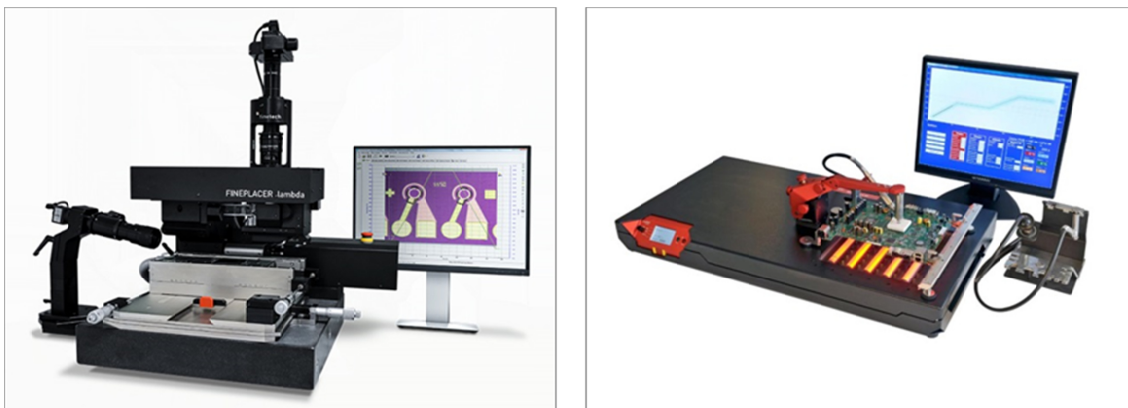


Figure 25 – Manual assembly machine (left) and rework station (right) (Finetech 2016; Martin 2016)

4.2.2 Semi-automatic assembly machines

Semi-automatic assembly machines require an operator to load and unload the machine. The assembly process can be carried out by either remote control of the machine or by executing previously entered assembly programs (Tresky 2016; Finetech 2016).

As far as productivity is concerned, semi-automatic machines can be classified between manual systems and fully automated high-performance systems. The precision, and particularly the variance, are superior to manual systems and the throughput is significantly higher, though still not economically viable for mass-production processes.

Curing equipment is typically not integrated into semi-automatic machines; the processes are usually performed in separate machines. An example of a semi-automatic assembly machine is presented in Figure 26 (left).

4.2.3 SMT placement machines

Pick-and-place machines perform serial placement operations of components onto a substrate. The components are fed from magazines or reels before being placed onto the substrate. The performance of pick-and-place machines ranges between several hundred and several thousand placement operations per hour. The achievable accuracy ranges between 20 μm and 50 μm (4σ confidence interval, with σ describing the standard deviation) (Siemens AG 1999; Höhn 2001; Jacob 2002).

Chip-shooting machines are high-performance placement machines that are optimized for placement performance. Through parallelization of pickup processes and the integration of revolver heads, up to 50,000 units per hour can be achieved. The increased performance slightly affects the accuracy, which ranges between 50 μm and 90 μm with a confidence interval of 4σ (Siemens AG 1999; Höhn 2001).

Soldering and curing processes are not integrated into SMT placement machines. Usually the assembly is transported by a conveyor belt to the next machine, e.g. a reflow oven.

SMT placement machines require considerable investment. Due to their high performance, these machines are suitable for mass-production processes, i.e. serial processing assemblies with a high number of components.

A picture of an example SMT placement machine is shown in Figure 26 (centre).

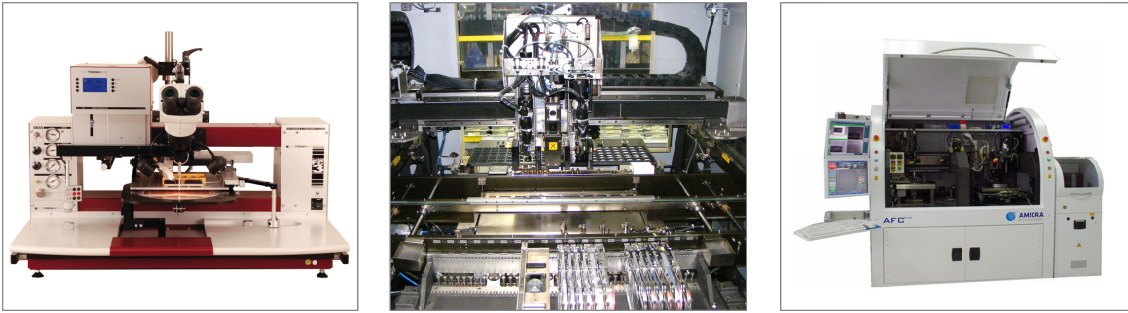


Figure 26 – Semi-automated assembly machine (left), SMT placement machine (centre), and automated die-bonding machine (right) (AMICRA 2016; Tresky 2016; Wikipedia 2016)

4.2.4 Automated die-bonding machines

For highly precise positioning of bare dies, die-bonding machines are used. These types of machine are typically precision robots in a Cartesian set-up (Siemens AG 1999; Höhn 2001). Die-bonding machines can be classified as high-speed die bonding, flexible die-bonding, precision die bonding, and automated flip-chip-bonding machines (Höhn 2001). Comprehensive descriptions of the different bonding systems can be found in the literature (Siemens AG 1999; Höhn 2001). Of particular relevance to this thesis, flip-chip die-bonding machines will be further explored.

Fully automated flip-chip-bonding machines are equipped with machine vision, which provides additional position information to achieve position accuracies of less than between 1 μm and 10 μm . Machines suitable for advanced packaging assembly processes, such as die stacking, have positioning accuracies of $\pm 5 \mu\text{m}$ or better. High-end flip-chip-bonding machines may produce between 200 and 300 units per hour (Blees 2011; Lee et al. 2011; Tung et al. 2014; Strothmann et al. 2016).

The investment costs of flip-chip-bonding machines are very high in relation to the other machine types. Therefore, a high degree of utilization is necessary to achieve a cost-effective operation.

There is normally no curing equipment integrated into automated die-bonding machines; these processes are performed within separate ovens.

An example of an automated die-bonding machine is depicted in Figure 26 (right).

4.2.5 Dispensing equipment

For laboratory purposes with low requirements on accuracy and repeatability, manual dispensing systems are used. These systems are typically time–pressure dispensers.

Regarding microelectronics packaging processes, these systems are particularly well-suited for glob-top encapsulation.

For applications with higher requirements on accuracy, robotic dispensing systems are used. Here, the dispensing system is positioned by a robot. As the properties of many adhesive materials change during pot time, and influences such as temperature, humidity and vibration can change the material's viscosity, numerous measures need to be undertaken in order to achieve a precise and repeatable dispensing result.

Dispensing equipment can be directly integrated into low-volume die-bonding machines. This is particularly used for the dispensing of die-attach materials, such as ECAs or solder paste. Underfill materials and encapsulants are typically dispensed in separate machines.

4.3 Assessment of the state of the art technologies

As the review of the existing state-of-the-art technologies shows, there are several heating and curing principles in use. There are also numerous types of assembly machines, which are designed for different production scenarios. An assessment of state-of-the-art assembly equipment is presented in Table 3.

Rework machines and SMT placement machines are targeted onto second-level packaging. Manual, semi-automated and automated assembly machines are, in principle, suitable for first- and second-level packaging, including flip chip on board. The throughput of rework stations is very low. Medium volumes can be achieved with manual and semi-automated machines. Automated machines achieve a high throughput. SMT placement machines are optimized for maximum throughput and very high volumes.

All of the reviewed machines provide pick-and-place processes supported by machine vision systems. Reflow and SMT machines do not integrate dispensing processes. Manual, semi-automated and automated machines can all, in principle, allow the implementation of all dispensing processes necessary for the flip-chip process described in Section 2.3.1.

Regarding the curing processes, the situation is different. Reflow soldering is available for all reviewed types of machines, except for SMT placement machines. Adhesive curing processes are not available, which prevents the implementation of the flip-chip process in a single machine. A review of the heating and curing equipment integrated in a state-of-the-art assembly system is presented in Table 4.

Integration of heating functionality into assembly equipment is typically performed with hot plates or heated stamps. Also typical are plane infrared heaters and spot heaters. A combination between a hot plate from the bottom and hot-air flow is often used in rework stations. Rare, but available, is the heating of the complete process space by convection heating. UV heating and laser heating are available as optional features if required. Microwave heating is yet to be integrated into microelectronics assembly equipment.

Table 3 – Process integration in microelectronics assembly equipment

Machine Type					
Properties	Rework Machine	Manual Assembly Machine	Semi-Automated Assembly Machine	Automated Die-Bonding Machine	SMT Placement Machine
Level of Electronic Packaging	x	✓	✓	o	x
First-level packaging (chip level)	x	✓	✓	✓	x
Second-level packaging (board level)	✓	✓	✓	o	✓
Flip chip on board	x	✓	✓	✓	x
Throughput (Thoben 1999)	Low	Medium	Medium	High	High
Low (10–250 units/day)	✓	✓	✓	✓	✓
Medium (250–500 units/day)	x	✓	✓	✓	✓
High (> 500 units/day)	x	x	x	✓	✓
Pick & Place Integration	✓	✓	✓	✓	✓
Pick & place process	✓	✓	✓	✓	✓
Machine vision	✓	✓	✓	✓	✓
Dispensing Process Integration	x	✓	✓	✓	x
Solder paste	x	✓	✓	✓	x
Conductive adhesive	x	✓	✓	✓	x
Underfill	x	Option	Option	Option	x
Encapsulant	x	Option	Option	Option	x
Cure Process Integration	x	x	x	x	x
Reflow	✓	Option	Option	✓	
Conductive adhesive	x	x	x	x	x
Underfill	x	x	x	x	x
Encapsulant	x	x	x	x	x
✓ – Fulfilled, o – Partly fulfilled, x – Not fulfilled, Option – Optionally available					

Table 4 – Heating and curing integration in microelectronics assembly equipment

Curing Equipment \ Assembly Equipment	Conv.		Indirect		Infrared		MW		UV	Laser Heating
	Convection Oven	Hot-air Flow	Hot Plate	Stamp	Infrared Spot	Infrared Heater	Microwave Oven	Microwave Spot		
Manual Workstations	-	o	✓	✓	✓	✓	-	-	o	-
Rework Stations	-	✓	✓	✓	✓	✓	-	-	o	-
Semi-Automated Machines	-	o	✓	✓	✓	✓	-	-	o	-
SMT Placement Machines	-	-	-	-	-	-	-	-	-	-
Automated Die-Bonding Machines	o	o	✓	✓	o	o	-	-	o	o

✓ – Typical solution, o – Optionally available, - – Not available

Conv. – Convection, MW – Microwave

4.4 Conclusions on state-of-the-art technology

Convection heating is still the prevalent method for the curing of polymer adhesives in microelectronics packaging. Closed or in-line ovens are typically used for the heating of polymer adhesives, although other technologies exist and are commercially available. The reviewed alternative technologies provide distinct advantages such as faster curing or selective heating. However, the benefits do not outweigh the increase in cost, particularly for low-cost applications. Furthermore, there is no solution that combines all of the required properties.

- All regarded thermal curing methods allow the curing to a defined temperature profile. The control should be based on the actual part temperature and not the temperature of the surrounding gas.
- By direct infrared heating, microwave, and UV, the curing cycle times can be reduced significantly compared to convection heating.

- UV and microwave curing offer material-selective curing, while infrared curing and convection curing allow focussing of the heat flow to a certain area.
- All studied curing methods can be applied, as long as the part is functional after the assembly process and it provides the necessary reliability according to relevant testing standards for the relevant field of application.
- Therefore, with respect to Requirements 1–4, promising approaches are available. In particular, microwave heating has notable beneficial properties.

In the field of placement machines, all processes required for the implementation of the full flip-chip process are available within one machine, except for the adhesive curing capability. Intermediate handling steps are therefore necessary for all the systems considered.

- For low- to medium-volume production, equipment with a higher degree of integration is available.
- A positioning accuracy of at least $\pm 5 \mu\text{m}$ is required.
- Manual and semi-automated equipment in particular provide dispensing steps combined with pick-and-place capabilities.
- For high-volume production, specialized high-performance equipment is used and just one or two functions per machine are carried out.
- An integration of heating equipment is found in specialized low-volume machines, specifically in rework stations, but is currently not suitable for adhesive curing processes.
- The prevalent set-up for both low- and high-volume production is separate pick-and-place and dispensing equipment with the necessary intermediate handling steps.

A system fulfilling all previously described requirements in a satisfactory way is not currently available, as the integrated adhesive curing capabilities are lacking. An integration of conventional heating processes would result in very low-performing machines, due to the long curing cycle times. A fast curing process integrated into an assembly system would provide distinct advantages in this regard and would help to overcome the previously identified limitations.

Therefore, a novel method for the rapid curing of adhesives in microelectronic assembly is required, which can be directly integrated into a precision placement machine.

5 Conception of a Potential Solution

5.1 Assessment and selection of curing method

As described in Section 4.1, different curing methods are already in industrial use and several others are potentially applicable, having distinct advantages. Requirement 1 calls for the reduction of curing times. A comparison of curing cycle times of three typical materials applied in electronic packaging is shown in Table 5.

Table 5 – Cycle duration with different curing methods
(Garard et al. 2002; Berga et al. 2011)

Curing Methods Materials	Convection	Indirect	Infrared	UV Light	Microwave
Epotek 353ND (at 120 °C)	300 s	300 s	30 s	-	45 s
Epotek H74 (at 120 °C)	90 min	90 min	-	-	3 min
Epotek OG142 (UV cure)	-	-	-	60 s	-
Claimed Reduction of Curing Cycle Duration	0%	0%	90%	-	95%

As can be seen in Table 5, infrared, UV light and microwave curing allow drastic reductions of curing cycle times, while indirect and convection heating do not provide substantial reductions.

An assessment of selective heating, material penetration and the applicability for flip-chip packaging is presented in Table 6.

Selective curing is possible with all the considered processes, except for convection heating, which is difficult to confine to a specific area. Microwave curing is a material-selective process, as different materials have different loss characteristics. UV curing is also a material-selective process, which leaves the surrounding material largely unaffected. Infrared curing can be confined to a specific area, but is not material selective.

The material penetration of convection and indirect heating is minimal and relies on the heat transfer inside the material (Deshmukh 2005). Infrared curing can be tuned to achieve increased material penetration by adjustment of the wavelength spectrum (Berga et al. 2011). Depending on the material, the radiation can then achieve depths between a few μm up to being transparent (Naganuma et al. 1999). UV-curable adhesives are typically transparent. The UV radiation is therefore well transmitted through the material and initiates the polymerization processes throughout the radiated volume. The microwaves almost fully saturate unfilled epoxy resins. A typical value for the penetration depth of epoxies is 300 mm (Mijović et al. 1990).

Table 6 – Assessment of relevant curing methods

Curing Method \ Properties	Convection	Indirect	Infrared	UV Light	Microwave
Selective Heating	x	o	o	✓	✓
Material selective	x	x	x	✓	✓
Focussed heating	x	✓	✓	✓	✓
Material Penetration	x	x	✓	✓	✓
Optical transmission	x	x	✓	✓	x
Electromagnetic	x	x	x	x	✓
Use Cases in Flip-Chip Assembly	✓	✓	✓	x	✓
ECA	✓	✓	✓	-	✓
Underfill	✓	✓	✓	-	✓
Encapsulant	✓	✓	✓	✓	✓
✓ – Fulfilled, o – Partly fulfilled, x – Not fulfilled					

Thermosetting polymers can be cured by convection, infrared and microwave curing. As this type of material dominates in microelectronics packaging, these three processes are applicable for the bulk of available materials. UV-curable materials are rather prevalent in dental and optical applications. Since conductive materials are not available, the applicability of UV-curable materials for microelectronics packaging is limited.

Based on the considered criteria, convection, indirect heating and UV curing all show significant drawbacks. Infrared and microwave heating offer, in comparison to the other considered methods, distinct advantages and are applicable, at least in principle, to all three curing use cases within the flip-chip process chain. Both infrared heating and microwave heating provide potentially drastic reductions in curing cycle duration. However, infrared heating requires an optical path in order to fully exploit its potential. Therefore, the potential field of applications is constrained. In contrast, microwave curing has been shown to be applicable to a broader range of applications, with distinct performance benefits.

Therefore, and with particular respect to Requirement 1 and Requirement 3, microwave heating is selected for application in the novel heating and curing system.

Metallic objects exposed to microwave radiation may cause arcing and sparking (Metaxas et al. 1983). These arcs and sparks may exert potentially hazardous and destructive effects on the exposed objects and their environment (Whittaker et al. 2000). The occurrence of arcing and sparking is depending on numerous factors such as the physical properties of the exposed materials and their geometry. The properties of the RF fields, including the frequency and the power, have significant impact on the arcing and sparking behaviour (Whittaker et al. 2000). With respect to Requirement 4, the yield and the reliability of the processed components may not be significantly affected by the curing process. Therefore, the proposed method must also provide measures to prevent the occurrence of arcing and sparking.

5.2 Conception of heating system

5.2.1 Microwave source

Microwave magnetrons are the most common microwave sources and are applied in hundreds of millions of microwave ovens all over the world. Magnetrons are high-power vacuum tubes that modify an electron beam by a magnetic field (Okress et al. 1957). They are very cheap and have very high efficiencies (over 80%). As the frequency is determined by the geometry, magnetrons have a single frequency, with some noisy adjacent bands (Neculaes et al. 2004).

Klystrons are also linear beam vacuum tubes. In a Klystron, microwaves are amplified by modulating the density within the electron beam by a number of resonant cavities (Adam et al. 1969). There are Klystrons available with very high gain and are therefore often used for high-power applications. Klystrons are not bound to a certain frequency,

but can operate in a defined, relatively small frequency range. They require regular maintenance.

In contrast to the Klystron, travelling wave tube (TWT) amplifiers do not use resonant cavities, but directly interact between the non-resonant transmission line and the electron beam (Adam et al. 1969). TWT amplifiers offer a wider bandwidth than Klystrons. They require regular maintenance, but provide high signal quality with low noise.

Solid-state power amplifiers (SSPAs) amplify RF signals with high-power transistor circuits (Adam et al. 1969). SSPAs were traditionally used for low-power applications, but with the improvement of transistor technology, SSPAs for high-power applications are now available (Boshnakov et al. 2012). They have a high reliability and need only a minimum of maintenance (Sechi et al. 2006). In contrast to TWTs, SSPAs can typically be pulsed rapidly. The cost is comparable to TWTs, while SSPAs occupy a smaller footprint than TWTs.

An assessment of different types of microwave amplifiers is shown in Table 7. The assessment is performed in the form of a weighted decision matrix (Bugdahl 1990; Haberfellner et al. 2012). Each criterion is weighted by a coefficient g . The fulfilment of each criterion is assessed on a scale from 1 to 10, with 1 representing lowest fulfilment and 10 the highest. The result is calculated by adding the weighed fulfilment points and ranking the options in ascending order. While magnetrons are cheap and solid, they provide just a single frequency. Klystrons and TWT amplifiers are suitable for high-power applications, but require maintenance and are relatively large. SSPAs are compact, reliable, can be pulsed and are available at a moderate cost.

Following the assessment, SSPAs are selected for further consideration in this thesis.

Table 7 – Assessment of microwave amplifiers

Criterion	Weight g	SSPA		Magnetron		TWT		Klystron	
		n	n·g	n	n·g	n	n·g	n	n·g
Reliability	5	9	45	8	40	3	15	3	15
Pulsing	5	10	50	3	15	4	20	4	20
Efficiency	4	8	32	8	32	5	20	3	12
Size	4	8	32	5	20	2	8	3	12
Frequency range	3	8	24	1	3	10	30	6	18
Signal quality	2	10	20	3	6	6	12	4	8
Maintenance	2	10	20	10	20	3	6	4	8
Cost	2	6	12	10	20	6	12	5	10
$\sum n \cdot g$		235		156		123		103	
Rank		1		2		3		4	

5.2.2 Microwave applicator

The dominating application for microwave heating is domestic heating of food. These microwave ovens are closed and isolated cavities. Handling is typically performed through a door. Such closed-cavity microwave ovens are also used in industrial applications, typically with higher performance regarding power and workspace. Bible *et al.* have proposed a closed-cavity microwave oven with variable frequency (Bible *et al.* 1992). The technology has been applied for a number of different electronics packaging applications, such as encapsulation (Wei *et al.* 2000; Mead *et al.* 2003; Diop *et al.* 2015), underfill (Mead *et al.* 2003; Diop *et al.* 2015) and soldering (Moon *et al.* 2004a; Moon *et al.* 2004b). However, there are alternative methods available to apply microwave radiation.

Antennas are typically used for communication purposes, but they can also be used to apply microwave energy for heating applications. A flat antenna has been shown to effectively heat up wet textiles in order to dry them (Vrba *et al.* 2011). Another application of antennas is hyperthermia treatment for medical purposes (Vrba 2005; Sangster *et al.* 2006). Typical antenna configurations for unfocussed emission are flat or beamformed antennas, focussed emission can be achieved with parabolic or beamformed antennas.

Waveguides are used to transfer electromagnetic power efficiently from one point in space to another, by restricting expansion to one or two dimensions (Orfanidis 2003). Typical types of waveguides are coaxial lines, two-wire lines, microstrip lines or hollow waveguides (Orfanidis 2003). The important factors for selection and choice of a structure are the amount of power to be transferred and the amount of transmission losses to be tolerated (Orfanidis 2003). However, waveguides can also be applied as applicators. Vrba *et al.* have proposed a waveguide applicator for textile drying (Vrba et al. 2011). Sangster proposed a waveguide cavity for hyperthermia treatment (Sangster et al. 2006) and Sinclair *et al.* proposed a microwave applicator based on an open-ended cavity for electronic packaging applications (Sinclair 2009).

A number of requirements must be fulfilled by the applicator:

- The heat energy provided by the applicator must be focussed onto the area of interest and spare the surrounding volume. Otherwise, the surrounding components are stressed unnecessarily, which may have a negative influence on their reliability (derived from Requirement 3).
- Since one of the main motivations of the integrated system is to reduce or eliminate handling steps, the applicator must reduce the need for intermediate handling steps (derived from Requirement 5).
- Microwave radiation is potentially harmful, especially when significant amounts of power are applied. The applicator should inherently shield as much power as possible and minimize any collateral radiation or other potentially harmful effects.
- The curing system is going to be integrated into a machine. To facilitate the integration, a minimum of adaptations on the machine shall be necessary. Ideally, the applicator can be integrated in the same manner as typical micro-assembly tools are already integrated (derived from Requirement 5).
- The design of the applicator has many implications on the subsequent dimensioning of the microwave source, amplifier and further components. If the applicator heats efficiently, then the requirements on the other components are reduced and the whole curing system can be made simpler and cheaper.
- The proposed curing system is designed to be applied in the field of electronics packaging. However, the spectrum of potential applications is very broad. Although many packaging applications are already highly standardized and very similar, the curing system may need to be adapted to a different type of application.

- As the system is planned to be applied in a production environment, economic aspects need to be taken into account. The hardware cost of the applicator should therefore be assessed.

Table 8 – Assessment of microwave applicators

Criterion	Weight g	Waveguide		Antenna		Oven	
		n	n·g	n	n·g	n	n·g
Selective Heating	5	3	15	8	40	8	40
Part Handling	5	2	10	10	50	7	35
Safety	5	10	50	2	10	6	30
Integration	4	3	12	7	28	6	24
Efficiency	3	4	12	6	18	9	27
Adaptation	3	3	9	7	21	8	24
Cost	2	4	8	5	10	7	14
$\Sigma n \cdot g$		194		177		116	
Rank		1		2		3	

An assessment of the three potential applicators is shown in Table 8. The same method as in Section 5.2.1 was used for the assessment. Antennas and waveguide resonators can provide selective heating, by focussing the microwave radiation onto a defined area. With closed-oven cavities, selective heating may be achieved by selecting materials with high loss tangents, although polymer components such as FR4-PCBs would be heated anyway. A closed-oven cavity requires intermediate handling steps, which negatively affect the assembly efficiency. These steps can be avoided when using alternative applicators such as antennas or waveguides. The oven, being an enclosed unit, is the safest of the three options, while the antenna requires additional safety measures. The waveguide resonator can be implemented as a safe applicator (Sinclair 2009), but still requires indirect safety measures. Integration of the oven is possible, but requires fundamental adaptation of the machine. Antennas and waveguide resonators can both be integrated as tools. The oven is the least-efficient option. With antennas, losses are also to be expected. The waveguide resonator is regarded as the most efficient applicator. While the adaptation of the oven is complicated, an exchange of the antenna or the waveguide resonator is, in principle, possible. However, the engineering and

manufacturing of a focussed antenna is regarded as more complicated than engineering the waveguide. This also has an impact on the cost. The oven is the most complex and expensive system. Design of the waveguide resonator is a complex task, but the manufacturing is comparatively simple.

Based on this assessment, a waveguide resonator is selected.

5.2.3 Open-ended microwave applicator

A waveguide resonator for the processing of microelectronic packages has been proposed by Sinclair *et al.* (Sinclair 2009). A schematic of the resonator is presented in Figure 27. A rectangular metal waveguide cavity is proposed, which is partially filled with a low-loss dielectric material, such as a ceramic or plastic. Electromagnetic energy will travel through a waveguide at frequencies above a critical cut-off frequency, which is a function of the cavity dimensions and the material it contains. As the waveguide cavity contains two materials, the cut-off frequency changes at the dielectric–air interface. The system is designed to operate at frequencies above the cut-off frequency of the ceramic section and below the cut-off frequency of the air-filled load section. In this case, a resonant field pattern is created within the dielectric portion of the cavity. The fields in the load section cannot propagate, and decrease exponentially in magnitude with distance from the interface.

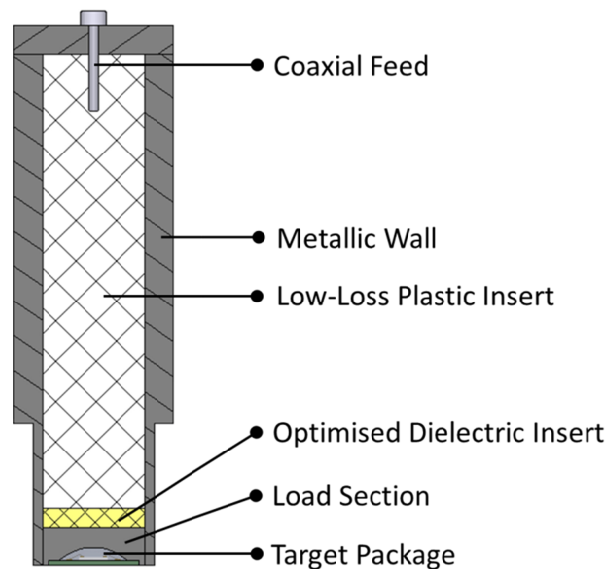


Figure 27 – Schematic of the open-ended microwave applicator

Load materials, such as thermosetting polymers, placed within the load section are exposed to these evanescent electromagnetic fields, inducing heating at a rate dependent upon the field strength, the material properties of the load and the frequency of excitation (Pavuluri et al. 2010a). Heating patterns generated in the load are therefore dependent upon the electric field distribution, which, in turn, depends on the operating frequency. The system can be operated at a large number of discrete harmonic resonant frequencies, each resulting in a differing modal structure within the dielectric. The heating pattern within the load can therefore be controlled through the choice of operating frequency. Through the integration of an optimized dielectric material, the field in the heating chamber can be enhanced significantly (Sinclair et al. 2008c).

The presented waveguide resonator is regarded to be suitable with respect to the requirements of selective heating and the integration into a precision assembly system. The dimensions of the open-ended microwave applicator are suitable for the processing of individual components. An adaptation to larger dimensions (e.g. for the processing of whole wafers) requires engineering effort, but is possible. Since the primary requirements for the envisaged task are met, this is therefore selected as the preferred applicator for further consideration.

5.3 Control concept

The operating frequency in the applicator determines the mode of operation and thereby the field distribution in the load section. This has a direct influence on the power distribution and therefore the heating pattern. The heating behaviour and curing cycle times are directly influenced by the frequency. In consequence, and with respect to Requirement 2, the frequency of the source is to be controlled.

Heating according to a defined temperature profile, as demanded by Requirement 1, requires information about the actual temperature of the heated product. This can, for example, be based on a model or on feedback from a sensor.

Arcing and sparking were identified as potentially detrimental effects. To reduce or eliminate the occurrence of arcs and sparks, different measures within the control system can be envisioned. With respect to Requirement 4, different methods to reduce these detrimental effects are considered.

5.3.1 Frequency control

When the open-ended cavity is excited at one of its resonant frequencies, the field intensity and thereby the transmitted energy is maximal. An example plot of the incident and the reflected power is shown in Figure 28.

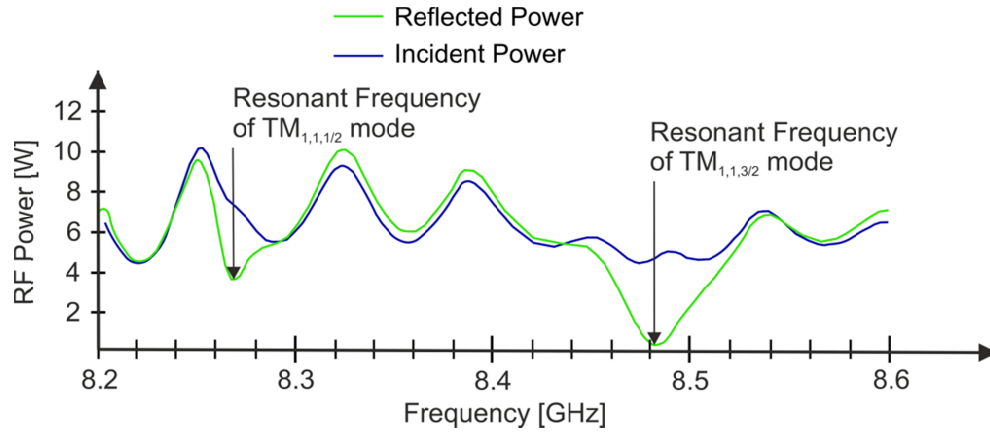


Figure 28 – Incident and reflected microwave power of an open-ended applicator

The actual amount of power dissipated in the heated material is determined by the difference between the incident and the reflected power. In the example at hand, there are two minima of reflected power. The difference between incident and reflected power becomes maximal at these minima, which correspond to the resonant frequencies of the oven cavity. The resonant frequencies can be calculated using Equation (3) (Sinclair 2009).

$$f_{m,n,p} = \frac{c}{2\pi\sqrt{\epsilon_r}} \sqrt{\left(\frac{m\pi}{a}\right)^2 + \left(\frac{n\pi}{b}\right)^2 + \left(\frac{p\pi}{d}\right)^2} \quad (3)$$

- m, n, p Mode indices
- c Speed of light in free space [m/s]
- ϵ_r Relative permittivity of the dielectric insert
- a, b, d Inner dimensions of the cavity [m]

This formula is only valid if the load section is empty and the geometry of the oven and the dielectric insert are considered ideal (Sinclair 2009). A real waveguide differs from an ideal waveguide in numerous aspects. The geometry of a real oven and its components inevitably vary and the physical properties, including dielectric properties, differ slightly. These factors lead to losses. Therefore, a real oven is less efficient than

its ideal counterpart. Additionally, the real applicator contains the assembly to be processed, which in turn influences the dielectric properties of the oven.

It cannot, therefore, be assumed that the calculated resonant frequencies match the resonant frequencies of a real oven. Tools like network analysers allow the measurement of the real resonant frequencies. However, the resonant frequencies shift according to the cure material and its degree of cure. Therefore, a set of measurements is needed to determine the resonant frequencies as a function of the material, temperature and degree of cure. This is impractical, as it would be time-consuming and would have to be done for every material and every oven. The resonant frequency should therefore rather be determined during the process. This can be performed by several methods. In the following paragraphs, two potential methods are discussed. Both methods rely on the approximate knowledge of the theoretical (or unloaded) resonant frequency.

The theoretical resonant frequencies for an oven with dimensions of $18 \times 18 \times 80 \text{ mm}^3$ were calculated according to Equation (3) and are presented in Table 10.

In the first method, the reflected power is measured while sweeping through a frequency band. Based on the measurements, the local minima next to the calculated resonant frequencies are determined. While this method has the advantage that the resonant frequencies can be found with a high likelihood, the sweep through the frequency band requires a considerable amount of time. Additionally, the procedure has to be carried out periodically to track changes during processing.

The time required for a frequency sweep can be calculated by:

$$T_{Sweep} = T_{Measure} \frac{\Delta f}{f_{Sample}} \quad (4)$$

T_{Sweep}	Total time required for the frequency sweep [s]
$T_{Measure}$	Time required to measure the current MW power [s]
Δf	Frequency band for the sweep [MHz]
f_{Step}	Step size for the sampling of the sweep [MHz]

With this formula, representative calculations of the sweep time can be performed. Three such calculations are shown in Table 9. The curing system by Sinclair *et al.* has a sampling rate of 50 Hz, which equates to $T_{Measure} = 20 \text{ ms}$ (Sinclair 2009). The step size of the sampling was assumed to be $f_{Step} = 1 \text{ MHz}$ for Cases 1 and 2. For Case 3, a step size of $f_{Step} = 2 \text{ MHz}$ was assumed. As can be seen, the time required for a frequency sweep T_{Sweep} , ranges between 0.5 s and 8 s. It is assumed that the heating is significantly

impaired during the sweep. The heating system may not therefore be able to provide the required energy output in this period. Additionally, the sweeping would have to be performed cyclically, e.g. every 10 s, and this would impair heating according to a defined temperature profile. However, this could be potentially tolerated, as, for example, Case 2 would only require a second sweep time.

Table 9 – Representative durations of frequency sweeps

Case No.	$T_{Measure}$	Δf	f_{Step}	T_{Sweep}
1	20 ms	400 MHz	1 MHz	8 s
2	20 ms	50 MHz	1 MHz	1 s
3	20 ms	50 MHz	2 MHz	0.5 s

Table 10 – Resonant frequencies of unloaded open-ended microwave applicator

m	n	p	Resonant Frequency f_{res} [GHz]
1	1	$\frac{1}{2}$	8.2817
1	1	$\frac{3}{2}$	8.4875
1	1	$\frac{5}{2}$	8.8847
1	1	$\frac{7}{2}$	9.4493
$\epsilon_r = 2.035$, dimensions $a \times b \times d = 18 \times 18 \times 80 \text{ mm}^3$			

A second method is illustrated in Figure 29. In this method, the frequency is set close to a known resonant frequency. The reflected power is then measured. The frequency is then increased by a defined step and the reflected power is measured again. The two measurements are compared and it is determined if the last step was moving towards the local minimum or away from it. If the reflected power increases, then the direction of the sweeping was wrong and a step in the alternate direction is made. If the reflected power decreases, then the direction was correct and another step in the same direction is made.

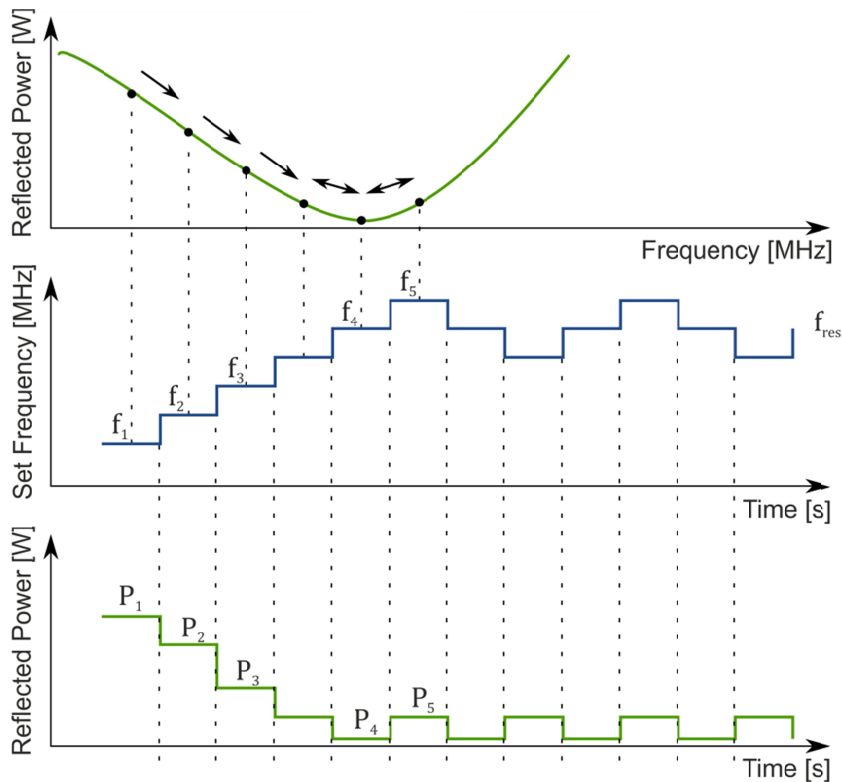


Figure 29 – Tracking of resonant frequency

The second method works, albeit with a number of limitations:

- The starting frequency must be close to a local minimum representing a resonant frequency.
- The reflected power must be strictly monotonic, decreasing between the start frequency and the resonant frequency.
- The step size must be small relative to the characteristics of the frequency, otherwise the local minimum may be missed.

As the measurement in Figure 28 shows, the two minima are about 15 MHz wide. There is no indication of other local minima nearby. The $TM_{1,1,3/2}$ minimum is the global minimum in this case.

The characteristics of the resonant frequencies may change with different loads placed in the open cavity. However, the shape of the local minima is assumed to be similar, according to preliminary experimental findings (Pavuluri et al. 2010a; Pavuluri et al. 2012). Therefore, the second method is applicable as long as its limitations are respected.

The first method the advantage of being very robust, but requires time to scan through the frequency band. The microwave power cannot be pulsed during the measurement,

which potentially interferes with the temperature control. If a sweep of 1 s is performed, then the surface temperature of a typical glob-top encapsulant would drop by approximately 0.7 °C to 0.9 °C in this period (Pavuluri et al. 2010a). If the sweep is performed during a ramp-up of the temperature, then the defined temperature ramp in this period would add up to the deviation. Thus, for a ramp rate of 1 °C/s, the total deviation would be between approximately 1.7 °C and 1.9 °C, which is quite significant.

In the second method, the frequency is changed gradually and requires just two consecutive RF power measurements and one change of frequency. With an assumed acquisition time of 20 ms, the frequency can, theoretically, be changed after 40 ms and then every 20 ms. The temperature control is almost entirely unimpaired in this period. The frequency set point remains close to the current resonant frequency during the whole process and the heating is therefore not impaired.

As the second method requires less time, allows the continuous tracking of the resonant frequency, and does not interfere with the temperature control it is selected for further consideration.

5.3.2 Temperature control

This section addresses the temperature control and the problems associated with it. In this context, an appropriate method for controlling the temperature is presented. Firstly, the relation between the microwave power that is fed into the oven and the change in temperature of the cure material is described. Secondly, two examples of heating experiments are used to discuss different options to control the temperature.

The main heating mechanism of the target material is dielectric heating (Pavuluri et al. 2012). For an ideal system, the load (cure material) would absorb the complete microwave power fed into the oven. If no load is present, an ideal oven would reflect all power.

In reality, neither the oven nor the load can be considered as ideal. Not all the power emitted by the source is absorbed by the polymer material; a fraction of the power is dissipated by the microwave components, such as cables and connectors, and another fraction is absorbed by the dielectric insert that fills the oven. The microwave components also account for a certain amount of reflected power. Figure 30 gives an overview of the energy balance of the oven.

The surrounding atmosphere also influences the target material by convective heat transfer. If the surrounding gas in the atmosphere has a lower temperature than the target material, it cools the target.

The heat applied to the target accelerates polymerization processes, which may be endothermal or exothermal; thermal energy is consumed or released by the target material (see Section 3.3.7 for details). The curing of epoxy compounds is typically dominated by exothermic reactions, which release a considerable amount of thermal energy (Morris et al. 2009).

Equation (5) provides an estimation of the temperature change based on absorbed electromagnetic energy P_{Absorb} , the amount of energy released into the oven, the energies released or consumed by the cure process as described by the enthalpies H_{Exo} and H_{Endo} , respectively, and the convective heat transfer Q_{Conv} .

$$\frac{d}{dt} T_{Poly} = \frac{P_{Absorb} + \frac{d}{dt} H_{Exo} + \frac{d}{dt} H_{Endo} + \frac{d}{dt} Q_{Conv}}{m_{Poly} C_{Poly}} \quad (5)$$

T_{Poly} temperature of the polymer [K];

$\frac{d}{dt} H_{Exo}$ change of internal energy due to the cure reaction [W];

$\frac{d}{dt} Q_{Conv}$ rate of the convective heat transfer [W];

C_{Poly} specific heat capacity [$\frac{J}{g \cdot K}$];

m_{Poly} mass of the polymer [g].

The load (polymer) is able to absorb only a certain fraction of microwave power per unit volume, as indicated by Equation (5). The remaining (not absorbed) energy is reflected. By taking losses due to mismatch and insertion losses into account, the power that is converted into heat can be determined. The heating rate does, however, not solely depend on the absorbed microwave power; it also depends on the convective heat transfer and the enthalpy of the cure process. Due to the number of influences and possible fluctuations, an estimate of these dynamic factors would be inaccurate and unreliable. Therefore, the current temperature of the material cannot currently be reliably estimated based on these thermodynamic considerations alone. An in-process measurement of the target temperature is needed.

A control of the temperature can be achieved by simply switching the microwave source on and off. If the switching is performed with a sufficient frequency, e.g. by pulse width modulation, then the average output power can be regulated.

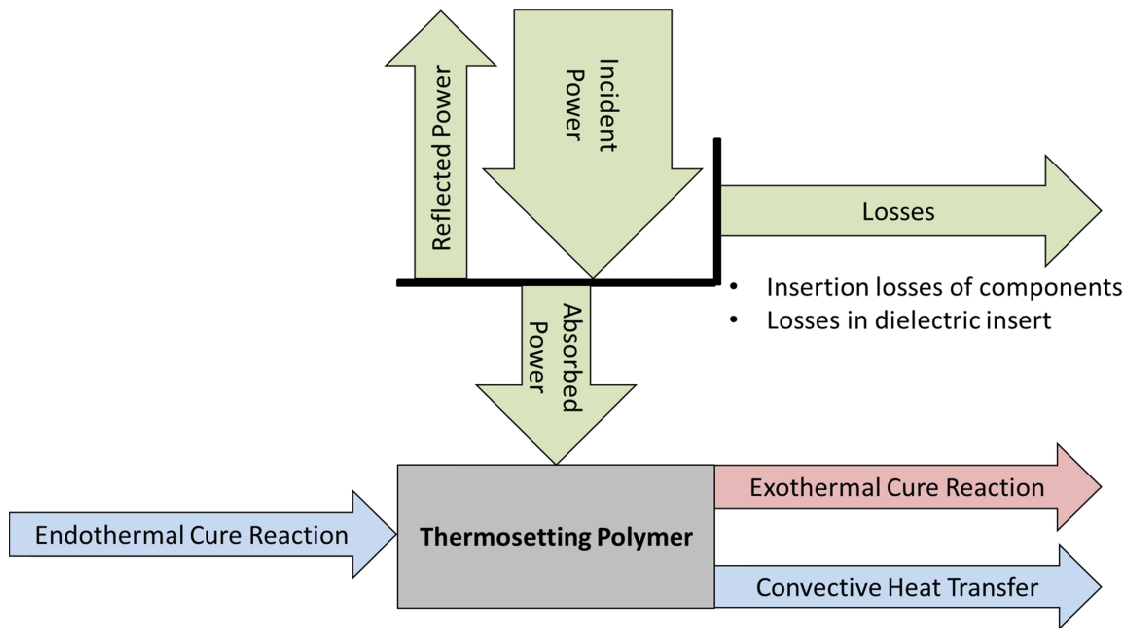


Figure 30 – Energy balance of the open-ended applicator

The absorbed electromagnetic power for an electrically non-conductive material is proportional to the dielectric loss ϵ'' . The dielectric loss is not constant; it changes with temperature and, more importantly, with the degree of cure (Jow et al. 1988; Zong et al. 2005). Experiments with epoxy resin showed that the dielectric loss decreases significantly once the epoxy is cured. Currently, the degree of cure cannot be measured directly. The data available on the relation between degree of cure and dielectric loss is very specific and is not yet applicable.

A potential approach to control the dynamic behaviour of the target material is to use a model-based adaptive controller. Such an adaptive controller would need to model the cure process in order to estimate the degree of cure and the changes to the material parameters. Such a model is very complex as it has to link several parameters that affect each other (Davis et al. 2008b). For example, the electric field in the load section affects the temperature of the load material, the temperature affects the dielectric properties of the material, and they in return affect the electric field. The same applies to the degree of cure, which is dependent on time and temperature but affects the temperature itself and the dielectric properties. A model capable of simulating this complex system has been proposed by Tim Tilford *et al.* (Tilford et al. 2007; Tilford et al. 2007; Tilford et al. 2008c; Tilford et al. 2008b; Tilford et al. 2009; Tilford et al. 2010c; Tilford et al. 2010e).

In order to design an appropriate temperature control system, two heating experiments, using a defined profile, were carried out. The experiments were carried out with Hysol

EO1080 (EO1080 2010), a commercial encapsulant material. For the experiments, a laboratory microwave curing system from Heriot-Watt University was used (Pavuluri et al. 2010a). A two-point controller was used for temperature control. The manufacturer recommends a curing temperature of 150 °C, which was followed in the two experiments.

A graph of the first cure experiment is presented in Figure 31.

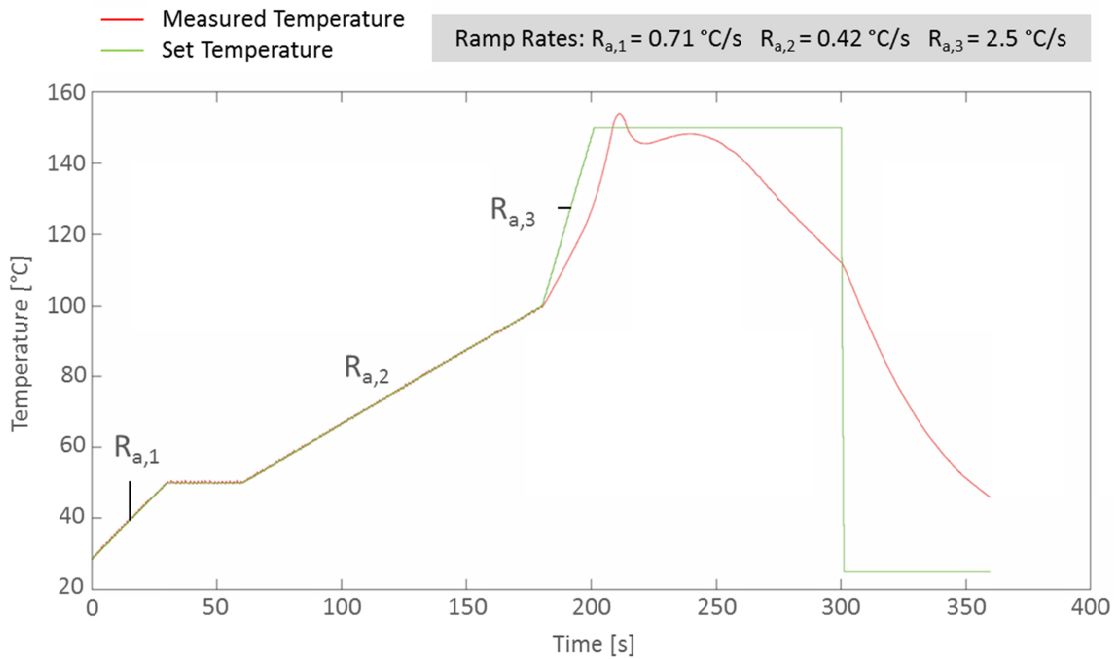


Figure 31 – Cure experiment with Hysol EO1080 with maximum ramp rate
 $R_{a,3} = 2.5 \text{ °C/s}$

The defined temperature profile is indicated by the green line, while the red line shows the actual measured temperature. Within the first 180 s, the controller is able to accurately follow the temperature profile ($R_{a,1} = 0.71 \text{ °C/s}$, $R_{a,2} = 0.42 \text{ °C/s}$). The ramp rate is then increased to $R_{a,3} = 2.5 \text{ °C/s}$. The heating system is not able to provide sufficient power to keep up with the defined profile. After about 210 s, an overshooting of the temperature can be seen. Directly after the maximum temperature is reached, the temperature drops below the set temperature. Afterwards, the temperature increases slightly and then falls monotonously since the microwave applicator has no active cooling capability. The microwave power was not pulsed during the process.

This behaviour corresponds to the changes in material properties during the cure process (as described in Section 3.3.7). With increasing degree of cure, the absorption of the microwave power decreases significantly (Sinclair et al. 2008d). The decreased amount

of microwave power does not then compensate for the convective heat transfer and endothermal cure reactions, resulting in a slow but steady reduction of temperature.

The overshooting at 210 s is caused by an exothermal cure reaction. This reaction starts at about 120 °C. Here the slope of the measured temperature increases, although the applied power remains constant. In this case the reaction eventually leads to an overshooting of the temperature. The overshooting could be theoretically prevented by either reduction of the microwave power once the slope increases or by active cooling.

The second cure experiment is shown in Figure 32. In this case a different temperature profile was used.

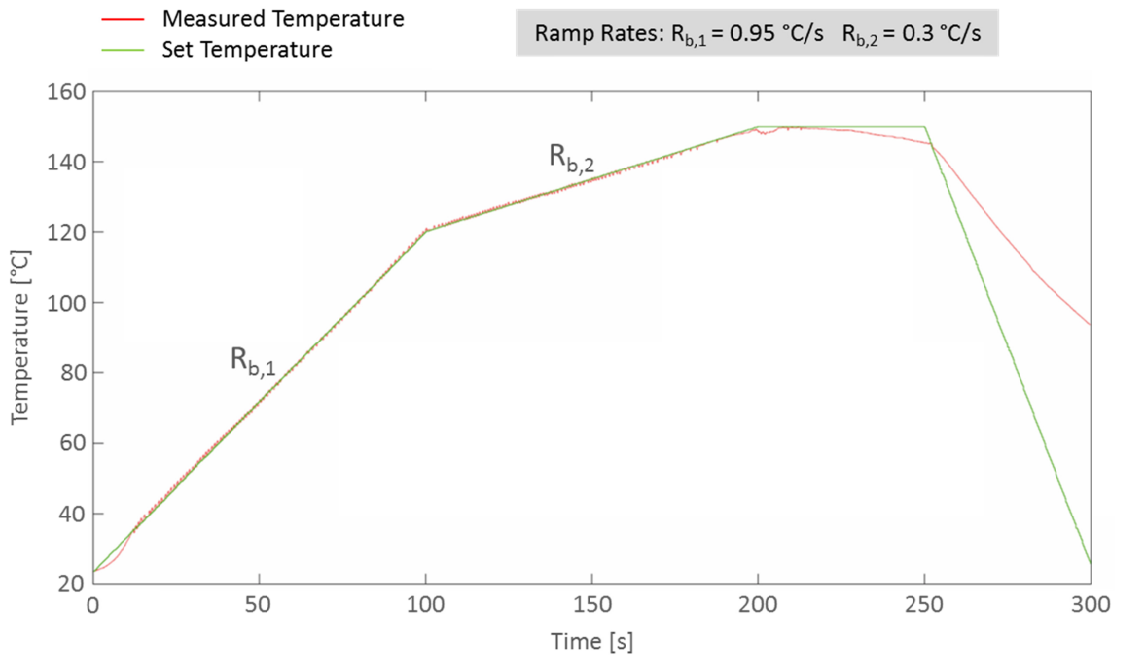


Figure 32 – Cure experiment with Hysol EO1080 and adjusted ramp rates

The ramp rate from 120 °C to 150 °C is $R_{b,2} = 0.3$ °C/s. The cure reaction is less intense and no overshooting can be observed. Additionally, the temperature drop in the subsequent endothermic reaction is less intense in this case.

In this experiment, the exothermic reaction appears to be less intense, allowing the controller to follow the temperature profile very closely. It seems that the intensity of the exothermic reaction is linked to the heating rate between 120 °C and 150 °C.

This behaviour can be explained by the dependence of the reaction rate on the temperature (Arrhenius law). If the cure process is expedited by a high ramp rate or

temperature, then the reaction rate is high and a high amount of uncured material starts to cure (crosslink). This results in a high release of thermal energy, which increases the temperature and speeds up the cure process. With increasing duration of the reaction, the degree of cure increases and therefore the reaction rate decreases. In turn, less thermal energy is dissipated and the temperature is reduced. If the ramp rate is low, then the reaction rate is also lower in turn, which results in lower exothermal energy dissipation. The latter case is easier to predict and to control.

As both experiments show, a two-point controller is, in principle, suitable for temperature control of microwave heating processes. Heating expedites the cure reaction, which may cause significant disturbances to the temperature control and thus exceed the control capabilities of the heating system. Preliminary experimental data suggests that this may be prevented by taking the complex chemistry and physics of the processed pastes into account and using temperature profiles which account for the cure reactions. Numerical models, such as the numerical multi-physics model by Tilford *et al.* (Tilford et al. 2008b), may be helpful in developing suitable temperature profiles.

5.4 Heating control

As pointed out before, microwave heating may cause arcing or sparking on conductive components. As microelectronic devices always have conductive elements, the potential for arcing or sparking needs to be prevented.

Three different heating methods have been considered with different frequency regimes and cure time durations. Two methods use variable-frequency microwave curing (Wei et al. 2000) and one uses a constant frequency. The overall cure time will be several minutes, depending on the process and heating method used. Based on experience from existing laboratory systems, maximum heating rates are expected to be around 5 °C/s (Pavuluri et al. 2010a). Comparable results to convection oven curing are expected by controlling the temperature to ± 2.5 °C (Pavuluri et al. 2011; Pavuluri et al. 2012).

5.4.1 Constant frequency

A signal with a starting frequency f_0 is used for heating. The starting frequency is close to a resonant frequency and cyclically adapted in order to track the continuously changing resonant frequency according to the algorithm presented in Chapter 5.3.1. The resulting frequency band is indicated as Δf_{max} .

To control the power output and to prevent arcing or sparking, the signal is pulsed with the frequency $f_{PWM} = \frac{1}{T_{PWM}}$. By adjustment of the pulse width, the power can be

controlled. The duty cycle $d = \frac{T_{On}}{T_{PWM}}$ describes the ratio between ‘On’ and ‘Off’ times. Temperature control is achieved by alternating between a duty cycle $0 < d_1 \leq 1$ and a duty cycle $d_2 = 0$. The control principle is illustrated in Figure 33.

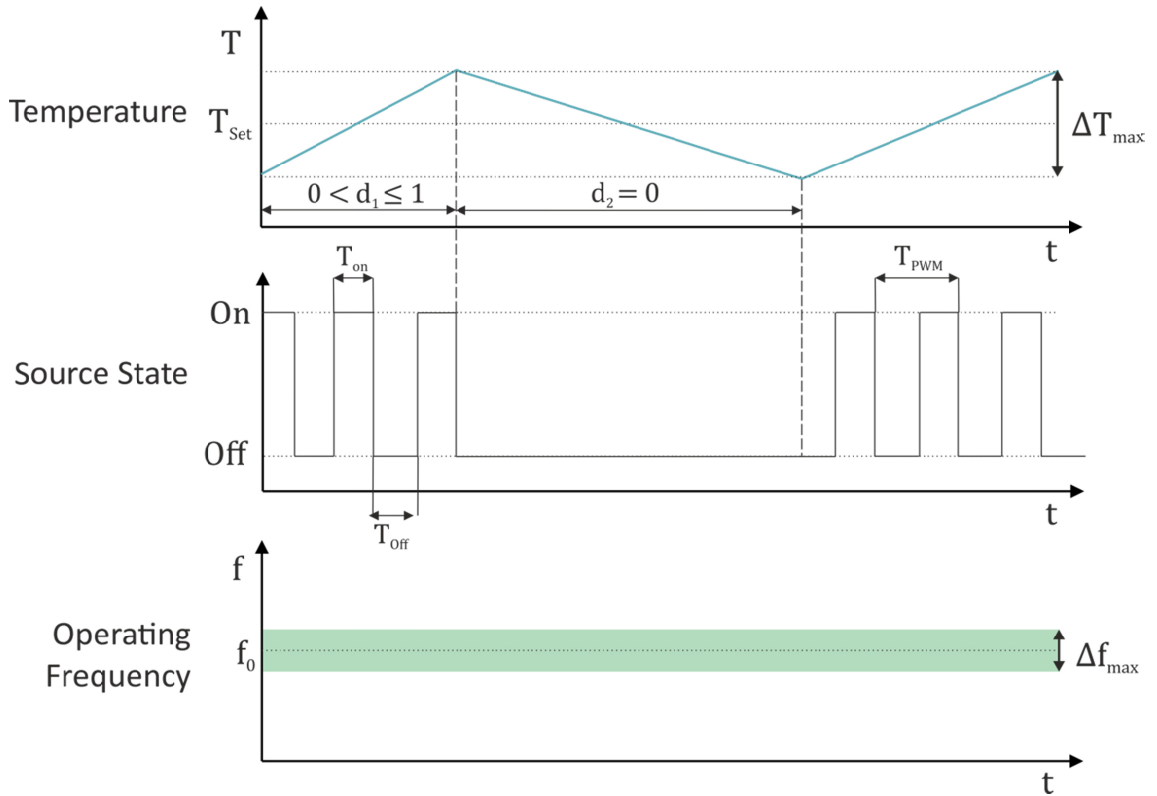


Figure 33 – Constant frequency control

5.4.2 Linear sweep

In this regime, the microwave frequency is swept periodically between a defined maximum frequency $f_{sweep,max}$ and a minimum frequency $f_{sweep,min}$. Different modes are excited during the sweep, which results in an effectively uniform heat distribution (Wei et al. 2000). Furthermore, this method effectively prevents arcing and sparking (Wei et al. 2000). Most of the time during the sweep, no modes are excited, which results in a low heating efficiency.

The temperature is regulated by switching the source on and off when the allowed temperature range ΔT_{max} is exceeded. The control principle is illustrated in Figure 34.

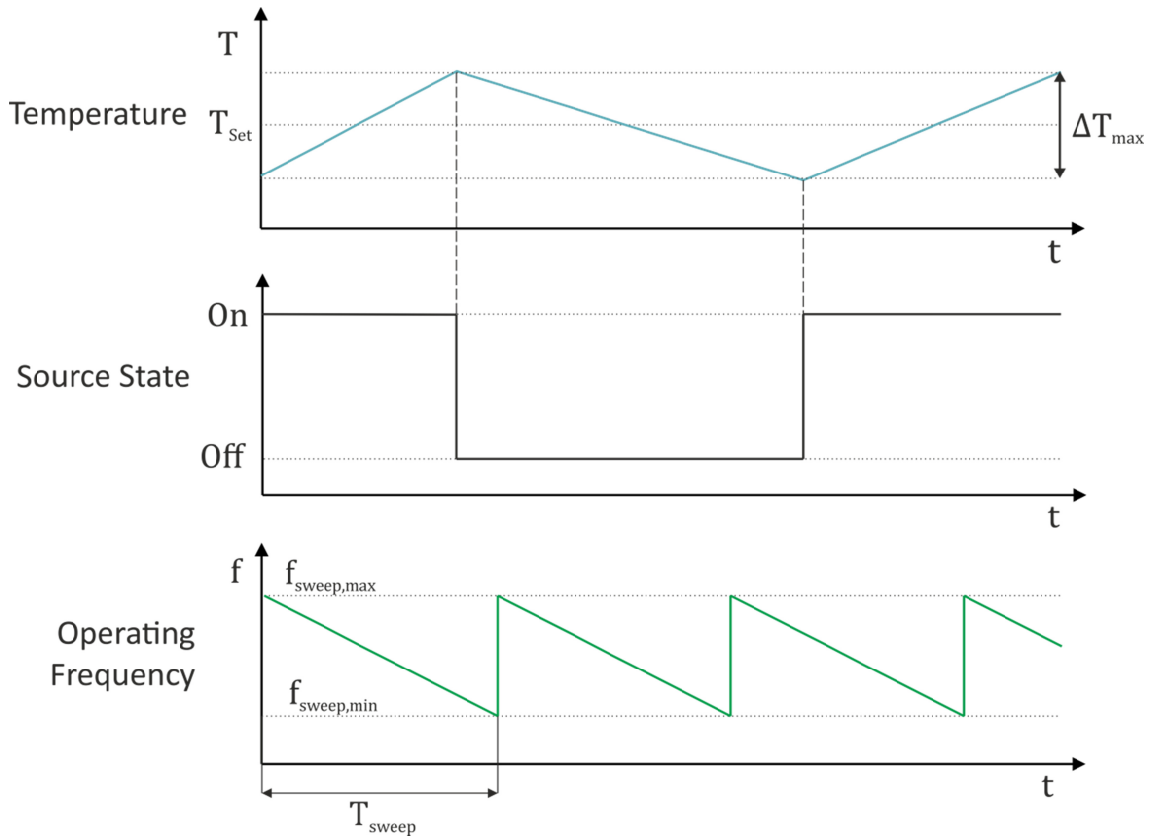


Figure 34 – Linear sweep

5.4.3 Frequency hopping

In this regime, the frequency is changed periodically between numerous discrete frequencies $f_{d,0} \dots f_{d,n}$. Ideally, each of these frequencies corresponds to a resonant frequency of the oven. By specifically changing between resonant frequencies, the power output is kept high compared to the conventional sweep. Arcing and sparking is prevented by the rapid change of the frequency. The temperature is again regulated by switching the microwave source on and off when the allowed temperature range ΔT_{max} is exceeded. The control principle is illustrated in Figure 35.

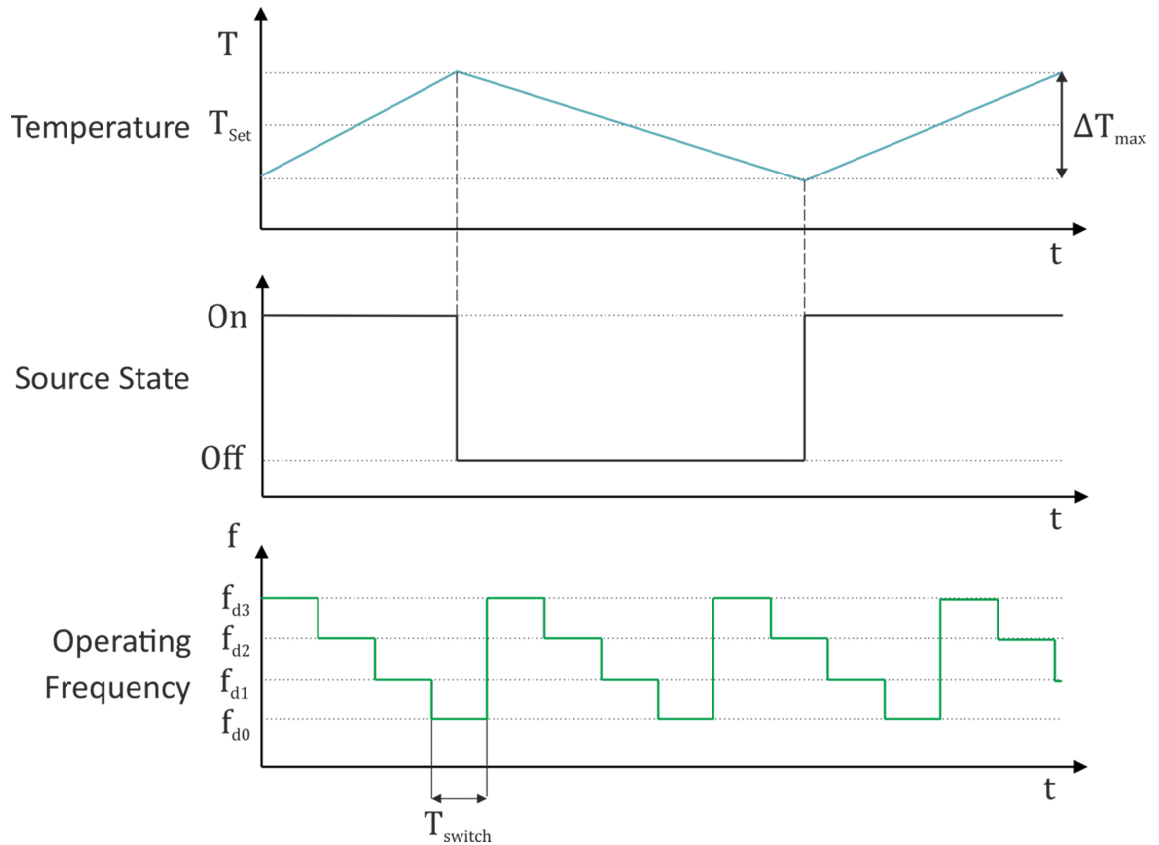


Figure 35 – Frequency hopping

5.4.4 Control system

The basic components of the curing system have been identified and a control concept of the curing system has been proposed. To realize the curing system, an appropriate control system is now required. The previously selected components and the control concept impose a set of requirements on the control system. In this section, four different control systems shall be assessed for their applicability to the curing system in order to select the most appropriate system.

An implication of the control concept is that all sensor values need to be read, processed and the set point values defined for the microwave system within a given time period, otherwise the required control of the temperature profile fails. This requirement is generally referred to as real-time capability and must be provided by the control system.

The proposed curing system is designed to be applied in the field of electronics packaging. However, the spectrum of potential applications is very broad. Although many packaging applications are already highly standardized and very similar, the curing system may need to be adapted to each type of application (e.g. from package processing to wafer processing). The control system must be flexible enough to allow

these changes or to allow the necessary adaptations. This may be applied from hardware, as a different microwave amplifier or a different temperature sensor may need to be installed, or alternatively, the adaptations need to be easily possible within the software.

For the first implementation of the system and for possible adaptations the available interfaces are very important. The control system must communicate with different superordinate control systems, most likely the pick and place or similar machines. Furthermore, over time, different sensors or sources may be integrated. The control system must therefore feature a wide spectrum of different interfaces and ideally allow the addition of further interfaces if necessary.

Another important requirement is acceptance by the end users. Typical direct end users of the curing system are machine-builders for the microelectronics packaging machines and indirectly, of course, companies applying microelectronics packaging processes. It should be taken into account that a potential user of the system will be more likely to integrate the system into a machine or into a production process if the system works with a control system that is already widely used in this industry.

Some control systems, particularly PC-based control systems, require regular maintenance, just like normal PCs. Dedicated control systems do not usually need to be maintained. The required maintenance effort should be low, especially considering that the system will be a subsystem of a larger machine.

The curing system is targeted towards industrial exploitation in the domain of electronics packaging. As in every industrial domain, economic aspects are to be considered; the hardware cost of the control systems must be taken into account.

The assessment is performed based on a decision matrix, analogous to the method used in Section 5.1. The result is presented in Table 11.

The four considered options are to use a microcontroller (μ -Contr.), an industrial PC (IPC) running a real-time operating system (RTOS), a programmable logic controller (PLC) or an IPC running a software PLC (Soft-PLC).

Microcontrollers are small computer systems and typically contain a processor core, RAM, program memory and IO interfaces within a single IC. A microcontroller can be considered a self-contained system and can be used as an embedded system (Heath 2002). Microcontrollers and kernels for real-time closed-loop applications are commercially available and are widely industrially exploited.

An alternative to microcontrollers are full-blown PCs. Such personal computers for industrial purposes are commonly referred to as industrial personal computers (IPC).

These systems typically run Microsoft Windows or Linux distributions. These operating systems are not real-time capable. To provide these capabilities on an industrial PC, a special RTOS can be applied, together with real-time capable programming languages. For example RTLinux, an extension to the Linux kernel, provides hard real-time and multiple threads, enabling it to control complex machinery (Yodaiken 1999; Ji et al. 2008).

According to Bolton, a PLC is a special form of microprocessor-based controller that uses programmable memory to store instructions and to implement functions such as logic, sequencing, timing, counting, and arithmetic in order to control machines and processes (Bolton 2015). PLCs are very common in automation technology, especially for motion and process control due to their real-time capabilities. PLCs have a high degree of standardization, particularly regarding the programming languages and interfaces.

Table 11 – Assessment of control systems

Criterion	Weight g	Soft-PLC		PLC		IPC		μ-Contr.	
		n	n·g	n	n·g	n	n·g	n	n·g
Flexibility of SW	5	10	50	7	35	10	50	6	30
Flexibility of HW	5	10	50	8	40	7	35	2	10
Maintenance Eff.	2	8	16	10	20	7	14	4	8
Real-time Capa.	4	8	32	8	32	8	32	10	40
Available	3	9	27	7	21	6	18	5	15
Hardware Cost	2	4	8	3	6	4	8	10	20
End User Accept.	3	7	21	9	27	6	18	7	21
$\sum n \cdot g$		204		181		175		144	
Rank		1		2		3		4	

Soft-PLC systems consist of a host PC, mostly embedded or industrial PCs, the PLC control software as well as PLC hardware components, which are connected to the PC via a field bus. The control software is embedded in a host operating system (e.g. Windows) and extends its kernel to include real-time capabilities. Soft-PLC systems like Codesys or TwinCAT apply the same standardized programming languages as conventional PLC systems. Soft-PLC systems offer a higher flexibility than

conventional PLC systems; however, as they are bound to their (unsafe) host system, they cannot be applied for safety-critical applications such as in aeroplanes or nuclear plants.

The decision matrix is shown in Table 11. A microcontroller is by far the cheapest solution; however, the main drawback is the lack of flexibility. An IPC with an RTOS has a high flexibility regarding software, but is deficient in interfaces and end-user acceptance. A pure PLC solution has high hardware costs and drawbacks in flexibility. Soft-PLC systems are relatively expensive, but offer a high flexibility regarding software and hardware, provide a wide range of interfaces and are still well accepted in the industry. According to this assessment, the appropriate control system is a Soft-PLC control, which is selected for further consideration.

5.4.5 Temperature sensor

A requirement imposed on the curing system is the control of the temperature profile (Requirement 1). Section 5.3.2 further underpinned the necessity of temperature control. Closed-loop control of the defined temperature profile requires a cyclic measurement of temperature.

Table 12 – Assessment of temperature measurement methods

Criterion	Weight g	Non-contact		Optical		Electrical	
		n	n·g	n	n·g	n	n·g
Temperature Range	5	10	50	8	40	6	30
Delay	5	10	50	5	25	4	20
Microwave Influence	5	8	40	10	50	2	10
Integration	3	7	21	7	21	10	30
Calibration	3	3	9	7	21	7	21
Resolution	2	6	12	10	20	8	16
Cost	2	4	8	3	6	10	20
$\sum n \cdot g$	25	190		183		147	
Rank		1		2		3	

Three classes of temperature sensors are considered: electrical; optical; and non-contact sensors. Electrical sensors include, for example, thermocouples and are contact-type

sensors. Optical sensors measure the optical parameters changing with temperature and include Fiber–Bragg sensors. They are also contact-type sensors. The non-contact sensors considered here are pyrometers and thermal imaging cameras.

An assessment of the different temperature measurement methods is shown in Table 12. Electric temperature sensors are very easy to integrate and very cheap, but also highly sensitive to electromagnetic fields. The sensor needs contact at or very close to the heated object. Optical sensors would need contact as well, but are not disturbed by electromagnetic fields. Non-contact measurements can measure from a distance and do not require a thermal equilibrium with the sensor. Their main drawback is the required calibration and the relatively high cost. Based on this assessment, non-contact temperature measurement is considered the most suitable solution.

5.4.6 Curing system concept overview and discussion

In Chapter 3, based on an analysis of electronic packaging, market needs, and the underlying processes, a first set of requirements for a novel method was formulated. The method should address the problem of intermediate handling processes in microelectronics packaging and improve the overall efficiency of microelectronic packaging processes.

By reviewing the state of the art, it was concluded that the imposed requirements are to be fulfilled by a novel curing system that was capable of integrated implementation.

The basic heating process has been discussed, assessed and microwave heating has been selected. The main components for the system have been identified. Viable options for these components have been assessed and individual selections have been carried out. Based on the components of the heating system, a control concept was developed, comprising frequency, temperature, and power control.

An overview of the features of the curing system concept is compiled in Table 13.

Table 13 – Curing system concept overview

Feature	Approach	Section
Curing Principle	Microwave curing	5.1
Microwave Source	Solid-state power amplifier (SSPA)	5.2.1
Microwave Applicator	Open-ended waveguide resonator	5.2.2
Control System	Soft-PLC	5.4.4
Temperature Sensor	Non-contact temperature sensor (pyrometer)	5.4.5
Control Methods	Frequency, temperature and heating control	5.3
Frequency control	Maximum power point tracking (MPP)	5.3.1
Temperature control	Two-point controller	5.3.2
Heating control	Three methods: constant frequency, linear sweep and frequency hopping	5.4

With the components known and the control concept described, the next step is the creation of a prototype curing system.

5.5 Concept of an assembly machine with microwave curing system

A concept for a microwave curing system has been proposed in the previous chapter. This system is targeted to microelectronics packaging processes. Now, based on the concept of the previously described curing system, a concept for a machine that integrates this curing system is developed.

The domain of microelectronic packaging has been analysed and a range of relevant products have been derived. With the products known, the key processes have been described and a set of relevant processes was derived.

With the principal products and processes known, numerous parameters of the machine are assessed and finally selected. Based on the choice of the individual components, a comprehensive concept is compiled and presented.

5.5.1 Machine requirements

The purpose of the machine is to develop a microelectronics assembly process with an integrated microwave curing process. This comprises the integration of all relevant components into one machine. Once the system is set up, validation and testing of the process under different conditions will be carried out on the machine.

Characterization of the developed process will provide knowledge to enable assessment of potential applications and to dimension further machines accordingly. For a reasonable machine layout, a production volume of 100 pieces per day is assumed, as a working hypothesis. This corresponds to a typical use case for assembly of complex products with high variance (Adamietz et al. 2010; Scholz et al. 2016).

Since the main purpose of the machine is for process research and development it should not be constricted to just one product or product variant. It should rather be designed to cover a range of products and process variants. Specifically, the machine should not be limited to a certain chip package with certain dimensions, but rather be suitable for a range of different products. The same applies for the processes, which should also provide a range of different process variants. If the provided flexibility is not sufficient, then at some point it should be possible to adapt the system with moderate effort.

The particular machine developed in the course of this thesis is not meant to be used in an industrial environment. Useful life, degree of utilization and amortization time are therefore not currently regarded as relevant requirements and are not defined at this point.

5.5.2 Product analysis

The reference for the product analysis is the flip-chip process described in Chapter 3.

Flip-chip processes are industrially implemented with both solder and conductive adhesive technologies.

Electrically conductive adhesives (ECAs) have advantages when compared to solder materials. ECAs are processed with significantly lower temperatures than solder materials, enabling them to be used with heat sensitive or non-solderable materials (Jagt et al. 1995). ECAs can be used for finer pitches than solder, as the materials have smaller particle sizes than solder pastes (Liu et al. 1998). The materials are also more flexible than solder materials, making them less sensitive to thermomechanical stresses (Jagt et al. 1995).

Solder materials have a significantly higher and steadier conductivity than ECA materials, especially regarding high-frequency applications (Coughlan et al. 2006). The curing times are significantly shorter (Jagt et al. 1995).

The processing of ECAs is relatively simple, as the materials can be dispensed quite easily. The high viscosity of solder pastes makes them very hard to dispense; in particular, achieving a precise application for fine pitches is complicated. Therefore, screen printing or solder balling is preferred for solder processing, which requires significantly more complicated and expensive equipment.

With respect to the method of microwave curing, both solder and adhesive materials are applicable. However, microwave heating of adhesive materials is more efficient, due to dielectric groups being present in the organic material.

With respect to machine and process flexibility, the achievable precision and the reliability properties, ECAs are preferred for the purposes of this thesis.

Dies are typically provided in a waffle pack tray for low-volume production, but can also be supplied from a blue tape with die ejector or from reel-to-reel feeding from foils or films (Reichl 1998). For the present conceptual design, waffle pack trays will be regarded as the preferred option, but the option of retrofitting to a different option will be taken into account as well.

The substrate can be a package such as a BGA, or a more complex SoC package. In this case the package will be typically provided on a tray. However, for higher throughputs, other feeding methods such as conveyor feeders, Auer boats or reel-to-reel feeders may be considered. The substrate may also be a board. In this case, it is either manually inserted or provided by a conveyor system. As the expected volumes are low, a manual insertion is appropriate for both the package and the board case. However, an optional tray system for packages will be considered, as well as an adaptation to a different feeding method.

Requirements on precision and reliability have been described previously: a precision assembly process with a precision of at least 20 μm and at least the same reliability as a comparable, industrially applied technology is required.

5.5.3 Assembly process

Approaches to micro assembly can be divided into serial and parallel assembly methods (Nelson et al. 1998; Lotter et al. 2006). The wafer-based production of MEMS applies mostly to batch processes. Parallel assembly strategies promise economic advantages, as with parallel assembly strategies, high throughputs can be achieved at the cost of a

significantly reduced flexibility. Serial micro-assembly methods perform the assembly one by one (Nelson et al. 1998; Lotter et al. 2006). This provides process flexibility and allows easy processing of different product variants. The proposed curing system concept is primarily designed for the processing of single components and selective processing of components on larger assemblies. Therefore, a serial micro-assembly strategy is considered to be suitable and will be further pursued.

SMD pick-and-place machines without sensor guidance achieve assembly accuracies of 35–40 μm under highest efforts (Fatikow 2000). Significantly higher accuracies are achieved by integration of sensor-guided positioning strategies (Fatikow 2000; Höhn 2001; Jacob 2002; Dittrich et al. 2004; Lotter et al. 2006). Two principles of sensor-guided positioning strategies are distinguished: relative; and absolute positioning (Höhn et al. 2001; Jacob 2002).

In relative positioning the position of the part and the assembly position on the substrate are measured at the same time with one measurement system (Raatz et al. 2012). This allows the direct determination of the relative pose difference, which can then be directly compensated by the positioning system (Höhn 2001). A challenge of relative positioning is the simultaneous measurement of features under the part and on the substrate, which prevents its application in electronic packaging, particularly flip-chip packaging.

Absolute positioning strategies measure the part and the assembly position on the substrate independently from spatially separate positions, which implies that two sensors are usually required (Raatz et al. 2012). The measurements of the individual sensors are both transferred into the joint base coordinate system, which allows a calculation of the pose difference. This difference can then be compensated by the positioning system. The measurement with two sensors has a negative impact on the precision of the assembly process, since the errors of the two sensor measurements are added. Due to the limitations of relative strategies, absolute positioning strategies are almost exclusively applied for surface-mount devices and for chip assembly (Höhn 2001).

Absolute positioning strategies require a higher material and integration effort and are less precise than relative strategies. However, the limitations described in this section impede an application for flip-chip packaging. Therefore, absolute positioning strategies are selected for further consideration.

5.5.4 Dispensing

Over the years, numerous methods for the precise dispensing of media have been developed. In Table 14 an assessment of prevalent micro-dispensing systems is presented.

Dispensing systems can be classified into contact and non-contact systems. Modern non-contact systems have a very good repeatability and very high throughput performance. However, these systems have limitations regarding the dispensing of high viscosity and filled materials.

Auger, time–pressure, piston and peristaltic dispensers are contact systems. These systems generally have a lower throughput, but are suitable for a wide range of materials, including filled materials.

While the performance of time–pressure dispensing systems is slightly below that of more sophisticated systems, they are cheap, easy to maintain, suitable for a wide range of materials and they still allow high-precision processes. Time–pressure systems are particularly suitable for low-volume production and are therefore further pursued for the dispensing processes in this conceptual design.

Table 14 – Assessment and selection of dispensing systems (Othman 2005; Wiedenhöfer 2009)

Principles / Properties	Auger	Time / Pressure	Piston	Peristaltic	Jet Pump	Piezo-Electric
Non-Contact	No	No	No	No	Yes	Yes
Repeatability	High	Medium	High	Medium	High	High
Low-Viscosity Materials	Good	Good	Good	Good	Good	Good
High-Viscosity Materials	Good	Good	Good	Good	Limited	Limited
Filled Materials	Limited	Yes	Yes	Yes	Limited	No
Feeding (Cartridge / Continuous)	x / x	x / -	x / -	x / x	x / x	x / x
Throughput	Low	Low	Low	Low	High	High
Maintenance	High	Low	Medium	High	Medium	High
Cost	High	Low	Medium	Medium	High	High
Process Development	Elaborate	Medium	Elaborate	Medium	Elaborate	Elaborate

5.5.5 Pick and place

The pick-and-place process deals with the problems of picking a part up, how it is positioned and how it can be released (van Brussel et al. 2000). Grippers are the interface between the handling or positioning system and the part and therefore have an important role during the handling process.

Macroscopic gripping processes deal mostly with mass-dependent forces, predominantly gravitational and inertial forces. In microscopic gripping processes, the relation changes towards electrostatic, van-der-Waals and surface tension forces, with smaller part dimensions (Fearing 1995). Picking up and holding the part are supported, but the part release is often more problematic, as the parts often strongly stick to the gripper. Therefore, for microscopic gripping problems, specialized grippers and release strategies are required (Bark et al. 1998).

Different gripping principles have been proposed and researched for microscopic parts. These comprise adhesive grippers (Westkämper et al. 1996; Grutzeck et al. 2002), electrostatic grippers (Oh 1998; Hesselbach et al. 2007), fluidic grippers (Nienhaus 1999) and miniaturized mechanical grippers with different actuation principles, such as piezo-actuation, shape-memory alloys or electromagnetic alloys (Höhn 2001). These systems have been experimentally tested and validated, but only a few of these systems are industrially established.

Vacuum grippers are the prevailing type of gripper in microelectronics packaging and SMT. It is a simple device, which consists of a thin tube connected to a vacuum (van Brussel et al. 2000). Its simplicity and low cost allow it to be exchanged frequently. To avoid stick effects on microscopic parts, the gripper should be designed to have a minimal contact area. Furthermore, the gripper should be made out of an antistatic or conductive material to minimize electrostatic adhesion effects. In microelectronics packaging processes, the part is typically placed onto adhesive or solder paste. The adhesion between paste and part supports the release from the gripper. In contrast to mechanical grippers, vacuum grippers are generally gentle to the parts, especially when rubber or other polymeric compounds are used as gripper materials.

As vacuum grippers are an industrially common technology that is cheap and flexible, vacuum grippers have been selected for use in this conceptual design.

5.5.6 Process analysis

In Chapter 5.5.3, a serial assembly process with an absolute positioning strategy has been selected. This assembly process relies on sensor feedback to measure part and substrate feature positions in a base coordinate system.

Three primary processes: dispensing; pick and place; and curing impose different requirements regarding positioning and orientation and auxiliary sensor feedback. An overview of these requirements is presented in Table 15.

Each of the processes requires translational positioning with three degrees of freedom (DoF). The pick-and-place process requires, in addition, a rotation of the gripped part to adjust its orientation.

The centre of the needle tip is the dominating feature of the dispensing process and has to be determined in the course of the process. For the gripper, the centre of gravity of the gripper geometry has to be determined. The pose of a gripped part may need to be determined in the course of the pick-and-place process. Relevant feature positions on the substrate are to be determined for both the dispensing and the pick-and-place

processes. These are primarily bond pad positions, but the pose of the assembled chip may also be helpful for the dispensing of underfill and encapsulant. A minimal distance between the needle tip and the substrate is needed for a reliable dispensing process. The vertical position of the substrate must therefore be determined. The curing process does not require position feedback, as the positioning accuracy of the applicator is only of secondary concern.

Table 15 – Requirements of the main processes

Process Properties	Dispensing	Pick and Place	Curing
Translation	3 DoF	3 DoF	3 DoF
Rotation	-	1 DoF	-
TCP-Measurement	Needle tip	Gripper Part on gripper	-
Measurement of Substrate Features	Bond pads Chip position	Bond pads	-
Other	Distance needle to substrate		

5.5.7 Sensor assessment and selection

The measurement of feature positions in the scale of micrometres for automated micro assembly is typically performed using machine vision systems (Höhn et al. 2001; Jacob 2002), as these instantly provide a planar image in contrast to a punctual measurement. Vision systems can be used in a versatile manner since a wide range of tasks can be covered through the variables of camera, optics and lighting. On the other hand, a vision system needs to be engineered to a specific task. Relevant factors in the engineering of vision systems are resolution, field of view, light intensity and cost. The quality of the optics has a significant impact on the image quality and thereby also on the measurement accuracy. Another factor is the image processing software. The image processing algorithms employed have a strong influence on the measurement accuracy (Davies 2004).

Cameras provide a two-dimensional image without depth information. If the exact focal distance of the camera is known, it can be used to determine depth information of the

feature. However, depending on the optical configuration employed, the focus tolerance might be between 10 μm and 100 μm , which is insufficient for the distance regulation of the dispenser needle and the pick-and-place processes. Stereo camera systems are another possibility to obtain additional 3D information, albeit of inferior quality regarding the accuracy compared to most dedicated sensors. Optical coherence tomography is available in the form of compact sensors. However, the high cost and the lack of software are currently impeding a broad industrial application.

A high-resolution 3D image of the surface would be advantageous, but is not compulsory. Punctual depth information is typically considered sufficient for microelectronics assembly processes. A dedicated distance sensor can be applied for the determination of the depth information.

An overview of distance measurement principles is shown in Table 16.

Table 16 – Distance measurement principles ($\mu\text{Epsilon}$ 2016; Häusler et al. 1999; Blais 2003; Hocken et al. 2011)

Principles \ Properties	Confocal	Interferometric	Laser Triangulation	Ultrasonic	Inductive	Capacitive	Tactile
Resolution	+	+	+	0	+	+	0
Accuracy	+	+	+	-	+	+	0
Measurement Time	+	+	+	0	+	+	-
Measurement Range	+	0	+	+	+	+	-
Materials	+	+	+	+	-	+	+
Distance to Object	0	0	+	0	0	-	-
Spot Size	+	+	+	-	0	0	0
Cost	0	-	0	+	0	0	+

Ultrasonic, inductive, capacitive and tactile sensors have significant drawbacks, which prevent their application in micro-assembly processes. Confocal, interferometric and laser triangulation are techniques that satisfy the requirement profile well.

Interferometric sensors are more expensive and have a relatively low measurement range. Confocal sensors require a relatively low distance to the measurement object compared to the laser triangulation sensor. Laser triangulation sensors provide a high resolution and measurement accuracy, while being suitable for different surfaces and allowing a high measurement distance. Based on this review, laser triangulation is selected as being most appropriate.

5.5.8 Absolute positioning strategy

To facilitate the calculation of positions, different coordinate systems are defined. These are shown in Figure 36. Additional tools, for example, further dispensers, may be necessary for the realization of the process.

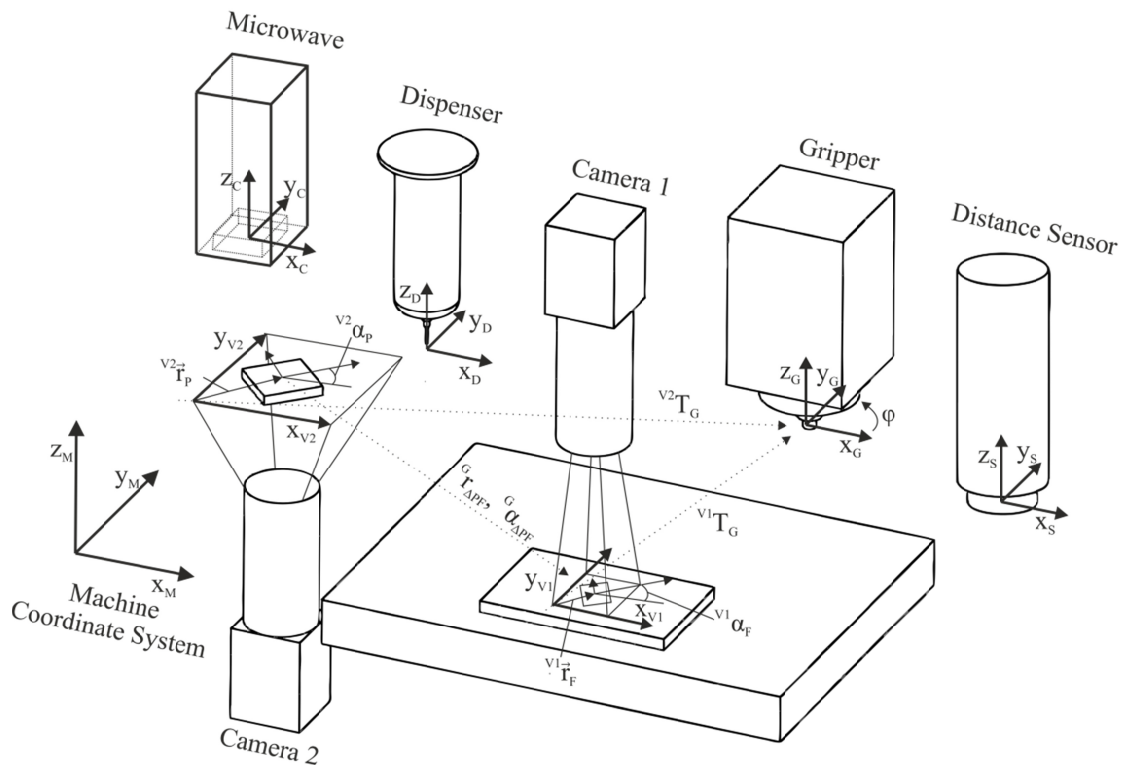


Figure 36 – Absolute assembly strategy

The transformation from a coordinate system C_I into a coordinate system C_J is a linear transformation, which can be represented by matrices. Homogenous coordinates are used to describe the transformation. The matrix ${}^I T_J$ is an example of a transformation matrix, which implements a rotation of angle α_{IJ} around the z-axis and a translation of t_{IJ} . Rotations around the x-axis and y-axis are typically not necessary for a 4D positioning system and are therefore neglected. Matrix ${}^I T_J$ is applied as a template for

the subsequent description of coordinate transformations. A position vector ${}^k\vec{r}_l$ is defined, with k indicating the used coordinate system and l indicating the associated function, e.g. ‘D’ for dispenser or ‘G’ for gripper. ${}^I\mathbf{T}_J$ and ${}^k\vec{r}_l$ are shown in Equation (6). The microwave applicator and its coordinate system are represented by ‘C’ for ‘curing’.

$${}^I\mathbf{T}_J = \begin{pmatrix} \cos \alpha_{IJ} & -\sin \alpha_{IJ} & 0 & t_{IJ,x} \\ \sin \alpha_{IJ} & \cos \alpha_{IJ} & 0 & t_{IJ,y} \\ 0 & 0 & 1 & t_{IJ,z} \\ 0 & 0 & 0 & 1 \end{pmatrix}, {}^k\vec{r}_l = \begin{pmatrix} r_{kl,x} \\ r_{kl,y} \\ r_{kl,z} \\ 1 \end{pmatrix} \quad (6)$$

A coordinate transformation from coordinate system C_I to C_J of position vector ${}^k\vec{r}_l$ can be described by Equation (7).

$${}^J\vec{r}_l = {}^I\mathbf{T}_J \cdot {}^I\vec{r}_l \quad (7)$$

With the prerequisites defined, the assembly strategy can be described.

Initially, feature position ${}^{V1}\vec{r}_F$ and orientation α_F are determined by Camera 1 in coordinate system C_{V1} . To measure the z position, the calibrated laser sensor is moved over the previously determined planar position with a known height, which allows the determination of the z position with the accuracy of the sensor.² Once the exact feature position is determined, it is transformed into the tool coordinate system C_T :

$${}^T\vec{r}_F = {}^{V1}\mathbf{T}_T \cdot {}^{V1}\vec{r}_F, \text{ with } \alpha_{IJ} = 0^\circ \quad (8)$$

With knowledge of the tool centre point ${}^T\vec{r}_{TCP}$, the relative vector between tool and feature position ${}^T\vec{r}_\Delta$ can be calculated and used to position the tool onto the feature position:

$${}^T\vec{r}_\Delta = {}^T\vec{r}_F - {}^T\vec{r}_{TCP} \quad (9)$$

This method can be applied for the positioning of the dispenser over the feature. An exact determination of the position is required for the dispensing of ECA on bond pads, e.g. for the flip-chip process. This method may also be applied for the laser sensor, the oven and for the pickup of a part with a gripper. During the pickup of a part, the part may be significantly dislocated on the gripper, impairing the precision of the overall pick-and-place process.

To compensate for the dislocation of the part on the gripper, a second camera is employed. The part is positioned with the gripper over the second camera and its position ${}^{V2}\vec{r}_P$ and orientation α_P on the gripper are determined within coordinate

² The calculation of the position is performed analogously for the other tools.

system $C_{V,2}$. The translational offset vector ${}^G\vec{r}_{\Delta P}$ can then be determined by Equation (10).

$${}^G\vec{r}_{\Delta PF} = ({}^{V1}T_G \cdot {}^{V1}\vec{r}_F) - ({}^{V2}T_G \cdot {}^{V2}\vec{r}_P) \quad (10)$$

The rotational offset ${}^G\alpha_{\Delta PF}$ is calculated by Equation (11), based on the absolute positions.

$${}^G\alpha_{\Delta PF} = ({}^{V1}\alpha_G + {}^{V1}\alpha_F) - ({}^{V2}\alpha_G + {}^{V2}\alpha_P) \quad (11)$$

Through knowledge of these two offsets, an absolute movement for the pick-and-place process can be determined.

Different strategies for the intrinsic calibration of vision sensors are described in the literature (Lenz 1987; Weng et al. 1992; Höhn 2001). In intrinsic calibration, the optical parameters of the camera and the optics are determined and compensated if necessary. This process is usually performed with the help of a reference object. Intrinsic camera calibration functionality typically forms part of state-of-the-art vision software packages.

Extrinsic calibration refers to the calibration of a vision sensor relative to the positioning system and process tools. This calibration process also has numerous strategies described in the literature (Wang 1992; Höhn et al. 2001).

5.5.9 Process chain

The previously described flip-chip assembly process (see Chapter 3.3.1) is used as a reference process for the machine concept. Based on the selected tools and the proposed assembly strategy, an example process chain for a flip-chip process including the microwave curing process is proposed. An overview of this process chain is presented in Figure 37.

The process chain comprises a total of 14 steps:

1. Initially, the substrate is transported to the process position. The part (die) is provided, sometimes in a magazine. Both processes may happen manually or automatically.
2. The pose of the bond pads on the substrate is determined by Camera 1. The height of the bond pads is measured using the distance sensor.
3. Based on the determined bond pad positions and the known calibration values, the dispensing positions are then calculated. On each of these positions, a defined volume of electrically conductive adhesive is applied using Dispenser 1.
4. Camera 1 is used to determine the exact part pose on the supply position. The height is additionally measured with the distance sensor.
5. The part is grabbed from the previously determined position using the gripper.
6. After moving the part over Camera 2, its pose on the gripper is determined.
7. With the poses of the part and the assembly position known, the relative position vector is calculated. The relative movement over the placement position is carried out and the part is then moved down and released from the gripper.
8. The microwave applicator is moved over the placed part. The adhesive is cured with the microwave applicator according to a defined temperature profile.
9. The pose of the part after curing is measured using Camera 1 and the distance sensor.
10. With respect to the pose of the part, underfill is applied between the part and the substrate using Dispenser 2.
11. Using the microwave applicator, the underfill is cured according to a defined temperature profile.
12. A glob of encapsulant is dispensed over the assembly using Dispenser 3.
13. The encapsulant is then cured using the microwave applicator according to a defined temperature profile.
14. The finished assembly is removed from the process position and transported away from the machine.

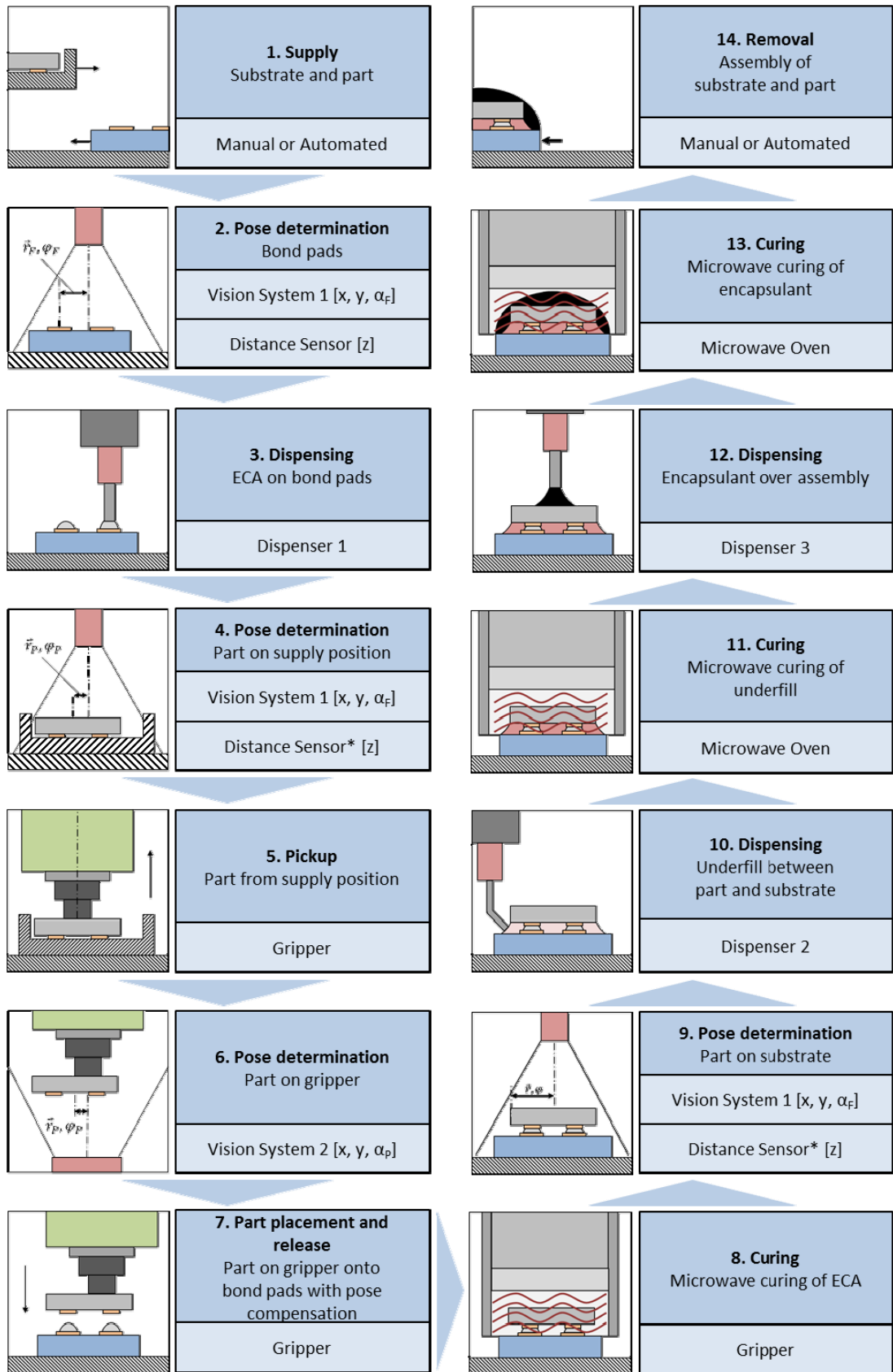


Figure 37 – Absolute assembly strategy with intermediate microwave curing steps. Process steps are described in anticlockwise direction.

With the above-described process chain, a combination of a typical assembly process with a microwave applicator is proposed. Based on this process chain, a machine concept can now be developed.

5.5.10 Machine concept

A concept for a flip-chip assembly process with intermediate microwave curing steps has been proposed. This will serve, together with the selected absolute assembly strategy, as main input variables for the conception of the machine. An overview of pre-selected kinematic configurations is shown in Figure 38.

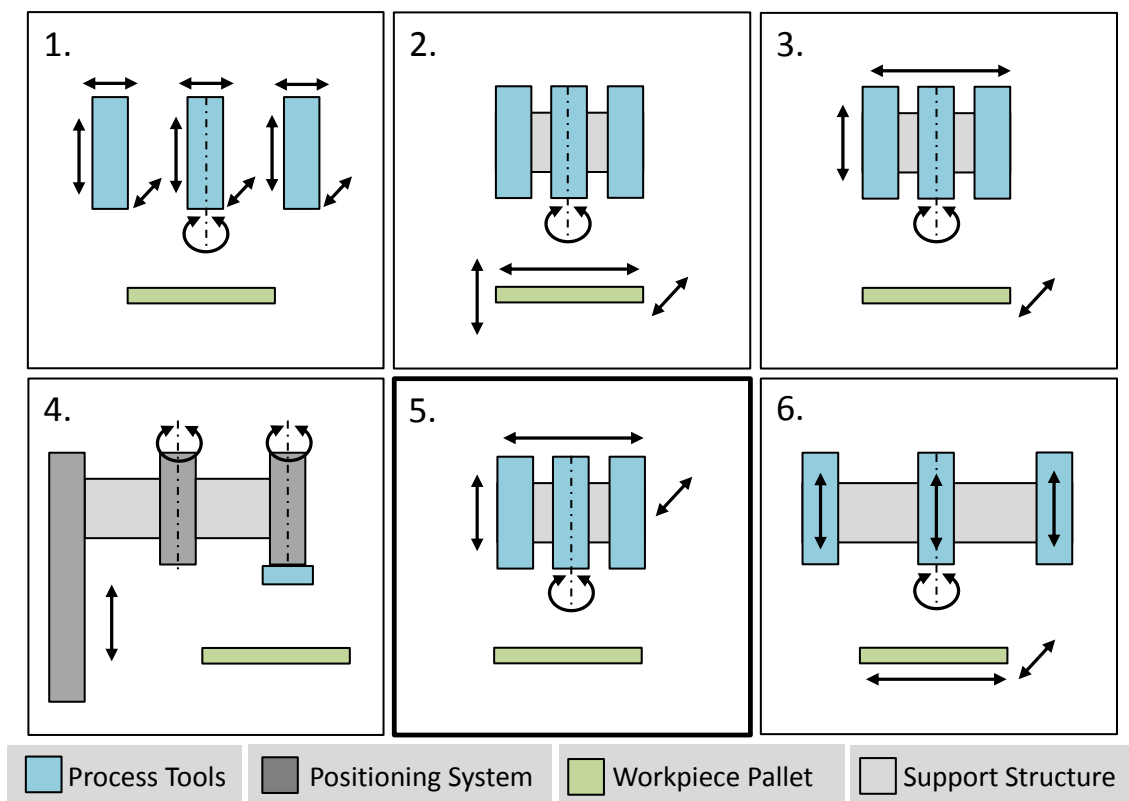


Figure 38 – Selection of kinematic configurations

Different parts of the system may be moved and others may remain stationary; the tools may be moved, the product may be moved or both may be moved in order to achieve the necessary relative movement. Since the workpieces are likely to be small and light, the moving mass may be reduced by moving the product. A drawback of such a configuration is that the positioning system might impair the integration of conveyor and feeding systems. Generally, the flexibility of the system is lower if the product is moved. Also, if positioning functions are on both the tools and the workpieces, then

flexibility is impaired. When considering flexibility of the process, a configuration with moving tools is preferred.

Potentially, each tool may be positioned individually. In this way, each positioning system may be optimally dimensioned to the requirements imposed by the individual processes and their hardware. However, the implementation of such a system is significantly more elaborate than a central positioning system in terms of the hardware and the control system. Additionally, the complexity of calibration and referencing is clearly higher. Therefore, a single central positioning system is preferred.

Robots are common for automated assembly tasks and robot systems with excellent positioning repeatability of less than 10 μm are available. However, the design of assembly robots, particularly SCARA robots, does not allow the robot to carry all the necessary process tools; a tool exchange would be required, which would negatively affect the assembly efficiency. Therefore, a Cartesian positioning system is preferred. In summary, a system with a central positioning system for all tools is preferred over the other option. Therefore, kinematic configuration 5 is selected.

5.5.11 Integration of the microwave curing equipment

The concept of the curing system consists of numerous basic components. It comprises the control system, a solid-state microwave source with integrated amplifier, power sensors, a temperature sensor and the open-ended microwave applicator.

As pointed out in Section 5.5.10, a set-up with a fixed product position and moving tools is pursued. With regard to the curing system components, the microwave applicator itself is regarded as a crucial tool to be on the moving part of the machine. To enable *in situ* temperature measurement during the heating process, the temperature sensor should also be integrated into the microwave applicator. The remaining components may be placed on fixed parts on the machine.

Splitting the components and their positioning within different sections of the machine provides the advantage that the moving mass of the machine, and thereby the load on the axes, can be reduced. In this way, an impairment of the dynamics and the positioning accuracy can be potentially circumvented. This may be important, because the microwave source is expected to have a large mass and will therefore present a significant load to the positioning system. Additionally, the size of the source takes up a considerable portion of the build space of the positioning system.

The transmission of the RF signal from the source to the applicator can, in practice, be implemented with a waveguide or a low-loss RF cable. Waveguides offer a transmission

with very low losses. Waveguides are rigid and are, in principle, suitable for a direct connection between source and applicator without relative movement. There are flexible waveguides available which allow for some relative movement; however, the high cost and the high implementation effort render this option undesirable.

Low-loss RF cables usually have worse transmission properties than waveguides, but with appropriate shielding, a transmission with relatively low losses can be achieved. RF cables are flexible, but there are no low-loss cables available that can be used within energy chains.

The transmission properties of RF cables and connectors (e.g. SMA) are impaired when forces are applied to them, for example by bending. The transmission losses then increase significantly. Therefore, the forces applied to the connectors and the cables must be minimized.

5.5.12 Machine concept overview and discussion

A concept for a machine integrating the curing system presented above is proposed. The specific requirements related to the machine were analysed. Processes needed for the assembly of microelectronic packages were considered and propositions for the specific subsystems to carry out these processes were made. With the proposed process tools, a positioning strategy has been developed. Based on the example of flip chip, an example process chain was developed. A first machine concept was then selected and the implications imposed by the microwave integration discussed.

The features and the solution approaches towards the machine are presented in Table 17.

Table 17 – Machine concept overview

Feature	Approach	Section
Process	Flip-chip process chain with intermediate microwave curing steps	5.5.9
Substrate	Microelectronic packages, PCBs, complex assemblies	5.5.2
Feeding	Preferably from magazine with optional modification to automated conveyor systems or feeders.	5.5.2
Pick and Place	Absolute positioning strategy with two vision sensors and laser triangulation sensor. Utilization of vacuum grippers for pick and place.	5.5.8
Dispensing	Time–pressure dispensers for ECA, underfill and encapsulant materials	5.5.4
Curing	Implementation and integration of proposed microwave curing system	5.5.11
Machine Type	Cartesian system with fixed product and feeding positions. Process tools are placed on the moving part of the machine.	5.5.10

With the concepts for both the curing system and the machine now available, the manufacturing of both systems can be carried out.

6 Design and Set-up of Prototype System

6.1 Integrable microwave curing system

6.1.1 Solid-state power amplifier

A solid-state power amplifier (SSPA) manufactured by RF Com Ltd and Freshfield Microwave Systems Ltd is used. The SSPA has been custom designed and built according to specifications provided by Heriot-Watt University, Edinburgh, Scotland.³ The microwave source is relatively compact, with dimensions of $180 \times 100 \times 50 \text{ mm}^3$. It has an integrated frequency generator and amplifier. The maximum output power is 11.2 W and the maximum power consumption is 100 W. Approximately 90 W are dissipated as heat, making active cooling necessary to prevent overheating. The operating frequency range is 7.5–8.7 GHz. The output power can be regulated by pulsing the source. The minimal pulse width specified by the manufacturer is 1 ms. A typical approach is to use pulse width modulation (PWM) with a fixed frequency of 10 kHz, giving a minimal duty cycle of 1% (1 ms ‘On’ and 99 ms ‘Off’) (Rupp 2011). The minimum time required for a frequency change is $2.15 \mu\text{s}$ (Rupp 2011).

6.1.2 RF power measurement

As described in Section 5.3, a satisfactory power output can be ensured by a frequency-tracking algorithm. To implement the tracking, a feedback of the power is necessary. Therefore, power measurement is required.

An overview of the microwave components and their insertion losses is shown in Figure 39.

The microwave source provides a signal to the directional coupler. Most of the power P_{12} is directly transferred via a low-loss RF cable and a rotary joint into the oven. A portion of the power is not absorbed and is reflected by the oven. This power P_{21} travels back through the rotary joint, the low-loss RF cable and the directional coupler into the source, where it is dissipated into heat (Rupp 2011).

³ The specifications and procurement of the microwave source were carried out by Dr. S. K. Pavuluri, HWU Edinburgh

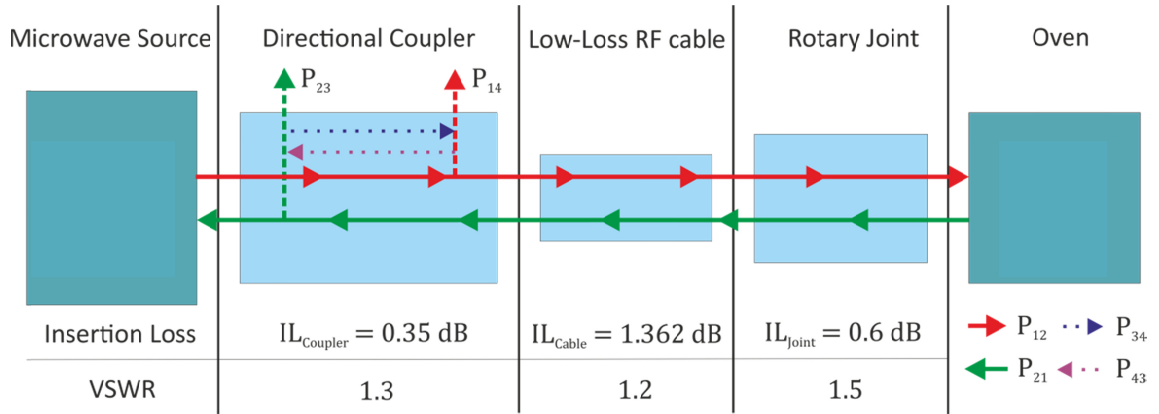


Figure 39 – Overview of microwave components and their insertion losses (IL)
(Rupp 2011)

Small portions of the incident and reflected energy are coupled out within the directional coupler. P_{23} is proportional to the reflected power P_{21} , while P_{14} is proportional to the incident power P_{12} (Rupp 2011). By measurement of P_{23} and P_{14} , the reflected and the incident power can be calculated (Rupp 2011). Equations (12)–(18) show how the power on the measuring ports can be approximated, dependent on the directivity of the coupler.

$$D_{Dir} = -10 \log_{10} \left(\frac{P_{23}}{P_{14}} \right), d_{Dir} = 10^{-\frac{D_{Dir}}{10}} \quad (12)$$

$$D_{Coupler} = -10 \log_{10} \left(\frac{P_{12}}{P_{14}} \right), d_{Coupler} = 10^{-\frac{D_{Coupler}}{10}} \quad (13)$$

$$P_{14} = d_{Coupler} P_{12} + d_{Dir} P_{23} \quad (14)$$

$$P_{23} = d_{Coupler} P_{21} + d_{Dir} P_{14} \quad (15)$$

with $D_{Dir} = 17 \text{ dB}$ and $D_{Coupler} = 30 \text{ dB}$

$$P_{23} = \frac{1}{1000} P_{21} + \frac{1}{50.12} P_{14} \quad (16)$$

$$P_{23} = \frac{1}{1000} P_{21} + \frac{1}{50.12} \left(\frac{1}{1000} P_{12} + \frac{1}{50.12} P_{23} \right)$$

$$P_{23} = \frac{1}{\underbrace{\left(1 - \frac{1}{2512}\right)}_{\approx 1}} \left(\frac{1}{1000} P_{21} + \frac{1}{\underbrace{50120}_{\approx 0}} P_{12} \right)$$

$$P_{14} = \frac{1}{1000} P_{12} + \frac{1}{\underbrace{50.12}_{\approx 0}} \frac{1}{1000} P_{21} \quad (17)$$

$$P_{23} \approx \frac{1}{1000} P_{21}, P_{14} \approx \frac{1}{1000} P_{12} \quad (18)$$

As can be seen from Equation (16) and Equation (17), the reflected power P_{21} must be very small in comparison to the incident power P_{12} to obtain a considerable error. However, to implement the frequency control, the measured values of the reflected power do not need to be exactly determined. It is regarded as sufficient if the measured values can be compared relative to each other. Therefore, a directivity of 17 dB is regarded as sufficient. The error caused by the power coupled from Port 4 to Port 3 can therefore be neglected.

The insertion loss is a measure of the power absorbed by a component in a signal path. Every microwave component and every connector absorbs signal power. The insertion losses of each component are shown in Figure 39. The sum of total insertion losses IL_{total} is given by Equation (19). The maximum output power of the source P_{Source} is 11.2 W (Equation (20)). Taking the losses of the coupler $IL_{coupler}$, the cable IL_{cable} and the rotary joint IL_{joint} into account, the maximum incident power at the oven P_{oven} is 6.6 W (Equation (21)). The reflected power is affected by losses in the cable and in the rotary joint before it reaches the directional coupler. The maximum reflected power at the direction coupler $P_{coupler}$ is 4.2 W (Equation (22)). The loss-induced difference between incident and reflected power has to be taken into account when a measurement of the absolute reflected power is performed.

$$IL_{total} = \sum IL = 2.312 \text{ dB} \quad (19)$$

$$P_{Source} = 11.2 \text{ W} = 40.5 \text{ dBm} \quad (20)$$

$$P_{Oven} = P_{Source} - IL_{Coupler} - IL_{Cable} - IL_{Joint} = 38.19 \text{ dBm} = 6.6 \text{ W} \quad (21)$$

$$P_{Coupler} = P_{Oven} - IL_{Cable} - IL_{Joint} = 36.23 \text{ dBm} = 4.2 \text{ W} \quad (22)$$

For the acquisition of the incident and reflected power, two suitable sensors are required. Pavuluri *et al.* used two Satori ST185SMA USB power meters for a comparable measurement (Pavuluri et al. 2010a). These sensors would, in principle, be applicable in this case, as they are suitable regarding frequency and power range and this type of sensor also directly provides a power value. However, the USB protocol in use has comparatively high latency times, resulting in sample frequencies in the range of 8–50 Hz.

An alternative to USB sensors are Schottky diode detectors. This type of sensor offers wide measurement ranges and requires a low amount of input power. Schottky diode detectors are very compact in comparison to the USB sensors. This type of sensor rectifies the RF signal into a DC signal. The measurement of the DC signal can be realized with an analogue control interface. This set-up provides much higher sampling rates than the USB sensors, which would be a clear advantage for the frequency-tracking algorithm. A drawback is that the signal has to be filtered from noise and amplified for the range of the analogue interface. Furthermore, the processing of the measured value, including calibration, has to be implemented in the control system. Considering the requirements on the quality of the frequency-tracking algorithm, which strongly depends on the sampling rate of the power sensors, Schottky diode sensors were selected.

The Schottky sensors have a frequency range of 2–18 GHz and a maximum input power of 100 mW. Since a maximum incident power of 11.2 mW and frequencies between 8 GHz and 9 GHz are expected, these sensors are appropriate for this application. A 16-bit analogue input interface for the Beckhoff control system with a measurement range of 0-10 V was used for the adaptation. The sensor output signal has a linear characteristic in the range 0-1 V. This signal needs to be amplified to obtain the required resolution. As with the signal amplification, an amplification of noise was also observed, which distorted the measurement. To counter this, two active low-pass filter boards with an amplification of 10 and a cut-off frequency of 4 kHz were built and integrated into the circuit.

6.1.3 Integration of temperature sensor

The open-ended microwave applicator by Sinclair *et al.* was designed for experiments in a laboratory environment (Sinclair 2009). For integration into a precision placement machine, an adapted design is necessary.

Sinclair *et al.* proposed an optimized dielectric insert to be integrated into the open-ended applicator (Sinclair et al. 2008c). This modification results in a field enhancement of up to 9.4 dB (Sinclair et al. 2008c). By analytical and experimental testing, a significant improvement of the heating performance could be demonstrated (Sinclair et al. 2008c). As this modification promised a remarkable productivity gain, it was implemented in the oven design.

According to Sinclair's proposal, the applicator is square-shaped with a cross-section of $18 \times 18 \text{ mm}^2$. The majority of the applicator is filled with a low-loss dielectric material. PTFE was chosen as the 'bulk' material since it has a low dielectric constant ($\epsilon_b = 2.1$)

and a low loss tangent ($\tan \delta = 10^{-4}$). In order to achieve the desired field enhancement, an intermediate layer with a higher dielectric constant is required. A ceramic with a dielectric constant $\epsilon_c = 6$ and a thickness of 3.5 mm was applied, following the findings of Sinclair *et al.* (Sinclair et al. 2008c) and Pavuluri *et al.* (Pavuluri et al. 2010b).

The need for temperature feedback was pointed out in Section 5.3.2. The subsequent assessment of different temperature sensors identified a pyrometer as a sensor that was, in principle, suitable. The pyrometer is going to be integrated into the applicator and placed on the moving part of the machine. The selected pyrometer has a sensor head that is separate from the control unit and can be fitted with a focussing lens. The temperature sensor has a measurement range from $-40\text{ }^{\circ}\text{C}$ to $600\text{ }^{\circ}\text{C}$. The measurement frequency is 50 Hz and the measurement accuracy is $\pm 1\text{ }^{\circ}\text{C}$ or $\pm 1\%$ (whichever is larger). Exact specifications can be retrieved from the manufacturer's data sheet (Sensortherm 2013).

Changes to the design were kept minimal in order not to affect the function of the applicator by the integration of the temperature sensor; negative effects on the sensor performance were possible. Figure 40 shows three concepts for the integration of the pyrometer.

In the first concept (Variant A), the pyrometer is integrated on top of the applicator. The angle is nearly ideal for measurements. However, a significant portion of the bulk dielectric material and the optimized dielectric insert has to be removed, which strongly influences the heating characteristics. The second concept (Variant B) integrates the pyrometer at an angle of 45° . This angle is not ideal, but still allows the measuring of the temperature during curing. In this case, small portions of the bulk dielectric and the optimized dielectric insert have to be removed. In the third concept (Variant C), the pyrometer observes the product from the bottom. The observation angle is ideal. The oven does not need to be adapted in this case. However, the temperature measurement is not a part of the oven itself in this case, which impairs its flexibility. Furthermore, the temperature of the substrate is measured primarily and not the temperature of the heated polymer. The measurement would therefore be highly inaccurate and most likely not be suitable for closed-loop control.

With respect to the requirement of closed-loop control of the temperature, the second concept (Variant B) with the pyrometer and a 45° angle is selected for further consideration.

As the oven is carried on the precision placement system as a tool, its mass affects the dynamics and possibly the precision of the machine. The mass of the oven should

therefore be minimal. Instead of copper, aluminium was used as the wall material, resulting in a total mass of the applicator (without temperature sensor) of 170 g.

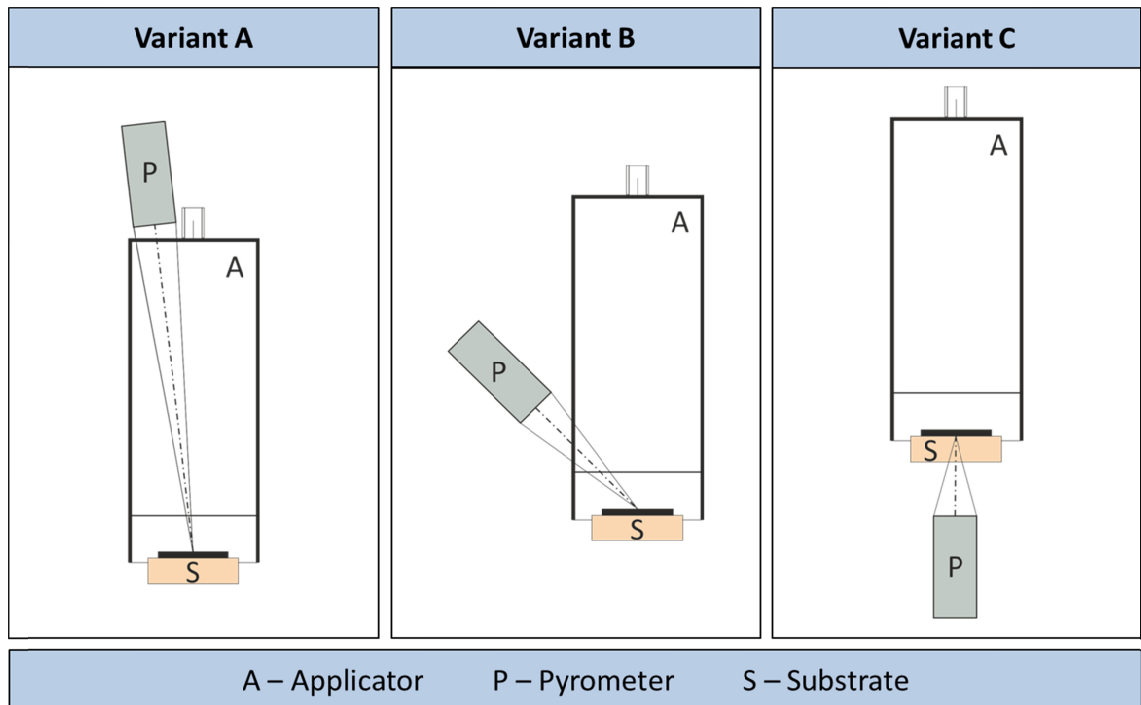


Figure 40 – Concepts for pyrometer integration

From the mechanical point of view, the prototype oven was still too heavy to be mounted onto the tool plate. The wall thicknesses were reduced to 5 mm, tapering down to 1.5 mm in the load area. The pyrometer is attached at an angle of 45°, as previously discussed. Small portions of wall material, bulk dielectric and optimized dielectric insert have been removed, as depicted in Figure 42. Due to the angle of observation, the projected measuring area is elliptic.

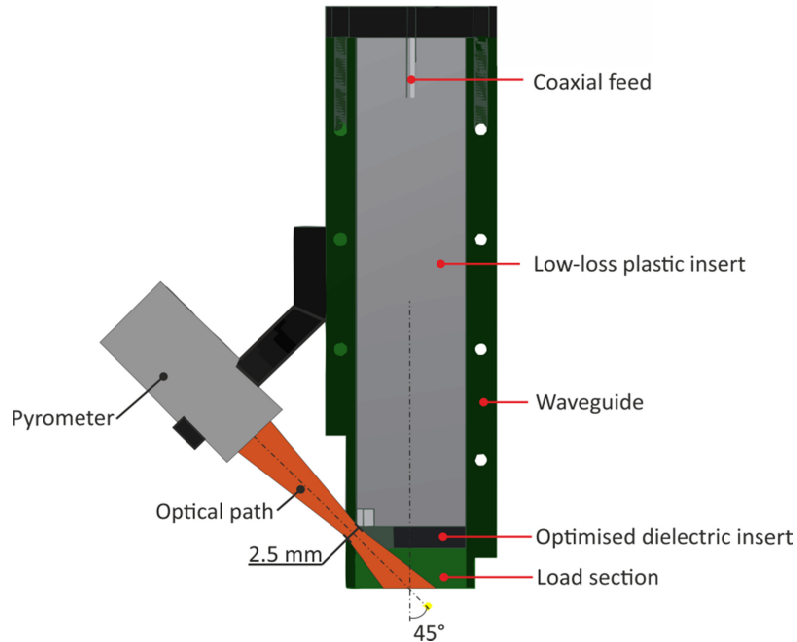


Figure 41 – Open-ended microwave applicator with integrated pyrometer

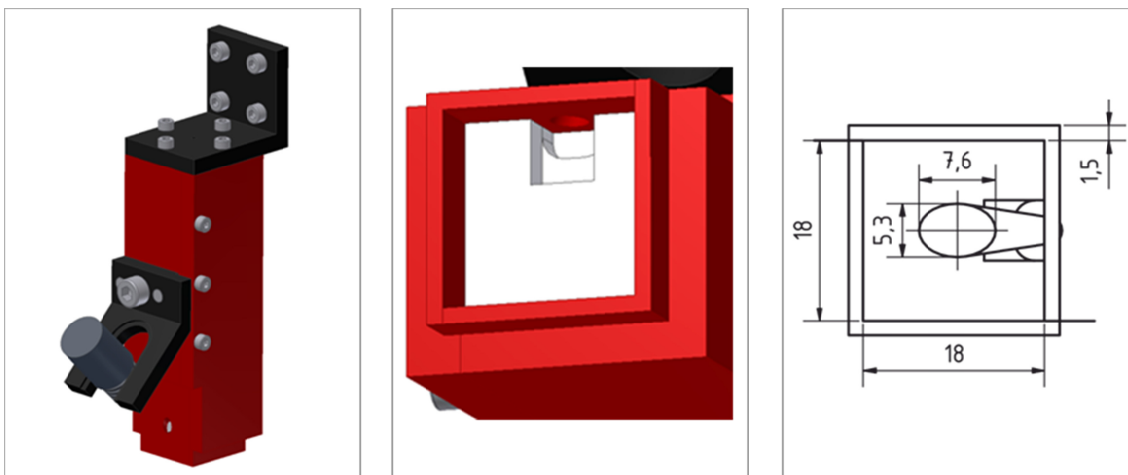


Figure 42 – Design of modified open-ended microwave applicator

To test the temperature measurement, a reference measurement was performed. As reference sensor, a Pt₁₀₀ thermocouple was put into a portion of EO1080 encapsulant. The modified microwave applicator with pyrometer was placed centrally over the encapsulant. The portion of encapsulant was heated stepwise up to 160 °C using a hot plate. The temperature was held at each level for at least one minute. Five

measurements were performed at each temperature level with both the Pt₁₀₀ and the pyrometer. Figure 43 shows the relative measured values between the pyrometer and the Pt₁₀₀ values (red plot – ‘Pyrometer Measurement’).

An ideal transfer function is shown as the green plot. According to this transfer function the values of the pyrometer would ideally correspond to the thermocouple values. However, the measured values cannot be simply corrected with a multiplying factor or an offset as the transfer function, shown as the red curve, has a strong curvature. Therefore, a correction function was applied to adjust the measured values.

$$T_{C,1} = \alpha \cdot T_{pyro}^{\gamma} + \beta \quad (23)$$

The function $T_{C,1}$ combines three typically applied correction parameters. The curvature is adjusted by the γ factor, the slope by the α factor and the offset by the β factor as can be seen in Equation (23). A correction with these three factors is sufficient in most cases. The median deviation after fitting the function was found to be 0.43 °C.

To further reduce the error, a second method for correcting the measured values was considered. The differences between the ideal transfer function and the measured values were determined. Different functions were fitted using a least square estimate to the difference values. It was found that a fitting with a seventh-order polynomial function produced no significant error (median deviation $9.4 \cdot 10^{-4}$ °C) and was therefore regarded as a suitable correction function. A plot of the difference function is shown in Figure 43. The measured temperature values can now be adjusted by adding the value of the difference function, as indicated in Equation (24).

$$T_{C,2} = T_{pyro} + f(T_{pyro}) \quad (24)$$

Both ways of compensation are applicable and both have advantages and drawbacks. While an adjustment according to Equation (23) allows better manual tweaking of the temperature values without the need for many values, it is relatively imprecise. However, it is still far better than the initial values. An adjustment according to Equation (24) is far more elaborate and requires a set of experimental values. However, the quality of the compensation is very good. This compensation method is appropriate where precision is needed and for series processes, especially when a precise temperature control is required. Numerous correction functions for different materials and surfaces may be stored within the control software, which would ease the set-up process of the temperature correction in the future.

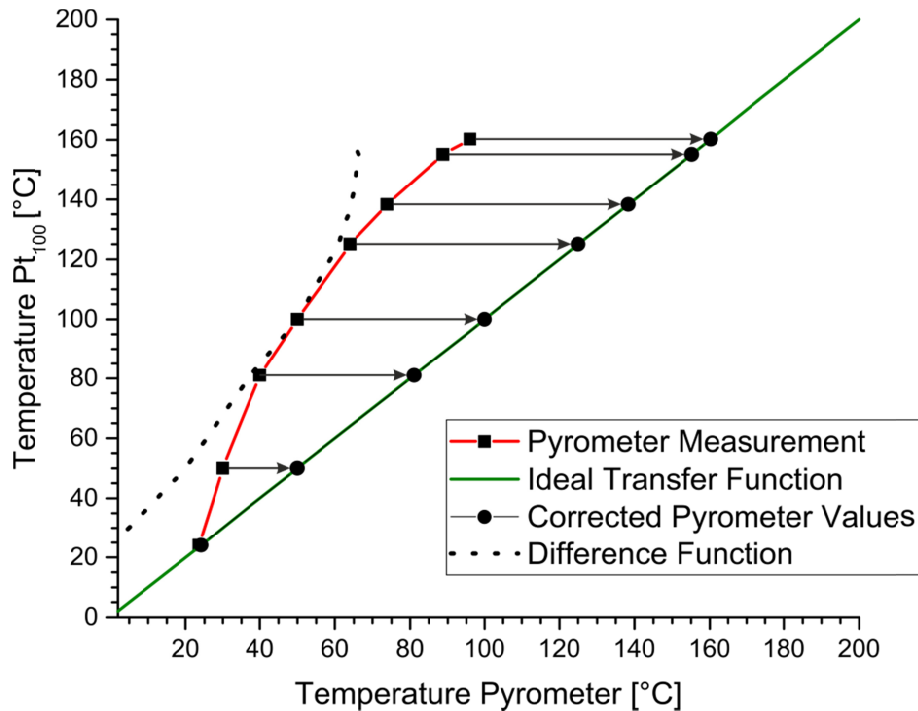


Figure 43 – Correction of pyrometer-measured temperature values

6.1.4 Control software

A real-time control software program for the microwave curing system has been written using Beckhoff TwinCat 2.11. One function of the software is the link between the hardware interfaces and the software component. The workflow of the programme can be programmed with programming languages compatible with IEC 61131. The basic structure of the control program is based on a state machine as shown in Figure 44.

When the program is started, the ‘PreInit’ state will be called, which waits for a trigger to start the program. Within the ‘Init’ state, the RF power sensors, the temperature sensor and the microwave source are initialized and the process parameters for the curing process are set. When the initialization process is complete, the program waits in the ‘Idle’ state for an external trigger to start the actual process. When the process is finished, the program jumps back to the ‘Init’ state. If an error occurs within the ‘Init’, ‘Idle’ or ‘Busy’ states, the program jumps into the fault mode. Once the error is handled, the program is reset to the ‘Init’ state.

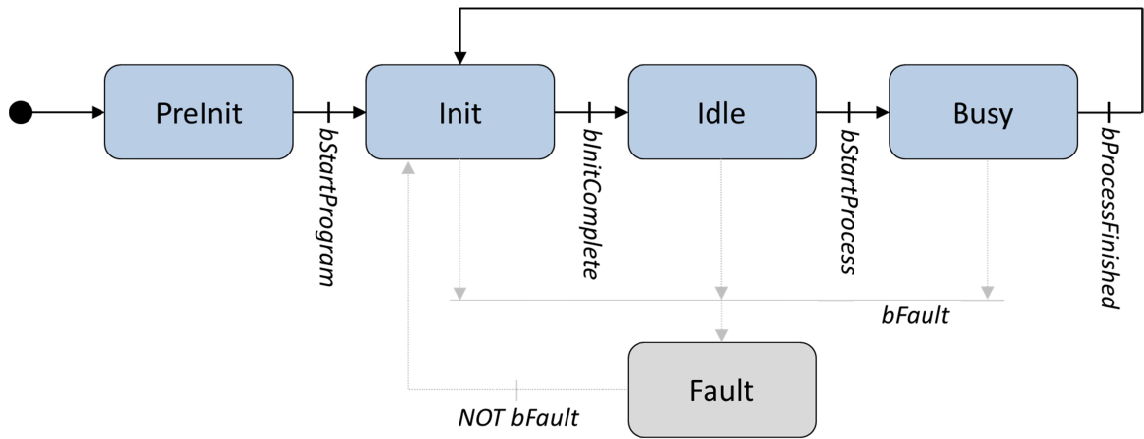


Figure 44 – PLC program state machine

The set-up of the parameters for the different control functions is performed according to a defined structure. It can be regarded as a ‘form’ for a certain cure profile. An overview of this structure is shown in Figure 45. Within the initialization phase, the parameters for temperature control, frequency control, the frequency tuning algorithm and the temperature measurement are set. If all parameters are not set within a given time frame, then the program will jump into the ‘Fault’ state. During the curing process, when the program is in the ‘Busy’ state, the temperature and frequency settings are transmitted, together with a timestamp, according to the current curing profile.

Cure Profile (STRUCT)		
Temperature Control - Control Algorithm {2-Point, PID} - 2-Point Control Parameters - PID-Control Parameters - Maximum Duty Cycle Init	Frequency Control - Frequency Control Mode {Constant, Hopping, VFM} - Frequency Cycle Time Init	Frequency Tuning - Frequency AutoTuning {On / Off} - Cycle Time - Frequency Band - Tuning Step Init
Temperature Measurement - Correction Function { $T_{c,1}$, $T_{c,2}$ } - Correction Function Parameters Init	Set Temperature Profile (Buffer) - Set Temperature over Time [ARRAY] Busy	Set Frequency Profile (Buffer) - Set Frequency over Time [ARRAY] Busy

Figure 45 – Cure profile structure

During the curing process, two main control functions are executed: frequency and temperature control. Furthermore, function blocks for the acquisition of RF power, temperature and the elapsed process time provide input data to the two control function blocks. The signals for the PWM and RF are set by two further function blocks. An overview of the program structure is shown in Figure 46. The structure has been slightly

simplified to make the basic mechanisms clearer; most superordinate start and stop variables are not shown.

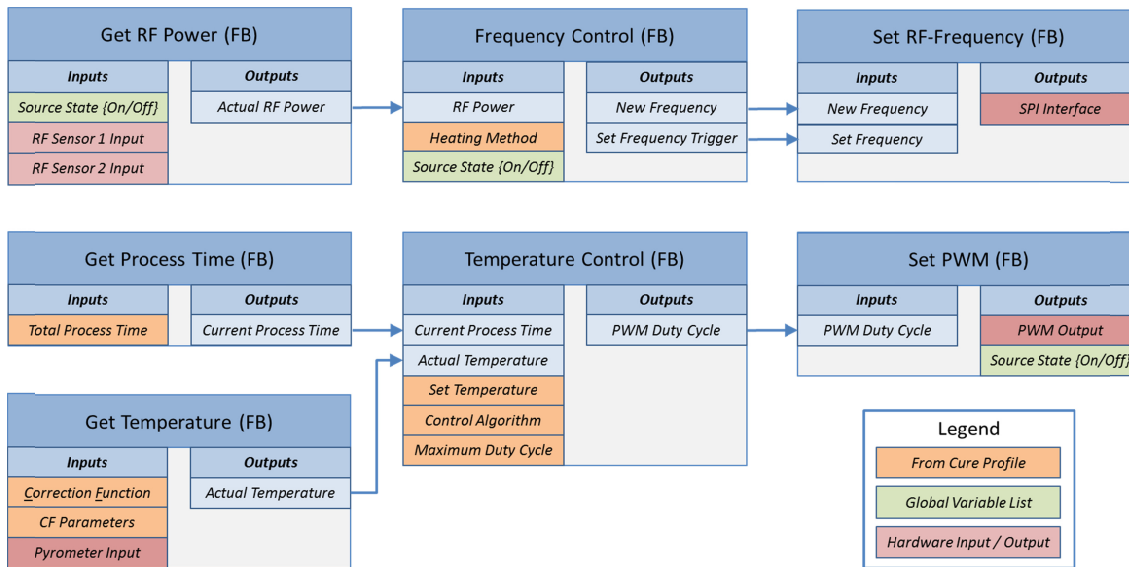


Figure 46 – Curing process program structure

With the ‘Get RF Power’ function block, the sensor values for both RF sensors are acquired if the source is switched on. Based on these sensor values, the actual RF power is calculated and provided to the ‘Frequency Control’ function.

The ‘Frequency Control’ function block implements the frequency control modes ‘Constant Frequency’, ‘Frequency Hopping’ and ‘Variable Frequency Microwave’. Additionally, the frequency tuning algorithm is implemented. The heating method and the frequency tuning parameters are set from the ‘Cure Profile’ structure. If the source is switched on, then the frequency is controlled according to the set frequency control algorithms. If a frequency change is necessary, then the new frequency is transferred to the ‘Set RF-Frequency’ function block.

The ‘Set RF-Frequency’ function block receives a set frequency and a trigger from the ‘Frequency Control’ function block. If the trigger is set, then the new frequency is transmitted to the solid-state source using the serial peripheral interface (SPI).

In the ‘Get Process Time’ function block, a timer is implemented that provides the current process time to the ‘Temperature Control’ function block.

Based on the sensor values received from the pyrometer and the correction function parameters from the ‘Cure Profile’ structure, the ‘Get Temperature’ function block provides the value of the actual temperature.

Current process time and current temperature are processed by the 'Temperature Control' function block. The 'Cure Profile' structure provides the parameters regarding maximum duty cycle and the control algorithm. The temperature set points are continuously provided from an external source and are buffered within an array. Actual and set temperatures are compared, and a PWM duty cycle is set as the output variable.

This PWM duty cycle is the input variable for the 'Set PWM' function block. The duty cycle value is converted into a compatible value for the PWM interface. The 'Source State' variable is set in the program's global variable list, according to the set duty cycle, which is either equal to zero or one, to indicate if the source is switched on or not.

6.1.5 Human machine interface

The aim of the human machine interface (HMI) is to provide the system user with the capability to set the parameters of a cure profile, to start and stop curing processes and to visualize important factors during processing. Therefore, the HMI is, in this particular case, an intermediate layer between the user and the programmable logic controller (PLC).

Numerous components are necessary to implement the HMI. The HMI needs to communicate with the PLC to send control commands and to receive status and process information. The user sets up cure profiles, may manually start and stop the curing process and needs to view the status of a running process. Functionality to save and load cure profiles and process data is also required. Components for PLC communication, user interaction and cure profile and data management are needed.

Based on the functional requirements, an initial class diagram of the HMI was designed, as shown in Figure 47. The main class is the 'Graphical User Interface'. It instantiates the 'PLCBase' class, a concrete class based on the abstract PLC class. From the 'PLCBase' class an arbitrary number of communication classes can be instantiated. The 'CureProfileList' class compiles the available cure profile data. These class relationships describe the relations between the three functional elements of graphical user interface, PLC communications and data management.

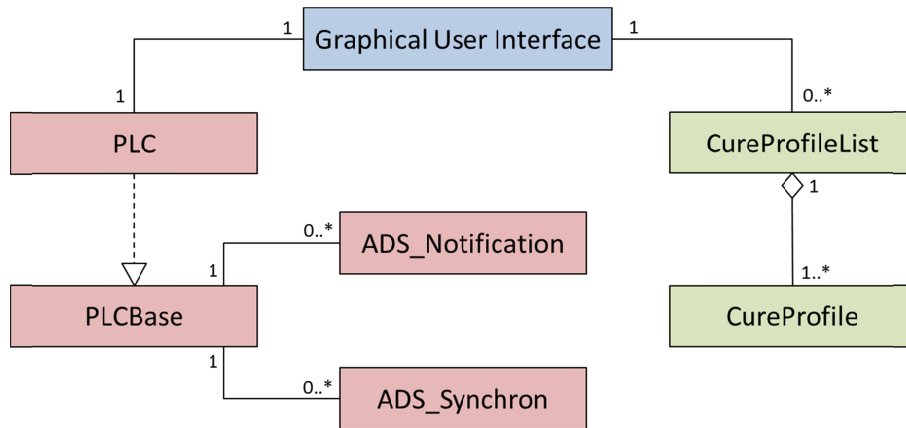


Figure 47 – HMI class diagram

Based on the defined relationships, an information flow was designed. A diagram illustrating the information flow is presented in Figure 48. The user interacts directly with the graphical user interface. The user sets the cure profile parameters, starts and stops the process and receives feedback about the process status. Process data can be saved to a hard disk. Management of the cure profile data is performed by the ‘CureProfileList’ class. One cure profile management function is saving and loading cure profile data to or from the hard disk. The ‘PLCBase’ class performs the management of the communication with the PLC. When the value of a variable in the PLC changes, a notification is sent to PLC interface the using the ADS protocol. Control variables are written in the PLC by the ADS synchronous access. Based on the design of the information flow, an implementation of the GUI can be created.

An example implementation of the workflow was performed with C# as a Windows Forms application. The ADS interface was integrated using the .NET interface provided by Beckhoff.

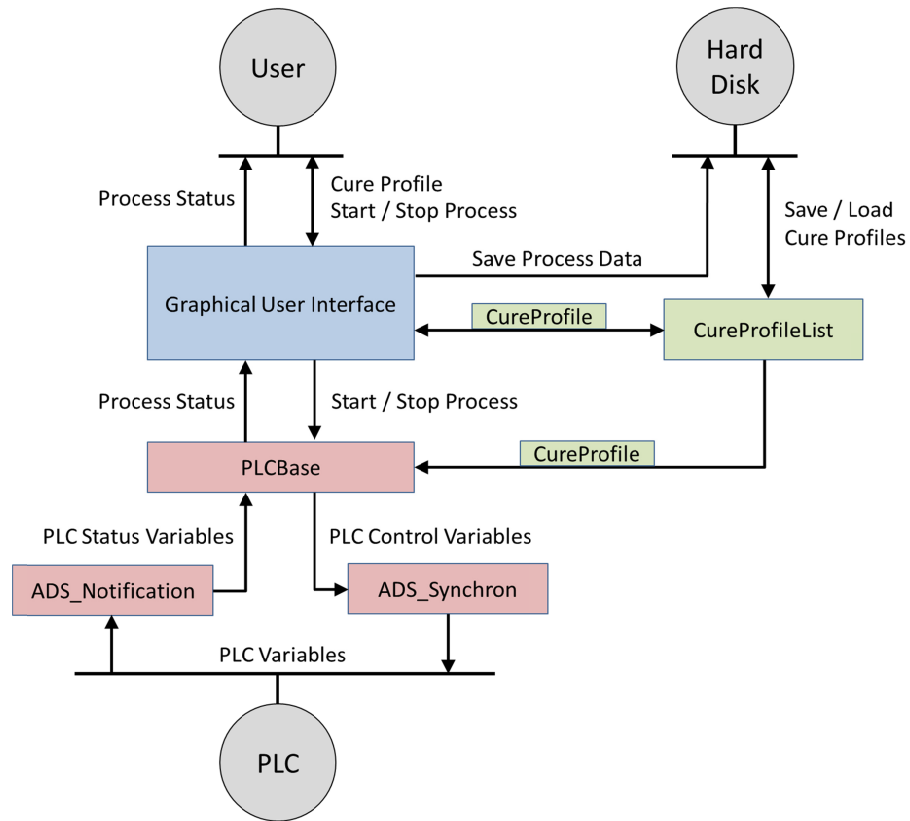


Figure 48 – HMI information flow

A screenshot of the GUI is shown in Figure 49. The application is structured into a configuration tab for the set-up of the process and a control tab for the visualization of the process. The cure profile management allows the management of cure profiles and implements the ‘CureProfileList’. The parameters for the cure profiles are set in the area to the right of the list. Temperature profiles with an arbitrary number of supporting points can be defined. Both the $T_{c,1}$ and the $T_{c,2}$ temperature correction functions can be chosen and parametrized by the frequency control tab as shown in Figure 50. Three available frequency control modes can be parametrized accordingly. The frequency tuning algorithm can be optionally selected and set up. Not depicted is the selection of the temperature control algorithm. The user may choose between the two-point control algorithm and the PID controller.

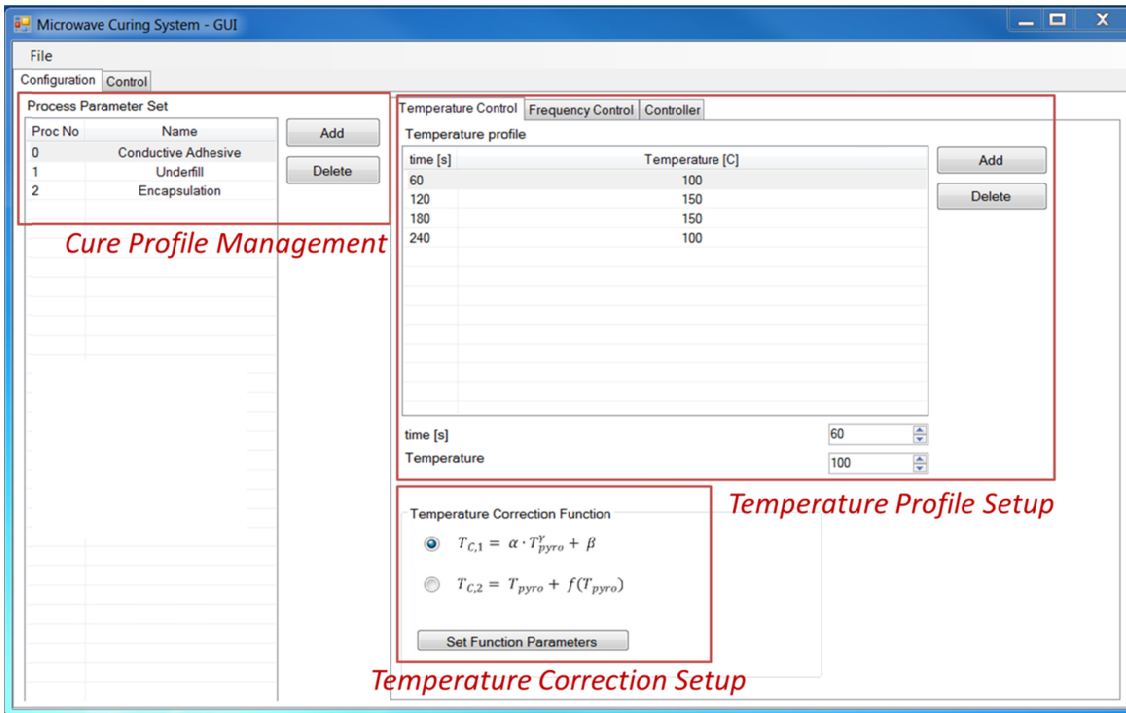


Figure 49 – Cure profile management and temperature control set-up

The user may start or stop the process from the ‘Control’ tab. A screenshot is shown in Figure 51. One graph visualizes the temperature control by plotting set and actual temperature. The other graph shows the set frequency and the RF power to display the function of the frequency control algorithms.

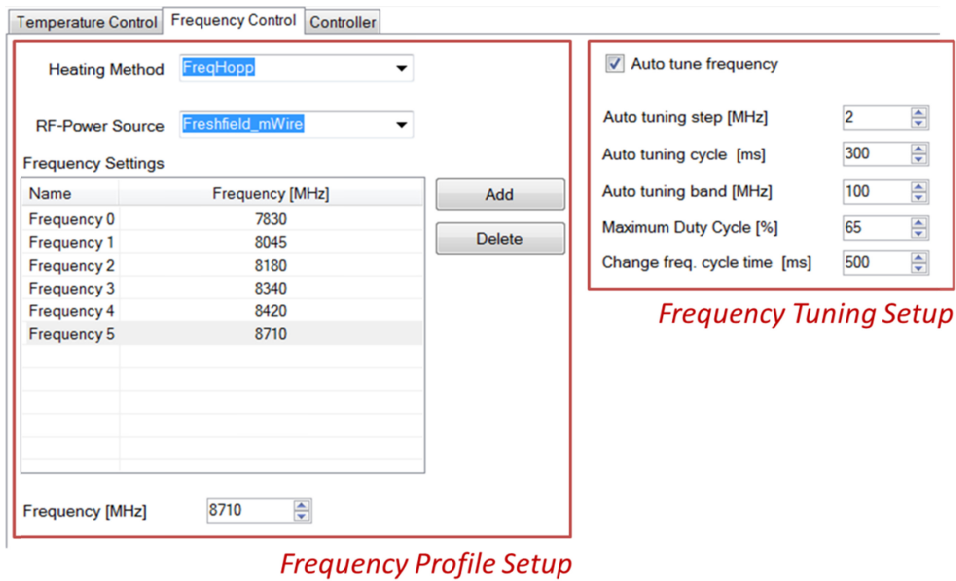


Figure 50 – Frequency set-up

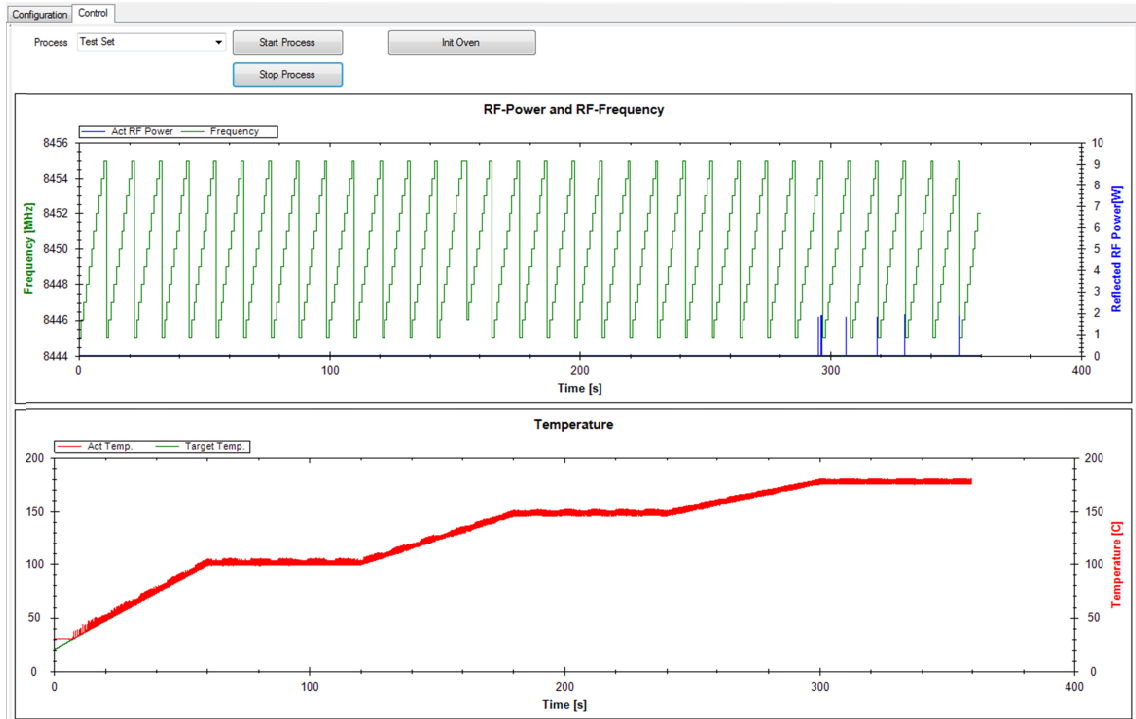


Figure 51 – Visualization of the curing process

6.1.6 Integrated microwave system set-up

With all components selected and available, the curing system can be integrated. An overview of the system is shown in Figure 52.

The system is controlled by an industrial personal computer. The user sets up and controls the process by the graphical user interface (Chapter 6.1.5). The PLC program controls the actual process as described in Chapter 6.1.4. It runs on a real-time kernel extension of the operating system.

The numerous interfaces for the different hardware components are provided by IO terminals. These are connected to the IPC with the EtherCAT field bus. The solid-state microwave source frequency is set by the SPI interface and the enabled PWM signal, as described in Chapter 6.1.1. The source provides an RF signal, which is fed to the directional coupler. The vast majority of the RF power is fed to the open-ended oven, while small amounts of incident and reflected power are directed to RF power sensors. The power feedback is required for a feedback of system efficiency and for the frequency tuning algorithm.

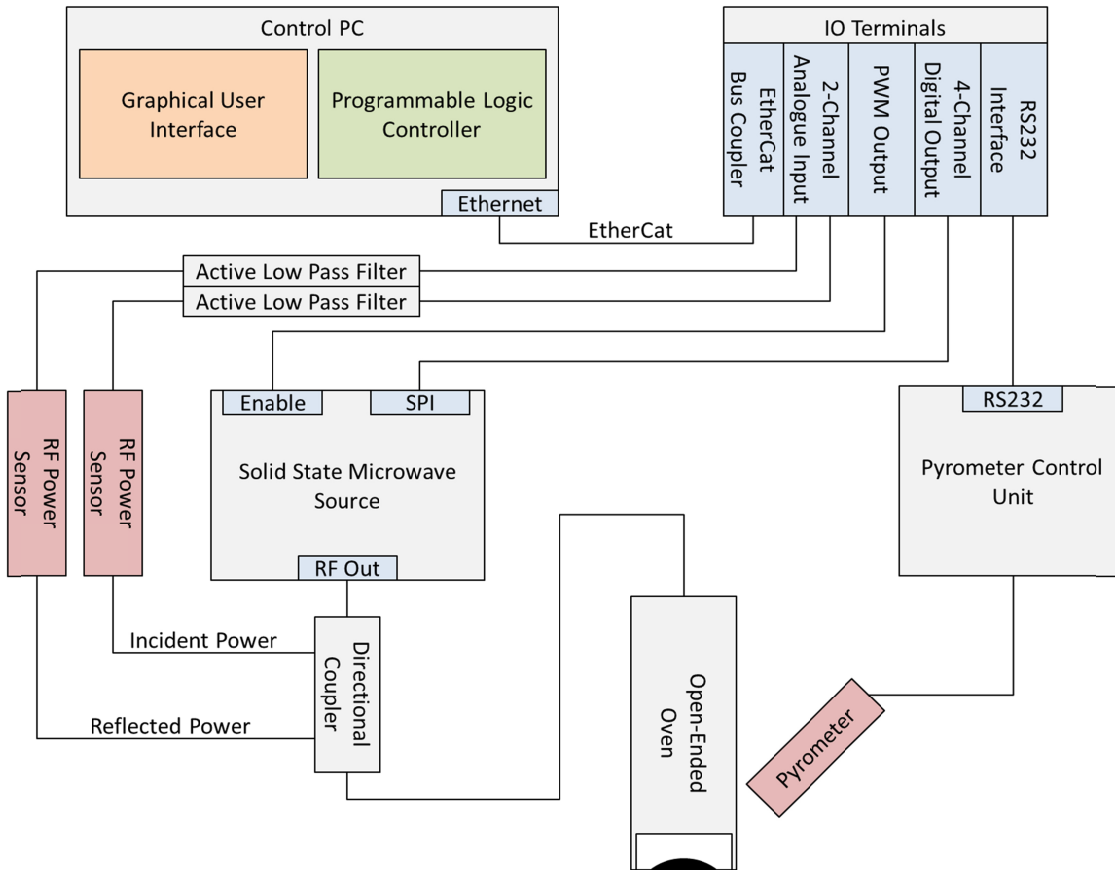


Figure 52 – Curing system overview

Temperature feedback is provided by a pyrometer, which is integrated into the open-ended microwave applicator, as described in Chapter 6.1.3. The pyrometer head is connected to a control unit, which is linked to the control system via a RS232 interface.

6.2 Design of process components

6.2.1 Dispensing system

Time–pressure dispensing has been selected for the dispensing of the three adhesive materials. The design of the time–pressure dispenser is presented in Figure 53.

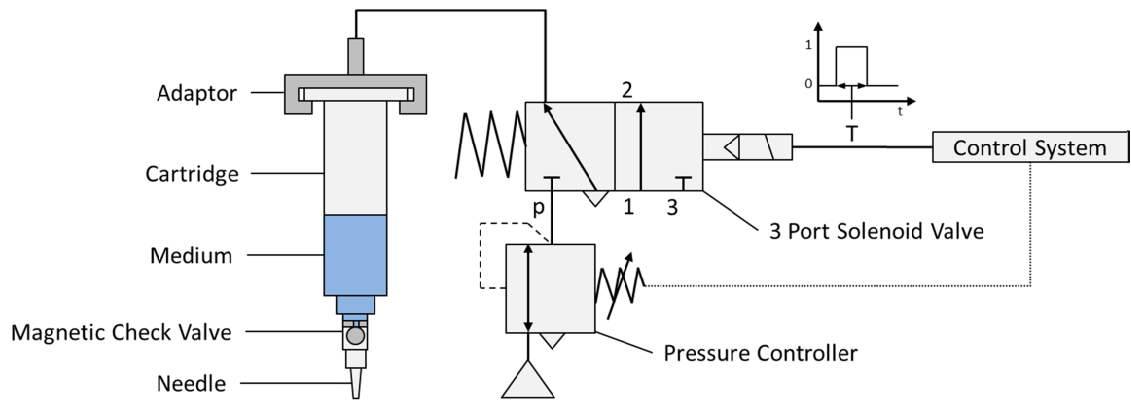


Figure 53 – Time–pressure dispensing system design

In this particular case, the control system sets the pressure on an electronic pressure controller. The dispense signal is a square-formed pulse with the time constant T and is used to switch a fast-acting 3-port solenoid valve ($T_{Switch} < 10$ ms). The pressure in the cartridge then builds up rapidly and displaces the medium through the needle onto the substrate. Unwanted dripping is prevented by a magnetic check valve between the needle and the cartridge.

6.2.2 Gripping system

The picking up and placement of the parts is performed with a vacuum gripper unit by Sysmelec. According to the machine concept, the gripper must also provide a rotational axis. The design principle of the gripping system is shown in Figure 54.

A hollow shaft is driven by a DC motor. The necessary transformation is achieved by a planetary gear. Position feedback is provided by an optical encoder. DC motor, gear and encoder are provided as an integrated unit by Faulhaber. On one end of the hollow shaft, vacuum or pressure impulses are applied, which are transported to the vacuum gripper on the bottom side of the tool. The gripper tool itself is elastically supported. The gripper tip is exchangeable; therefore, depending on the part to be handled, a matching gripper tip can be used.

The control system is connected to the motor drive via a field bus. The motor drive integrates the closed-loop control of the motor–encoder–drive system and provides a control signal to the motor.

Either vacuum or pressure impulses can be applied to the gripper by a fast-acting pneumatic solenoid valve as depicted in Figure 54. The valve is controlled by the control system using digital IO.

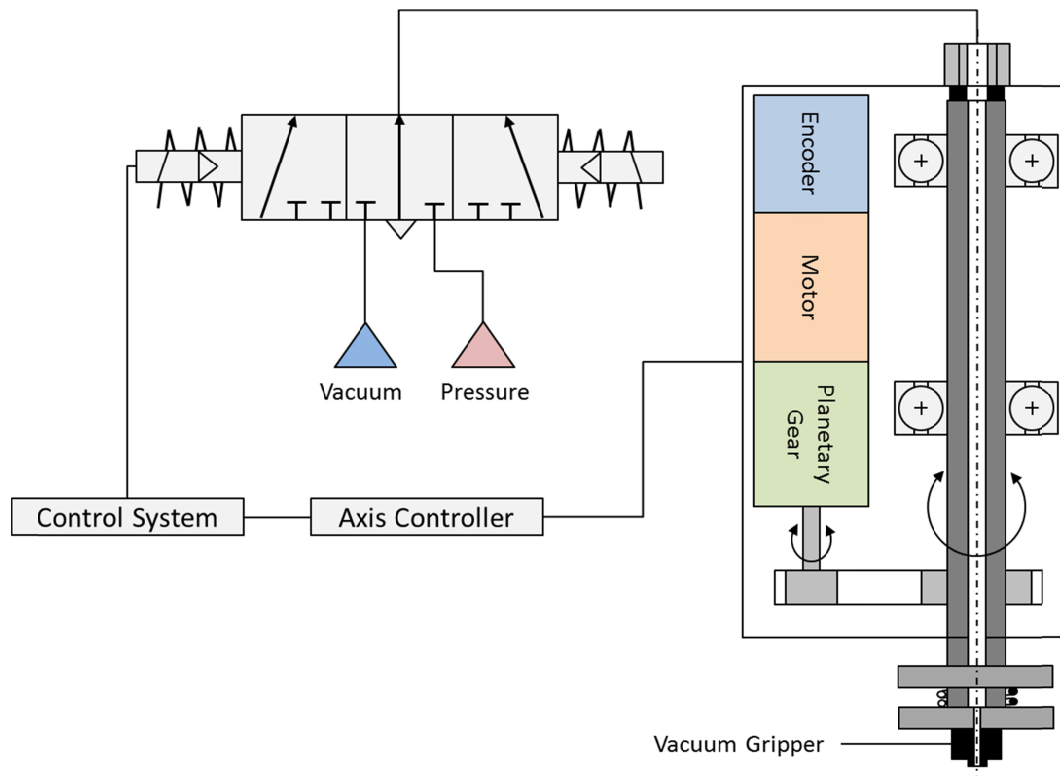


Figure 54 – Gripper system design

6.2.3 Vision system

According to the machine concept, measurement tasks are performed by a vision system with two cameras. Such a vision system has been designed; an overview is shown in Figure 55.

Cameras with a resolution of 1600×1200 pixels and a 1/1.8" CMOS chip have been selected (AVT Manta G-201). Both cameras are combined with a telecentric lens, which provides a magnification of 2 (Vision & Control T45/2.01). A white LED on-axis lighting system with a semi-transparent mirror is used for the feature camera, while the object camera provides lighting with a white LED ring. Both camera configurations have a focal distance $f = 70$ mm. The resulting field of view is 3.55×2.7 mm² for both cameras. This corresponds to 2.2×2.2 μm²/pixel.

The cameras are connected to the control PC via the GigE Vision interface. The vision software acquires and processes the image. Calibration parameters are stored in the program. The measurement result is then passed to the central machine control software using TCP/IP.

The two lighting devices are open-loop controlled by the central control software. Two analogue outputs provide a voltage between 0 V and 10 V. The signal is fed to a lighting driver circuit, which feeds a controlled supply current to the lighting devices.

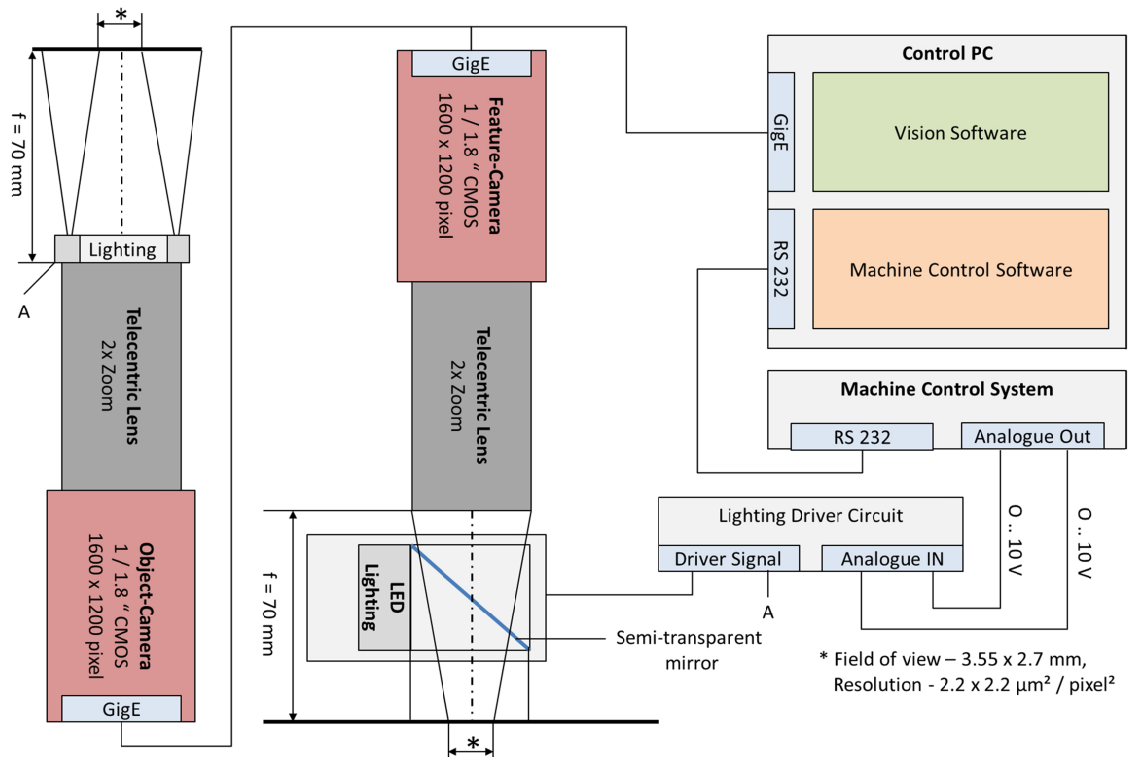


Figure 55 – Vision system design

6.2.4 Distance measurement sensor

A displacement sensor based on the laser triangulation principle was selected (Keyence LK-H052 with LK-5001P control unit). The integration of the sensor is performed as presented in Figure 56.

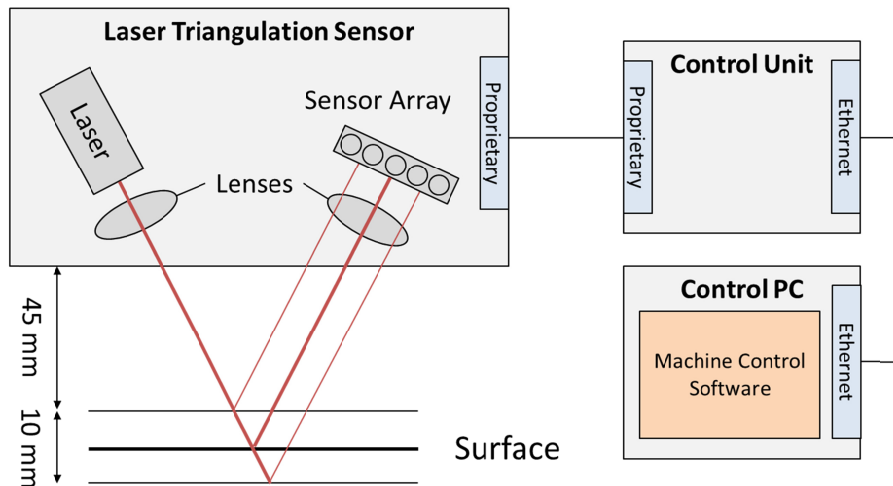


Figure 56 – Displacement sensor

The main components of the triangulation sensor are a solid-state laser and a sensor array. The laser beam is focussed by a lens and projected onto a surface, from which the beam is reflected. The reflected beam is again focussed by a lens and projected on to a linear sensor array. The distance to the surface can be determined from the position of the laser beam on the sensor array. According to the manufacturer, the sensor has a repeatability of 0.025 μm and an accuracy of 1 μm .

The laser triangulation sensor is connected to a control unit via a proprietary interface. The control unit controls the sensor and performs data acquisition, buffering and processing in addition to providing an Ethernet interface. The machine control software on the control PC communicates with the control unit via the Ethernet interface.

6.2.5 Workpiece holder

The assembly process requires that the magazines and the parts are supplied from defined poses. A defined process position is necessary. A construction with receptacles for chip and package magazines has been designed, as shown in Figure 57.

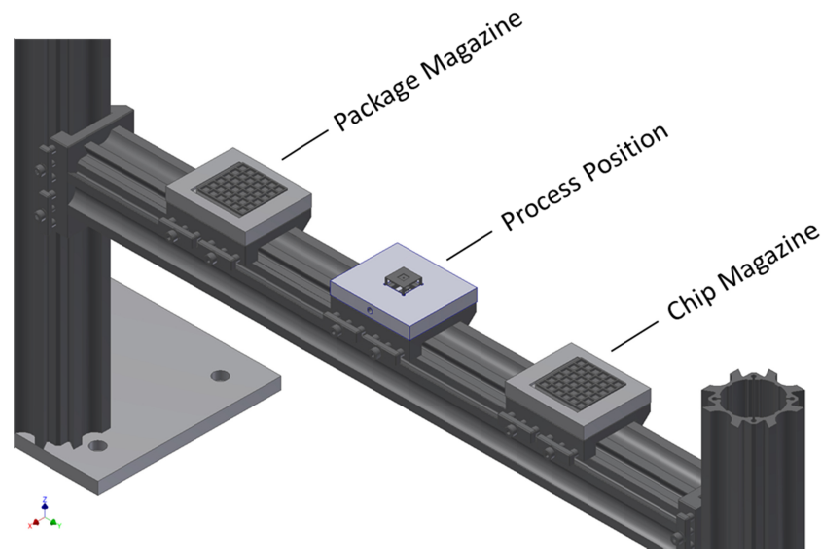


Figure 57 – Package and chip magazines and process position

Packages and chips are supplied in the form of waffle pack magazines. These are inserted into receptacles. On the process position, a customized fixture can be inserted into a receptacle. The parts are held in their position by vacuum.

6.3 Surface-mount assembly machine with integrated microwave curing system

6.3.1 Mechanical design

Based on the concept presented in Section 5.5, a pilot machine has been designed. The machine is based on a commercially available three-axis pick-and-place machine by Sysmelec. The base machine has a positioning repeatability of $\pm 2 \mu\text{m}$ per axis. According to the manufacturer, the system is capable of achieving positioning accuracies of less than $\pm 5 \mu\text{m}$, as demanded in Chapter 4. The system has an effective working space of $660 \times 200 \times 200 \text{ mm}$. An overview of the machine is shown in Figure 58. The solid-state microwave source is placed on the top of the long vertical axis, enabling the load of the source to be driven by one axis and not by all the axes.

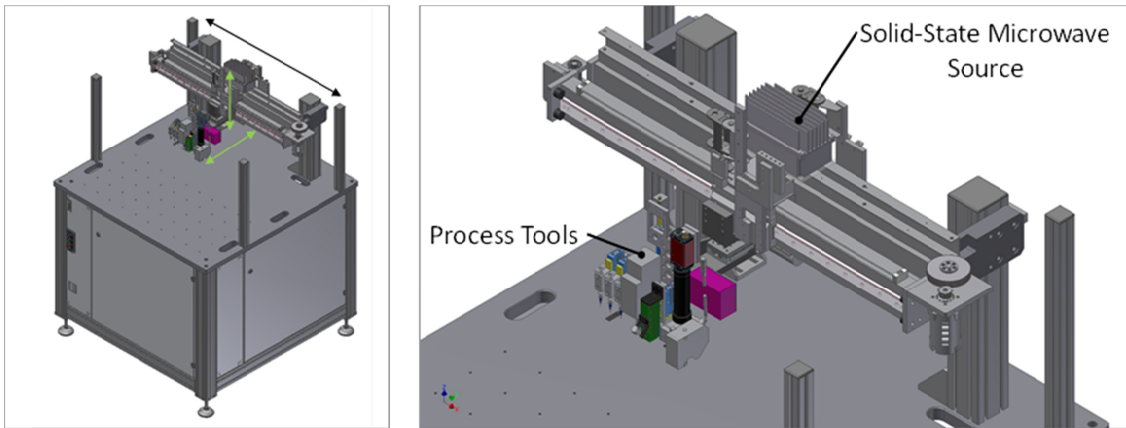


Figure 58 – Machine design overview

The process tools are mounted on a plate, which is connected to the vertical axis. The tools are shown in Figure 59.

Three time–pressure dispensers are mounted on precision-guided pneumatic linear slides. For dispensing with a particular dispenser, it is moved down to the working plane and can be moved up again when the dispenser is no longer needed.

A controlled rotatable axis with a vacuum gripper provides the gripping functionality. The axis is driven by a DC motor, which is connected to a planetary gear. The orientation is determined by an encoder with 512 steps per revolution.

The microwave applicator with temperature sensor is also mounted on a precision-guided pneumatic linear slide. The microwave signal is provided by a low-loss microwave cable, between the oven and the solid-state microwave source.

Additionally, the camera, with on-axis lighting and a distance sensor, is mounted on the tool plate.

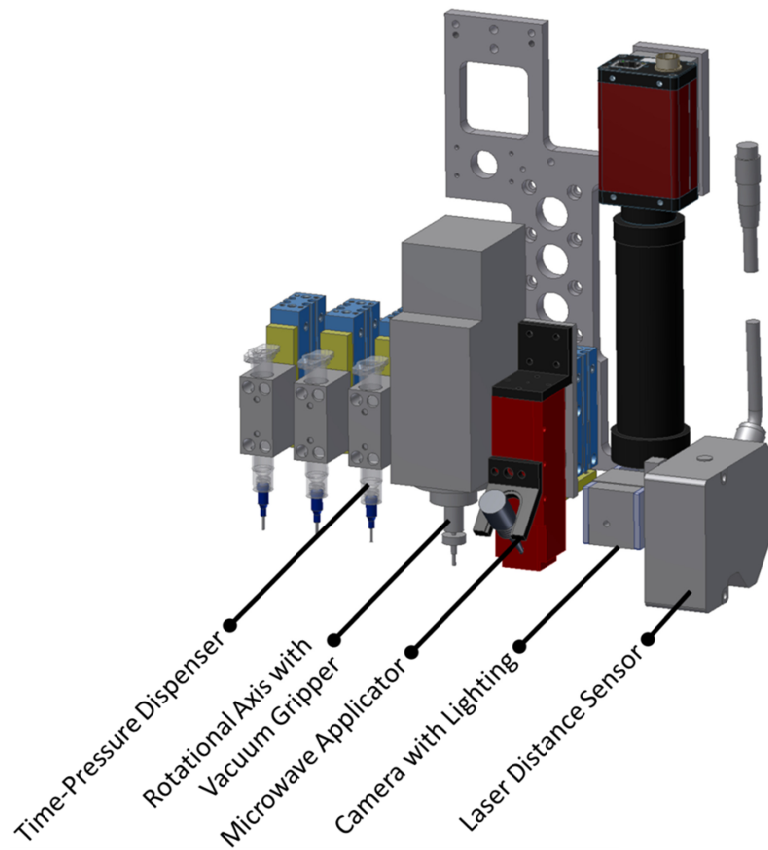


Figure 59 – CAD model of the process tools

6.3.2 Chip fixture

To process single chip packages, a fixture is required that needs to be suitable for the assembly and the microwave curing processes. A fixture has been designed as shown in Figure 60.

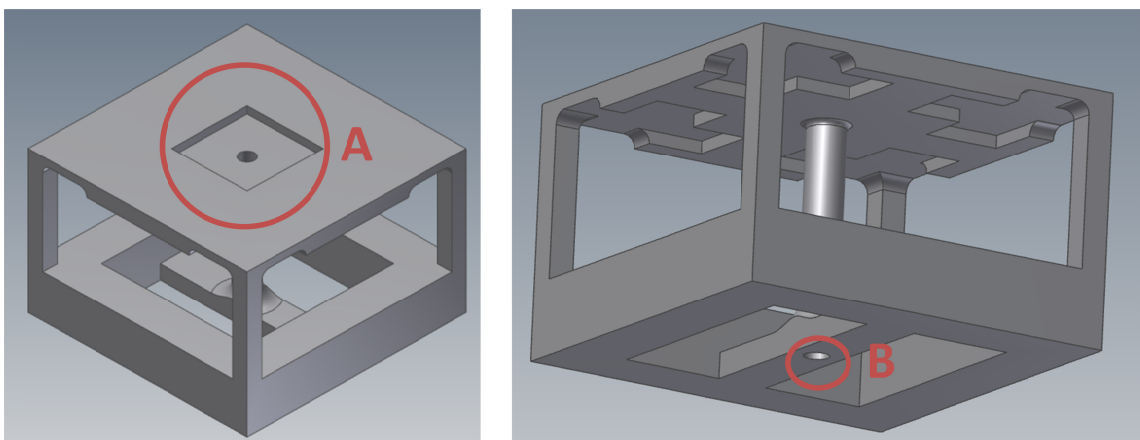


Figure 60 – CAD model of fixture for single chip

The fixture has a pocket for a microchip package on top, as indicated by ‘A’. The chip is held in position by vacuum suction in the centre of the pocket. An external vacuum supply is provided on the bottom of the fixture, as indicated by ‘B’.

One design criterion was minimization of mass. When the fixture is covered by the microwave applicator, the mass inside the applicator should be minimal in order to prevent energy loss. A design with reduced mass is proposed. Furthermore, a material with a low loss tangent is advised. A low loss, organic material is advantageous.

A prototype of the fixture for a $5 \times 5 \text{ mm}^2$ chip has been produced with polymer jetting from an ABS-type material ($\epsilon_b = 2.5$, $\tan \delta = 10^{-2}$) and is presented in Figure 61. The design can be easily altered to different geometries and then be produced by rapid prototyping techniques.

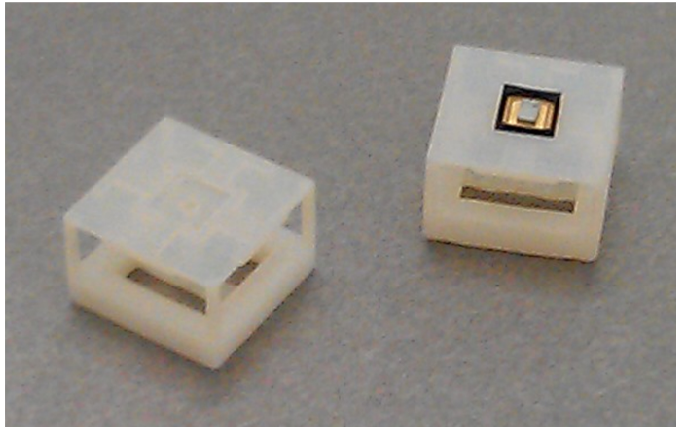


Figure 61 – 3D-printed fixture for a single chip

6.4 Control system for integrated machine

6.4.1 Control system architecture

The design of the process components has been described in the previous sections. Control of these components is necessary to realize the flip-chip process as explained in Section 5.5.9. A control system architecture for the machine and the process components for the prototype system is proposed. An overview of the control system architecture is presented in Figure 62.

Superordinate control of the process sequence is performed by the machine control GUI. The user sets up the parameters of the process and the process components and can start and stop assembly processes in the GUI. The software is programmed in C#.

The two cameras are controlled using dedicated machine vision software. In this case, National Instruments Labview Vision Assistant has been used to develop the machine vision application. The software is interfaced with the machine control GUI using a TCP/IP interface.

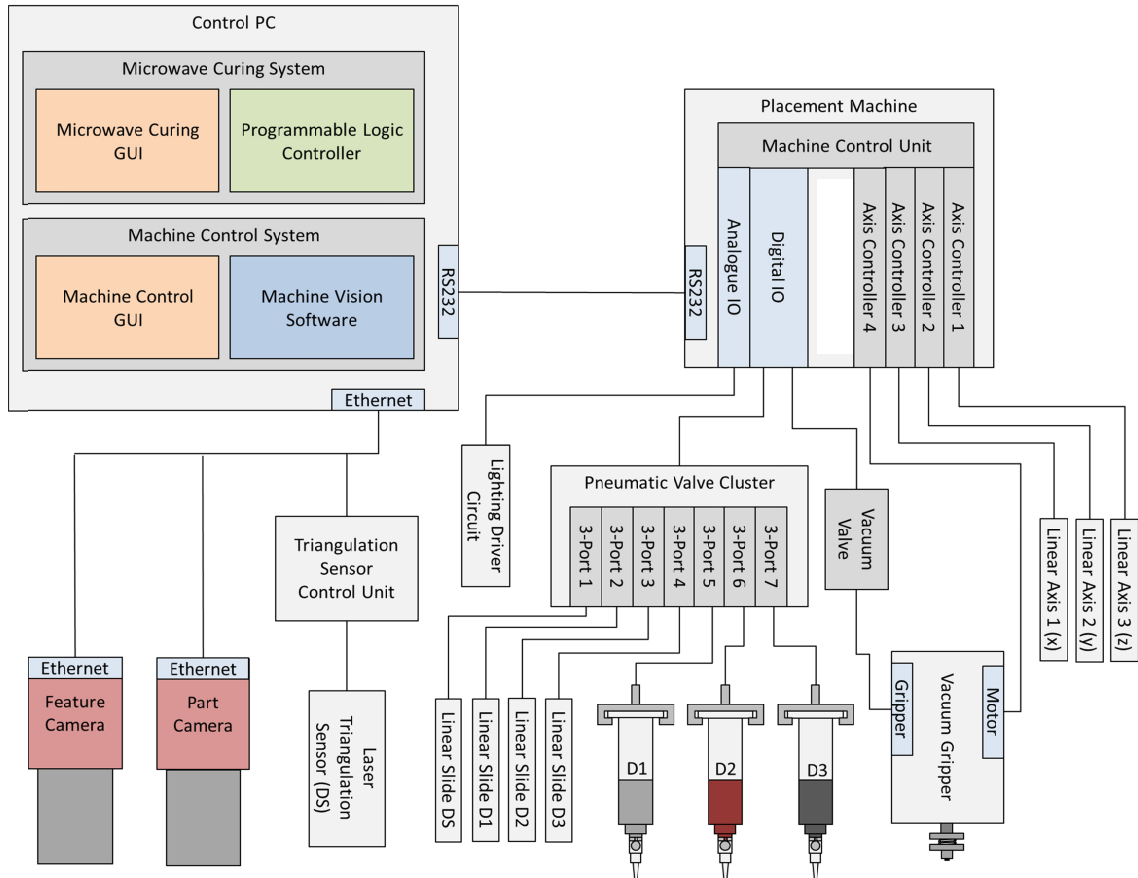


Figure 62 – Control system architecture

The two cameras and the laser triangulation sensors are connected by a Gigabit Ethernet interface network with the PC. Communication with the cameras is performed using the GigE interface. The laser sensor communicates using TCP/IP protocol.

Within the base machine, an integrated machine control unit performs the control of the positioning axes and provides digital and analogue output functionality. The machine control GUI communicates with the machine control unit by an RS232 interface.

The machine control unit provides four axis controllers for the three linear axes and the rotational axis on the vacuum gripper tool. The control unit has analogue and digital inputs and outputs. The lighting driver is controlled by the analogue outputs. Numerous digital outputs control the four linear slides, the time–pressure dispensers and a vacuum

valve, which switches the vacuum for the gripper tool. Additionally, each linear slide is equipped with two limit sensors in order to determine the slide positions, which are interfaced over digital inputs on the machine control unit.

6.4.2 Process control software

With respect to the machine control system architecture, process control software has been developed. The architecture of the program is shown in Figure 63.

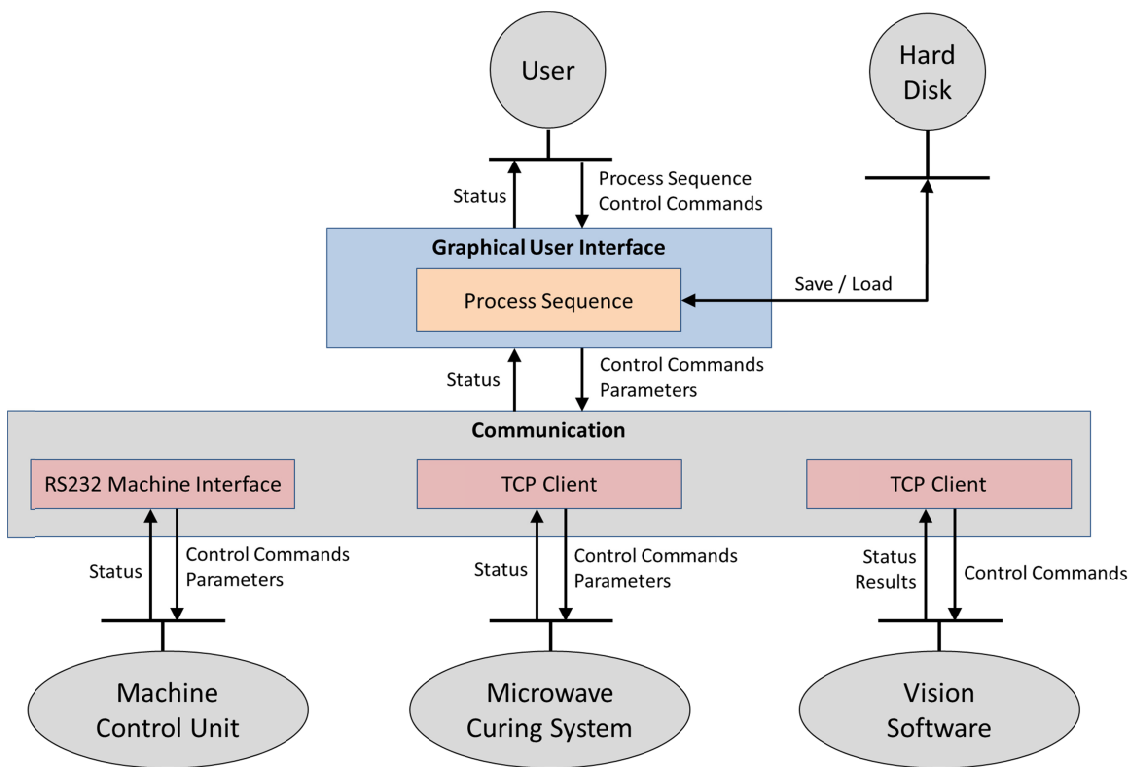


Figure 63 – Process control software architecture

The user interacts with the GUI, setting up the process sequence and giving control commands to the machine. The user receives status information from the GUI. Process sequences may be loaded from and saved to the hard drive. The GUI incorporates sequential process control functionality.

Communication with the hardware is implemented through several interfaces. The machine is connected to the process control software via an RS232 interface. The microwave curing system and the vision software are connected to the GUI by a TCP interface. The process control software acts in both cases as a TCP client.

The connected systems receive control commands and parameters from the process control software. The connected systems report their status and process results. The communication with the machine is enacted by polling, while the microwave curing system and the vision software have an event-based behaviour.

Prototype software has been developed with Visual C++ as Windows Forms applications. A screenshot of the program is shown in Figure 64.

The visualization is structured in six different tabs. Each of these tabs provides a specific functionality. The first tab establishes a connection to the placement machine control system and allows reading of the current machine parameters. A console provides feedback on the current communication status and shows errors if they occur.

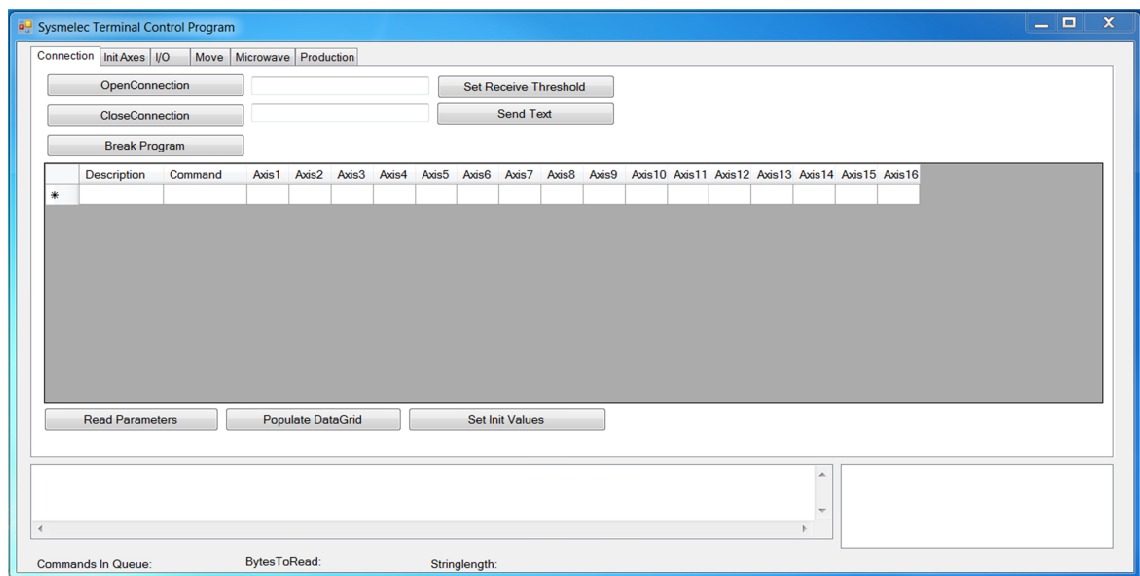


Figure 64 – Process control software screenshot

In the following tab, the four axes in the placement machine can be initialized, the amplifiers can be switched on and the servo control can be activated. The 'I/O' tab provides information about the current IO status and allows for manual switching the outputs. Within the 'Move' tab, the axes may be moved in a stepwise manner. Furthermore, pre-defined points may be approached. The 'Microwave' tab provides connectivity with the microwave curing system to parametrize and to start the curing process. In the 'Production' tab, a process chain may be set up and started. Process chains can be loaded and saved in this tab.

6.4.3 Vision software

The machine vision processes are controlled by the vision software. A machine vision process consists of multiple steps, an example of which, the pose determination of a semiconductor die, is shown in Figure 65.

First, the image is acquired by one of the two cameras. The image is typically filtered in order to reduce noise and disturbing features. In this case, the brightness and the contrast are modified to reduce shadows on the die. Then, an edge detection algorithm is used to determine the orientation of the semiconductor die. In the next step, an object detection algorithm is used to determine the centre of gravity of the die. The measured values are directly converted from the image coordinate system into the camera coordinate system based on the calibration values. The pose values are then saved in a file, together with a timestamp, and the superordinate control system is informed by a TCP message that the measurement is done.

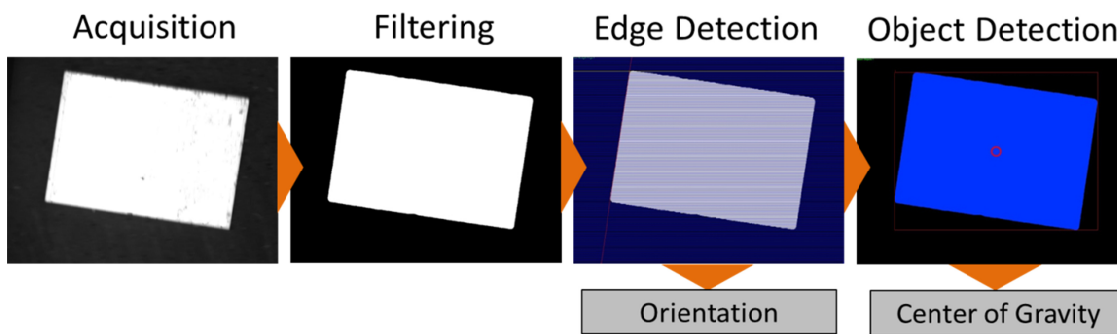


Figure 65 – Pose determination of a semiconductor die

The vision software comprises several such vision programs for different measurement tasks. To coordinate the behaviour of the program, its structure is based on a state machine. The program behaviour has a number of distinct states and external control of the programs is facilitated. A simplified illustration of the state machine is shown in Figure 66.

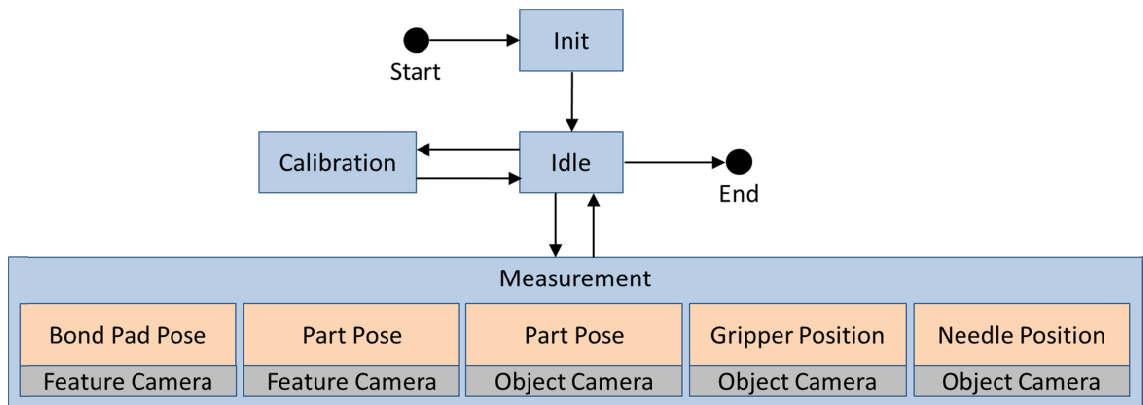


Figure 66 – Vision software state machine

As the state machine illustration shows, the vision system is initialized first. The system is then idle and therefore ready to accept commands. The vision system provides a set of calibration functions, which can be accessed in the ‘Calibration’ state. Here, for example, the position of the camera relative to a feature on the machine, a fiducial or a scale, can be determined. In the ‘Measurement’ state, numerous measurement functions are implemented. These are measurements of bond pad poses, part poses with both cameras and the measurement of tool centre-point positions.

6.5 System integration

The developments described in this chapter were realized. Figure 67 shows a picture of the precision placement machine with microwave curing system.

The main process tools, including the microwave applicator, have been integrated on the moving part of the machine (‘A’). The solid-state microwave source has been placed on the main axis (‘B’). The ultra-low-loss cable connects the source with the oven (‘C’). The workpiece holder and the object camera are placed right under the process tools (‘D’).

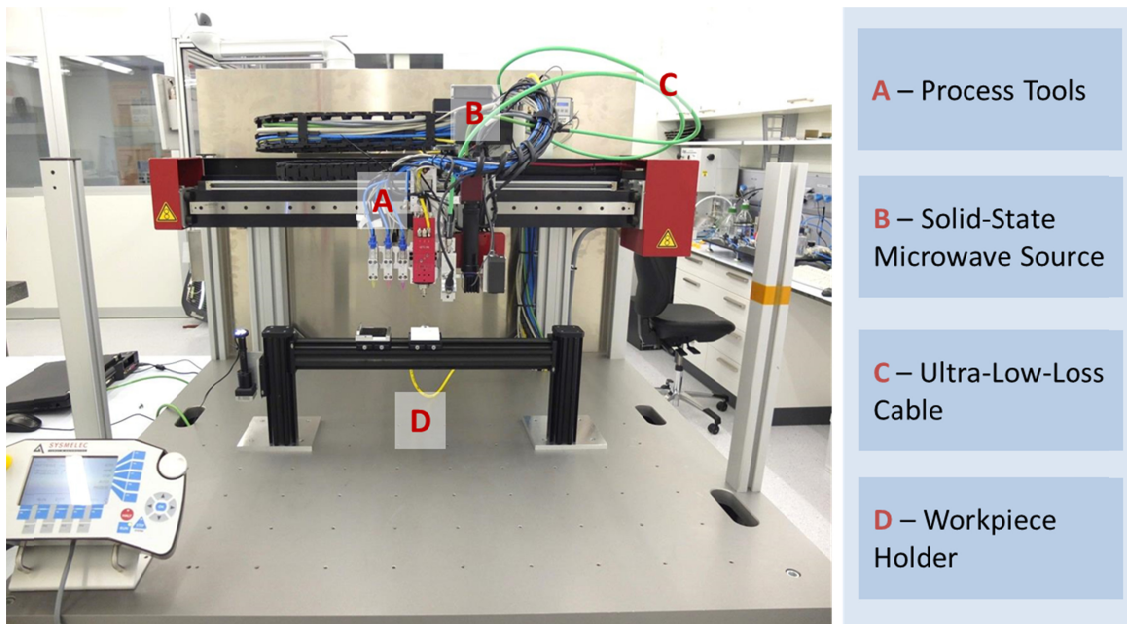


Figure 67 – Integrated machine

In Figure 68, a close-up picture of the process tools is shown. As can be seen from the pictures, the process tools, the solid-state microwave source and its components have been built. The process tools were built as described in Section 6.3.1. All tools were mechanically integrated as shown in Figure 68. Pneumatic circuits and control of the dispensers, the pneumatic slides and vacuum gripper were created and installed. The vision and the laser displacement sensor systems were integrated both electrically and from the control system point of view.

The PLC control software, the GUI and the vision software were installed on an IPC. Network interface cards for GigE and EtherCAT were installed along with the required network infrastructure.

All subsystems were tested individually and found to be functional. The communication between the subsystems could be successfully established. All in all, the integration of the pick-and-place machine with the integrated microwave curing system was a success.

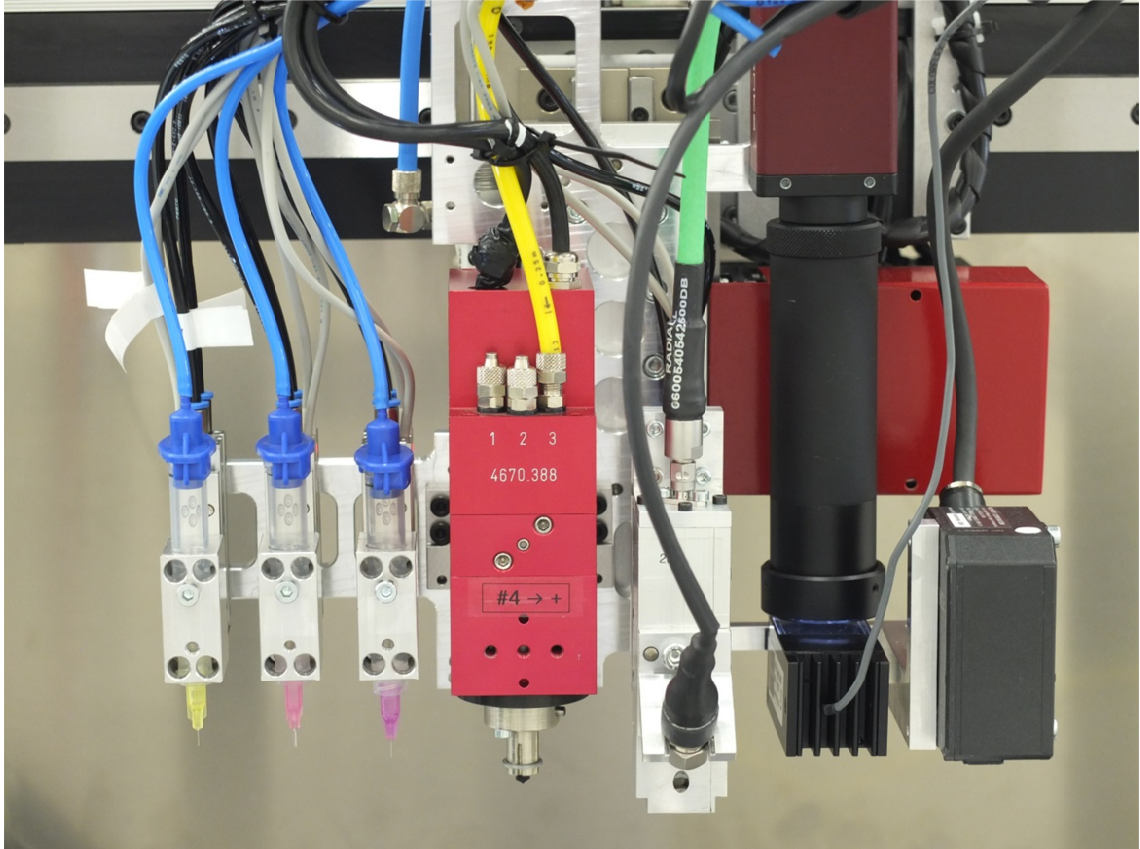


Figure 68 – Realized process tools

6.6 Conclusion

Based on the concept proposed in Chapter 5, a prototype microwave curing system was built. In the course of the process, the necessary components were selected. The open-ended resonator was modified to integrate a pyrometer for *in situ* temperature measurement. A control system was implemented that incorporated the proposed temperature and frequency control methods.

Table 18 gives an overview of the curing system set-up with respect to the approach proposed in Chapter 5. It can be concluded that the curing system was fully realized in accordance with the proposed concept.

Following the machine concept from Section 5.5, the components of the integrated machine with microwave heating system were selected and an integrated machine was designed. A control system for the integrated machine was developed. The developed pick-and-place machine was then implemented.

Table 19 presents an overview of the building of the machine with respect to the concept proposed in Chapter 5. The proposed machine provides all features as worked

out within the machine concept. The resulting machine represents the first of its kind in having an integrated pick-and-place machine with embedded microwave curing system.

Table 18 – Curing system implementation overview

Feature	Approach	Implementation	Section
Curing Principle	Microwave curing	Prototype of microwave curing system	6.1
Microwave Source	Solid-State Power Amplifier (SSPA)	Custom designed and built SSPA	6.1.1
Microwave Applicator	Open-ended waveguide resonator	Open-ended waveguide resonator with integrated pyrometer	6.1.3
Control System	Soft-PLC	Beckhoff TwinCAT Soft-PLC	6.1.4
Temperature Sensor	Non-contact temperature sensor (pyrometer)	Integration of pyrometer into applicator	6.1.3
Control Methods	Frequency, temperature and heating control	Implemented in TwinCAT Soft-PLC	6.1.4

Now that the curing system and the machine are available, their functions and their capabilities can be evaluated.

Table 19 – Machine implementation overview

Feature	Approach	Implementation	Section
Process	Flip-chip process chain with intermediate microwave curing steps	Machine is, in principle, capable of performing the desired process	5.5.9
Substrate	Microelectronic packages, PCBs, complex assemblies	Flexible set up allowing the processing of the desired substrates. Adaptation to other substrates possible	5.5.2
Feeding	Preferably from magazine with optional modification to automated conveyor systems or feeders	Magazine feeding has been implemented. Adaptation to other feeding systems is possible	5.5.2
Pick and Place	Relative positioning strategy with two vision sensors and laser triangulation sensor. Utilization of vacuum grippers for pick and place	Process tools and sensors for proposed relative positioning strategy have been developed and integrated	5.5.8
Dispensing	Time–pressure dispensers for ECA, underfill and encapsulant materials	Three separate time–pressure dispensers have been integrated	5.5.4
Curing	Realization and integration of proposed microwave curing system	Microwave curing system has been integrated	5.5.11
Machine Type	Cartesian system with fixed product and feeding positions. Process tools are placed on the moving part of the machine	Machine has been fully realized according to the proposed concept	5.5.10

In the next step, the proposed method and developed machine are to be experimentally validated. Figure 69 shows the necessary tests derived to assess performance against the previously defined set of requirements.

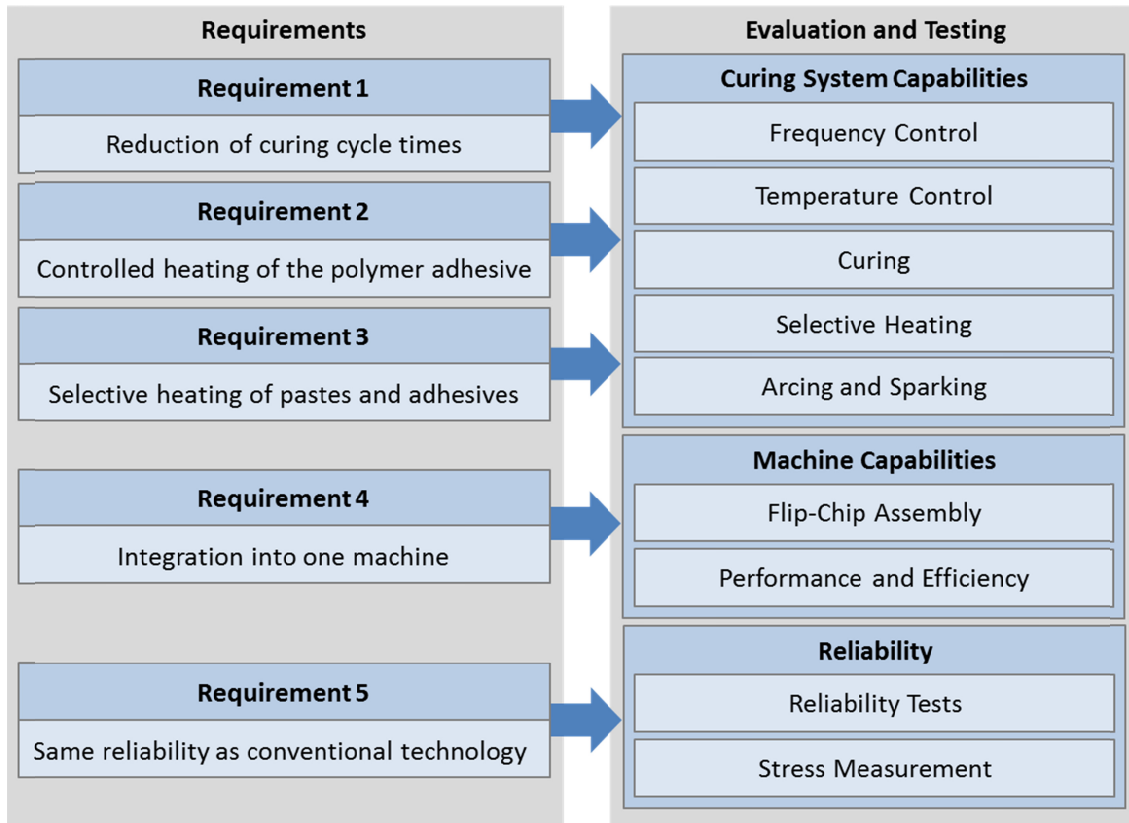


Figure 69 – Derivation of tests from requirements

The first three requirements directly concern the curing system. First, the temperature control and the frequency control are tested for their capabilities. Then, actual curing tests are performed on different relevant materials, enabling the testing of Requirements 1 and 2. Requirement 3 demands selective heating of pastes and adhesives; therefore, additional tests are performed. As discussed in the conception of the curing system, arcing and sparking were identified as potentially detrimental effects for the assembly process, and specific tests are carried out to determine the likelihood and effect of arcing and sparking during the process.

The integration of the process equipment formed Requirement 5. To prove this capability, the assembly process is experimentally tested. The performance and efficiency of the prototype system are investigated.

Requirement 4 demands reliability testing according to industrially relevant standards. These standard industrial tests are performed. Additionally, the effect of the curing mode on residual stresses within electronic packages is investigated.

7 Validation of the Proposed Solution Approach

This chapter investigates whether the proposed method fulfils the previously identified requirements. This validation is performed by a number of experiments as outlined at the end of the previous chapter.

7.1 Curing system capabilities

A number of tests have been carried out to evaluate the heating capabilities of the proposed microwave heating system. To perform these tests, three different materials have been selected: an ICA; an underfill; and an encapsulant material. The selection has been performed based on the flip-chip process chain. For each of the required pastes, a suitable material was considered. The particular materials were selected with respect to prior work performed on microwave curing of polymer adhesives, whereby research was carried out on the properties during and after cure (Tilford et al. 2008b; Tilford et al. 2008a; Tilford et al. 2010e; Tilford et al. 2010b).

7.1.1 Frequency control

The three frequency control methods of constant frequency, variable-frequency microwave and frequency sweeping have been implemented and tested. All methods were found to be functional (Rupp 2011).

Optimal heating results require the oven to be operated as close as possible to a resonant frequency. Perturbations, such as temperature or dielectric materials placed inside the load section, cause the resonant frequencies to change slightly, but not in a significant manner. As the temperature and the dielectric properties of the oven, and particularly the material placed in the oven, change during processing, the resonant frequencies also change. Therefore, in order to track a set resonant frequency, an auto-tuning algorithm has been implemented. Figure 70 shows a heating process with a set starting frequency, which is autotuned during the process (Rupp 2011).

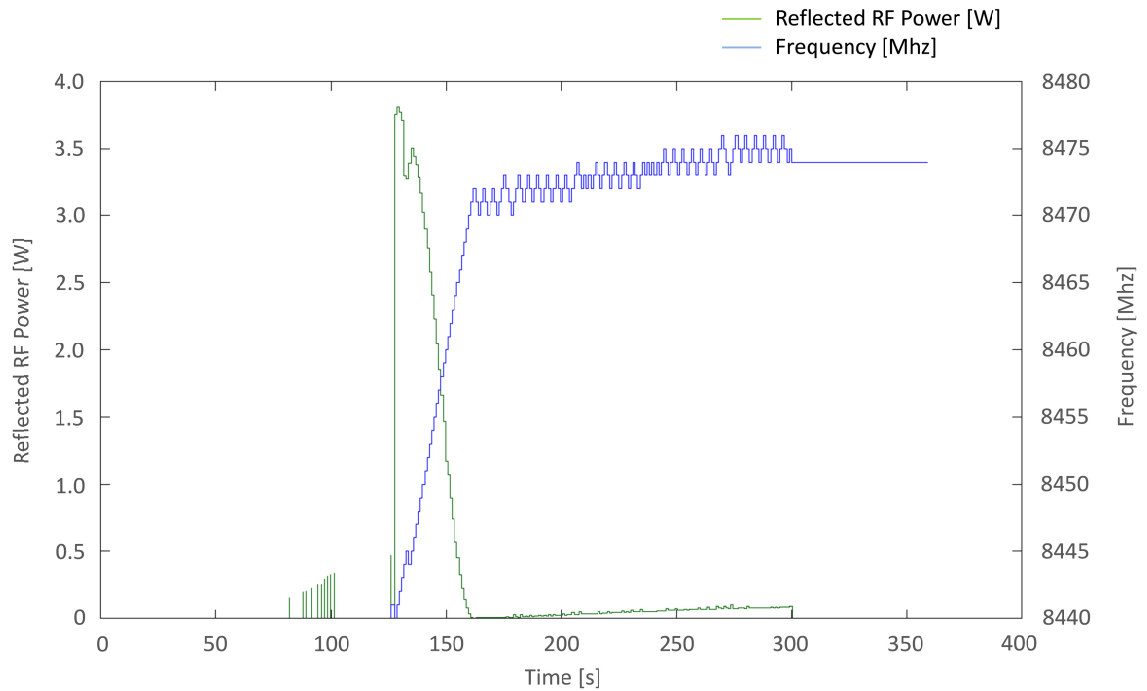


Figure 70 – Frequency auto-tuning algorithm

The ideal resonant frequency of the applicator is 8.4 GHz. The plot shows that a considerable amount of power is reflected (3.7 W) at this frequency. Once the power is fully switched on, the auto-tuning algorithm is able to tune the microwave frequency to a resonant frequency in approximately 30 s, after which, the reflected power stays below 100 mW. The microwave source is pulsed using 10 kHz PWM to prevent the damage of sensitive devices due to, for example, arcing and sparking. The PWM duty cycle can be adjusted within its configurable limits to regulate the microwave source power.

The frequency hopping algorithm was tested. A plot of the frequency and the resulting power output is presented in Figure 71. As can be seen, the frequency is set cyclically between the six frequencies $f_{h,1}$ to $f_{h,6}$. A frequency change is performed every second.

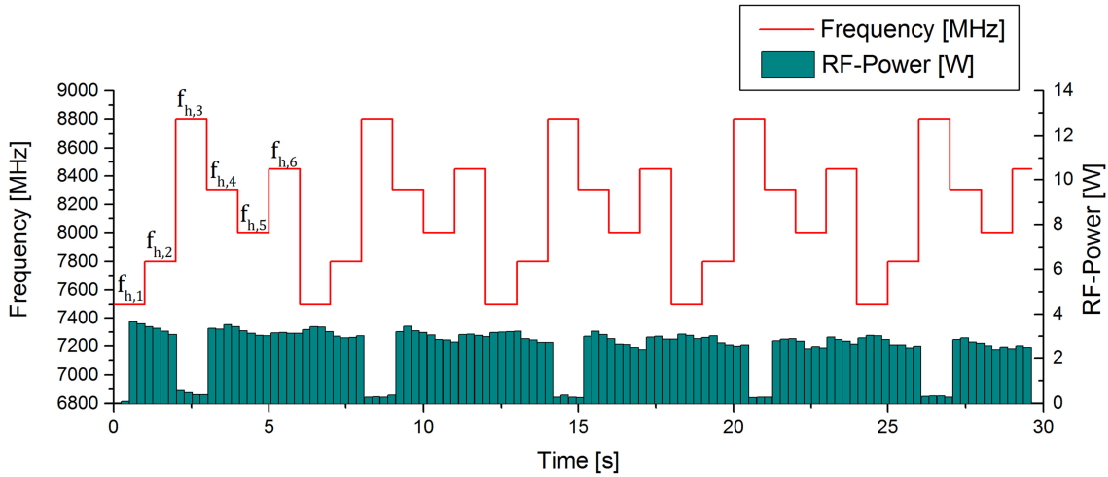


Figure 71 – Frequency hopping

A plot of the frequency sweep and the resulting power output is presented in Figure 72. Sweeping was performed between the frequencies $f_{s,1}$ and $f_{s,2}$. The cycle time in this case was 1.3 s.

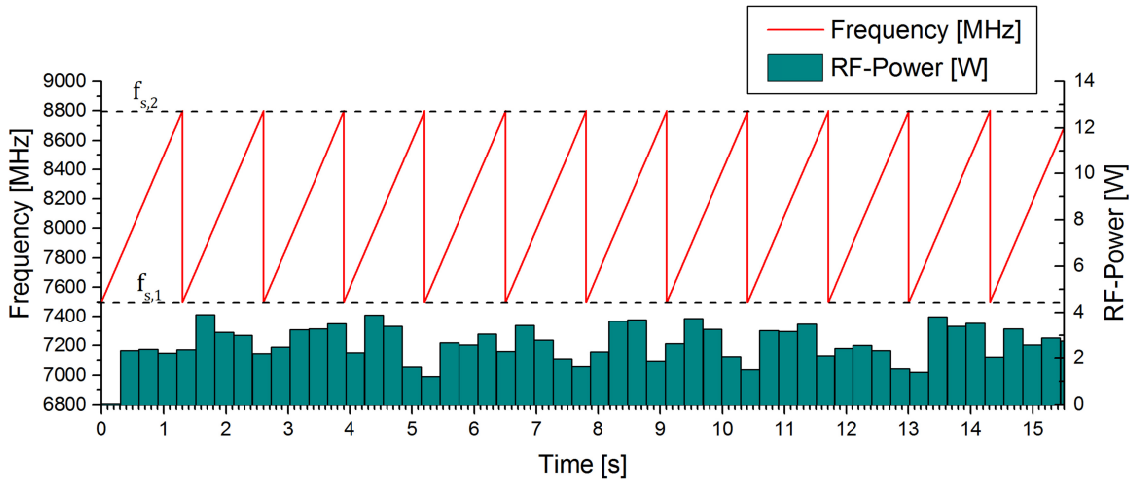


Figure 72 – Linear frequency sweep

All three frequency control algorithms have been implemented and tested with positive outcome. Additionally, the auto-tuning algorithm for the frequency has been implemented. Testing of the algorithm revealed the effectiveness of the algorithm at optimizing the energy output of the system. The proposed frequency control functionality was therefore successfully implemented.

7.1.2 Temperature control

Experiments were carried out to investigate the heating and curing capabilities. Sample holders have been fabricated for these experiments. A picture of such a sample is shown in Figure 73 (left). The encapsulant Hysol EO1080 has been used for the curing experiments.

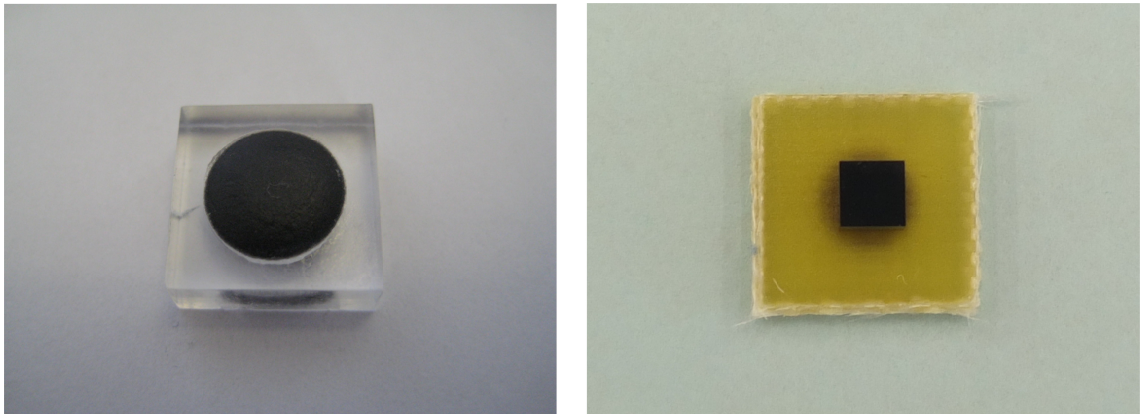


Figure 73 – Specimen for heating tests

Figure 74 shows a graph of the curing of EO1080 according to a defined temperature profile. As can be seen, the two-point controller is able to follow the defined temperature profile. Deviations within the hold period are less than ± 2 °C.

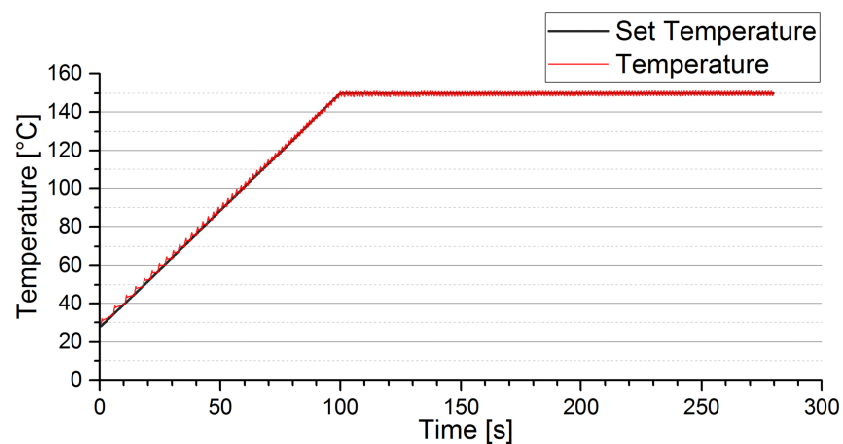


Figure 74 – Curing of encapsulant Hysol EO1080

A second experiment was performed in order to test the temperature control algorithm on a reflow profile. For this experiment, a silicon die with dimensions of $3 \times 3 \times 1.5$ mm was placed onto a 10×10 mm² FR4 board, shown in Figure 73 (right).

The temperature measurement was carried out on the silicon die with a calibrated pyrometer.

The specimen was heated up with ramp rate $\Phi_1 = 3 \text{ }^\circ\text{C/s}$ up to a soak temperature of $150 \text{ }^\circ\text{C}$. After a hold period of 100 s , the specimen was further heated up with ramp rate $\Phi_2 = 3 \text{ }^\circ\text{C/s}$ to temperature $T_{max} = 280 \text{ }^\circ\text{C}$. This temperature was held for 60 s before cooling down of the specimen was carried out with a ramp rate of $\Phi_3 = -6 \text{ }^\circ\text{C/s}$. A plot of the experiment is presented in Figure 75.

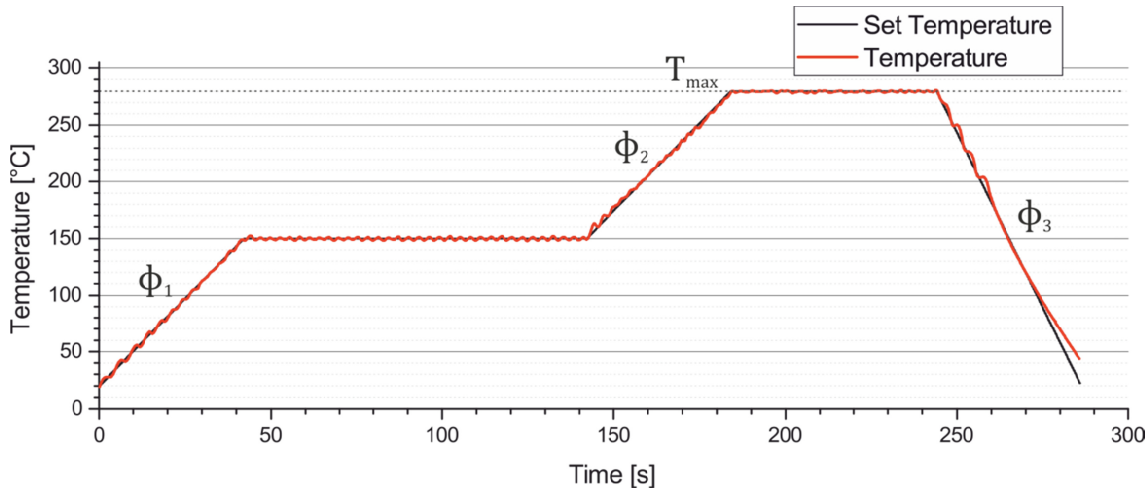


Figure 75 – Heating of silicon with reflow profile

The curing system was well able to follow the set temperature profile. The deviation during hold periods was less than $\pm 5 \text{ }^\circ\text{C}$ – meeting the specification. Within the ramp-up and ramp-down phases, the deviation increased slightly compared to the hold period. During the ramp-down phase, the system was not able to follow the defined profile in the final seconds. As discussed in Chapter 4, additional active cooling would be necessary to ideally follow the defined profile, but is not relevant for the curing of polymer adhesives. Overall, the criteria compiled in Table 1 are met.

In summary, the system is capable of performing controlled heating of the polymer adhesive according to a defined temperature profile within an industrially relevant range of process parameters, as demanded by Requirement 2.

7.1.3 Curing tests

For the three materials, curing profiles for convection heating are proposed by the manufacturer. Findings from the literature indicate that these profiles are not appropriate or applicable for microwave heating. For Hysol EO1080 it was found that a 100% degree of cure using microwave curing can be achieved with drastically reduced curing times (Pavuluri et al. 2010a). For FP4511, extensive experimental analysis and

modelling of the cure kinetics were performed (Tilford et al. 2010e; Tilford et al. 2010a). Results indicate that the cure time could be reduced from 2 hours, as proposed by the manufacturer, to several minutes (Tilford et al. 2010a; Tilford et al. 2010d). For CE3103WLV the total profile time is in the order of three minutes. Cure kinetic analysis and modelling indicates that the required time for curing can also be significantly reduced by microwave curing (Tilford et al. 2010a; Tilford et al. 2010b). However, preliminary testing of conductivity showed that the material could not be satisfactorily cured with hold times less than 180 s using the proposed curing system. Therefore, the hold times were not reduced for this material. An overview of the cure profiles is presented in Table 20.

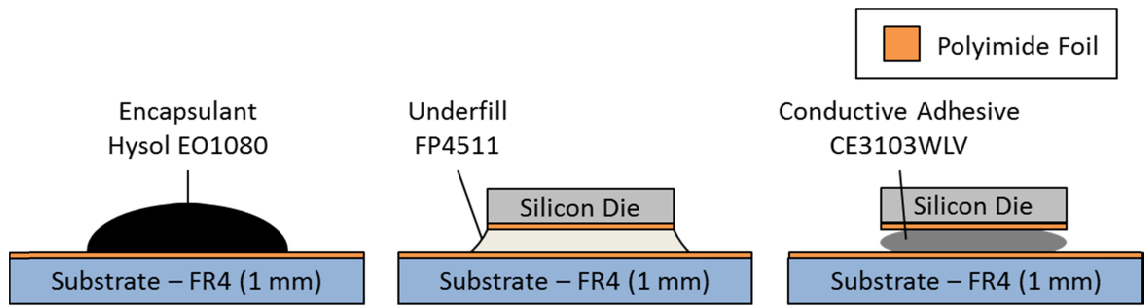


Figure 76 – Test set-ups for curing tests

Samples of the materials were prepared according to the three set-ups shown in Figure 76. The dimensions of the substrate were $10 \times 10 \times 1$ mm, while the dimensions of the die were $3 \times 3 \times 1.5$ mm. The open cavity was set up with the load section on top and the samples were placed in the centre of the load section. Curing was carried out according to the profiles from Table 20. Temperature control was performed using a two-point controller. Frequency control was set to constant frequency with the auto-tuning algorithm switched on.

To determine if the specimens had been sufficiently cured, DSC measurements were performed – according to IPC-TM-650, method 2.4.35 – on all three materials. Each specimen was heated at a ramp rate of 20 °C/min from a minimum temperature of -50 °C up to 180 °C, before they were each subsequently cooled back down to a temperature of -50 °C at a ramp rate of 200 °C/min. Afterwards, another heating cycle with identical parameters was performed. Intermediate hold times were 3 minutes. Initial and final glass transition temperatures T_{gI} and T_{gF} , initial and final heat capacity change ΔC_{pI} and ΔC_{pF} , as well as the cure factor ΔT_g were determined. Glass transition temperatures were determined with the $\frac{1}{2} \Delta C_p$ method. The degree of cure (DoC) has

been determined by the ratio of T_gI and T_gF .⁴ The results of the DSC measurements are shown in Table 21.

Glass transition temperature T_g is considered to be a sensitive probe for the DoC beyond 95%, at which point regular DSC curves cannot predict a complete cure of the material (Zhang et al. 2004). The cure factor ΔT_g can be regarded as a relative measure of DoC; the lower the cure factor, the higher the DoC of the specimen. The reference specimen U3 and C2 were prepared according to manufacturer specifications and can therefore be regarded as sufficiently cured.

Table 20 – Cure profiles (MW: microwave, Convection: convection heating)

ID	Material	Method	Ramp Rate [°C/s]	Hold Time [s]	Temp [°C]	Source
E1	Hysol EO1080	MW	1.5	180	150	[1]
E2	Hysol EO1080	MW	1.5	360	150	[1]
E3	Hysol EO1080	Convection	-	1200	150	[2]
U1	FP4511	MW	1.5	360	150	[3]
U2	FP4511	MW	1.5	720	150	[3]
U3	FP4511	Convection	-	7200	150	[4]
C1	CE3103WLV	MW	1.5	180	150	[5]
C2	CE3103WLV	Convection	-	180	150	[5]
[1] (Pavuluri et al. 2010a), [2] (EO1080 2010), [3] (Tilford et al. 2010a), [4] (FP4511 2010), [5] (CE3103WLV 2011)						

Sample E1 and E2, the microwave-cured samples of encapsulant exhibit practically the same behaviour during the first and the second pass. The glass transition temperatures are also very similar between the two passes. These materials are almost fully cured. The reference encapsulant sample E3 had a significantly higher cure factor.

Sample U1 of the underfill showed a chemical reaction in the first pass; therefore, the glass transition temperature could only be preliminarily determined. The material

⁴ This calculation method is not accurate, but supports the illustration of the results.

sample U2 exhibited a slightly lower glass transition temperature and a slightly higher cure factor than the conventionally cured sample.

The samples C1 and C2 show comparable glass transition temperatures and cure factors. The microwave-cured sample was exposed to heat for slightly longer, due to the controlled ramp-up, which might explain the slightly lower cure factor and higher DoC.

It was possible to cure the adhesives according to the defined temperature profiles with the proposed curing system. After finding applicable parameters, the defined temperature profiles could be ideally followed in practice – fulfilling Requirement 2.

Table 21 – DSC measurements

ID	Material	Method	T _{gI} [°C]	ΔC _{pI} [J/g·°C]	T _{gF} [°C]	ΔC _{pF} [J/g·°C]	ΔT _g [°C]	DoC
E1	EO1080	MW	114.73	0.197	115.30	0.208	0.57	99.5%
E2	EO1080	MW	117.34	0.152	117.72	0.198	0.38	99.7%
E3	EO1080	Conv.	107.02	0.256	114.75	0.209	7.73	93.3%
U1	FP4511	MW	(128.30)	-	143.11	0.108	(14.8)	(90%)
U2	FP4511	MW	132.49	0.155	139.92	0.108	7.43	94.7%
U3	FP4511	Conv.	140.67	0.110	145.2	0.084	4.53	96.9%
C1	CE3103	MW	85.30	0.073	87.69	0.088	2.39	97.3%
C2	CE3103	Conv.	85.83	0.075	88.62	0.089	2.79	96.9%

All three materials could be successfully cured. The results obtained from DSC testing and from the literature show that materials EO1080 and FP4511 can be cured to at least the same degree in drastically shorter times compared to the profiles proposed for convection ovens. Although no general statement about the reduction of curing cycle times can be made, it could be shown that curing cycles can be significantly reduced for certain materials with the proposed system. Requirement 1 is therefore regarded as fulfilled.

7.1.4 Selective heating

Open-ended cavity design is specifically designed to apply energy within the load section. Since the RF power is solely applied within the load section, heating processes

are confined to this designated volume (Sinclair 2009). The oven therefore supports selective heating of individual components on a substrate by design.

The power absorbed per unit volume due to dielectric loss within a material exposed to an electric field is defined by Equation (25):

$$P_D = \frac{f_{res}\pi\varepsilon'' \int_V \vec{E} \cdot \vec{E} dV}{V} \quad (25)$$

where

- f_{res} resonant frequency of the coupled mode [Hz];
- ε'' imaginary component of the complex permittivity;
- \vec{E} electric field [$\frac{V}{m}$];
- V volume of the material [m^3].

In order to maximize the dielectric power loss, and therefore the heating potential, the target sample should have a high dielectric loss tangent relative to the dielectric filling material within the cavity. Typical values for the dielectric constant of an epoxy/encapsulant range from 4 to 13. Typical values of $\tan \delta$ at X band and at 24 °C for the epoxy range from $2 \cdot 10^{-4}$ to $5 \cdot 10^{-1}$ (Sinclair et al. 2008a; Sinclair et al. 2008d; Sinclair 2009). Therefore, for the application of the proposed curing system, materials with a high loss tangent at the applied microwave frequencies should be used. If, for example, an encapsulant with a very high loss tangent is applied onto an assembly with lower loss properties, then the encapsulant will be mainly heated.

Silicon has a comparatively high loss tangent of 0.02 in the X band and can be effectively heated with the proposed system. To assess the selectivity of the system, an experiment was performed. A silicon block with dimensions of $3 \times 3 \times 1.5$ mm was placed onto an FR4 circuit board with dimensions of $10 \times 10 \times 1$ mm. A silicon block of height 1.5 mm was selected as the worst-case model for a silicon die.⁵ Eight SMD LEDs (Kingbright KP2012SGD) were placed at an approximate distance of 2 mm from the edge of the silicon. The LEDs were used as representative examples of temperature-sensitive components. The oven was set up upside down, with the pyrometer pointing onto the silicon surface. Pictures of the experimental set-up are presented in Figure 77.

⁵ Silicon dies are typically significantly thinner (< 0.8 mm) and have a much lower mass.

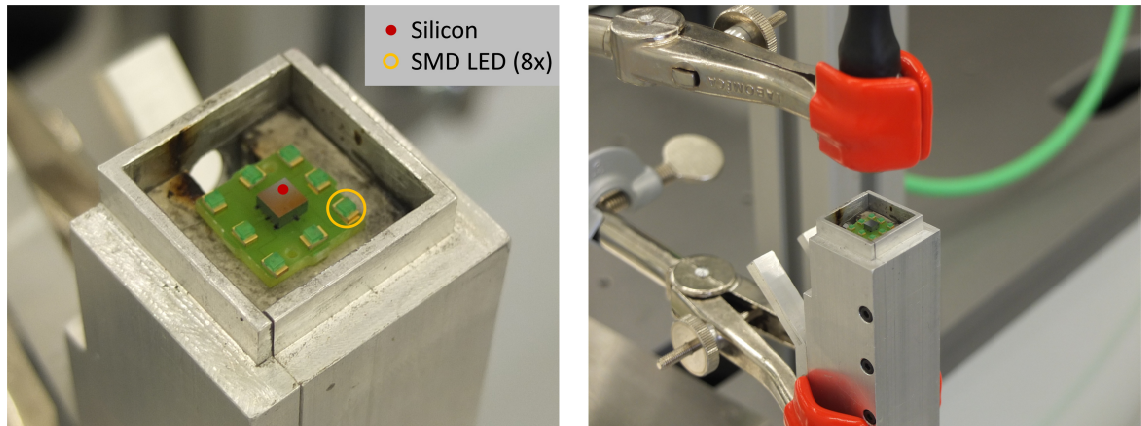


Figure 77 – Experimental set-up for selective heating

The specimen was heated according to the reflow temperature profile shown in Figure 75. At the peak temperature of 280 °C a thermal camera image was taken (Figure 78). As can be seen clearly on the thermal image, the silicon block is heated significantly more strongly than the substrate and the LEDs.

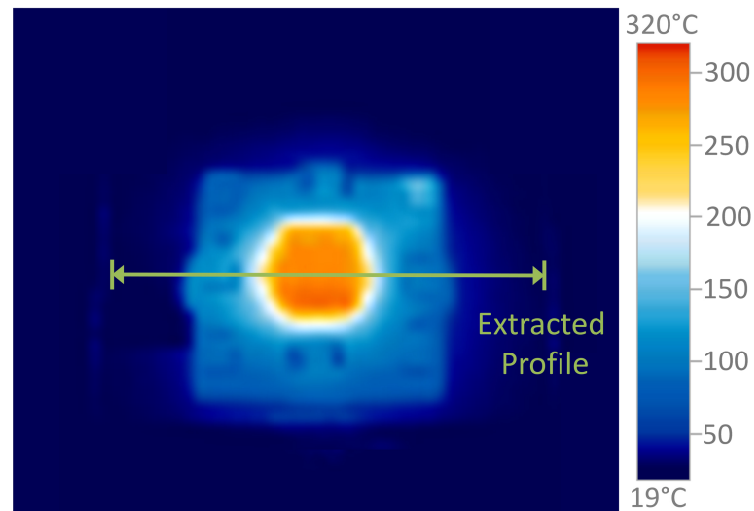


Figure 78 – Thermal image of silicon die and 8 LEDs on FR4 circuit board

As indicated in Figure 78, a profile was extracted from the thermal image. This profile is shown in Figure 79. The positions of the heated components are included on the image. As can be seen, the die has a temperature of 280 °C. The LEDs are exposed to temperatures between 90 °C and 125 °C. With increasing distance from the die, the temperature drops rapidly. For both depicted sides, the target area for selective heating, as was described in Figure 20, is shown in light blue. The target temperature is reached

at a distance of 1.4 mm on both sides – clearly within the target area as demanded by Requirement 3.

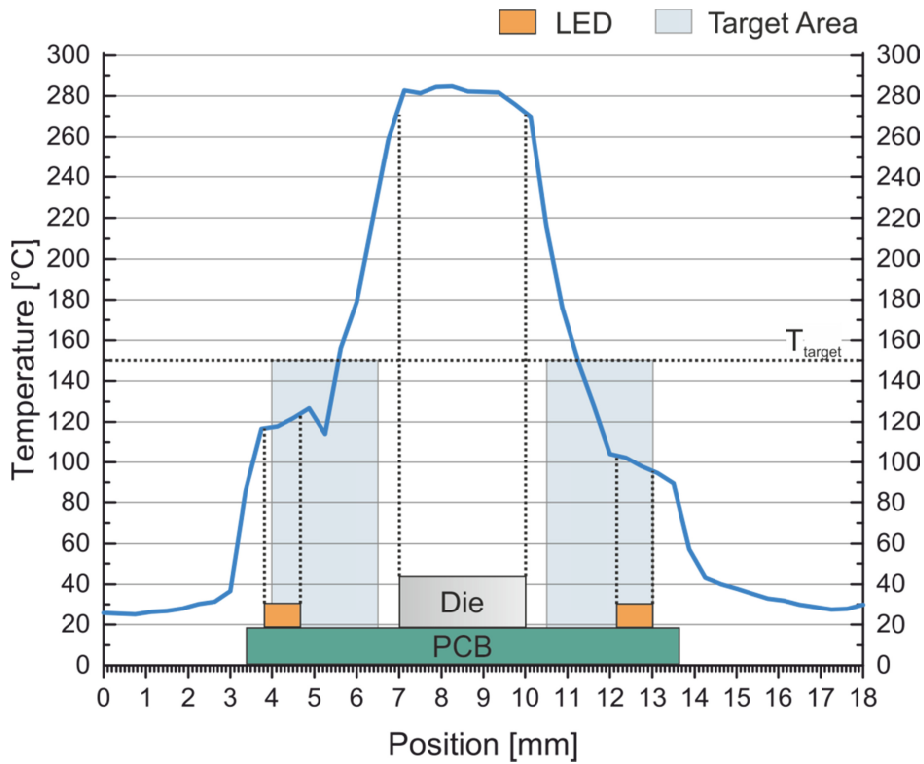


Figure 79 – Temperature profile in tested specimen

Two sets of 16 LEDs were exposed to three reflow cycles analogous to Figure 75. One set was processed in a reflow oven (LPKF Protoflow S), and the other set was processed in the curing system with the set-up shown in Figure 77. One representative sample of each set is presented in Figure 80.

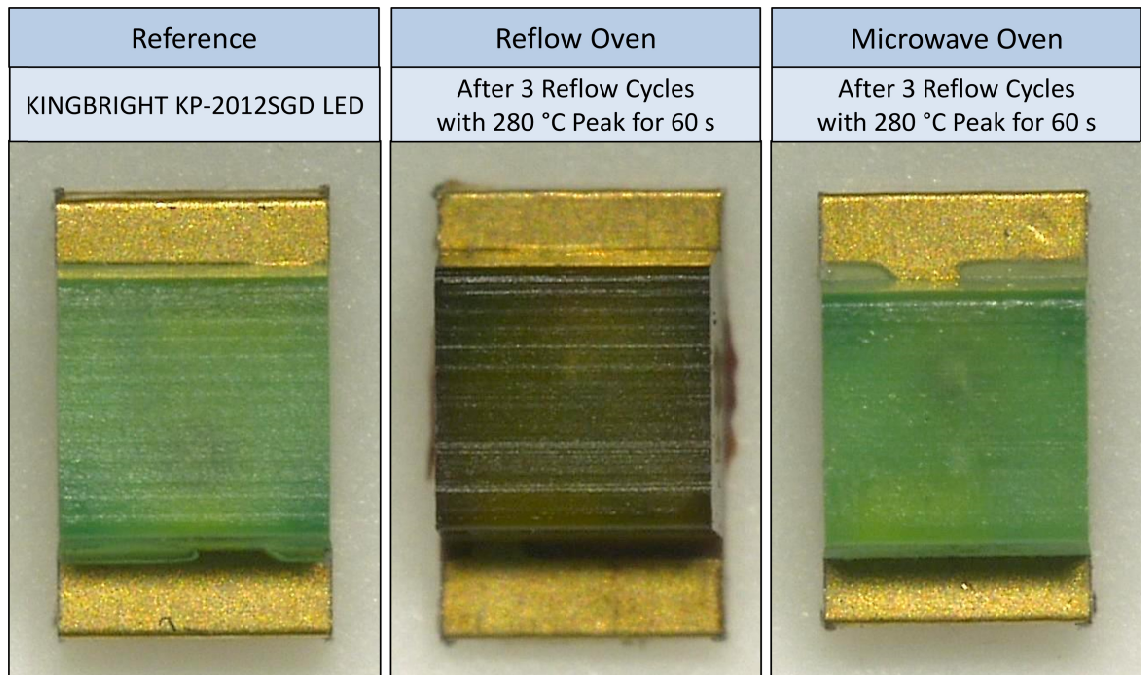


Figure 80 – LEDs after three reflow cycles

According to the manufacturer’s data sheet, the KP-2012SGD LEDs may be exposed to a maximum of two reflow cycles with a peak temperature of 260 °C (Kingbright 2007). The allowed time at peak temperature is 5 s. The LEDs tested in this case were exposed to far more demanding profiles with 280 °C peak and 60 s at peak temperature.

The set exposed to the reflow oven was functional after the three reflow cycles. However, the optical properties of the LED had changed significantly. As can be seen clearly in Figure 80, the light green colour changed to a darker, nearly brown colour. The LEDs processed in the microwave applicator were also functional after the three reflow cycles. However, due to the significantly lower thermal exposure, the optical properties of the microwave-processed components remained unchanged.

The selective heating capability has been successfully demonstrated. Due to its material properties, the silicon die can be heated according to a defined profile, while the surrounding components are spared. The slope of the temperature reduction is well within the targeted corridor. Additionally, it was successfully demonstrated that a typical temperature-sensitive component can be effectively protected from detrimental temperatures – fulfilling the criteria of Requirement 3.

7.1.5 Arcing and sparking

The application of microwave heating may cause arcing or sparking on electrically conductive components, especially highly conductive materials such as gold, silver or copper.

A simple printed circuit board (see Chapter 7.2.1) was placed inside the load section of the microwave applicator. The PCB has small contact pads in the centre of the board, which are lead individually to the outer section of the board. The contacts leading to two of the closest contact pads were connected to an oscilloscope.

With the PCB and the oscilloscope probes placed inside the oven, the oven was operated with different parameters at full duty cycle. For all three frequency modes, no significant signals could be measured. Also, no arcing or sparking could be visually observed.

It was still, however, possible that arcing and sparking was happening during microwave exposure, but that this could not be visually observed. The arcs and sparks could be either too small or might appear and disappear too fast to be observed with conventional camera equipment. Additionally, it could be possible that the measurement circuit could prevent electrical loads from building up.

Therefore, an alternative set-up with a high-speed camera was employed. A Photron FASTCAM SA4 model 500K-M1 with a frame rate of up to 500,000 frames per second and an adjustable 1–12× magnification lens was used. Preliminary testing of the set-up was carried out by application of a voltage of 1000 V between two of the closest contacts on the circuit board. This way arcing and sparking could reliably be provoked and the high-speed camera could reliably capture the arcing and sparking processes. Three screenshots of the preliminary experiment are shown in Figure 81.

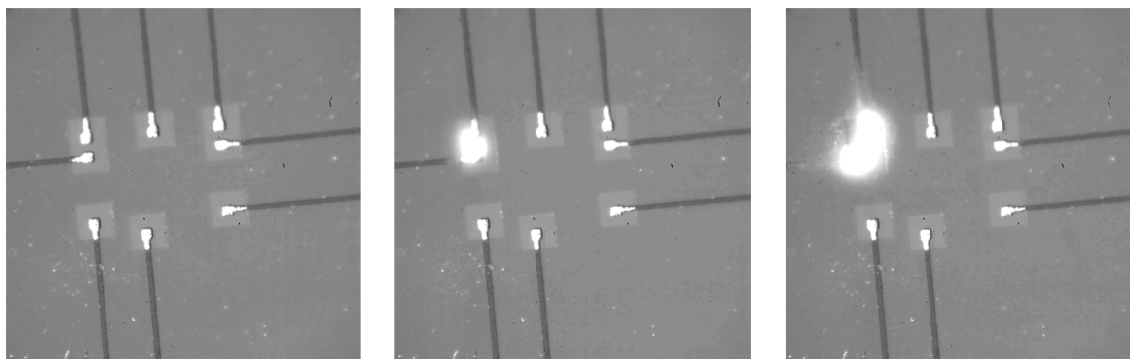


Figure 81 – Arcing and sparking induced by 1000 V signal

One of the before-mentioned 10×10 mm circuit boards, a LM2940C voltage regulator die, and an open quad flat-pack package with no leads (QFN) with a wire-bonded voltage regulator die were placed inside the oven. Microwave heating at full duty cycle was observed at 6750 frames per second. All three frequency control modes were tested. Screenshots are shown in Figure 82. In none of the cases was an arc or a spark detected.

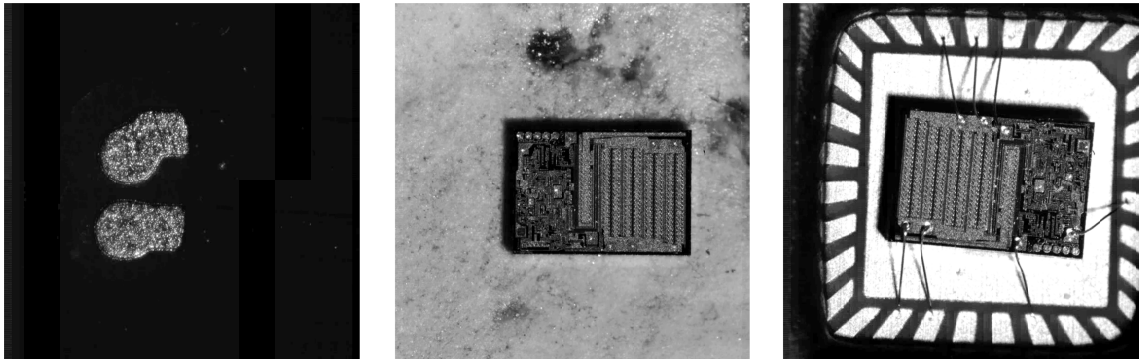


Figure 82 – Circuit board, bare die and open QFN observed with high-speed camera during microwave heating

The experimental results indicate that no arcing or sparking was induced by the microwave heating set-up. Measurement of the induced voltages did not reveal any extraordinary values. Neither visually, nor with a high-speed camera, could any arcing or sparking provoked by microwave heating be observed. In addition, no damage to the exposed components was found. These preliminary results suggest that microwave heating of microelectronic components with the proposed set-up can be carried out without arcing and sparking.

7.2 Flip-chip bonding

To investigate the capability of the proposed assembly system to perform a flip-chip process, a sample assembly is proposed. Based on this sample, a process close to industrial standards is suggested. The results are then closely examined to determine the industrial applicability, with particular attention paid to the microwave curing process.

7.2.1 Assembly

An LM358A bipolar operations amplifier has been chosen for flip-chip testing. It is a fully functional chip that is also not too complex and does not impose any special requirements regarding its assembly. The small contact pads, however, do still pose a significant challenge for assembly with ECA.

The chip has a floating back potential and is thus suitable for the flip-chip mode of die attach (TI 2015). The silicon-based die has dimensions of $1.35 \times 1.09 \times 0.64 \text{ mm}^3$ and eight contact pads, each with dimensions of $90 \times 90 \mu\text{m}^2$. A simple printed circuit board, based on FR4 material, serves as the substrate for the flip-chip sample. A picture of the board is depicted in Figure 83.

The board has outer dimensions of $10 \times 10 \text{ mm}^2$. In the centre, there are eight bond pads ($90 \times 90 \mu\text{m}^2$) for connection with the LM358. Eight contact pads for external connection ($1 \times 1 \text{ mm}^2$), each connected to a small bond pad, are designated for external contacting and testing. The circuit paths are $75 \mu\text{m}$ wide. The surface is covered with solder resist.

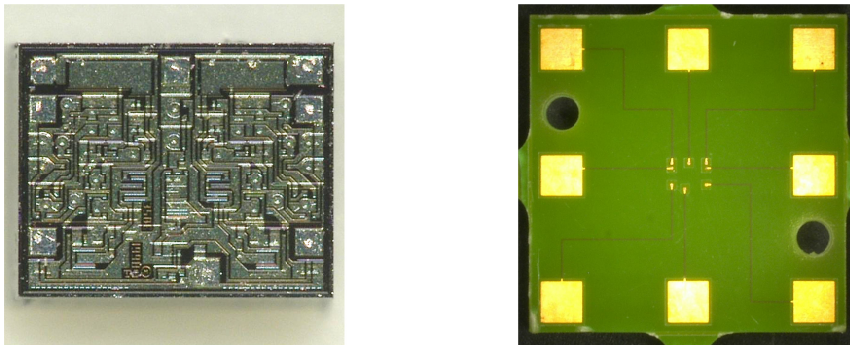


Figure 83 – LM358 die (left) and PCB (right)

7.2.2 Process

The flip-chip assembly approach adopted in this study is depicted in Figure 84. The PCB is placed on the process position. An unwanted displacement of the PCB is avoided by mechanical fixing. Since the board position, orientation and geometry may vary, the position of the bond pads is determined using the vision system. To contact the board and the die, a dot with a diameter of between $80 \mu\text{m}$ and $100 \mu\text{m}$ of CE3103WLV is dispensed on each of the PCB bond pads. Subsequently, the bare die is picked up from the wafer pack and placed precisely onto the PCB. The conductive adhesive is then cured. Afterwards, a portion of underfill encapsulant is dispensed between the PCB and the die. The underfill encapsulant FP4511 is cured. Next, the PCB is covered with EO1080 glob-top encapsulant, which is then also cured. The flip-chip assembly is then removed from the machine and tested for its functionality. Pictures of the process chain on the actual machine are presented in Appendix III.

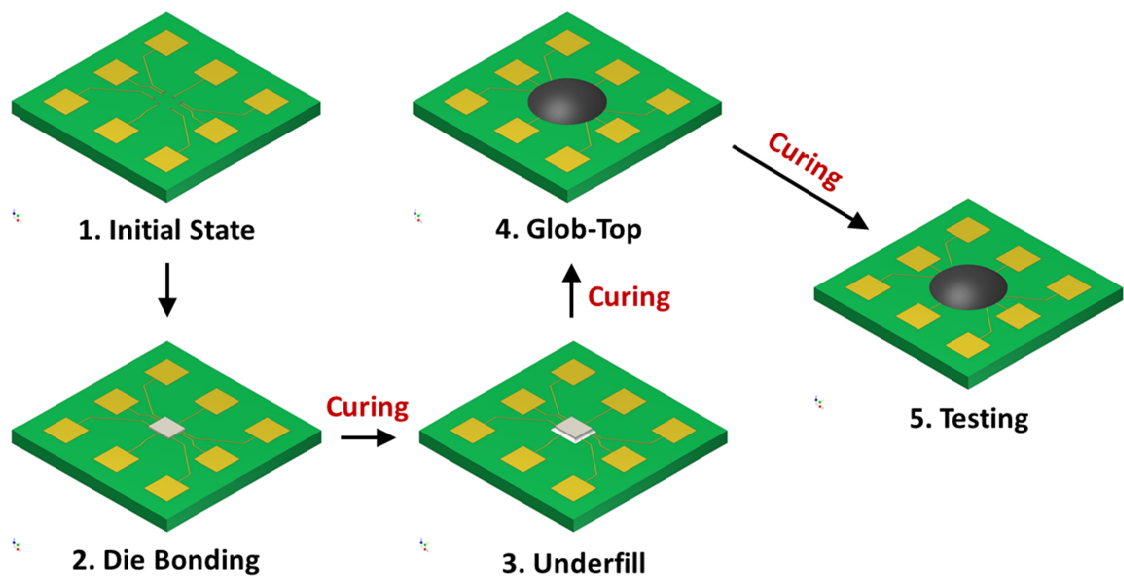


Figure 84 – Flip-chip test assembly process with test board

7.2.3 Die bonding

Eight dots of electrically conductive adhesive CE3103WLV have been dispensed onto the substrate. The average diameter of the dots was approximately 80 μm . The material has a high viscosity, a pasty consistency and is highly filled with silver particles. After a number of initial tests, a dispensing needle with a diameter of 110 μm was chosen. A pressure of 4.5 bar was applied for about 1 s onto the time–pressure dispenser. After this time, a drop formed on the needle tip. This drop was then precisely positioned onto the bond pad.

In the next step, the die was picked and placed from the waffle pack onto the bond pads and pressed against the PCB with a force of 5 N.

Initial testing of the curing process was performed with non-pulsed heating in the $\text{TM}_{1,1}$ mode with the temperature profile according to manufacturer’s data sheet (150 $^{\circ}\text{C}$ for 3 minutes). The duty cycle was initially set to 100% using the auto-tuning algorithm. Heating with the high duty cycle lead to extreme overshooting of the temperature and eventually melted the PCB (Figure 85 left).

Further tests were performed and the duty cycle was reduced stepwise. The conductive tracks on the PCB were extremely heated with duty cycles around 60% and melted the surrounding material. Burned tracks were observed with duty cycles over 40%.

Empirical testing eventually showed that a duty cycle around 30% was appropriate in this case, as the curing system was very capable of following the set temperature without overshooting (Figure 85 right).

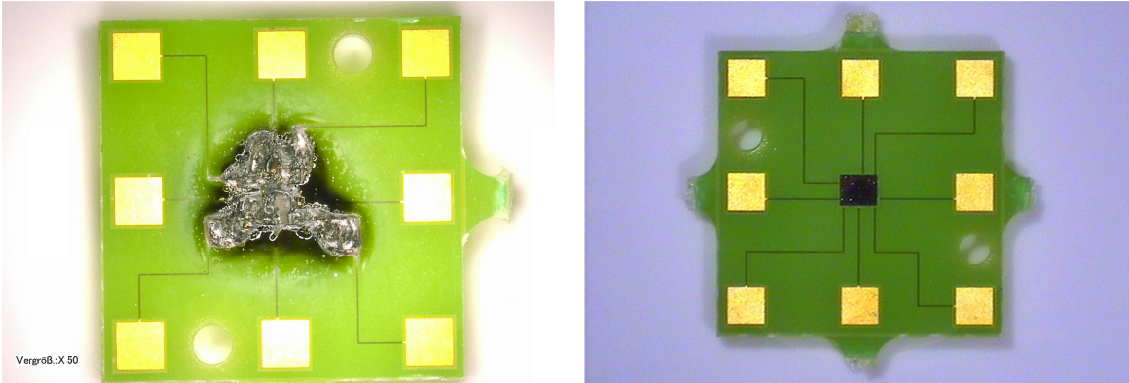


Figure 85 – Destroyed assembly (left) and flipped LM358 die on PCB (right)

The results of the die-bonding experiments show that the power output of the curing system needs to be controlled and adjusted to suit the application. With a suitable set of parameters, a rapid curing process can be achieved – providing the potential for low cycle times.

7.2.4 Underfill

The dispensing of underfill was performed with a 140 μm diameter needle. The underfill encapsulant FP4531 is suitable for gaps larger than 25 μm (FP4511 2010). The gap between the die and the PCB was between 26.3 μm and 31.4 μm .

Dots of underfill were dispensed on each of the four corners. The material was then cured with a temperature of 150 $^{\circ}\text{C}$ for 720 s, using a duty cycle of 30%. The material could be successfully cured. Figure 86 shows an assembly before and after cure of the underfill material.

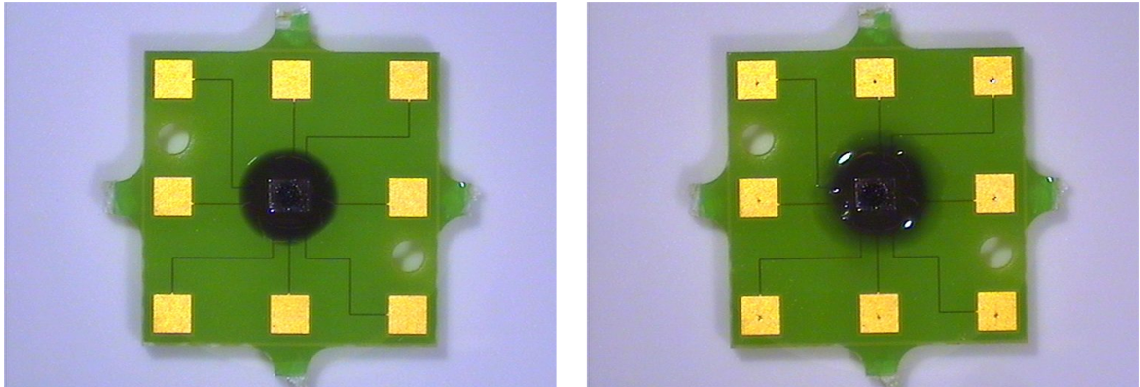


Figure 86 – Underfill on assembly before (left) and after (right) cure

7.2.5 Encapsulation

EO1080 encapsulant was applied on top of the centre of the chip with a 500 μm needle. The chip was fully covered with the encapsulant.

The chip was successfully cured for 480 s at 150 °C with a duty cycle of 75%. An assembly before and after curing of the encapsulant is shown in Figure 87.

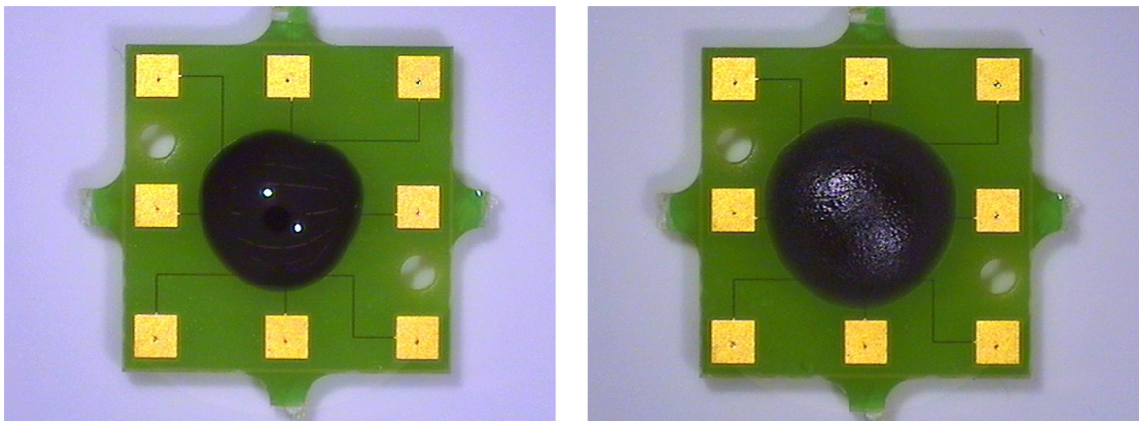


Figure 87 – Encapsulant on assembly before (left) and after (right) cure

7.2.6 Functional testing

Twelve chips were assembled in total using the microwave processes (samples ‘1’ to ‘12’). Additionally, two control samples using a convection oven were produced (C_1 and C_2). The chips were tested after each assembly step. An overview of the chip functionality is presented in Table 22. The testing was performed with an inverter circuit, whereby an input voltage of 10 V was inverted to -10 V. Deviations of the output voltage of 10% were tolerated, as these are normal variations according to the manufacturer’s data sheet (TI 2015).

Table 22 – Functionality of flip-chip samples

Sample No.	1	2	3	4	5	6	7	8	9	10	11	12	C ₁	C ₂
Process Step														
Die Bonding	✓	✓	✓	✓	✓	✓	✓	✓	✗	✓	✓	✓	✓	✓
Underfill	✓	✓	✓	✓	✓	✓	✗	✓	✗	✓	✓	✓	✓	✓
Encapsulation	✓	✓	✓	✓	✓	✓	✗	✓	✗	✓	✗	✓	✓	✓

Nine out of twelve samples were functional after the process. In sample 7, one of the two amplifiers did not survive the underfill process. In sample 9, no signal was obtained directly after die bonding. In sample 11, one amplifier was working normally after the encapsulation process, while the other amplifier was not found to be functional. The curing profiles of all chips were inspected, but did not show any significant deviations from the set cure profiles. Both control samples survived all processes.

For the microwave-cured samples, 91.7% of the assembly operations per process step were successful. Defect rates in this order are common for new processes and are always subject to optimization. The results show that the attempted flip-chip assembly was successful and that the proposed system is, in principle, applicable for flip-chip assembly.

7.3 Performance and effort comparison of microwave and reference heating methods

An assessment of the assembly performance and handling effort is performed on the representative flip-chip process described in Section 3.3.1. The handling times within the machine were assumed to be 3 s. The handling times between assembly machine and oven were assumed to be 60 s. The curing cycle time assumptions were as indicated in Table 23.

The convection curing cycle times correspond to the manufacturer’s guidelines. The microwave curing cycle times were derived from the findings described in Section 7.1.3. Underfill curing allows for slightly incomplete curing in the first pass, which is permissible according to JEDEC J-STD-030.

Table 23 – Assumed process durations for convection and microwave heating

Material Process	ECA (CE3103WLV 2011)	Underfill (FP4511 2010)	Encapsulant (EO1080 2010)
Convection	180 s	7200 s	1200 s
Microwave	240 s	360 s	240 s

7.3.1 Serial processing

The total process durations for the representative flip-chip process have been determined for convection and microwave heating. The results are shown in Figure 88 and Table 24.

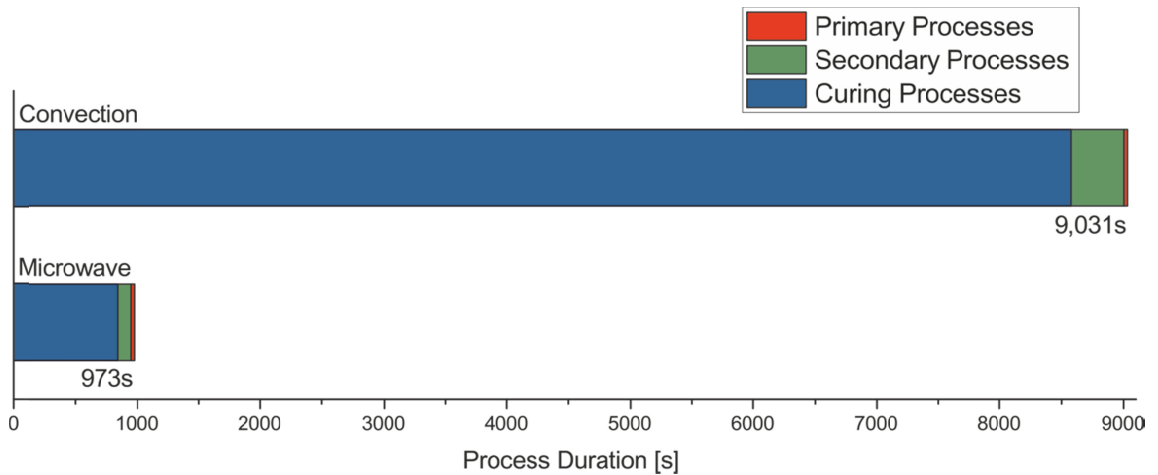


Figure 88 – Process durations of convection and microwave heating for single-piece processing

With the integration of the proposed microwave curing system, a drastic reduction of the overall processing time can be achieved. The microwave process requires 89.2% less time compared to the convection heating process. The convection heating process has a throughput of 0.4 parts per hour, while the microwave process provides a throughput of 3.7 parts per hour. A primary–secondary analysis is presented in Appendix II.

Table 24 – Process durations for serial processing

Process Type Process	Total Process Duration	Total Duration Of Primary Processes	Total Duration Of Secondary Processes	Total Duration Of Curing Processes
Convection	9031 s	8607 s	424 s	8580 s
Microwave	973 s	867 s	106 s	840 s

The time expenditure for primary processes consists of assembly operations and curing processes. Curing processes are regarded as primary processes, but are separately presented in this graph. As can be seen from Figure 88, the vast majority of the primary process duration is required for curing processes. The main reason for the reduced processing time lies in the drastically shorter curing cycle times of microwave curing processes. The assembly times were equal for both the convection and microwave heating processes.

The secondary processes are the handling processes. In this case, the machine with integrated curing system was compared to an external convection oven. The handling time between machine and oven was determined to be 60 s. The handling time within the machine was determined to be significantly lower with 3 s. In this case the handling times were reduced by the machine with integrated microwave curing system by 75%. In reality, the target product-handling effort between the individual processes could be completely eliminated.

Overall, the calculation shows strong advantages to the microwave process compared to the convection heating process for single-piece processing. The proposed microwave process has a higher performance, requires lower handling effort than conventional processes and requires less space.

7.3.2 Batch processing

Convection heating processes in microelectronics are typically performed in batches. The proposed microwave heating process is a serial process. To assess the performance of a serial microwave process relative to convection heating batch processes, the throughput for both cases has been calculated. The results are shown in Table 25.

With increasing batch size, the overall throughput of the convection process increases. A batch size of ten has approximately the same throughput as the microwave process.

For batch sizes larger than 10, the convection heating process has a higher performance than the microwave process.

The dimensions of the waveguide resonator can be adapted to larger sizes. In this way, batch processing would also be possible with the microwave process. For example, a waffle pack could be processed in one step with this method. To assess the performance of a batch microwave system, the throughput has been calculated for different batch sizes. Figure 89 shows the throughput for microwave and convection heating for different batch sizes.

The microwave process has, for all batch sizes considered, a significantly higher throughput than the convection heating process. The difference in throughput performance is particularly large in batch sizes below 1000. This corresponds to the capacity of typical magazines used in microelectronic packaging, such as waffle packs.

The serial microwave process is particularly suitable for low-volume scenarios, such as prototyping. A variant of the curing system, suitable for batches, would have distinct performance advantages and would require less handling effort.

Table 25 – Process durations for batch processing

Properties Process	Batch Size	Throughput [parts/h]	Total Primary Processes	Total Secondary Processes	Total Duration Of Curing Processes
Microwave	1	3.70	867 s	106 s	840 s
Convection	1	0.40	8607 s	424 s	8580 s
Convection	2	0.79	8634 s	458 s	8580 s
Convection	4	1.56	8688 s	526 s	8580 s
Convection	8	3.05	8796 s	662 s	8580 s
Convection	10	3.76	8850 s	730 s	8580 s
Convection	16	5.79	9012 s	934 s	8580 s
Convection	32	10.55	9444 s	1478 s	8580 s

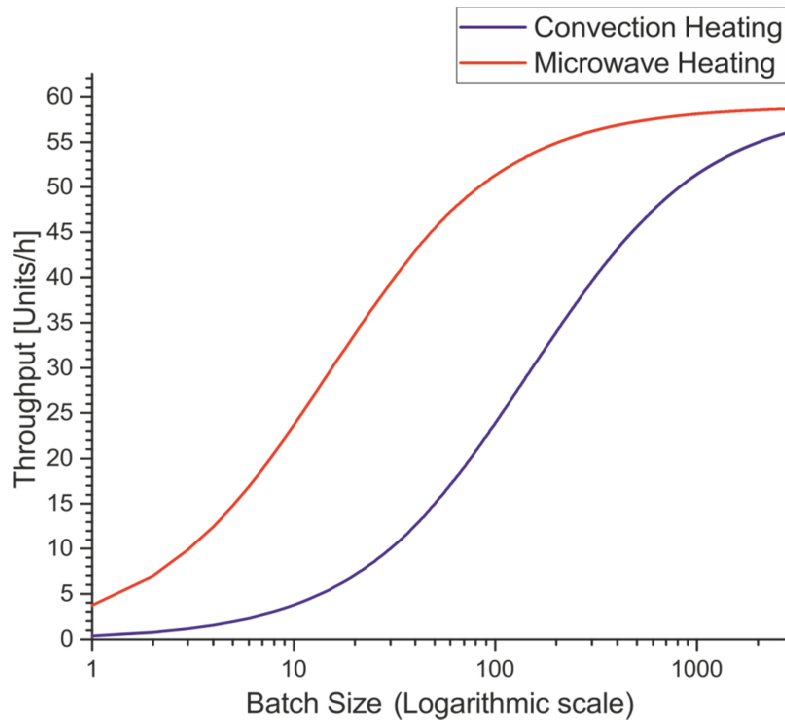


Figure 89 – Throughput for different batch sizes for microwave and convection heating

7.3.3 Conclusions

In single-piece processing, the performance of the reference process is drastically improved by a factor of 9.25 when applying microwave rather than convection heating. This can be mainly attributed to the drastic reduction in curing cycle times, which are now in the range of reflow processes. By integration of the curing equipment into a single machine, the product-handling effort between the individual processes has been completely eliminated. The system would be therefore particularly suitable for an implementation into existing lines to perform flip-chip-on-board assemblies. Since the integration criteria have been met, Requirement 5 is considered to be fulfilled.

In addition, batch processes were considered. A batch curing system would, hypothetically, provide distinct performance advantages, particularly for batch sizes up to approximately 1000 pieces per batch. This indicates potential for a system with an applicator capable of directly processing a whole magazine.

7.4 Reliability tests

To investigate the influence of microwave curing processes on the reliability of microelectronic components, a number of test samples have been produced and subjected to temperature cycling and highly accelerated stress testing. This has been

carried out in order to evaluate the performance of the method with regards Requirement 4.

7.4.1 Production of test samples

Within the flip-chip process, several bonding and curing processes take place. When investigating the reliability of the curing, these impose a high number of parameters. However, in order to assess the impact of the curing mode on the reliability of the resulting package, the number of parameters should be as low as possible. The number of processes is reduced by focussing the encapsulation process onto one process. Furthermore, a well-known and reliable package in combination with a reliable die are used in order to reduce their potential influence.

A commercial LM2940C 12 V voltage regulator, assembled in a QFN package, with dimensions of $5 \times 5 \times 0.9 \text{ mm}^3$, was chosen as a test product. An electrically conductive adhesive (CE3103WLV) was used as die-bonding agent. The voltage regulator die has six bond pads, which have been connected to the package using gold wires with a diameter of $25 \text{ }\mu\text{m}$. A dam, made out of an epoxy-based material, was applied by the package manufacturer. The chip, in this state, is ready for a cavity-fill encapsulation process. The assembly of the open chip was performed by Micros Components.

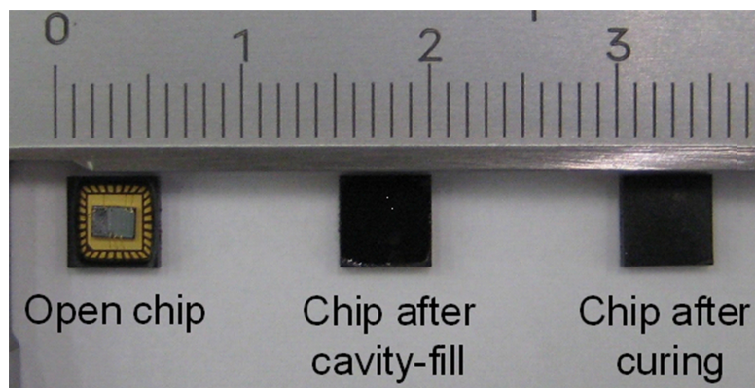


Figure 90 – Encapsulation of open QFN package

Eighty samples have been produced by dispensing Hysol EO1080 using a time–pressure dispenser. The samples were cured according to the profiles in Table 26. Profile 1 and Profile 2 were chosen based on experimental experience (Pavuluri et al. 2010a; Pavuluri et al. 2010b; Pavuluri et al. 2011). Profile 3 was chosen according to results from numerical simulation by Tilford *et al.*, which predicts a DoC above 99.9% (Tilford et al. 2010d; Tilford et al. 2011). Profile 4 was the reference profile in the convection oven according to the encapsulant manufacturer’s datasheet. The tests have been carried out

with the curing system set-up at Heriot-Watt University Edinburgh, which was used with a 50 W laboratory source (Pavuluri et al. 2012).

Table 26 – Produced samples for reliability tests

Profile Number	Type of Cure	No. of Samples	Ramp Rate [°C/s]	Set Temp [°C]	Hold Time [s]	Function After Cure
1	MW	20	1.66	150	100	OK
2	MW	20	0.65	150	180	OK
3	MW	20	0.4	150	669	OK
4	Oven	20	-	150	1200	OK

Each chip was tested once before curing and three times after curing. All samples were found to be functional before and after curing.

7.4.2 Temperature cycling test

Ten chips per profile have been subjected to a temperature cycling test based on JEDEC JESD22-A104. Figure 91 shows the parameters of the applied temperature cycle. These parameters correspond to ‘Test Condition H’. The high-temperature set point T_1 was 150 °C, while the low-temperature set point T_2 was -55 °C. A dwell time t_d of 600 s was chosen. The ramp rate was not controlled, as it is regarded as non-critical for component testing (JEDEC 2015). A total of 1000 cycles were conducted in tests carried out by IMT Bucharest. Intermediate functionality measurements were carried out every 50 cycles.

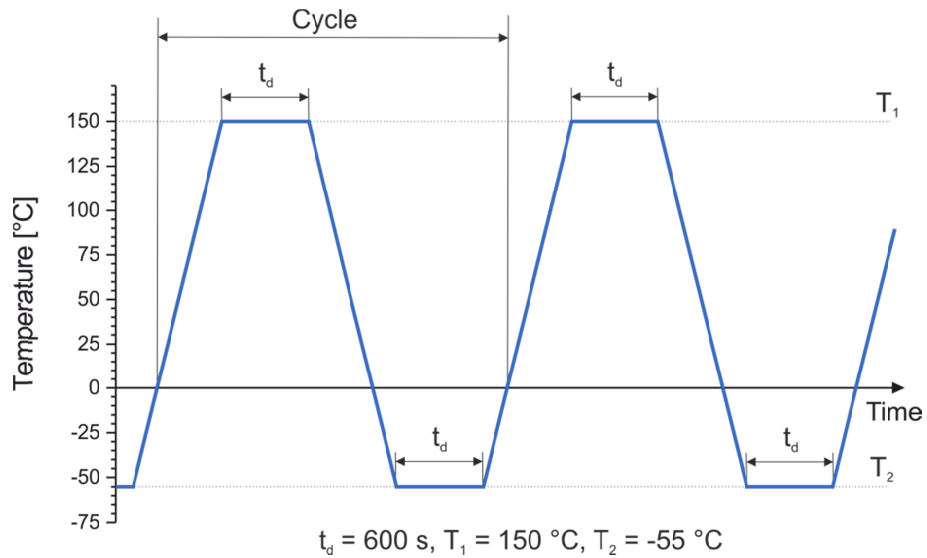


Figure 91 – Thermal cycling profile

The failure instances for each profile are depicted in Figure 92. After completion of the 1000 cycles, a total of 19 samples had failed. There were five failures for Microwave Profile 1, four failures each for Microwave Profile 2 and Profile 3. For the conventionally cured samples six failures were determined in total.

Two types of failures were identified: open circuit; and intermittent failures. Some of the components showing intermittent failures recovered temporarily after further thermal cycling before they completely failed. Visual inspection was performed on the failed components. A number of failed components displayed visually identifiable mechanical defects.

Figure 93 and Figure 94 show cracks on two different failed packages. The mechanical stresses induced by the temperature changes lead to propagation of cracks until eventually the electrical connection was broken.

Figure 95 shows a different kind of failure. This specimen shows a pore and a vaporized material that is scattered around the pore, covering the electrical contact.

Based on the analysis of the failures, a single failure mechanism can be identified: the continuity of the electrical contact.

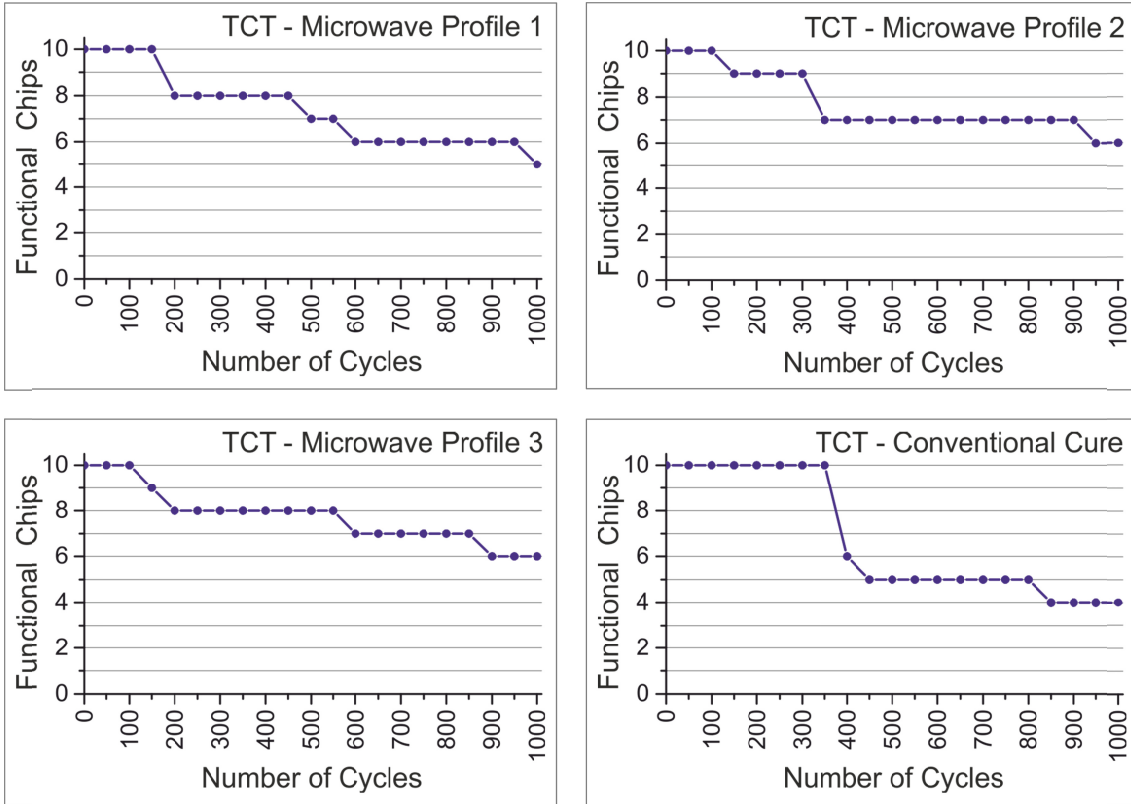


Figure 92 – Failures during the temperature cycling test

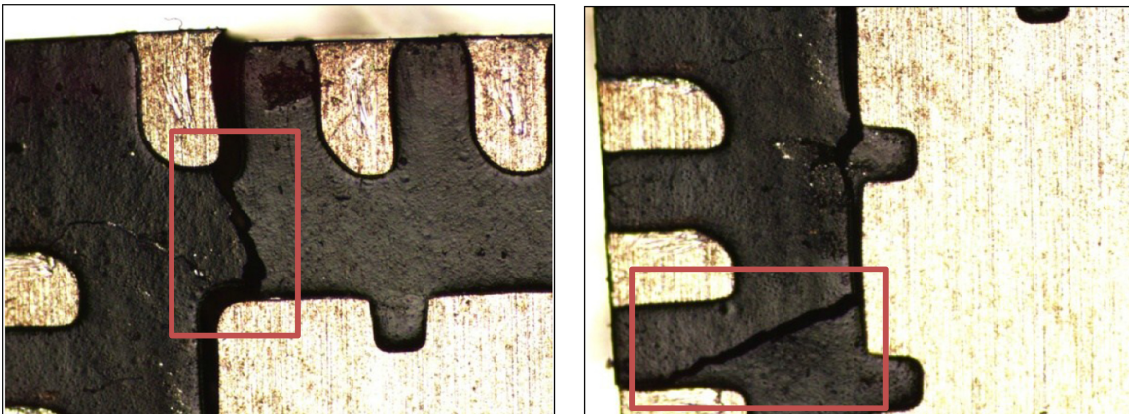


Figure 93 – Cracks on failed package – Microwave Profile 1, defect after 150 cycles (Sikiö et al. 2012)

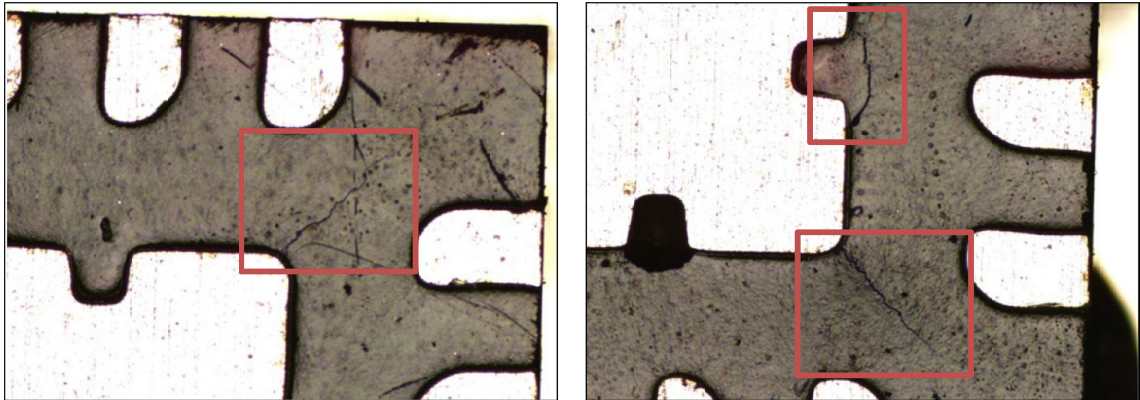


Figure 94 – Cracks on failed package – Microwave Profile 2, defect after 350 cycles (Sikiö et al. 2012)

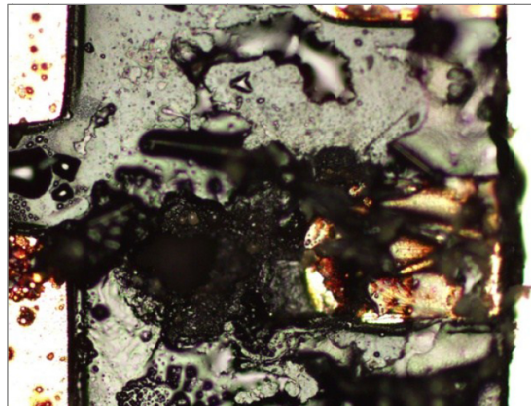


Figure 95 – Vaporized connection on failed package – Profile 3, defect after 150 cycles (Sikiö et al. 2012)

Based on the failure instances, the cumulative failures over the number of cycles have been calculated. According to Bajenescu and Bazu, the statistical distribution can be effectively approximated with a lognormal distribution (Bajenescu et al. 2012). Based on the method described by Bajenescu and Bazu (Bajenescu et al. 2012), the median values μ and the variance σ for all four cases were calculated. The approximations and the cumulative failures are presented in Figure 96.

The microwave-cured profiles show significantly higher median values compared to the conventionally cured samples ($\mu = 450$ cycles, $\sigma = 1.5$). Microwave Profile 1 showed a median value of $\mu = 1000$ cycles with a variance $\sigma = 1.8$. The median values of Microwave Profile 2 ($\mu = 1400$ cycles, $\sigma = 2$) and Microwave Profile 3 ($\mu = 1500$ cycles, $\sigma = 2.1$) showed further-improved reliability compared to Microwave Profile 1.

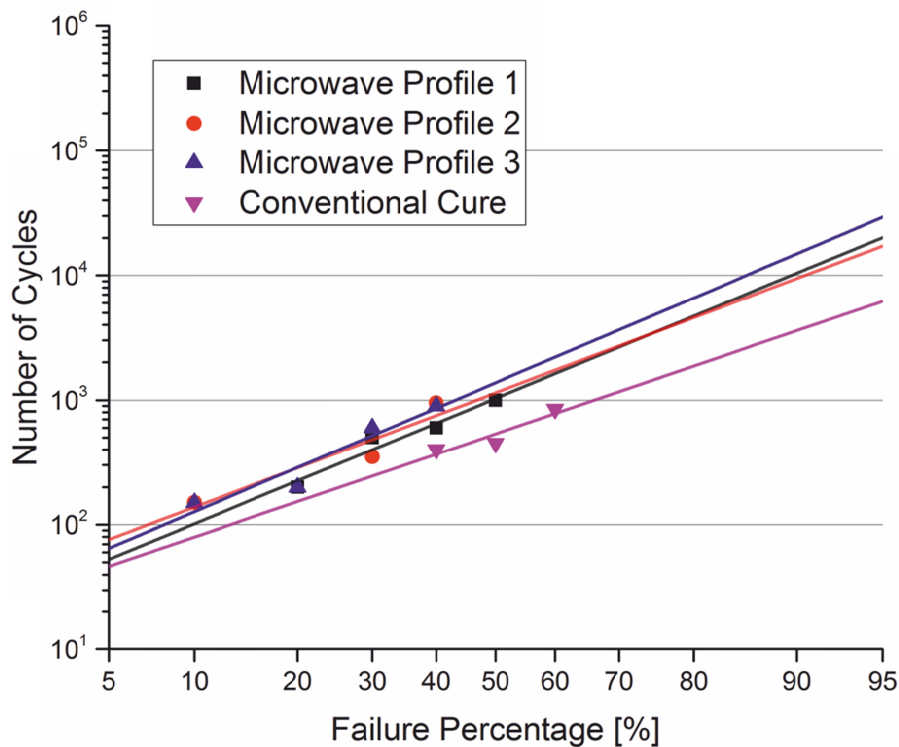


Figure 96 – Cumulative failures against number of cycles

7.4.3 Highly accelerated stress test

A highly accelerated temperature and humidity stress test (HAST) is performed for the purpose of evaluating the reliability of non-hermetic-packaged solid-state devices in humid environments (JEDEC 1999). It employs severe conditions of temperature, humidity, and bias, which accelerate the penetration of moisture through the external protective material (encapsulant or seal) or along the interface between the external protective material and the metallic conductors which pass through it (JEDEC 1999). The test is performed at a specified temperature and relative humidity, or pressure.

Ten chips per profile have been subjected to a HAST based on JEDEC JESD22-A110 (JEDEC 1999). The 40 test specimens were exposed to a temperature of 130 °C and 85% relative humidity for 96 hours. Initial and final measurements were performed. The tests were carried out by IMT Bucharest.

Before and after the test, all devices were functional. Therefore, no significant differences between the different curing methods and profiles were apparent. The microwave-cured samples passed the same test as the conventionally cured samples.

All 40 samples were then subjected to a temperature cycling test with the same parameters as described in Chapter 7.4.2. The failure instances for each profile are depicted in Figure 97. After completion of the 1000 cycles, a total of 18 samples had

failed. There were three failures for Microwave Profile 1, and five failures each for Microwave Profile 2 and 3. For the conventionally cured samples, seven failures occurred.

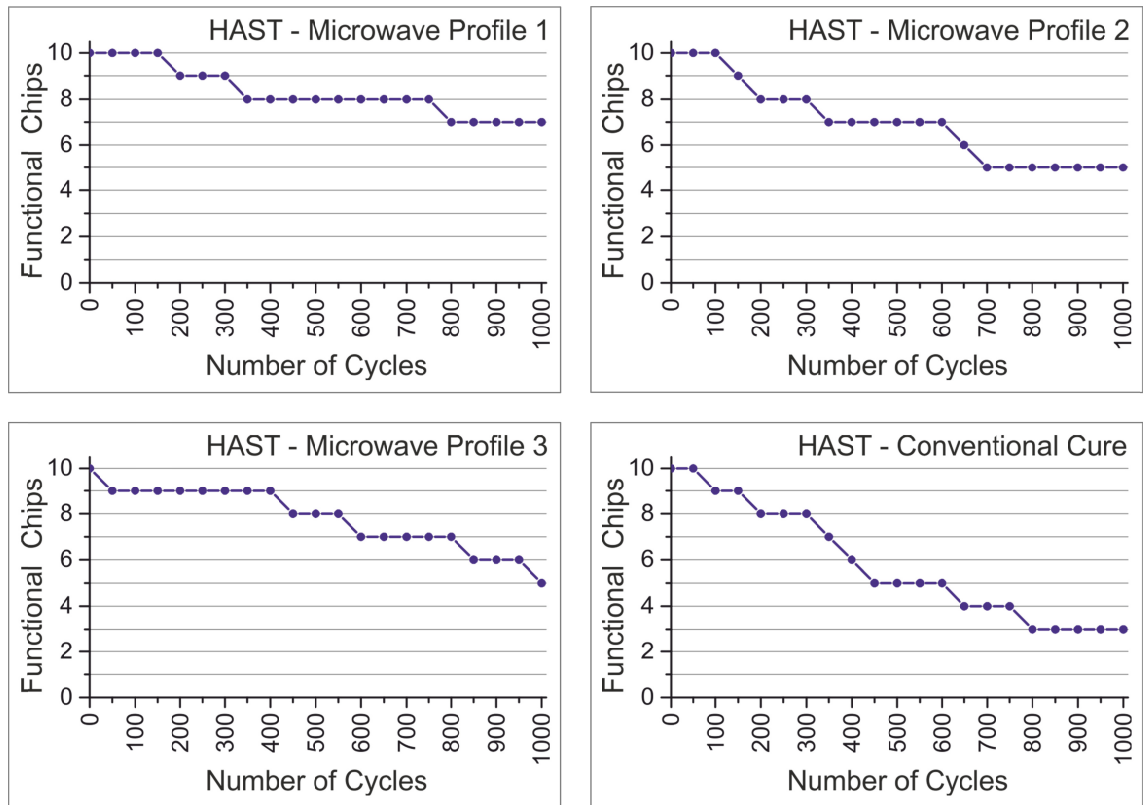


Figure 97 – Failures during HAST test

The cumulative failures over the total number of cycles have been calculated with the same method as in Chapter 7.4.2. The median values μ and the variance σ for all four cases were calculated. The approximations and the cumulative failures are presented in Figure 98.

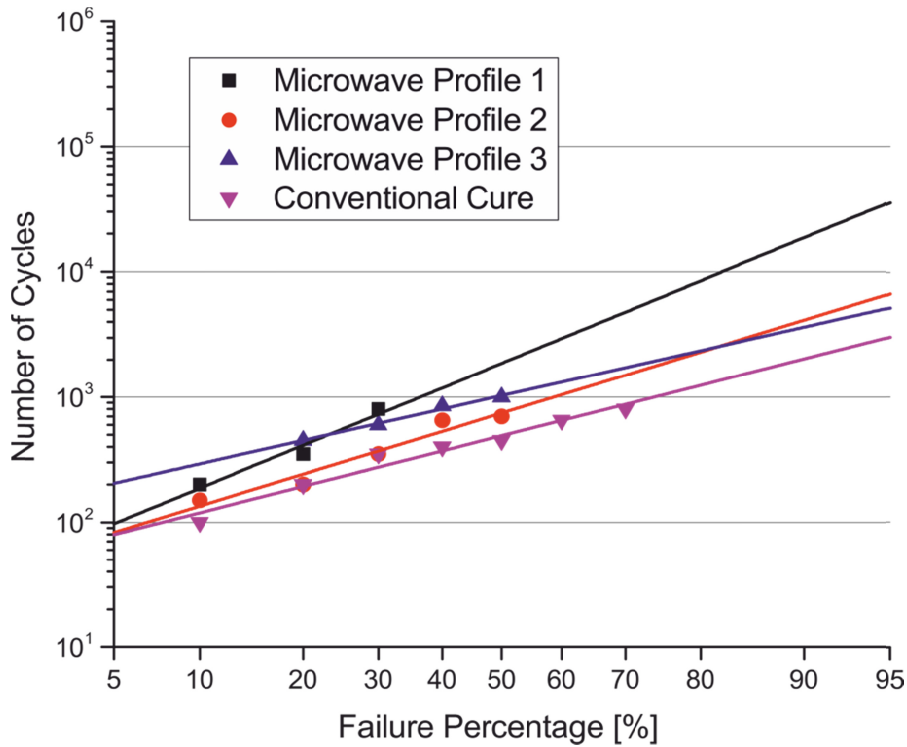


Figure 98 – Cumulative failures against number of cycles after HAST

Similarly to the temperature cycling tests, the microwave-cured profiles show a significantly higher median value compared to the conventionally cured samples ($\mu = 450$ cycles, $\sigma = 1.2$). Microwave Profile 1 showed a median value of $\mu = 1600$ cycles with a variance $\sigma = 1.7$. The median values of Microwave Profile 2 ($\mu = 700$ cycles, $\sigma = 1.3$) were significantly lower compared to the other microwave profiles. Microwave Profile 3 ($\mu = 1000$ cycles, $\sigma = 1$) showed a significantly higher median time than Microwave Profile 2, but a lower median time than Microwave Profile 1.

7.4.4 Overview of reliability tests

The temperature cycling test results obtained indicate a significantly higher reliability than conventionally cured samples. An overview of the test results is shown in Table 27. An extended version of the table including Weibull analysis is presented in Appendix IV. The results show, despite the comparatively small sample size, a significant effect with high magnitude on the reliability according to the applied, industrially accepted, testing methods. Therefore, it is preliminarily concluded that Requirement 4 is fulfilled.

Table 27 – Overview of reliability test results

Profile	Microwave Profile 1	Microwave Profile 2	Microwave Profile 3	Conventional Profile
Reliability Tests				
HAST Test (130 °C, 85% RH for 96 hours)	✓	✓	✓	✓
Number of defective parts	0	0	0	0
TCT (Lognormal)				
Mean life μ [cycles]	1000	1400	1500	450
Standard deviation σ	1.8	2	2.1	1.5
TCT after HAST (Lognormal)				
Mean life μ [cycles]	1600	700	1000	450
Standard deviation σ	1.7	1.3	1	1.2
✓ – Fulfilled, o – Partly fulfilled, ✗ – Not fulfilled				

7.5 Stress measurement

Results from reliability testing have shown a significantly improved reliability of microwave-cured packages compared to conventionally cured packages. A potential explanation could be reduced residual stresses caused by microwave curing compared to those of oven curing. As microwave curing provides volumetric heating, it is suspected that it thereby provides a more uniform curing process, with lower residual stresses compared to convection heating.

7.5.1 Stress-measurement chips

To measure and to subsequently optimize these residual stresses, a number of stress-measurement chips have been developed within the last decade (Jaeger et al. 2000; Schwizer et al. 2003; Chen et al. 2006; Hirsch et al. 2006; Kittel et al. 2008b; Majcherek et al. 2009; Niehoff et al. 2009; Gieschke et al. 2010).

One of these systems has been developed at Fraunhofer IZM as part of the BMBF-funded project iForceSens (Kittel et al. 2008a). The main components of the system are a calibrated test chip and an ASIC control unit (Schreier-Alt et al. 2013).

The test chip itself was fabricated using CMOS technology and contains orthogonal stress-sensitive current mirrors (Kittel et al. 2008a). An external mechanical load causes an asymmetry of the current mirrors (Majcherek et al. 2009). The change in the drain current within these orthogonal Si-MOSFETs is described by the theory of piezoresistivity of silicon:

$$R_{ij}(\sigma) = R_0 \cdot \left(1 + \sum_{k,l} \pi_{i,j,k,l} \cdot \sigma_{k,l} \right) \quad (26)$$

where σ is the stress, π is the piezoresistive tensor and R is resistance (Suhling et al. 2001). By a series of four-point bending tests of silicon strips with defined orientations and at various temperatures, the piezoresistive tensors have been determined as part of the project iForceSens (Kittel et al. 2008a).

The stress sensor ASIC is structured with an array of orthogonally oriented nMOS and pMOS structures. The nMOS transistor channels are oriented along the [010] and [100] silicon crystal directions and are used to calculate the in-plane shear stress τ_{xy} as described by Equation (27) (Schreier-Alt et al. 2013). The pMOS transistor channels are aligned in the [-110] and [110] direction and are used to determine the in-plane normal stress $\sigma_{xx} - \sigma_{yy}$ as described by Equation (28) (Schreier-Alt et al. 2013).

$$\tau_{xy} \approx \frac{-1}{\pi_{11}^{(n)} - \pi_{12}^{(n)}} \frac{I_{out} - I_{in}}{I_{out} + I_{in}} \quad (27)$$

$$\sigma_{xx} - \sigma_{yy} \approx \frac{2}{\pi_{44}^{(p)}} \frac{I_{out} - I_{in}}{I_{out} + I_{in}} \quad (28)$$

$$\sigma_{xx} + \sigma_{yy} \approx \frac{2}{\pi_{11}^{(n)} + \pi_{12}^{(n)}} \left(1 - \frac{I_{in} + I_{out}}{2I_0} - \pi_{12}^{(n)} \sigma_{zz} \right) \quad (29)$$

By determination of the sum of the in-plane normal stresses as described by Equation (29), it becomes possible to calculate the normal in-plane stress components σ_{xx} and σ_{yy} (Schreier-Alt et al. 2013). The calculation of the components can be performed with an accuracy of 13%, while shear stress and normal stress differences can be calculated with an accuracy down to 4.5% and 1.2%, respectively (Kittel et al. 2008a). These accuracies apply as long as the stress component σ_{zz} normal to the chip surface is negligible (< 10 MPa) or is known and the temperature is measured correctly (Schreier-Alt et al. 2013). The measurement accuracy further depends on the integration time during measurement (Suhling et al. 2001).

7.5.2 Preparation of samples for stress-measurement tests

Different versions of this particular stress chip are available, which offer different arrays of measuring cells (Schreier-Alt et al. 2013). A version with dimensions $1.13 \times 1.11 \text{ mm}^2$, was chosen for further experiments, as the dimensions of the chip are comparable to those of the previously used voltage regulator die. A total of 104 stress-measurement dies were packaged in the same open QFN packages as were used for the reliability tests. The chips were die-bonded to the package using Henkel CE3103WLV isotropically conductive adhesive. The four die contacts were wire bonded to the chip casing using $25 \text{ }\mu\text{m}$ gold wire.

The initial stresses on the open packages were measured as a zero-level reference. In summary, 95 packages were encapsulated with the same four curing profiles as used for the reliability tests. The curing system from Heriot-Watt University was used for these experiments with a 50 W source (Pavuluri et al. 2012). For each of the microwave profiles, 25 samples were produced and 20 chips were cured using the conventional profile. A total of four chips were discarded as these had either visible voids or strongly irregular surfaces (three from Profile 1, and one from Profile 2). Table 28 shows an overview of the produced samples and the cure profiles applied.

Table 28 – Produced samples for stress-measurement tests

Profile Number	Type of Cure	No. of Samples	Ramp Rate [°C/s]	Set Temp [°C]	Hold Time [s]
1	MW	25	1.66	150	100
2	MW	25	0.65	150	180
3	MW	25	0.4	150	669
4	Convection	20	-	150	1200

The stress was measured for each of the encapsulated chips. One stress chip from Profile 2 was not readable and was discarded. All other stress chips were readable.

7.5.3 Results

The distributions of the in-plane normal stresses σ_{xx} and σ_{yy} , as well as the distributions of shear stresses τ_{xy} were determined for each chip. All components of the plain stress tensor σ are thereby known. Based on the individual components of the stress tensor, an equivalent stress can be calculated – facilitating a comparison of the stress between

different chips. Different hypotheses for the calculation of the equivalent stress were considered. The previously identified failure mechanisms are the cracking of polymer structures and subsequent breaking of wire bonds (see Chapter 7.4.2). The silicon die itself is not affected; therefore, the relevant materials for the equivalent stress are the surrounding polymers and the metallic wires. Both of these materials can be regarded as ductile (Callister et al. 2012). For these type of materials, the equivalent stress σ_v can be calculated according to the von Mises formula for equivalent stress (Dowling 1993). The planar distributions of the von Mises equivalent stress σ_v have been calculated for each chip.

The arithmetic mean distributions for each profile and their standard deviations (SD) are presented in Figure 99, Figure 100, Figure 101 and Figure 102.

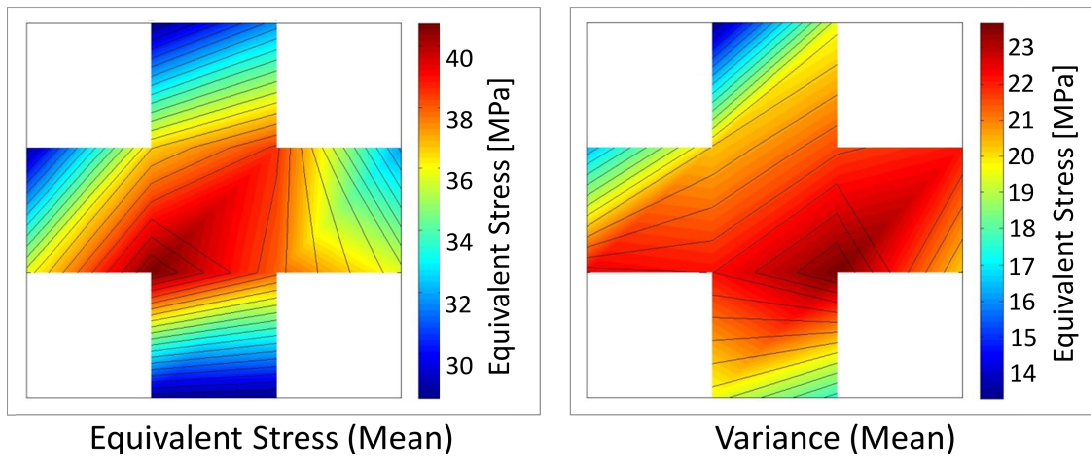


Figure 99 – Equivalent stress (left) and SD of Microwave Profile 1 (right)

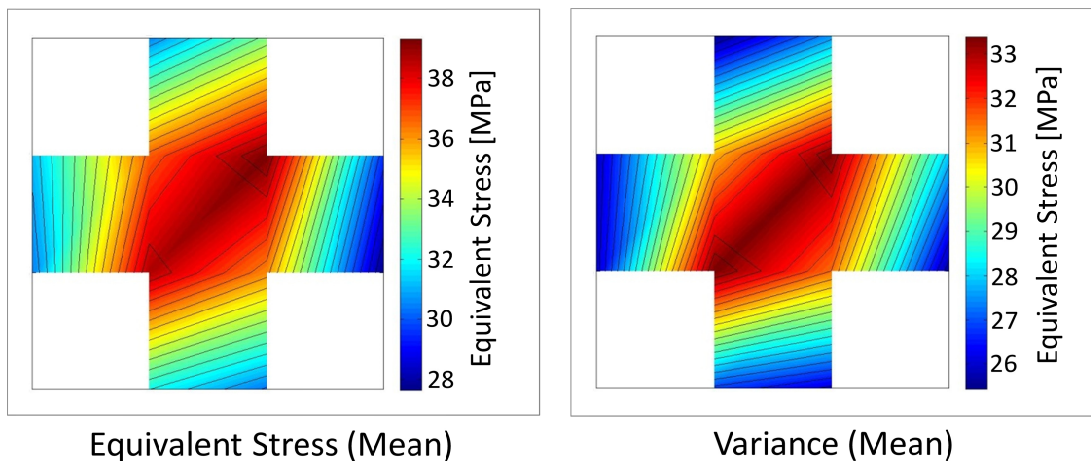


Figure 100 – Equivalent stress (left) and SD of Microwave Profile 2 (right)

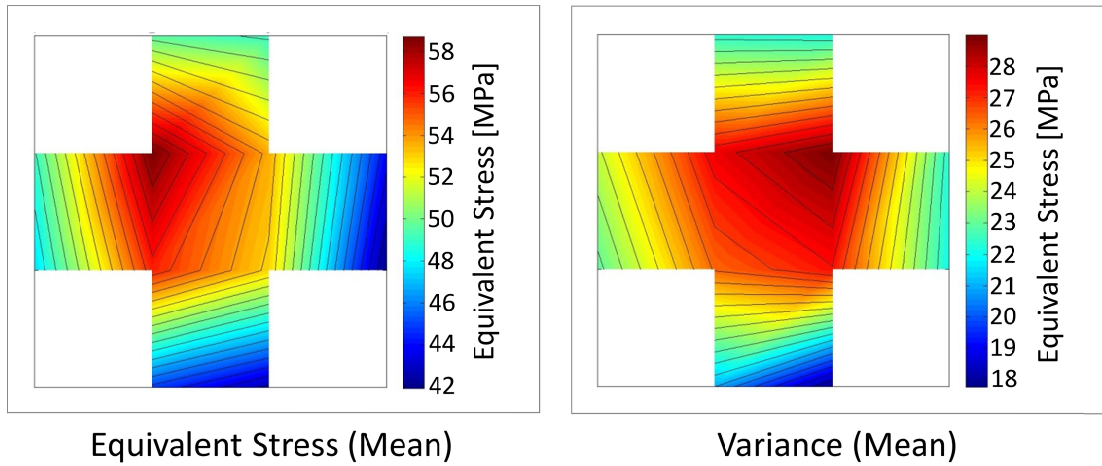


Figure 101 – Equivalent stress (left) and SD of Microwave Profile 3 (right)

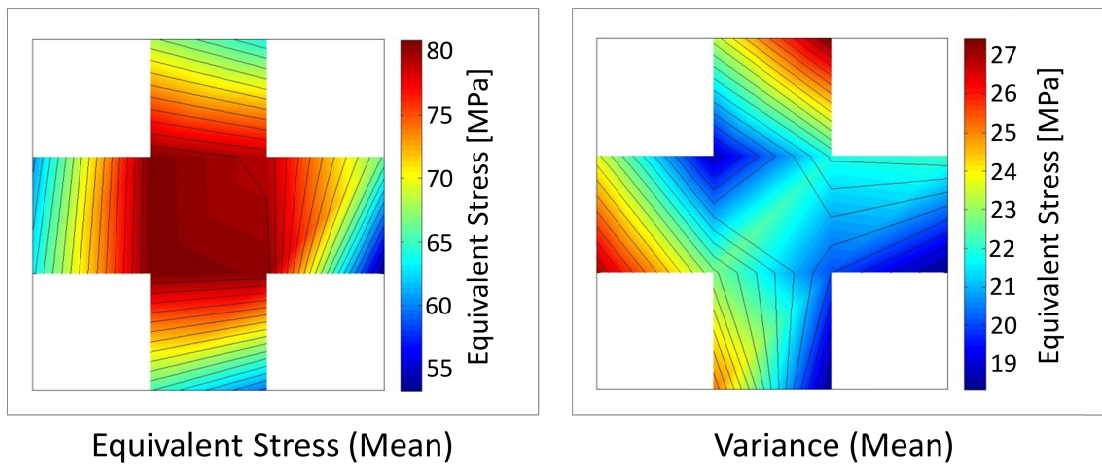


Figure 102 – Equivalent stress (left) and SD of conventional cure profile (right)

The mean distributions of all four cure profiles show a maximum stress in the centre of the chip and reduced stress towards the edge. This corresponds roughly to the previously described model of a uniformly loaded beam, supported at its ends (Kittel et al. 2008a).

An overview of the stresses measured in all four profiles is presented in Figure 103. Microwave Profile 1 shows stress values between 29 MPa and 40.5 MPa. The measurements of Microwave Profile 2 result in values between 26 MPa and 39 MPa. Microwave Profile 3 shows significantly higher values of between 42 MPa and 58.3 MPa. The conventionally cured reference profile yields values between 54 MPa and 80.5 MPa.

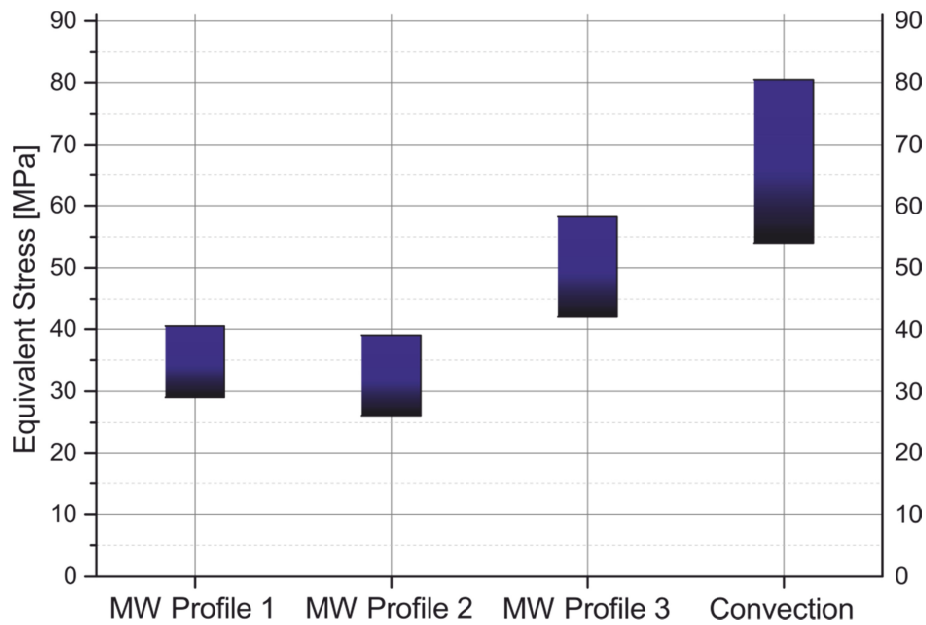


Figure 103 – Overview of measured stresses

The stresses occurring in the microwave-cured profiles are therefore significantly lower compared to the stresses in the conventionally cured samples. While the stresses in the packages cured with Profile 1 and Profile 2 are in the same range, Profile 3 shows a significantly higher stress compared to the first two profiles.

The variances are large compared to the measured values for both the microwave-cured samples and the oven-cured samples. This suggests that the distribution of stresses varies largely, due to the assembly process. Potential sources for this variance are:

- Die dimensions.
- Position and orientation of die after bonding.
- Amount of conductive adhesive used for die bonding.
- Amount of encapsulant.
- Residual stresses in the open package.
- Dimensions of the open package.
- Stress induced by the test socket.
- Defects in the package, such as delamination.

Since the variances for microwave and conventionally cured packages are in the same range and a high number of plausible causes exist, they can likely be attributed to the assembly process and the test socket.

The significantly lower stresses within the microwave-cured packages correlate with the improved reliability determined in the TCT and HAST tests. It can therefore be concluded that the proposed method of microwave curing induced less stress than

convection oven curing. The results of the conventional cured packages are in a comparable range as values obtained for transfer moulding of QFN packages (Schreier-Alt et al. 2013).

7.6 Assessment of results

In this chapter, it has been experimentally demonstrated that the proposed microwave heating system can be successfully applied to cure typical adhesives in electronic packaging. Furthermore, the integration of this system into precision assembly systems was successfully demonstrated, reducing the number of handling steps, which is particularly beneficial for lower volumes or prototyping. Microwave curing was successfully applied for the intermediate curing steps of flip-chip assemblies. Thermal cycling and HAST tests indicated an improved reliability compared to conventional curing.

The requirements identified in Chapter 3 are manifest in the design and build of the system and have been fulfilled. Table 29 illustrates the fulfilment of each requirement.

Table 29 – Assessment of fulfilment of requirements

Requirement	Description	Status
1	Reduction of curing cycle times down to the duration of reflow processes according to J-STD-020E	Fulfilled ✓ → Section 7.1
→ ECA, underfill and encapsulant materials can be cured with the proposed microwave curing system with drastically reduced cycle times – below 420 s – compared to convection oven curing, albeit with potential for process optimization.		
2	Controlled heating of the polymer adhesive according to a defined temperature profile within an industrially relevant range of process parameters	Fulfilled ✓ → Section 7.1
→ Heating processes can be performed with the proposed microwave curing system according to the defined range of temperature profiles, with closed-loop control of temperature and resonant frequency, and without the occurrence of arcing and sparking.		
3	Selective heating with reduction to target temperature within clearance area	Fulfilled ✓ → Section 7.1.4
→ Selective heating is achieved by the confined geometry of the applicator and a potential selectivity by materials with a high loss tangent. Reduction to target temperature within specified distance was achieved.		
4	At least the same reliability as conventional technologies	Fulfilled ✓ → Sections 7.4, 7.5
→ Microwave-cured QFN packages have lower internal stresses than packages cured in a convection oven, which significantly improves performance in thermal cycling and HAST tests.		
5	Integration of all process components into a single machine, particularly the curing equipment	Fulfilled ✓ → Sections 6.5, 7.2
→ The combination of automated assembly and microwave curing equipment is possible, enabling microelectronic packaging processes such as flip chip to be implemented, with distinct advantages regarding process performance.		

Prior to an industrial exploitation, an economic assessment of the proposed method and the connected machinery against potential alternatives is to be carried out. This requires target definitions to be performed beforehand, as these mainly define the functionality and properties of the applied process and machinery. Only then the application of the prototype in an industrial setting is possible.

7.7 Progress beyond the state of the art

The method proposed in this work integrates a novel microwave curing system into a precision assembly machine.

Within this work a machine-integrable microwave curing system is developed. In contrast to existing microwave heating and curing systems, the presented concept applies an open-ended microwave applicator. This novel approach enables the effective processing of single components, without the necessity for intermediate handling steps.

The control system implements temperature control, power control functionalities and novel methods for the frequency control, which allow optimization of the efficiency of the system and enables preventive measures against arcing and sparking. The concept and the realization of the curing system – capable of being integrated into a machine – are novel and represent significant progress beyond the current state-of-the-art equipment. The novel control system exceeds the capabilities provided by existing microwave curing systems and therefore represents significant progress.

A concept of a machine integrating the proposed curing system has been developed. Using the example of a flip-chip assembly process, a process chain with intermediate microwave curing steps was developed. A prototype precision assembly machine was built, integrating the microwave curing system to provide the proposed process chain. The proposed system is the first of its kind and represents significant progress beyond the state of the art as there is currently no precision assembly machine with integrated microwave curing equipment available.

In the course of the experimental validation of the system, several new aspects have been investigated. For the first time, experimental tests have been performed to discover the occurrence of arcing or sparking and investigate its possible prevention. The proposed novel flip-chip assembly process has been experimentally verified. For the first time, a number of QFN packages have been prepared using the open-ended applicator and tested for reliability. In another experiment, stress-measurement chips have been packaged, cured with the microwave curing system, and subsequently

analysed. The experiments carried out with the proposed microwave curing system are novel and represent a significant progress beyond the current state of the art.

A summary of the achieved progress is compiled in Table 30 (for the microwave curing system), Table 31 (for the machine with integrated curing system) and Table 32 (for the experimental validation).

Table 30 – Progress beyond state of the art regarding curing system

Microwave Curing System	
State of the Art	Progress Beyond State of the Art
Commercial batch microwave curing systems and laboratory-scale microwave curing system with open-ended resonator (Section 4.1.4)	Machine-integrable microwave curing system with open-ended microwave resonator and solid-state microwave source (Section 5.2)
No integrated temperature measurement in open-ended resonator. Temperature measurement inside heated material (Section 4.1.4)	Integration of pyrometer into open-ended resonator. Non-contact measurement of temperature (Section 6.1.3)
Frequency control strategies comprise constant frequency, pulsing and frequency sweeping (Section 4.1.4)	Implementation of constant frequency, pulsing, frequency sweeping and frequency hopping (Section 5.4)
No tracking of resonant frequency (Section 4.1.4)	Auto-tuning of the resonant frequency for maximum power output (Section 5.3.1)

Table 31 – Progress beyond state of the art regarding the proposed machine

Precision Assembly Machine with Integrated Microwave Curing System	
State of the Art	Progress Beyond State of the Art
Precision assembly and microwave curing are performed in separate machines (Sections 4.2 and 4.3)	Assembly machine with integrated microwave curing process has been proposed (Sections 6.3, 6.4 and 6.5)
There is currently no combined precision assembly and microwave curing strategy (Section 4.1.4)	An absolute assembly strategy with intermediate microwave curing steps for flip-chip assemblies has been proposed (Section 5.5.9)
Product handling between process steps is usually necessary, particularly between the assembly and curing steps (Sections 4.2 and 4.3)	No intermediate product handling necessary (Section 7.2)

Table 32 – Progress beyond state of the art regarding experimental validation

Experimental Validation	
State of the Art	Progress Beyond State of the Art
Open-ended resonator shown to cure EO1080 encapsulant and FP4511 underfill (Section 4.1.4, (Pavuluri et al. 2012))	It was demonstrated that encapsulant, underfill and ICA can be cured with the proposed system. Microwave curing has significantly reduced curing cycle times for selected materials (Section 7.1.3)
Occurrence of arcing and sparking with open-ended resonator has not yet been investigated (Section 4.1.4)	Experiments with high-speed camera have been performed. No arcing or sparking occurred during processing of several microelectronic parts. Occurrence cannot be fully excluded, but preliminary results indicate no detrimental effects due to microwave curing (Section 7.1.5)
Commercial batch processing systems achieve partial selectivity through material properties, mainly the loss tangent. Effect is weakened by frequency sweeping (Section 4.1.4, (Mead et al. 2003))	Open-ended resonator allows application of energy in confined area. Also, due to loss tangents, material-selective heating is possible. Has been proven by thermal imaging (Section 7.1.4)
No assembly of microelectronic packages performed with open-ended resonator system. Broad spectrum performed with batch system (Section 4.1.4)	Flip-chip process chain with intermediate microwave curing steps has been performed with proposed machine. Process is not fully stable yet, but feasibility has been demonstrated (Section 7.2)
Reliability of components cured with open-ended microwave resonator system unknown (Section 4.1.4)	TCT and HAST testing of microwave-cured and conventionally cured QFN was performed. Microwave-processed parts showed improved reliability compared to control (Section 7.4)
Possible influence of microwave curing on the residual stresses of cured materials is unknown. Positive influence and hence lower residual stresses are suspected (Section 4.1.4)	Encapsulation of stress-measurement chips into QFN packages was performed. Microwave-cured packages show significantly lower stresses than conventionally cured packages (Section 7.5)

8 Summary and Outlook

8.1 Summary

Driven by the continuous trend for miniaturization with concurrent functional integration, the field of advanced electronic packaging continues to gain prevalence. The processes in use today are efficient for mass production, but are not suitable for the purposes of low volume and prototype production.

The need for expensive masks and tooling in advanced packaging processes can be obviated by the application of adhesives, where bonding processes can be employed with significantly greater flexibility, particularly for lower-volume production. A significant drawback of adhesive bonding is the duration of the curing processes.

A typical assembly process of an electronic package (a flip-chip process, for example) requires numerous heating cycles to cure the adhesive and encapsulant materials. These heating cycles extend from several minutes to several hours, representing a clear bottleneck in the production of microelectronic assemblies.

Moreover, the system technology typically applied in electronics packaging today is implemented by a number of separate stations, with each station carrying out one part of the process chain. While this approach is efficient for batch production, when considering lower-volume production, a number of drawbacks become apparent.

To overcome these problems, a novel method for the assembly of electronic packages and MEMS is required, one that improves the efficiency of assembly processes and reduces the handling effort between the separate process steps.

The domain of electronic packaging was analysed in Chapter 3 and surface-mount devices were identified as being of particular interest. Since flip-chip assemblies involve the same characteristic base processes as complex multi-chip assemblies, the flip-chip process is an appropriate reference process. A detailed analysis of the flip-chip process revealed ECA interconnects, underfill and encapsulation as key adhesive-application processes within the flip-chip assembly process. Curing of the respective pastes requires precise control according to defined temperature profiles and these curing cycles often last for several hours – this was identified as the main subject for optimization. Another important aspect is reliability; the assembly should be exposed to minimal stress, which

should ideally be confined to the volume of interest – the cured paste itself. Reliability of the electronic assembly must not be affected.

The assembly process is analysed from the production perspective. Through means of a primary–secondary analysis, a considerable number of handling processes were identified, the majority of which involved the transport of the product assembly to an oven for curing. This drastically reduces the performance of the process for low-volume production carried out using separate stations.

A review of the current state of the art in Chapter 4 revealed that, besides convection heating, which is in common usage, numerous other methods exist for the curing of pastes in electronic packaging. Each of the methods has distinct advantages, but none currently provide a solution to the requirement profile identified in the present study. A review of state-of-the-art packaging machines showed that integration of curing equipment into the assembly machines is not currently available.

The concept of a curing system and its machine integration was developed in Chapter 5, where basic heating processes were discussed and assessed and microwave heating was selected. The main components for the system were identified and viable options for these components were assessed and selected according to the requirements. An open-ended cavity was selected for the applicator. A control concept was developed around the components of the heating system comprising frequency, temperature and power control.

The machine concept was developed based on the curing system and the specific requirements of the machine were analysed. The processes needed for the assembly of microelectronic packages were studied and proposals were made for specific subsystems to carry out these processes. A positioning strategy was developed with the proposed process tools and, based on the example of flip chip, an example process chain was proposed. An initial machine concept was then derived.

A prototype for an integrable microwave curing system was developed and implemented; this is described in Chapter 6. The RF power was provided by a solid-state microwave source and an applicator with integrated pyrometer sensor was designed and built. Diode sensors for measurement of inbound and outbound power were integrated and a PLC control system was developed that implemented different algorithms for temperature and frequency control.

Based on an existing precision placement system, a machine providing assembly and curing processes in one system and the associated process tools were designed and built. The curing system was integrated physically and interfaced with the control system. A

control software for the complete integrated system was developed. In so doing, a first-of-its-kind assembly machine with integrated microwave curing system was proposed.

The basic function of the curing system is evaluated in Chapter 7. Testing showed all of the temperature and frequency control functionality to be operational.

Three representative materials were selected for the curing tests: an ECA; an underfill; and an encapsulant material. All three materials were successfully cured using the proposed microwave curing system and all three saw improved cure rates compared to conventional methods.

The occurrence of arcing and sparking was experimentally tested with different parameters on different relevant components. Neither by electrical measurement, nor by a high-speed camera, could arcing or sparking be observed. The occurrence of arcing and sparking, and their potentially detrimental effects, cannot, however, be fully excluded, although there is no indication of undesired destructive arcs or sparks during microwave processing with the proposed curing system.

The proposed flip-chip process with microwave curing was subject to testing with twelve sample assemblies and it was shown that the complete process chain could be successfully realized. The principal feasibility of the proposed flip-chip process with intermediate microwave curing was proven.

A series of reliability tests (thermal cycling, HAST) were carried out on QFN packages encapsulated with EO1080. Three microwave profiles and a reference conventional profile were used. The results showed that the microwave-cured samples delivered a significantly higher level of reliability.

To investigate the improved reliability of the microwave-cured packages, another set of samples was prepared with the same curing profiles, but with packaging stress-measurement chips. The results showed that the microwave-cured profiles have consistently lower internal stresses than conventionally cured samples. A possible explanation for this is that volumetric heating causes significantly lower residual stresses, as predicted by multi-physical modelling.

The performance of the proposed microwave process relative to a convection heating process was calculated. In a one-piece-flow scenario, the proposed microwave process provided significantly better performance. When comparing a one-piece-flow microwave process to a convection oven batch process, the microwave process provided better performance up to batch sizes of ten. A microwave batch system was then investigated and the results showed that a microwave batch system would provide distinct performance benefits, with a particularly strong performance gain for batch

sizes of up to 1000 pieces per batch. An applicator suitable for a whole magazine would therefore provide a strong performance improvement compared to convection heating processes.

8.2 Outlook

In this work, the microwave curing of three different materials were studied. The materials used were commercially available and not specifically optimized for microwave heating. To obtain further-increased heating rates and improved process stability, as well as increased selectivity during heating, materials with high loss tangents need to be either identified or developed. Additives with high loss tangents, such as carbon black, carbon nanotubes, graphenes, fullerenes or silicon powder may be applied to increase the susceptibility of the processed pastes.

The proposed curing system provides curing according to defined temperature profiles. It has been shown that the chemistry of the processed pastes is similar to that of conventionally cured pastes. However, the involved gelation and vitrification processes are performed faster and with different dynamics, which may lead to different material properties. Further research and development is necessary to identify temperature profiles that are optimized for microwave curing, including optimization for specific assemblies. The polymer cure modelling performed by Tilford *et al.* may be further exploited for this purpose (Morris *et al.* 2009; Tilford *et al.* 2010d).

The experiments performed in this work indicate that microwave-cured assemblies are more reliable than conventionally cured assemblies due to having lower residual stress. The experiments were carried out with relatively small sample sizes and just one encapsulant material. Further research and development is advised to reproduce and to statistically substantiate the findings. Additional research is necessary to investigate whether the beneficial effects extend to other materials and assemblies.

The machine developed, constructed and tested in this work shows how microwave curing can be directly integrated into an assembly machine to provide an integrated process chain without intermediate handling steps. In so doing, the overall performance of the process has been significantly improved. In this work, the flip-chip assembly process was used as an example of an advanced packaging process. In order to further exploit the benefits of the proposed technology, the assembly of complex 2D and 3D packages should be investigated.

Finally, the performance of the microwave curing system has clear advantages in comparison to convection heating systems. A modification of the curing system for

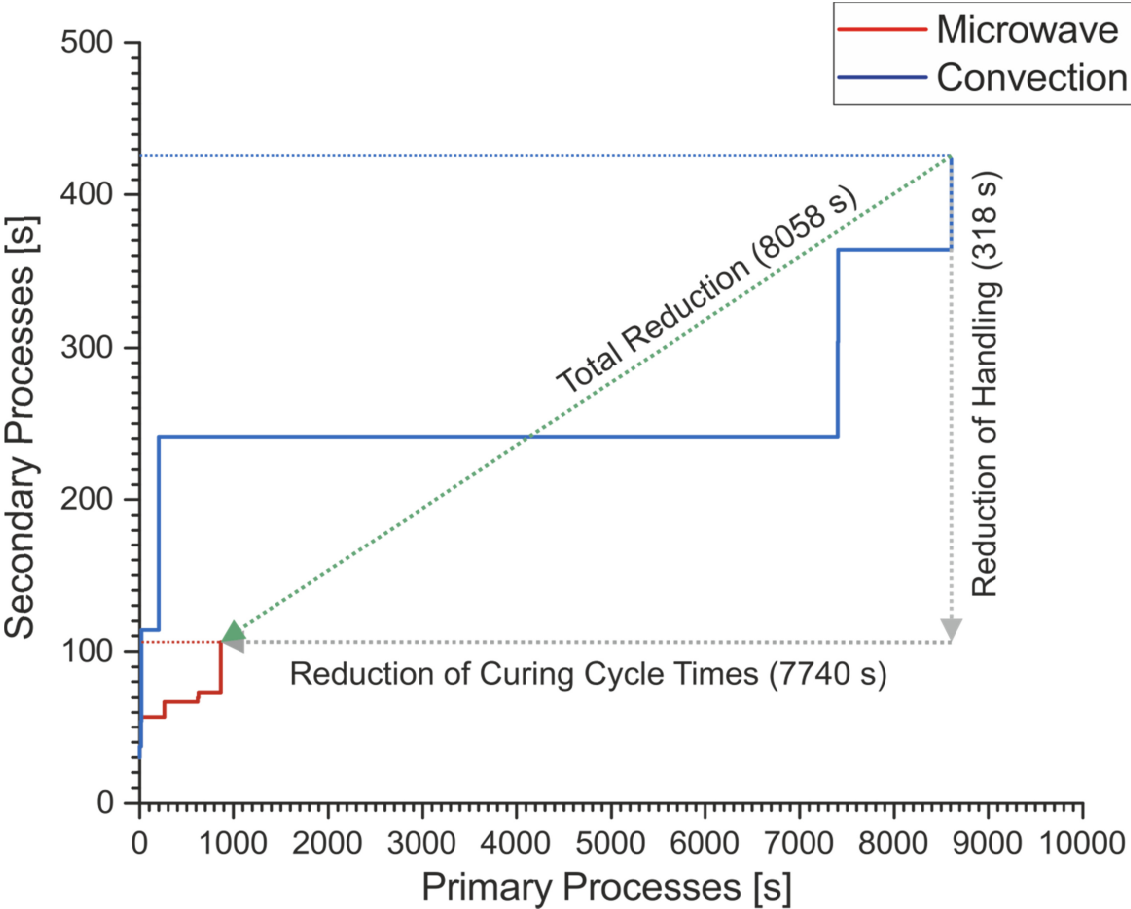
batch processing would potentially provide even further performance gains. Therefore, the development of a curing system with a larger waveguide resonator would be a possible next step towards an industrially exploitable microwave curing system.

Appendix

I. Flip-chip-on-board process

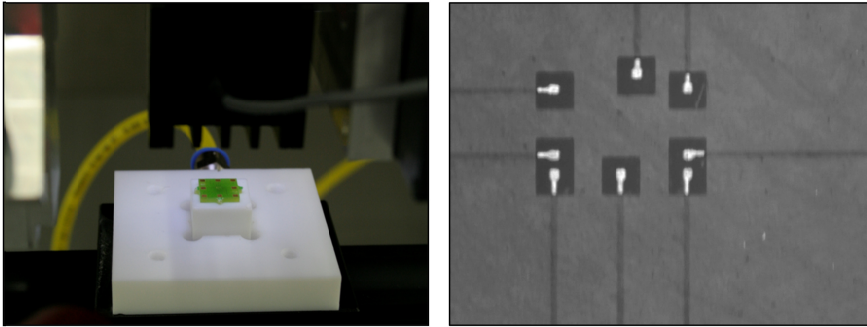
Duration and Throughput Processes	Process Duration [s]	Throughput [parts/hour]
SMT Process* [Harper 2004]		
Solder paste printing*	420	8.57
Solder paste inspection*	420	8.57
Component placement*	420	8.57
Pre-reflow optical inspection*	420	8.57
Reflow soldering [JEDEC 2015]	420	8.57
Post-reflow optical inspection*	420	8.57
Flip-Chip-On-Board Process		
Dispensing ECA	60	60.00
Placement of die	60	60.00
Curing of ECA (Epotek 377H)	3600	1.00
Dispensing of underfill	60	60.00
Curing of Underfill (FP4511)	7200	0.50
Dispensing of ECA	60	60.00
Curing of Encapsulant (EO1080)	1200	3.00
Throughput Without Flip-Chip-On-Board		8.57
Throughput With Flip-Chip-On-Board		0.5
*SMT processes are all assumed to have the same duration (serial process, bottleneck: reflow)		

II. Primary–Secondary analysis

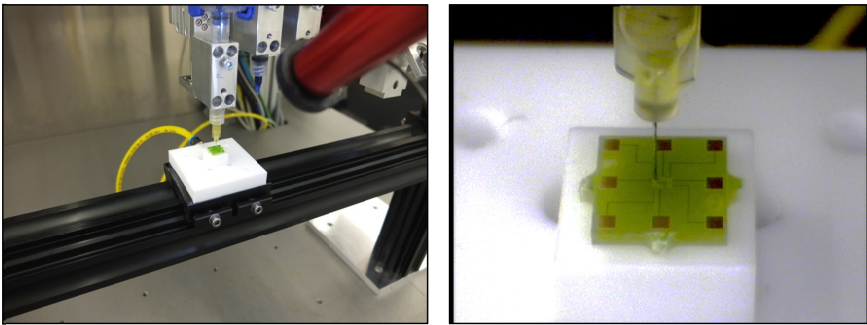


III. Flip-chip assembly process

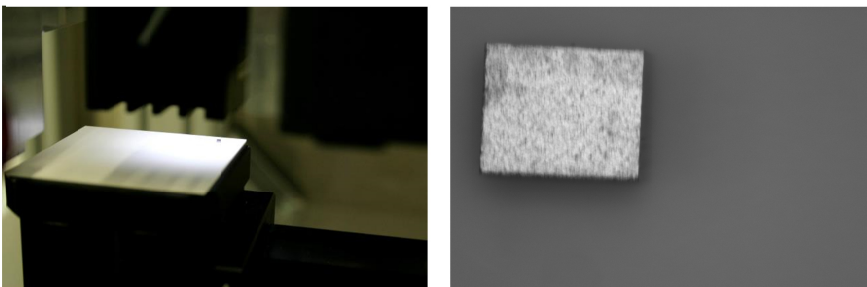
1. Supply of substrate and die



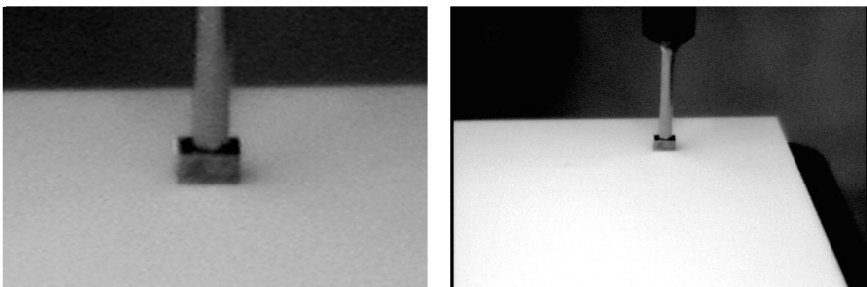
2. Pose determination of bond pads on substrate



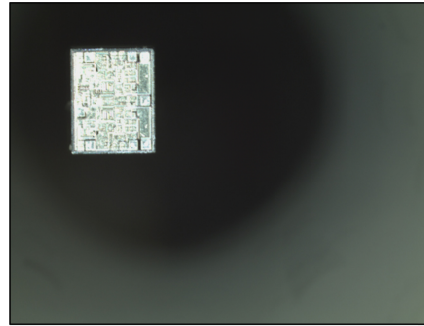
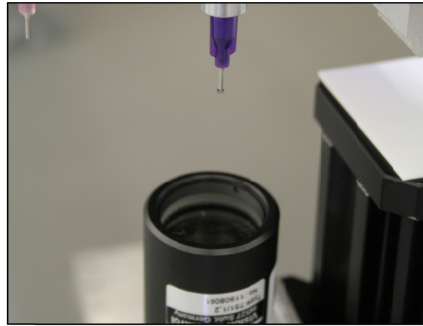
3. Dispensing of ECA on bond pads



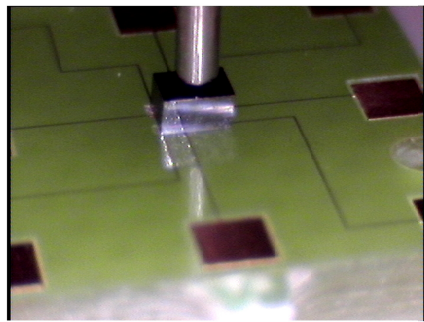
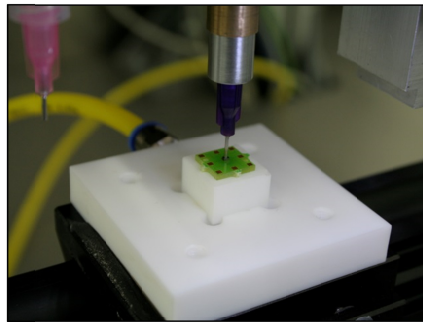
4. Pose determination of part on supply position



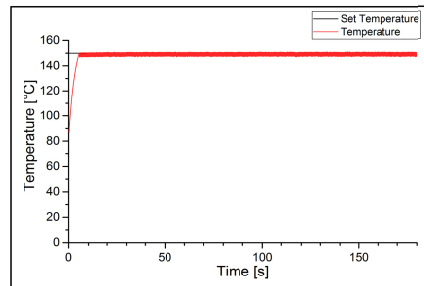
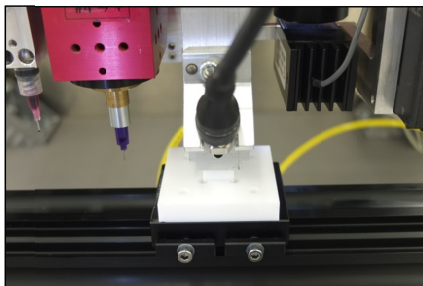
5. Pickup of part on supply position



6. Pose determination of die on gripper

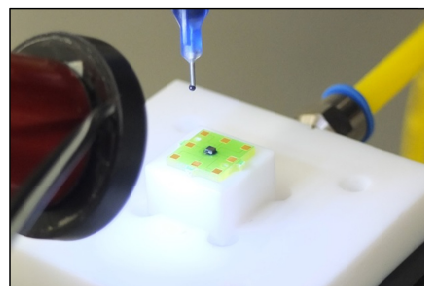
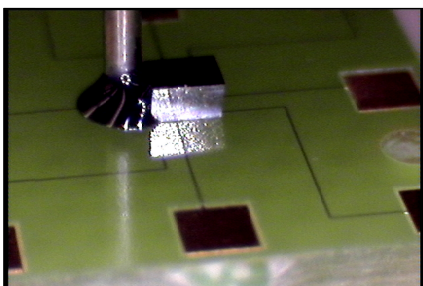


7. Part placement and release

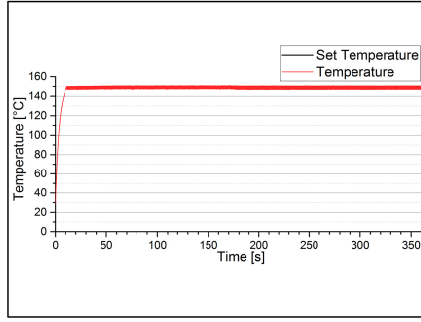
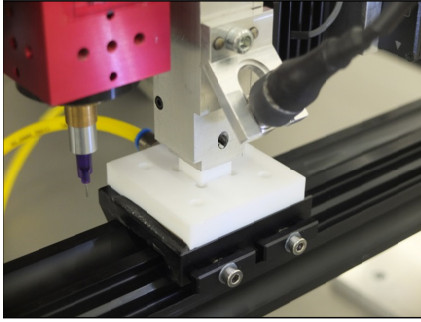


8. Microwave curing of ECA

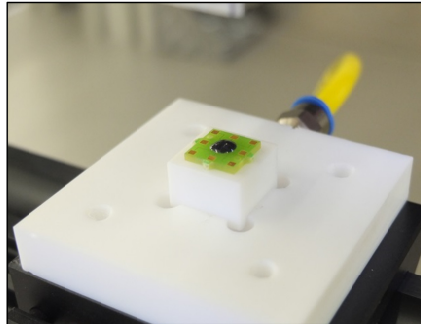
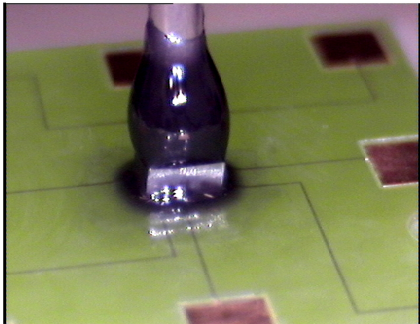
9. Pose determination of part on substrate



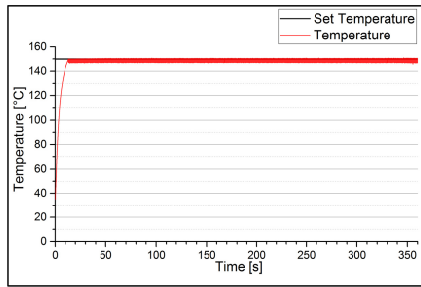
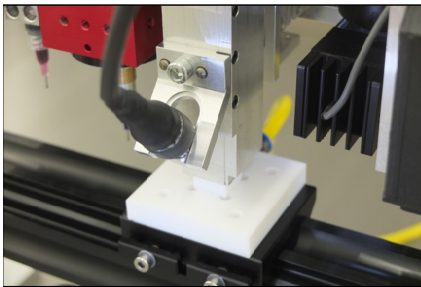
10. Dispensing of underfill



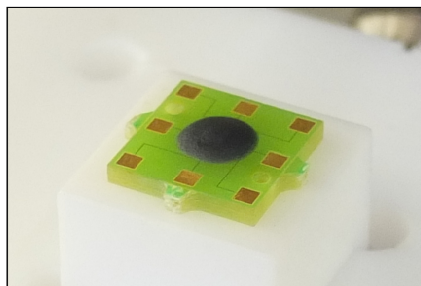
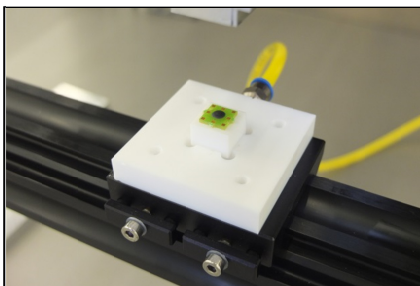
11. Microwave curing of underfill



12. Dispensing of encapsulant



13. Microwave curing of encapsulant



14. Removal of finished product

IV. Extended reliability test results

Microwave Profile	Microwave Profile 1	Microwave Profile 2	Microwave Profile 3	Conventional Profile
Reliability Tests				
HAST Test (130 °C, 85% RH for 96 hours)	✓	✓	✓	✓
Number of defective parts	0	0	0	0
Temperature Cycling Test (Weibull)				
Shape parameter β	1.09	0.98	0.87	1.77
Characteristic life η [cycles]	1467.58	1858.14	2260.74	907.68
Mean life μ [cycles]	1421.75	1874.16	2425.77	808.28
Variance σ^2	$1.68 \cdot 10^6$	$3.65 \cdot 10^6$	$7.83 \cdot 10^6$	$2.21 \cdot 10^5$
TCT After HAST (Weibull)				
Shape parameter β	1.02	1.16	0.66	1.31
Characteristic life η [cycles]	2366.50	1239.87	3291.67	762.88
Mean life μ [cycles]	2346.87	1176.25	1313.15	702.90
Variance σ^2	$5.29 \cdot 10^6$	$1.02 \cdot 10^6$	$1.11 \cdot 10^6$	$2.96 \cdot 10^5$
Temperature Cycling Test (Lognormal)				
Mean life μ [cycles]	1000	1400	1500	450
Standard deviation σ	1.8	2	2.1	1.5
TCT After HAST (Lognormal)				
Mean life μ [cycles]	1600	700	1000	450
Standard deviation σ	1.7	1.3	1	1.2
✓ – Fulfilled, o – Partly fulfilled, ✗ – Not fulfilled				

Bibliography

- μEpsilon 2016** Micro-Epsilon Messtechnik GmbH & Co. KG.
Technote - Präzise berührungslose Wegsensoren.
Ortenburg : μEpsilon,
zuletzt geprüft am 10. November 2016.
Verfügbar: <http://www.micro-epsilon.de/download/products/T001--de--Praezise-beruehrungslose-Sensoren.pdf>
- Adam et al. 1969** Adam, Stephen F. & Packard, Hewlett. 1969.
Microwave theory and applications.
Upper Saddle River, USA : Prentice-Hall.
ISBN 013581488X
- Adamietz et al. 2010** Adamietz, R., Iseringhausen, T. & Zapp, M. 2010.
Modulare Montageanlage.
wt Werkstattstechnik online **100** (3), S. 156–161
- AMICRA 2016** AMICRA Microtechnologies GmbH. 2016.
AFC Plus - Die Bonder and Flip Chip Bonder.
Regensburg : AMICRA,
zuletzt geprüft am 10. November 2016.
Verfügbar: <http://amicra.com/products/die-flip-chip-bonder/afc-plus-die-bonder-and-flip-chip-bonder>
- Anguiano et al. 2011** Anguiano, C., *et al.* 2011.
Heating capacity analysis of a focused infrared light soldering system.
In: *IECON 2011 - 37th Annual Conference on IEEE Industrial Electronics Society*,
November 7-10, 2011, Melbourne, Australia, S. 2136–2140
- ASE Group 2012** ASE Group. 2012.
ASE Package Handbook.
Kaohsiung, Taiwan : ASE Group
- ASE Group 2016** ASE Singapore Pte Ltd. 2016.
ASE Singapore.
Singapore, Singapore : ASE Group,
zuletzt geprüft am 12. Juli 2016.
Verfügbar: <http://www.aseglobal.com.sg>

- Bajenescu et al. 2012** Bajenescu, Titu-Marius & Bazu, Marius I. 2012. *Reliability of electronic components: a practical guide to electronic systems manufacturing*. Berlin, Germany : Springer. ISBN 3642585051
- Bark et al. 1998** Bark, C., *et al.* 1998. Gripping with low viscosity fluids. In: *The Eleventh Annual International Workshop on Micro Electro Mechanical Systems MEMS 98*, January 25-29, 1998, Heidelberg, Germany, S. 301–305
- Bechtold 2009** Bechtold, Franz. 2009. A comprehensive overview on today's ceramic substrate technologies. In: *European Microelectronics and Packaging Conference (EMPC)*, June, 15-18, 2009, Rimini, Italy, S. 1–12
- Beica 2015** Beica, Rozalia. 2015. 3D integration. In: *2015 International 3D Systems Integration Conference (3DIC)*, August 31-September 2, 2015, Sendai, Japan, TS5.1.1–TS5.1.7
- Beica et al. 2014** Beica, Rozalia, Buisson, Thibault & Pizzagalli, Amandine. 2014. 3D Packaging Technologies and Applications, Latest Challenges and Supply Chain Activities. *ECS Transactions* **61** (6), S. 11–16
- Berga et al. 2011** Berga, Ruben & Saad, Mohammed. 2011. *Thermal Spot Curing of Adhesives with Photonic Energy: A novel fiber delivery method of radiant heating to accelerate the polymerization of thermally active adhesives*. Hamden, USA : IR Photonics, zuletzt geprüft am 11. November 2016. Verfügbar: <https://www.smtnet.com/library/files/upload/thermal-spot-curing-adhesives.pdf>
- Beyne 2006** Beyne, Eric. 2006. The rise of the 3rd dimension for system integration. In: *2006 International Interconnect Technology Conference*, June 5-7, 2006, Burlingame, Canada, S. 1–5

- Bible et al. 1992** Bible, D. W., Lauf, R. J. & Everleigh, C. A. 1992. Multikilowatt variable frequency microwave furnace. *MRS Proceedings* 77 (269). DOI: 10.1557/PROC-269-77
- Blackwell 2002** Blackwell, Glenn R. 2002. *The electronic packaging handbook*. Boca Raton, USA : CRC Press. ISBN 0849385911
- Blais 2003** Blais, François. 2003. Review of 20 years of range sensor development. In: *Stuttgarter Impulse : Zukunft gestalten - Zeichen setzen*, October 13-15, 2003, Stuttgart, Germany, S. 62–76
- Blees 2011** Blees, Christoph. 2011. *Eine Methode zur Entwicklung modularer Produktfamilien* : Universitätsbibliothek. ISBN 3941492357
- Blundell 1987** Blundell, D. J. 1987. On the interpretation of multiple melting peaks in poly (ether ether ketone). *The International Journal for the Science and Technology of Polymers* 28 (13), S. 2248–2251
- Bolton 2015** Bolton, William. 2015. *Programmable logic controllers*. Oxford, UK : Newnes. ISBN 0081003536
- Boshnakov et al. 2012** Boshnakov, Ivan, Wood, Anna & Taylor, Simon. 2012. RF and microwave solid-state power amplifiers design requires specialised engineering. *Microwave Engineering Europe* (July-August), S. 14–16
- Bugdahl 1990** Bugdahl, Volker. 1990. *Methoden der Entscheidungsfindung*. Würzburg : Vogel. Management Wissen. ISBN 9783802304163
- Callister et al. 2012** Callister, William D. & Rethwisch, David G. 2012. *Fundamentals of materials science and engineering: An integrated approach*. Hoboken, USA : John Wiley & Sons. ISBN 1118061608

- CE3103WLV 2011** Henkel Electronic Materials. 2011.
Hysol ECCOBOND CE3103WLV Data Sheet.
Düsseldorf, Germany : Henkel
- Chen et al. 2006** Chen, Yonggang, Jaeger, Richard C. & Suhling, Jeffrey C. 2006.
Multiplexed CMOS sensor arrays for die stress mapping.
In: *Proceedings of the 32nd European Solid-State Circuits Conference 2006,*
September 18-22, 2006, Montreux, Switzerland, S. 424–427
- Chen et al. 2010** Chen, Yibo, *et al.* 2010.
Cost-effective integration of three-dimensional (3D) ICs emphasizing testing cost analysis.
In: *2010 IEEE/ACM International Conference on Computer-Aided Design (ICCAD),*
November 7-11, 2010, San Jose, USA, S. 471–476
- Chryssolouris 2013** Chryssolouris, ELKE. 2013.
Laser machining: Theory and practice.
Berlin, Germany : Springer Science & Business Media.
ISBN 1475740840
- Cohn et al. 1998** Cohn, Michael B., *et al.* 1998.
Microassembly technologies for MEMS.
In: *SPIE Conference on Micromachining and Microfabrication Process,*
September 20, 1998, Santa Clara, USA, S. 2–16
- Coughlan et al. 2006** Coughlan, F. M. & Lewis, H. J. 2006.
A study of electrically conductive adhesives as a manufacturing solder alternative.
Journal of electronic materials **35** (5), S. 912–921
- Davies 2004** Davies, E. Roy. 2004.
Machine vision: Theory, algorithms, practicalities.
Amsterdam : Elsevier.
ISBN 0080473245
- Davis et al. 2002** Davis, C., *et al.* 2002.
Neural network modeling of variable frequency microwave curing.
In: *Proceedings of the 52nd Electronic Components and Technology Conference, 2002.,*
May 28-31, 2002, San Diego, USA, S. 931–935

- Davis et al. 2007** Davis, Cleon E., *et al.* 2007.
An Acoustic Temperature Sensor to Monitor Variable Frequency Microwave Curing of Polymer Dielectrics.
In: *IEEE SENSORS 2007 Conference*, October 28-31, 2007, Atlanta, USA, S. 832–835
- Davis et al. 2008a** Davis, Cleon E., *et al.* 2008.
In Situ Acoustic Temperature Measurement During Variable-Frequency Microwave Curing.
IEEE Transactions on Electronics Packaging Manufacturing **31** (4), S. 273–284
- Davis et al. 2008b** Davis, Cleon E. & May, Gary S. 2008.
Neural network control of variable-frequency microwave processing of polymer dielectric curing.
IEEE Transactions on Electronics Packaging Manufacturing **31** (2), S. 104–113
- DeHaven et al. 1994** DeHaven, Keith & Dietz, Joel. 1994.
Controlled collapse chip connection (C4)- an enabling technology.
In: *Proceedings of the 44th Electronic Components and Technology Conference*, May 1-4, 1994, Washington DC, USA, S. 1–6
- Deshmukh 2005** Deshmukh, Yeshvant V. 2005.
Industrial heating: principles, techniques, materials, applications, and design.
Boca Raton, USA : CRC Press.
ISBN 1420027557
- Dickerhof et al. 2013** Dickerhof, Markus, *et al.* 2013.
An additive manufacturing and eprinting based approach for flexible scalable manufacturing of microsystems.
In: *10th International Conference on Multi-Material Micro Manufacture*, October 8-10, 2013, San Sebastian, Spain, S. 288–291
- Diop et al. 2015** Diop, Mamadou Diobet, *et al.* 2015.
Void-Free Underfill Process With Variable Frequency Microwave for Higher Throughput in Large Flip Chip Package Application.
IEEE Transactions on Device and Materials Reliability **2** (15)
- Dittrich et al. 2004** Dittrich, S. & Schlaich, P. 2004.
Sensorguided micro-assembly.
Microsystem technologies **10** (3), S. 199–201

- Dohda et al. 2004** Dohda, Kuniaki, Ni, Jun & Rooij, Nico de. 2004. Micro/Meso-scale Manufacturing. *Transactions of the ASME-B-Journal of Manufacturing* **126** (4), S. 641
- Dong et al. 2009** Dong, Xiangyu & Xie, Yuan. 2009. System-level cost analysis and design exploration for three-dimensional integrated circuits (3D ICs). In: *14th Asia and South Pacific Design Automation Conference*, January 19-22, 2009, Yokohama, Japan, S. 234–241
- Dowling 1993** Dowling, Norman E. 1993. *Mechanical behavior of materials: Engineering methods for deformation, fracture, and fatigue*. Upper Saddle River, USA : Prentice-Hall. ISBN 0135790468
- Dreiza et al. 2007** Dreiza, Moody, *et al.* 2007. High density PoP (package-on-package) and package stacking development. In: *Proceedings of the 57th Electronic Components and Technology Conference*, May 29 - June 01, 2007, Sparks, USA, S. 1397–1402
- Enns et al. 1983** Enns, John B. & Gillham, John K. 1983. Time–temperature–transformation (TTT) cure diagram. *Journal of Applied Polymer Science* **28** (8), S. 2567–2591
- EO1080 2010** Henkel Electronic Materials. 2010. *Hysol EO1080 Encapsulant Data Sheet*. Düsseldorf, Germany : Henkel
- EPO-TEK 2013** Epoxy Technology Inc. 2013. *EPO-TEK Adhesives Applications*. Billerica, USA : Epotek
- Eveloy et al. 2005** Eveloy, Valérie, *et al.* 2005. Are you ready for lead-free electronics? *IEEE Transactions on Components and Packaging Technologies* **28** (4), S. 884–894
- Famsworth et al. 2001** Famsworth, K. D., *et al.* 2001. Variable frequency microwave curing of photosensitive polyimides. *IEEE Transactions on Components and Packaging Technologies* **24** (3), S. 474–481

- Fatikow 2000** Fatikow, Sergej. 2000.
Mikroroboter und Mikromontage: Aufbau, Steuerung und Planung von flexiblen mikroroboterbasierten Montagestationen.
Berlin, Germany : Springer.
ISBN 351906264X
- Fatikow et al. 2013** Fatikow, Sergej & Rembold, Ulrich. 2013.
Microsystem technology and microrobotics.
Berlin, Germany : Springer.
ISBN 3662034506
- Fearing 1995** Fearing, Ronald S. 1995.
Survey of sticking effects for micro parts handling.
In: *Proceedings 1995 IEEE/RSJ International Conference on Intelligent Robots and Systems,*
August 5-9, 1995, Pittsburgh, USA, S. 212–217
- Felix et al. 2012** Felix, Marco, *et al.* 2012.
Infrared thermography of integrated circuits heated by focused IR light soldering system.
In: *Latin America Optics and Photonics Conference,*
November 10-13, 2012, Sao Sebastiao, Brazil
- Finetech 2016** Finetech GmbH & Co. KG. 2016.
Finetech.
Berlin, Germany : Finetech,
zuletzt geprüft am 11. November 2016.
Verfügbar: <http://www.finetech.de>
- Folmar 2000** Folmar, Patrick. 2000.
The truth about placement accuracy.
San Francisco, USA : Extension Media LLC,
zuletzt geprüft am 11. November 2016.
Verfügbar: <http://electroiq.com/blog/2000/04/the-truth-about-placement-accuracy/>
- FP4511 2010** Henkel Electronic Materials. 2010.
FP4511 Underfill Encapsulant Data sheet.
Düsseldorf, Germany : Henkel
- Frost & Sullivan 2017** Frost & Sullivan. 2017.
Global Market for MEMS and NEMS Sensors, Forecast to 2022: MEMS & NEMS Sensors are Enabling Smart Devices and IoT Applications Across Vertical Markets.
Mountain View, USA : Frost & Sullivan

- Fu et al. 2000** Fu, Ying, *et al.* 2000. Experimental and theoretical characterization of electrical contact in anisotropically conductive adhesive. *IEEE Transactions on Advanced Packaging* **23** (1), S. 15–21
- Gabbott 2008** Gabbott, Paul. 2008. *Principles and applications of thermal analysis*. Hoboken, USA : John Wiley & Sons. ISBN 0470698128
- Gad-el-Hak 2001** Gad-el-Hak, Mohamed. 2001. *The MEMS handbook*. Boca Raton, USA : CRC Press. ISBN 1420050907
- Garard et al. 2002** Garard, Richard S. & Adams, Bruce A. 2002. "Curing" low yields & reliability issues in photonics assembly. In: *Symposium on Design, Test, Integration, and Packaging of MEMS/MOEMS 2002*, March 19, 2002, Mandelieu-La Napoule, France
- Ghaffarian 2000** Ghaffarian, Reza. 2000. Accelerated thermal cycling and failure mechanisms for BGA and CSP assemblies. *Journal of Electronic Packaging* **122** (4), S. 335–340
- Ghaffarian et al. 2014** Ghaffarian, Reza & Evans, John W. 2014. Enabling More than Moore. In: *2014 Accelerated Stress Testing and Reliability Workshop*, September 10-12, 2014, Saint Paul, USA
- Ghosal et al. 2001** Ghosal, Balaram, Sigliano, Richard & Kunitatsu, Y. 2001. Ceramic and Plastic Pin Grid Array Technology: *Area Array Interconnection Handbook*. Berlin, Germany : Springer, S. 551–576. ISBN 146135529X
- Gibbs et al. 1958** Gibbs, Julian H. & DiMarzio, Edmund A. 1958. Nature of the glass transition and the glassy state. *The Journal of Chemical Physics* **28** (3), S. 373–383
- Gieschke et al. 2010** Gieschke, P. & Paul, O. 2010. CMOS-integrated Sensor chip for in-plane and out-of-plane shear stress. *Procedia Engineering* **5**, S. 1364–1367

- Gilleo 1998** Gilleo, Ken. 1998.
The Chemistry & Physics of Underfill.
In: *Proceedings of NEPCON West*,
March 1-5, 1998, Anaheim, USA, S. 280–292
- Gomatam et al. 2008** Gomatam, Rajesh & Mittal, Kash L. 2008.
Electrically Conductive Adhesives.
Boca Raton, USA : CRC Press.
ISBN 9004187820
- Gongora-Rubio et al. 2001** Gongora-Rubio, Mario Ricardo, *et al.* 2001.
Overview of low temperature co-fired ceramics tape
technology for meso-system technology (MsST).
Sensors and Actuators A: Physical **89** (3), S. 222–
241
- Gopalakrishnan et al. 1998** Gopalakrishnan, L., *et al.* 1998.
Encapsulant materials for flip-chip attach.
In: *Proceedings of the 48th Electronic Components
& Technology Conference*,
May 25-28, 1998, Seattle, USA, S. 1291–1297
- Greitmann 1998** Greitmann, Georg. 1998.
*Micromechanical tactile gripper system for micro
assembly*.
Zürich, Doctoral Thesis,
zuletzt geprüft am 11. November 2016.
Verfügbar: [http://e-
collection.library.ethz.ch/eserv/eth:22833/eth-
22833-01.pdf](http://e-collection.library.ethz.ch/eserv/eth:22833/eth-22833-01.pdf)
- Grutzeck et al. 2002** Grutzeck, Helmut & Kiesewetter, Lothar. 2002.
Downscaling of grippers for micro assembly.
Microsystem technologies **8** (1), S. 27–31
- Haberfellner et al. 2012** Haberfellner, Reinhard & Becker, Mario. 2012.
Systems Engineering: Methodik und Praxis.
12., völlig neu bearb. u. erw. Auflage.
Zürich : Verl. Industrielle Organisation.
ISBN 9783857439988
- Harman 2010** Harman, George G. 2010.
Wire bonding in microelectronics.
New York, USA : McGraw-Hill.
ISBN 0071476237
- Harper 2004** Harper, Charles. 2004.
*Electronic packaging and interconnection
handbook*.
New York, USA : McGraw-Hill.
ISBN 0071430482

- Häusler et al. 1999** Häusler, G., *et al.* 1999.
Limits of optical range sensors and how to exploit them.
In: Asakura, T. (Hrsg.): *International Trends in Optics and Photonics*.
Berlin, Germany : Springer, S. 328–342.
ISBN 3662142120
- Heath 2002** Heath, Steve. 2002.
Embedded systems design.
Oxford, UK : Newnes.
ISBN 0080477569
- Heller 2017** Heller Industries, Inc. 2017.
Heller Industries.
Florham Park, USA : Heller Industries,
zuletzt geprüft am 5. Februar 2018.
Verfügbar: <http://www.hellerindustries.com/>
- Henkel 2011** Henkel Electronic Materials. 2011.
Electronics Assembly Solutions.
Düsseldorf, Germany : Henkel
- Hesselbach et al. 2002** Hesselbach, J. *et al.* 2002.
Untersuchung zum internationalen Stand der Mikroproduktionstechnik.
Essen, Germany : Vulkan Verlag.
Schriftenreihe des Instituts für Werkzeugmaschinen und Fertigungstechnik der TU Braunschweig
- Hesselbach et al. 2007** Hesselbach, J., Wrege, J. & Raatz, A. 2007.
Micro handling devices supported by electrostatic forces.
CIRP Annals of Manufacturing Technology **56** (1),
S. 45–48
- Hirsch et al. 2006** Hirsch, Soeren, *et al.* 2006.
A new test device for characterization of mechanical stress caused by packaging processes: *Journal of Physics: Conference Series*, vol. 34 : IOP Publishing, p. 39.
ISBN 1742-6596
- Hivision 2017** Guilin Hivision Technology Co., Ltd. 2017.
Hivisi.
Guangxi, China : Guilin Hivision,
zuletzt geprüft am 5. Februar 2018.
Verfügbar: <http://www.hivisi.com>
- Hocken et al. 2011** Hocken, Robert J. & Pereira, Paulo H. 2011.
Coordinate measuring machines and systems.
Boca Raton, USA : CRC Press.
ISBN 1420017535

- Höhn 2001** Höhn, Michael. 2001.
Sensorgeführte Montage hybrider Mikrosysteme,
Doctoral Thesis.
München, Germany : Herbert Utz Verlag.
ISBN 3831600120
- Höhn et al. 2001** Höhn, Michael & Jacob, Dirk. 2001.
Verfahren und Methoden für die kosteneffiziente
Montage hybrider Mikrosysteme.
In: Reinhart, Günther (Hrsg.): *Automatisierte
Mikromontage - Werkzeuge und Fügetechnologien
für die automatisierte Mikrosystemtechnik*, vol. 59.
München, Germany : Herbert Utz Verlag, 2-15
- Hsiung et al. 1997** Hsiung, J-C & Pearson, R. A. 1997.
Processing diagrams for polymeric die attach
adhesives.
In: *Proceedings of 47th Electronic Components and
Technology Conference 1997*,
May 18-21, 1997, San Jose, USA, S. 536–543
- Hsu 2006** Hsu, Tai-Ran. 2006.
Reliability in MEMS packaging.
In: *2006 IEEE International Reliability Physics
Symposium Proceedings 44th Annual*,
March 26-30, 2006, San Jose, USA, S. 398–402
- Hu et al. 2014** Hu, Yi, *et al.* 2014.
Research Reviews and Prospects of MEMS
Reliability.
Integrated Ferroelectrics **152** (1), S. 8–21
- Huang 1996** Huang, Chien-Yi. 1996.
*Process research in the encapsulation of direct chip
attach components*.
New York, USA, Doctoral Thesis
- Huang et al. 2012** Huang, Yunhan, *et al.* 2012.
MEMS reliability review.
*IEEE Transactions on Device and Materials
Reliability* **12** (2), S. 482–493
- Hubbard et al. 2004** Hubbard, R. L., *et al.* 2004.
Low temperature curing of polyimide wafer
coatings.
In: *29th International Electronics Manufacturing
Technology Symposium*,
July 14-16, 2004, San Jose, USA, S. 149–151

- Hubbard et al. 2006** Hubbard, Robert L., *et al.* 2006.
Area array encapsulation with stencil printing and microwave curing.
In: *Proceedings of the 56th Electronic Components and Technology Conference*,
May 30-June 2, 2006, San Diego, USA
- Hubbard et al. 2010** Hubbard, Robert L., Zappella, Pierino & Zhu, Pukun. 2010.
Flip-chip process improvements for low warpage.
In: *Proceedings of the 60th Electronic Components and Technology Conference*,
June 1-4, 2010, Las Vegas, USA, S. 25–30
- Hubbard et al. 2011** Hubbard, Robert Lane & Zappella, Pierino. 2011.
Low warpage flip-chip under-fill curing.
Components, Packaging and Manufacturing Technology, IEEE Transactions on **1** (12), S. 1957–1964
- Imanaka 2005** Imanaka, Yoshihiko. 2005.
Multilayered low temperature cofired ceramics (LTCC) technology.
Berlin, Germany : Springer.
ISBN 0387231307
- IPC 7351** IPC. 2005.
IPC-7351 - Generic Requirements for Surface Mount Design and Land Pattern Standard.
Bannockburn, USA : IPC
- IRDS 2016** IEEE IRDS. 2016.
International Roadmap for Devices and Systems: 2016 Edition, More Moore White Paper.
Piscataway, USA : IEEE,
zuletzt geprüft am 7. März 2017.
Verfügbar: <http://irds.ieee.org/reports>
- Jacob 2002** Jacob, Dirk. 2002.
Verfahren zur Positionierung unterseitenstrukturierter Bauelemente in der Mikrosystemtechnik, Doctoral Thesis.
München, Germany : Herbert Utz Verlag.
ISBN 3831601429
- Jaeger et al. 2000** Jaeger, Richard C., *et al.* 2000.
CMOS stress sensors on [100] silicon.
Solid-State Circuits, IEEE Journal of **35** (1), S. 85–95

- Jagt 1998** Jagt, Jannes C. 1998.
Reliability of electrically conductive adhesive joints for surface mount applications.
IEEE Transactions on Components, Packaging, and Manufacturing Technology **21** (2), S. 215–225
- Jagt et al. 1995** Jagt, J. C., Beris, P. J.M. & Lijten, G. 1995.
Electrically conductive adhesives.
IEEE Transactions on Components, Packaging, and Manufacturing Technology **18** (2), S. 292–298
- JEDEC 1999** JEDEC Solid State Technology Association. 1999.
Highly Accelerated Temperature and Humidity Stress Test.
Arlington, USA : Electronic Industries Alliance
- JEDEC 2015** JEDEC Solid State Technology Association. 2015.
Moisture/Reflow Sensitivity Classification or Nonhermetic Surface Mount Devices.
Arlington, USA : JEDEC Solid State Technology Association
- Jenton 2016** Jenton Group. 2016.
Jenton Group - Capability in Packaging, UV, Converting.
Whitchurch, UK : Jenton,
zuletzt geprüft am 10. November 2016.
Verfügbar: <http://www.jentonuv.co.uk/>
- Ji et al. 2008** Ji, Hua, Li, Yan & Wang, Jian. 2008.
A software oriented CNC system based on Linux/RTLinux.
The International Journal of Advanced Manufacturing Technology **39** (3-4), S. 291–301
- Jow et al. 1988** Jow, J., et al. 1988.
Dielectric analysis of epoxy/amine resins using microwave cavity technique.
Polymer Engineering & Science **28** (22), S. 1450–1454
- Kada 2015** Kada, Morihito. 2015.
R&D overview of 3D Integration Technology using TSV Worldwide and in Japan.
ECS Transactions **64** (40), S. 1–8
- Karkanias et al. 2000** Karkanias, Panagiotis I. & Partridge, Ivana K. 2000.
Cure modeling and monitoring of epoxy/amine resin systems. I. Cure kinetics modeling.
Journal of Applied Polymer Science **77** (7), S. 1419–1431

- Karnezos 2004** Karnezos, Marcos. 2004.
3D packaging - Where all technologies come together.
In: *29th International Electronics Manufacturing Technology Symposium*,
July 14-16, 2004, San Jose, USA, S. 64–67
- Kim et al. 1993** Kim, Hansoo, *et al.* 1993.
Processing, structural and electrical properties of electrically conductive adhesives.
In: *Proceedings of 43rd Electronic Components and Technology Conference*,
June 1-4, 1993, Orlando, USA, S. 311–319
- Kingbright 2007** Kingbright. 2007.
Kingbright KP-2012SGD 2.0x1.25mm SMD CHIP LED LAMP.
New Taipeh City, Taiwan : Kingbright
- Kinstle 1990** Kinstle, James F. 1990.
Electron-Beam Curing of Polymeric Materials.
In: Hoyle, Charles E. & Kinstle, James F. (Hrsg.):
Radiation Curing of Polymeric Materials.
Washington DC, USA : American Chemical Society, S. 17–23
- Kittel et al. 2008a** Kittel, Hartmut *et al.* 2008.
iForceSens – Entwicklung eines integrierten Stressmesssystems zur Quantifizierung der 3D-Verformung von Sensorbauelementen in Abhängigkeit des Verpackungsprozesses.
Gerlingen, Germany : Robert Bosch GmbH
- Kittel et al. 2008b** Kittel, Hartmut, *et al.* 2008.
Novel stress measurement system for evaluation of package induced stress.
In: *2nd European Conference & Exhibition on Integration Issues of Miniaturized Systems-MEMS, MOEMS, ICS and Electronic Components (SSI)*,
April 9-10, 2008, Berlin, Germany, S. 1–8
- Kristiansen et al. 1998** Kristiansen, Helge & Liu, Johan. 1998.
Overview of conductive adhesive interconnection technologies for LCDs.
IEEE Transactions on Components, Packaging, and Manufacturing Technology **21** (2), S. 208–214

- Lambda 2016** Lambda Technology. 2016.
Lambda Technology - Produkte.
Hohenbrunn, Germany : Lambda Technology,
zuletzt geprüft am 10. November 2016.
Verfügbar:
<http://www.lambdatechnology.de/de/produkte.html>
- Lambda Technologies 2007** Lambda Technologies. 2007.
Lambda Technologies.
Morrisville, USA : Lambda Technologies,
zuletzt geprüft am 11. November 2016.
Verfügbar: <http://www.microcure.com/>
- Lau 1994** Lau, John H. 1994.
Chip on Board: Technology for Multichip Modules.
Berlin, Germany : Springer.
ISBN 0442014414
- Lau 1996** Lau, John H. 1996.
Solder joint reliability of flip chip and plastic ball
grid array assemblies under thermal, mechanical,
and vibrational conditions.
*IEEE Transactions on Components, Packaging, and
Manufacturing Technology* **19** (4), S. 728–735
- Lau 2010** Lau, John H. 2010.
TSV manufacturing yield and hidden costs for 3D
IC integration.
In: *Proceedings of the 60th Electronic Components
and Technology Conference*,
June 1-4, 2010, Las Vegas, USA, S. 1031–1042
- Lau et al. 1997** Lau, John H. & Pao, Yi-Hsin. 1997.
*Solder joint reliability of BGA, CSP, flip chip, and
fine pitch SMT assemblies.*
New York, USA : McGraw-Hill.
ISBN 0070366489
- Lau et al. 2003** Lau, J. H., Wong, C. P., Lee, N. C. & Lee, S.
RickyW. 2003.
*Electronics manufacturing with lead-free halogen-
free, and conductive–adhesive handbooks.*
New York, USA : McGraw-Hill.
ISBN 0071386246
- Lee et al. 2011** Lee, Sang Hwui, Chen, Kuan Neng & Lu, James
Jian Qiang. 2011.
Wafer-to-Wafer Alignment for Three-Dimensional
Integration: A Review.
Journal of Microelectromechanical Systems **20** (4),
S. 885–898.
DOI: 10.1109/JMEMS.2011.2148161

- Lee et al. 2012** Lee, Y. C. & Chen, W. T. 2012.
Manufacturing challenges in electronic packaging.
London : Chapman & Hall.
ISBN 9780412620300
- Lenz 1987** Lenz, Reimar. 1987.
Linsenfehlerkorrigierte Eichung von
Halbleiterkameras mit Standardobjektiven für
hochgenaue 3D-Messungen in Echtzeit.
In: *Mustererkennung 1987*, Braunschweig,
Germany, S. 212–216
- Li et al. 1997** Li, Li & Morris, James E. 1997.
Electrical conduction models for isotropically
conductive adhesive joints.
*IEEE Transactions on Components, Packaging, and
Manufacturing Technology* **20** (1), S. 3–8
- Lim 2005** Lim, Sung Kyu. 2005.
Physical design for 3D system on package.
IEEE Design & Test of Computers **22** (6), S. 532–
539
- Liu 2012** Liu, Yong. 2012.
*Power electronic packaging: design, assembly
process, reliability and modeling*.
Berlin, Germany : Springer.
ISBN 1461410533
- Liu et al. 1998** Liu, Johan, *et al.* 1998.
Overview of conductive adhesive joining technology
in electronics packaging applications.
In: *Proceedings of 3rd international Conference on
Adhesive Joining and Coating Technology in
Electronics Manufacturing*,
September 30, 1998, Binghamton, USA, S. 1–18
- Liu et al. 1999** Liu, Johan, *et al.* 1999.
A reliable and environmentally friendly packaging
technology-flip-chip joining using anisotropically
conductive adhesive.
*IEEE Transactions on Components and Packaging
Technologies* **22** (2), S. 186–190
- Loos et al. 1983** Loos, Alfred C. & Springer, George S. 1983.
Curing of epoxy matrix composites.
Journal of composite materials **17** (2), S. 135–169
- Lotter 1982** Lotter, Bruno. 1982.
The economic design of assembly processes.
Assembly automation **2** (3), S. 153–157

- Lotter 1985** Lotter, Bruno. 1985.
Primary secondary assembly analysis as a planning method for assembly lines.
Werkstattechnik - Zeitschrift für industrielle Fertigung **75** (1), S. 9–14
- Lotter 2013** Lotter, Bruno. 2013.
Manufacturing assembly handbook.
Oxford, UK : Butterworth-Heinemann.
ISBN 1483163385
- Lotter et al. 2006** Lotter, Bruno & Wiendahl, Hans-Peter. 2006.
Montage in der industriellen Produktion: Ein Handbuch für die Praxis.
Berlin, Germany : Springer-Verlag.
ISBN 3540366695
- Lu et al. 2009** Lu, Daniel & Wong, C. P. 2009.
Materials for advanced packaging.
Berlin, Germany : Springer.
ISBN 0387782184
- Mahajan et al. 2017** Mahajan, Ravi & Sankman, Bob. 2017.
3D Packaging Architectures and Assembly Process Design.
Berlin, Germany : Springer
- Majcherek et al. 2009** Majcherek, Soeren, Leneke, Thomas & Hirsch, Soeren. 2009.
A silicon test chip for the thermomechanical analysis of MEMS packagings.
Microsystem technologies **15** (1), S. 191–200
- Martin 2016** Martin GmbH. 2016.
Martin - A Finetech Company.
Germering, Germany : Martin GmbH,
zuletzt geprüft am 11. Oktober 2016.
Verfügbar: <http://www.martin-smt.de>
- Masterbond 2015** Masterbond. 2015.
Adhesives, Sealants & Coatings for the Electronic Industry.
New Jersey, USA : Masterbond
- Mead et al. 2003** Mead, Patricia F., *et al.* 2003.
Variable frequency microwave processing of underfill encapsulants for flip-chip applications.
Journal of Electronic Packaging **125** (2), S. 302–307

- Menz et al. 2008** Menz, Wolfgang, Mohr, Jürgen & Paul, Oliver. 2008.
Microsystem technology.
Hoboken, USA : John Wiley & Sons.
ISBN 3527613013
- Meredith 1998** Meredith, Roger J. 1998.
Engineers' handbook of industrial microwave heating.
London, UK : IET; 25.
ISBN 0852969163
- Metaxas et al. 1983** Metaxas, A., Metaxas, C. & Meredith, Roger J. 1983.
Industrial microwave heating.
London, UK : IET; 4.
ISBN 0906048893
- Miettinen et al. 2004** Miettinen, Jani, *et al.* 2004.
System design issues for 3D system-in-package (SiP).
In: *Proceedings of the 54th Electronic Components and Technology Conference*,
June 1-4, 2004, Las Vegas, USA, S. 610–615
- Mijović et al. 1990** Mijović, Jovan & Wijaya, Jony. 1990.
Review of cure of polymers and composites by microwave energy.
Polymer composites **11** (3), S. 184–191
- Moon et al. 2004a** Moon, Kyoung-Sik, *et al.* 2004.
A novel technique for lead-free soldering process using variable frequency microwave (VFM).
In: *Proceedings of the 9th International Symposium on Advanced Packaging Materials: Processes, Properties and Interfaces*,
March 24-26, 2004, Atlanta, USA, S. 118–125
- Moon et al. 2004b** Moon, Kyoung-Sik, *et al.* 2004.
Lead-free solder interconnect by variable frequency microwave (VFM).
In: *Proceedings of the 54th Electronic Components and Technology Conference*,
June 1-4, 2004, Las Vegas, USA, S. 1989–1995
- Morris 2011** Morris, J. E. 2011.
Isotropic conductive adhesives in electronics.
Cambridge, UK : Woodhead Publishing Ltd.

- Morris et al. 2007** Morris, James E. & Liu, Johan. 2007. Electrically conductive adhesives. In: Suhir, E., Lee, Y. C., & Wong, C. P. (Hrsg.): *Micro-and Opto-Electronic Materials and Structures: Physics, Mechanics, Design, Reliability, Packaging*. Berlin, Germany : Springer, 527-570. ISBN 0387279741
- Morris et al. 2009** Morris, James E., *et al.* 2009. Polymer cure modeling for microelectronics applications. In: *32nd International Spring Seminar on Electronics Technology (ISSE)*, May 13-17, 2009, Brno, Czech Republic, S. 1–6
- Mounier 2012** Mounier, Eric. 2012. MEMS Markets & Applications. In: *Proceedings of 2nd Workshop on design, control and software implementation for distributed MEMS (dMEMS)*, April 2-3, 2012, Besancon, France
- Naganuma et al. 1999** Naganuma, T. & Kagawa, Y. 1999. Effect of particle size on light transmittance of glass particle dispersed epoxy matrix optical composites. *Acta materialia* **47** (17), S. 4321–4327
- Neculaes et al. 2004** Neculaes, V. Bogdan, *et al.* 2004. Low-noise microwave oven magnetrons with fast start-oscillation by azimuthally varying axial magnetic fields. *IEEE Transactions on Plasma Science* **32** (3), S. 1152–1159
- Negrea 2011** Negrea, D. 2011. Hochpräzise Montage von elektro-optischen System. In: *MikroMontage 2011*, May 10-11, 2011, Stuttgart, Germany
- Nelson et al. 1998** Nelson, Bradley J., Zhou, Yu & Vikramaditya, Barmeshwar. 1998. Sensor-based microassembly of hybrid MEMS devices. *IEEE Control Systems* **18** (6), S. 35–45
- Niehoff et al. 2009** Niehoff, Katrin, *et al.* 2009. Thermo-mechanical stress analysis. In: *European Microelectronics and Packaging Conference (EMPC)*, June, 15-18, 2009, Rimini, Italy, S. 1–5

- Nienhaus 1999** Nienhaus, M. 1999.
Zur Montage hybrider Mikrosysteme am Beispiel von Radarsensoren und Umlaufrädergetrieben.
Düsseldorf, Germany : VDI Verlag; No. 501.
ISBN 3183501023
- O’Sullivan 1990** O’Sullivan, Colm T. 1990.
Newton's law of cooling-A critical assessment.
American Journal of Physics **58** (12), S. 956–960
- Ogochukwu 2014** Ogochukwu, Ezeonu Stella. 2014.
Laser Soldering.
In: Mastai, Yitzhak (Hrsg.): *Materials science - advanced topics.*
Rijeka, Croatia : INTECH.
ISBN 953511140X
- Oh 1998** Oh, Hyeon-Seok. 1998.
Elektrostatische Greifer für die Mikromontage.
Düsseldorf, Germany : VDI-Verlag.
ISBN 3183702088
- Okress et al. 1957** Okress, E. C., *et al.* 1957.
Design and performance of a high power pulsed magnetron.
IRE Transactions on Electron Devices **4** (2), S. 161–171
- Orfanidis 2003** Orfanidis, Sophocles J. 2003.
Electromagnetic Waves and Antennas: Waveguides.
Upper Saddle River, USA : Prentice-Hall.
ISBN 0130938556
- Othman 2005** Othman, Nabih. 2005.
Entwicklung eines Verfahrens zum präzisen Punkt- und Linienauftrag von hochviskosem Leitleber mit einem geregelten Mikrodosiersystem.
Heimsheim, Germany : Jost-Jetter.
IPA-IAO-Forschung und Praxis; 428.
ISBN 3936947732
- Ozawa 1971** Ozawa, T. 1971.
Kinetics of non-isothermal crystallization.
Polymer **12** (3), S. 150–158
- Palaniappan et al. 1999** Palaniappan, Prema, *et al.* 1999.
Correlation of flip chip underfill process parameters and material properties with in-process stress generation.
IEEE Transactions on Electronics Packaging Manufacturing **22** (1), S. 53–62

- Parker et al. 1979** Parker, D. & Stafford, J. W.D. 1979. Development of an 18 PIN premolded plastic DIP. *Semiconductor International* **2** (9), S. 49–61
- Pavuluri et al. 2010a** Pavuluri, S. K., *et al.* 2010. Experimental investigation of open-ended microwave oven assisted encapsulation process. In: *Proceedings of the 3rd Electronic System-Integration Technology Conference (ESTC)*, September 13-16, 2010, Berlin, Germany, S. 1–6
- Pavuluri et al. 2010b** Pavuluri, Sumanth K., *et al.* 2010. Advances in the design and test of a novel open ended microwave oven. In: *Proceedings of the 2010 Symposium on Design Test Integration and Packaging of MEMS/MOEMS (DTIP)*, May 5-7, 2010, Sevilla, Spain, S. 247–252
- Pavuluri et al. 2011** Pavuluri, S. K., *et al.* 2011. Post cure behaviour of encapsulants for QFN packages processed by an open-ended single mode resonant microwave applicator. In: *Proceedings of the 13th Electronics Packaging Technology Conference (EPTC)*, December 7-9, 2011, Singapore, Singapore, S. 573–578
- Pavuluri et al. 2012** Pavuluri, Sumanth Kumar, *et al.* 2012. Encapsulation of microelectronic components using open-ended microwave oven. *IEEE Transactions on Components, Packaging and Manufacturing Technology* **2** (5), S. 799–806
- Peercy 2000** Peercy, Paul S. 2000. The drive to miniaturization. *Nature* **406** (6799), S. 1023–1026
- Pizzagalli et al. 2014** Pizzagalli, Amandine, Buisson, Thibault & Beica, Rozalia. 2014. 3D technology applications market trends & key challenges. In: *25th Annual SEMI Advanced Semiconductor Manufacturing Conference (ASMC 2014)*, May 19-21, 2014, Saratoga Springs, USA, S. 78–81
- Popa et al. 2004** Popa, Dan O. & Stephanou, Harry E. 2004. Micro and mesoscale robotic assembly. *Journal of manufacturing processes* **6** (1), S. 52–71

- Powell et al. 1993** Powell, D. O. & Trivedi, A. K. 1993.
Flip-chip on FR-4 integrated circuit packaging.
In: *Proceedings of 43rd Electronic Components and Technology Conference*,
June 1-4, 1993, Orlando, USA, S. 182–186
- Prasad 2013** Prasad, Ray. 2013.
Surface mount technology: principles and practice.
Berlin, Germany : Springer Science & Business
Media.
ISBN 1461540844
- Pymonto et al. 2008** Pymonto, L. G., *et al.* 2008.
Process development with temperature sensitive
components in server applications.
In: *IPC - IPC Printed Circuits Expo, APEX and the
Designers Summit 2008*,
April 1-3, 2008, Las Vegas, USA
- Qu et al. 1998** Qu, Jianmin & Wong, C. P. 1998.
Effective elastic modulus of underfill material for
flip-chip applications.
In: *Proceedings of the 48th Electronic Components
& Technology Conference*,
May 25-28, 1998, Seattle, USA, S. 848–850
- Raatz et al. 2012** Raatz, Annika, *et al.* 2012.
Mikromontage.
In: Lotter, Bruno & Wiendahl, Hans-Peter (Hrsg.):
Montage in der industriellen Produktion.
Berlin, Germany : Springer, S. 443–471.
ISBN 3642290604
- Raeis-Zadeh et al. 2012** Raeis-Zadeh, Mehrsa, *et al.* 2012.
Variable-Frequency Microwave Curing of
Photosensitive Polynorbornene Dielectric.
ECS Journal of Solid State Science and Technology
1 (1), S. N6-N13
- Reichl 1998** Reichl, Herbert. 1998.
*Direktmontage - Handbuch über die Verarbeitung
ungehäuster ICs*.
Heidelberg, Germany : Springer.
ISBN 354064203X
- Rösner et al. 1996** Rösner, Bela, Liu, Johan & Lai, Zonghe. 1996.
Flip chip bonding using isotropically conductive
adhesives.
In: *Proceedings of the 46th Electronic Components
and Technology Conference (ECTC)*,
May 28-31, 1996, Orlando, USA, S. 578–581

- Rosu et al. 2003** Rosu, B., Reyes-Turcu, P. & Simion-Zanescu, D. 2003.
Thermal management system for reflow oven.
In: *26th International Spring Seminar on Electronics Technology: Integrated Management of Electronic Materials Production*,
May 8-11, 2003, High Tatras Slovakia, S. 306–309
- Rupp 2011** Rupp, Johannes. 2011.
Development of an Embedded Control System for an Open-ended Microwave Oven.
Stuttgart, Master Thesis
- Sakai et al. 1994** Sakai, Noboru & Hanzawa, Tamotsu. 1994.
Applications and advances in far-infrared heating in Japan.
Trends in Food Science & Technology **5** (11), S. 357–362
- Sangster et al. 2006** Sangster, A. J. & Sinclair, K. I. 2006.
Multimode degenerate mode cavity for microwave hyperthermia treatment.
IEE Proceedings - Microwaves, Antennas and Propagation **153** (1), S. 75–82
- Scholz et al. 2016** Scholz, Steffen, *et al.* 2016.
A modular flexible scalable and reconfigurable system for manufacturing of Microsystems based on additive manufacturing and e-printing.
Robotics and Computer-Integrated Manufacturing **40**, S. 14–23
- Schreier-Alt et al. 2013** Schreier-Alt, Thomas, *et al.* 2013.
Piezoresistive stress sensor for inline monitoring during assembly and packaging of QFN.
In: *Proceedings of the 63rd Electronic Components and Technology Conference (ECTC)*,
May 28-31, 2013, Las Vegas, USA, S. 2126–2131
- Schwizer et al. 2003** Schwizer, Jiirg, *et al.* 2003.
Packaging test chip for flip-chip and wire bonding process characterization.
In: *12th International Conference on TRANSDUCERS, Solid-State Sensors, Actuators and Microsystems*,
June 8-12, 2003, Boston, USA, S. 440–443

- Sechi et al. 2006** Sechi, F. N. & Bujatti, M. 2006.
Broadband high power amplifiers for instrumentation.
In: *Proceedings of the 67th ARFTG Conference 2006*,
June 16, 2006, San Francisco, USA, S. 61–67
- Seelert et al. 2012** Seelert, W. & Pyschny, N. 2012.
Herausforderungen und erste Ergebnisse auf dem Weg zur automatisierten Montage von miniaturisierten Lasersystemen.
In: *MikroMontage 2012*,
June 12-13, 2012, Leinfelden-Echterdingen, Germany
- Sensortherm 2013** Sensortherm. 2013.
Miniature Pyrometer CT84 Data Sheet.
Sulzbach, Germany : Sensortherm
- Serway et al. 2013** Serway, Raymond A., Beichner, Robert J. & Jewett, John W. 2013.
Physics for scientists and engineers with modern physics.
Boston USA : Cengage Learning.
ISBN 1133954057
- Siemens AG 1999** Siemens AG. 1999.
Die Welt der Surface Mount Technology - Das Technologiehandbuch aus der Praxis für die Praxis.
München, Germany : Siemens AG
- Sikiö et al. 2012** Sikiö, Vili *et al.* 2012.
Famobs Deliverable 6.2 – Report on the reliability of the bonded components and experimental validation of simulated results.
Talinn, Estonia : Eesti Innovatsiooni Instituut (EII)
- Simon et al. 1994** Simon, S. L. & Gillham, J. K. 1994.
Thermosetting cure diagrams - calculation and application.
Journal of Applied Polymer Science **53** (6), S. 709–727
- Sinclair 2009** Sinclair, Keith Ian. 2009.
Focussed microwave heating using degenerate and non-degenerate cavity modes.
Edinburgh, UK, Doctoral Thesis,
zuletzt geprüft am 3. April 2017.
Verfügbar:
<http://www.ros.hw.ac.uk/handle/10399/2288>

- Sinclair et al. 2008a** Sinclair, Keith, *et al.* 2008.
Polymer curing within an optimised open-ended microwave oven.
In: *Proceedings of the 38th European Microwave Conference (EuMC) 2008*,
October 27-31, 2008, Amsterdam, Netherlands, S. 17–20
- Sinclair et al. 2008b** Sinclair, K. I., *et al.* 2008.
Open ended microwave oven for packaging.
In: *Proceedings of the Symposium on Design, Test, Integration and Packaging of MEMS/MOEMS 2008*,
April 9-11, 2008, Nice, France, S. 16–20
- Sinclair et al. 2008c** Sinclair, Keith, *et al.* 2008.
Optimization of an open-ended microwave oven for microelectronics packaging.
IEEE Transactions on Microwave Theory and Techniques **56** (11), S. 2635–2641
- Sinclair et al. 2008d** Sinclair, Keith I., *et al.* 2008.
Advanced microwave oven for rapid curing of encapsulant.
In: *Proceedings of the 2nd Electronics System-Integration Technology Conference (ESTC)*,
September 1-4, 2008, London, UK, S. 551–556
- Singh et al. 2012** Singh, Pratap & Viswanadham, Puligandla. 2012.
Failure modes and mechanisms in electronic packages.
Berlin, Germany : Springer.
ISBN 1461560292
- Smolka et al. 2004** Smolka, G., *et al.* 2004.
Micro electron beam welding and laser machining–potentials of beam welding methods in the micro-system technology.
Microsystem technologies **10** (3), S. 187–192
- Strothmann et al. 2016** Strothmann, Tom & Clauberg, Horst. 2016.
High throughput thermocompression bonding enabled with a flexible manufacturing platform.
In: *2016 China Semiconductor Technology International Conference (CSTIC)*,
March 13-14, 2016, Shanghai, China, S. 1–3
- Suhling et al. 2001** Suhling, Jeffrey C. & Jaeger, Richard C. 2001.
Silicon piezoresistive stress sensors and their application in electronic packaging.
IEEE Sensors Journal **1** (1), S. 14–30

- Szendiuch 2011** Szendiuch, Ivan. 2011.
Development in electronic packaging—moving to 3D system configuration.
Radioengineering **20** (1), S. 214–220
- Tanikella et al. 2002** Tanikella, Ravindra V., Allen, Sue A. Bidstrup & Kohl, Paul A. 2002.
Novel low-temperature processing of polymer dielectrics on organic substrates by variable frequency microwave processing.
In: *Proceedings of the 8th International Symposium on Advanced Packaging Materials*,
March 3-6, 2002, Stone Mountain, USA, S. 254–259
- Tanikella et al. 2006** Tanikella, Ravindra V., *et al.* 2006.
Rapid curing of positive tone photosensitive polybenzoxazole based dielectric resin by variable frequency microwave processing.
IEEE Transactions on Components and Packaging Technologies **29** (2), S. 411–419
- Taweplengsangsuksue et al. 2000** Taweplengsangsuksue, J. & Pearson, R. A. 2000.
Development of processing diagrams for underfill resins.
In: *Proceedings of the 4th International Conference on Adhesive Joining and Coating Technology in Electronics Manufacturing*,
June 18-21, 2000, Espoo, Finland, S. 174–181
- Teutsch et al. 2004** Teutsch, T., *et al.* 2004.
Laser assisted soldering and flip-chip attach for MEMS packaging.
In: *Proceedings of the 19th Annual Meeting of the American Society for Precision Engineering*,
October 24-29, 2004, Orlando, USA
- Thoben 1999** Thoben, Ralf. 1999.
Parallelroboter für die automatisierte Mikromontage.
Düsseldorf, Germany : VDI-Verlag.
ISBN 3183758083
- Thomas 2005** Thomas, Leonard C. 2005.
An introduction to the techniques of differential scanning calorimetry (DSC) and modulated DSC.
Eschborn, Germany : TA Instruments.
ISBN 8497491009,
zuletzt geprüft am 13. November 2016.
Verfügbar:
<http://ruc.udc.es/dspace/bitstream/handle/2183/11493/CC-80%20art%202.pdf?sequence=1>

- TI 2015** Texas Instruments. 2012.
LM358A Bipolar Operational Amplifier Data Sheet.
 Dallas, USA : Texas Instruments,
 zuletzt geprüft am 11. November 2016.
 Verfügbar:
<http://www.ti.com/lit/ds/symlink/lm358.pdf>
- Tilford et al. 2007** Tilford, Tim, *et al.* 2007.
 Variable frequency microwave curing of polymer materials in microelectronics packaging applications.
 In: *Proceedings of the 9th Electronics Packaging Technology Conference (EPTC)*,
 December 10-12, 2007, Singapore, Singapore
- Tilford et al. 2008a** Tilford, Tim, *et al.* 2008.
 Comparison of encapsulant curing with convection and microwave systems.
 In: *Proceedings of the 33rd IEEE/CPMT International Electronic Manufacturing Technology Symposium (IEMT)*,
 November 4-6, 2008, Penang, Malaysia, S. 1–6
- Tilford et al. 2008b** Tilford, Tim, *et al.* 2008.
 Numerical simulation of encapsulant curing within a variable frequency microwave processing system.
 In: *International Conference on Thermal, Mechanical and Multi-Physics Simulation and Experiments in Microelectronics and Micro-Systems (EuroSimE 2008)*,
 April 20-23, 2008, Freiburg, Germany, S. 1–8
- Tilford et al. 2008c** Tilford, Tim, *et al.* 2008.
 Numerical analysis of thermal stresses induced during VFM encapsulant curing.
 In: *Proceedings of the 31st International Spring Seminar on Electronics Technology*,
 May 7-11, 2008, Budapest, Hungary, S. 348–353
- Tilford et al. 2008d** Tilford, T., *et al.* 2008.
 Impact of assembly process technologies on electronic packaging materials.
 In: *Electronic Packaging Technology & High Density International Conference on Packaging, 2008. ICEPT-HDP 2008.*, S. 1–6

- Tilford et al. 2009** Tilford, Tim, *et al.* 2009.
On variable frequency microwave processing of heterogeneous chip-on-board assemblies.
In: *Proceedings of International Conference on Electronic Packaging Technology & High Density Packaging (ICEPT-HDP) 2009*, August 10-13, 2009, Beijing, China, S. 927–931
- Tilford et al. 2010a** Tilford, Tim, *et al.* 2010.
Application of particle swarm optimisation to evaluation of polymer cure kinetics models.
Journal of Algorithms & Computational Technology 4 (1), S. 121–146
- Tilford et al. 2010b** Tilford, Tim, *et al.* 2010.
Numerical analysis of polymer cure kinetics in isotropic conductive adhesives.
In: *Proceedings of 33rd International Spring Seminar on Electronics Technology (ISSE) 2010*, May 12-16, 2010, Warsaw, Poland, S. 412–416
- Tilford et al. 2010c** Tilford, Tim, *et al.* 2010.
Numerical analysis of microwave-assisted encapsulation processes for ball grid array packages.
In: *International Microwave Power Institute's 44th Annual Symposium 2010*, July 14-16, 2010, Denver, USA, S. 30–35
- Tilford et al. 2010d** Tilford, Tim, *et al.* 2010.
On model fitting methods for modeling polymer cure kinetics in microelectronics assembly applications.
In: *Proceedings of the 3rd Electronic System-Integration Technology Conference (ESTC)*, September 13-16, 2010, Berlin, Germany, S. 1–6
- Tilford et al. 2010e** Tilford, Tim, *et al.* 2010.
Numerical analysis of microwave underfill cure in ball-grid packages.
In: *Proceedings of the 3rd Electronic System-Integration Technology Conference (ESTC)*, September 13-16, 2010, Berlin, Germany, S. 1–6
- Tilford et al. 2011** Tilford, Tim, *et al.* 2011.
Assessment of the accuracy of cure kinetics models and fitting approaches utilised in analysis of microelectronics encapsulation materials.
In: *Proceedings of the 13th Electronics Packaging Technology Conference (EPTC)*, December 7-9, 2011, Singapore, Singapore, S. 262–267

- Tipler et al. 2007** Tipler, Paul A. & Mosca, Gene. 2007.
Physics for scientists and engineers.
London, UK : Macmillan.
ISBN 142920124X
- Tong 2011** Tong, Xingcun Colin. 2011.
*Advanced Materials for Thermal Management of
Electronic Packaging.*
Berlin, Germany : Springer.
ISBN 9781441977588
- Tresky 2016** Dr. Tresky AG. 2016.
Micro Assembly with motorized Bond Axis.
Thalwil, Switzerland : Dr. Tresky AG,
zuletzt geprüft am 13. November 2016.
Verfügbar: <http://www.tresky.com/>
- Tummala et al. 1997** Tummala, Rao, Rymaszewski, Eugene J. &
Klopfenstein, Alan G. 1997.
Microelectronics Packaging Handbook.
Cambridge, UK : Cambridge University Press.
ISBN 9781461560371
- Tung et al. 2014** Tung, Bui Thanh, *et al.* 2014.
Flip-chip bonding alignment accuracy enhancement
using self-aligned interconnection elements to
realize low-temperature construction of ultrafine-
pitch copper bump interconnections.
In: *2014 IEEE 64th Electronic Components and
Technology Conference (ECTC)*,
May 27-30, 2014, Orlando, USA, S. 62–67
- Ulrich et al. 2006** Ulrich, Richard K. & Brown, William D. 2006.
Advanced electronic packaging.
Hoboken, USA : Wiley.
ISBN 0471754501
- Urbaniak et al. 2007** Urbaniak, Magdalena & Grudziński, Karol. 2007.
Time-temperature-transformation (TTT) cure
diagram for EPY® epoxy system.
Polimery **52** (2), S. 117–126
- van Brussel et al. 2000** van Brussel, Hendrik, *et al.* 2000.
Assembly of microsystems.
CIRP Annals-Manufacturing Technology **49** (2), S.
451–472
- VDI 2860** VDI. 1990.
*VDI 2860 - Montage- und Handhabungstechnik -
Handhabungsfunktionen,
Handhabungseinrichtungen; Begriffe, Definitionen,
Symbole.*
Berlin, Germany : Beuth Verlag GmbH

- Vrba 2005** Vrba, Jan. 2005.
Microwave Applicators for Medical Applications.
Mikrotalasna revija **June 2005**, S. 43–46
- Vrba et al. 2011** Vrba, Jan, *et al.* 2011.
Microwave Applicators for Industrial Purposes.
In: *Progress In Electromagnetics Research Symposium Proceedings (PIERS) 2011*,
March 20-23, 2011, Marrakesh, Morocco, S. 1825–1829
- Wang 1992** Wang, Ching-Cheng. 1992.
Extrinsic calibration of a vision sensor mounted on a robot.
IEEE Transactions on Robotics and Automation **8** (2), S. 161–175
- Wang et al. 2010** Wang, Yuming, Cui, Zengwei & Wang, Beibei. 2010.
Test and Assessment of the Heating System of Reflow Ovens.
In: *11th International Conference on Electronic Packaging Technology & High Density Packaging (ICEPT-HDP)*,
August 16-19, 2010, Xi'an, China, S. 798–804
- Wei et al. 2000** Wei, J. Billy, *et al.* 2000.
Use of microwave technology for rapid cure of chip-on-board glob top encapsulants.
In: *Proceedings of 3rd Electronics Packaging Technology Conference (EPTC)*,
December 7, 2000, Singapore, Singapore, S. 181–185
- Weng et al. 1992** Weng, Juyang, Cohen, Paul & Herniou, Marc. 1992.
Camera calibration with distortion models and accuracy evaluation.
IEEE Transactions on Pattern Analysis & Machine Intelligence (10), S. 965–980
- Westkämper et al. 1996** Westkämper, E., *et al.* 1996.
Adhesive Gripper-a new approach to handling MEMS.
In: *Actuator 96 - 5th International Conference on New Actuators Conference Proceedings*,
June 26-28, 1996, Bremen, Germany, S. 100–103
- Whittaker et al. 2000** Whittaker, A. Gavin & Mingos, D. Michael P. 2000.
Arcing and other microwave characteristics of metal powders in liquid systems.
Journal of the Chemical Society, Dalton Transactions (9), S. 1521–1526

- Wiedenhöfer 2009** Wiedenhöfer, Markus. 2009.
Prozessgeregeltes Mikrodosieren hochviskoser Klebstoffe.
Heimsheim, Germany : Jost-Jetter.
IPA-IAO-Forschung und Praxis; 482.
ISBN 978-3-939890-43-0
- Wikipedia 2016** Wikimedia Foundation. 2016.
SMT Placement Equipment.
Saint Petersburg, USA : Wikimedia Foundation,
zuletzt geprüft am 11. Oktober 2016.
Verfügbar:
https://en.wikipedia.org/wiki/SMT_placement_equipment
- Woegerer et al. 2014** Woegerer, Christian, *et al.* 2014.
A modular flexible scalable and reconfigurable
system for manufacturing of Microsystems based on
additive manufacturing and e-printing.
In: *Proceedings of the International Conference on
Flexible Automation and Intelligent Manufacturing
(FAIM)*,
May 20-23, 2014, San Antonio, USA
- Wolter 2012** Wolter, Klaus-Jürgen. 2012.
System integration by advanced electronics
packaging.
In: Gerlach, Gerald & Wolter, Klaus-Jürgen (Hrsg.):
*Bio and Nano Packaging Techniques for Electron
Devices.*
Berlin, Germany : Springer, S. 31–48.
ISBN 364228521X
- Xie et al. 2010** Xie, Yuan, Cong, Jason & Sapatnekar, Sachin S.
2010.
Three-dimensional integrated circuit design.
Berlin, Germany : Springer.
ISBN 144190784X
- Yasuda et al. 2003a** Yasuda, K., *et al.* 2003.
New process of self-organized interconnection in
packaging by conductive adhesive with low melting
point filler.
Japanese Journal of Applied Physics Part 1 **43**, S.
390–391

- Yasuda et al. 2003b** Yasuda, K., *et al.* 2003.
Joining Mechanism and Joint Property by Polymer Adhesive with Low Melting Alloy Filler.
In: *Stuttgarter Impulse : Zukunft gestalten - Zeichen setzen*,
October 13-15, 2003, Stuttgart, Germany, S. 149–154
- Ye et al. 1999** Ye, Lilei, *et al.* 1999.
Effect of Ag particle size on electrical conductivity of isotropically conductive adhesives.
IEEE Transactions on Electronics Packaging Manufacturing **22** (4), S. 299–302
- Yodaiken 1999** Yodaiken, Victor. 1999.
The RTLinux manifesto.
In: *Proceedings of the 5th Linux Expo*,
May 20-22, 1999, Raleigh, USA
- Yole 2016** Yole Développement.
Status of the MEMS Industry 2016.
Lyon, France : Yole Développement
- Zhang 2011** Zhang, Rongwei. 2011.
Novel Conductive Adhesives for Electronic Packaging Applications – A Way Towards Economical, Highly Conductive, Low Temperature and Flexible Interconnects.
Atlanta, USA, Doctoral Thesis
- Zhang et al. 2004** Zhang, Zhuqing & Wong, C. P. 2004.
Study and characterizations on the post cure behavior of underfill.
In: *Proceedings of the 9th International Symposium on Advanced Packaging Materials: Processes, Properties and Interfaces*,
March 24-26, 2004, Atlanta, USA, S. 208–214
- Zhang et al. 2009** Zhang, J., Xu, Y. C. & Huang, P. 2009.
Effect of cure cycle on curing process and hardness for epoxy resin.
Express Polymer Letters **3** (9), S. 534–541,
zuletzt geprüft am 28. Februar 2017.
DOI: 10.3144/expresspolymlett.2009.67
- Zong et al. 2005** Zong, Liming, Kempel, Leo C. & Hawley, Martin C. 2005.
Dielectric studies of three epoxy resin systems during microwave cure.
Polymer **46** (8), S. 2638–2645

Kurzfassung

Durch den anhaltenden Trend der Miniaturisierung bei gleichzeitiger Funktionsintegration steigt die Komplexität in der Aufbau- und Verbindungstechnik stetig. Die dabei eingesetzten Fertigungsverfahren sind ausgelegt auf eine Massenproduktion und nur bedingt geeignet für kleinere Stückzahlen. Durch den Einsatz von Klebstoffen in der Aufbau- und Verbindungstechnik kann die aufwändige und für die Massenproduktion typische Herstellung von Werkzeugen umgangen werden. Die dabei eingesetzten Fügeprozesse weisen eine deutlich höhere Flexibilität auf, insbesondere bei kleinen und mittleren Stückzahlen. Ein deutlicher Nachteil ist jedoch die häufig lange Dauer der Aushärteprozesse im Verhältnis zu den übrigen Montageprozessen. Im Zuge dieser Arbeit wird daher ein neues Verfahren beschrieben, welches den Durchsatz der Montageprozesse erhöht und den Wirkungsgrad des Gesamtmontageprozesses steigert. Dabei wird insbesondere eine Reduzierung der Aushärtezeiten adressiert.

Es wird zunächst eine Anforderungsanalyse der Aufbau- und Verbindungstechnik mit Fokus auf die Anforderungen des Aushärtens von Klebstoffen durchgeführt. Anschließend wird der relevante Stand der Technik analysiert und die Notwendigkeit eines neuen Verfahrens erörtert. Es wird ein Konzept eines neuartigen Mikrowellen-Aushärtesystems unter Einsatz eines einseitig offenen Wellenleiters beschrieben. Verschiedene Konzepte zur Regelung des Heizprozesses werden beschrieben. Zur Realisierung des gesamten Mikromontageprozesses wird eine Montageanlage mit integriertem Mikrowellen-Aushärtesystem konzipiert. Beide Systeme werden anschließend prototypisch umgesetzt. Im Folgenden wird das Verfahren experimentell evaluiert. In diesem Zuge wird eine Flip-Chip-Baugruppe mit dem neuen Verfahren aufgebaut. Um den Einfluss auf die Zuverlässigkeit zu bestimmen werden an einer repräsentativen Baugruppe Thermozyklentests durchgeführt. Weiterhin werden Einflüsse des Verfahrens auf Zuverlässigkeit, Durchsatz und Montagewirkungsgrad untersucht.

Mit dem beschriebenen Verfahren können die Aushärtezeiten deutlich reduziert und somit der Durchsatz gesteigert werden. Der Montagewirkungsgrad kann durch die Verringerung des Handhabungsaufwands stark verbessert werden. Weiterhin konnte gezeigt werden, dass die Zuverlässigkeit der montierten Baugruppen durch reduzierte innere Spannungen innerhalb des Klebstoffs erhöht werden kann.

Short Summary

Advanced electronic packaging continues to gain prevalence, driven by the continuous trend for miniaturization with concurrent functional integration. Processes in use today are typically efficient for mass production, but are not suitable for the purposes of low volume and prototype production. Adhesive bonding circumvents the elaborate tooling typical for mass production and provides a higher degree of flexibility. Disadvantages lie in long curing cycle times and high handling effort. To overcome these problems, a novel method for the assembly of electronic packages is proposed, one that improves the performance and efficiency of the assembly processes and reduces the handling effort between the separate process steps by integration of assembly and curing process equipment into a single machine.

An analysis of the field of electronic packaging with particular respect to adhesive curing processes is performed. Then the relevant state-of-the-art is reviewed and the need of a novel method is identified. The conception and realization of a microwave curing system, based on an open-ended waveguide resonator are carried out. Different concepts for the control of the curing process are described. A machine integrating the curing system and the assembly process equipment is designed and prototypically realized. This is followed by extensive evaluation and testing of the novel method. In the course of the evaluation a representative flip-chip assembly is realized. In order to assess the influence on reliability, a series of temperature cycling tests is performed. Additionally, stress-measurement dies are packaged and the influence of the proposed method onto residual stresses is studied. The influence of the proposed method on throughput and assembly efficiency is investigated.

The proposed method provides reduction of curing cycle times for three different adhesive materials and therewith an increase of the overall throughput. By reduction of handling effort, the overall process efficiency could be improved. Furthermore, by microwave curing with the proposed method, a higher reliability of the resulting electronic packages can be achieved. The experiments with the stress chips reveal lower residual stresses in the microwave-heated chips compared to convection heating.

Advanced electronic packaging continues to gain prevalence, driven by the continuous trend for miniaturization with concurrent functional integration. Processes in use today are efficient for mass production, but are not suitable for the purposes of low volume and prototype production. To overcome these problems, a novel method for the assembly of electronic packages is proposed, one that improves the efficiency of assembly processes and reduces the handling effort between the separate process steps by integration of assembly and curing process equipment into a single machine. An analysis of the field of electronic packaging with particular respect to adhesive curing processes is performed, the relevant state-of-the-art is reviewed and the need of a novel method is identified. The conception and realization of a microwave curing system, based on an open-ended waveguide resonator and a prototype machine integrating the curing system are carried out. This is followed by extensive evaluation and testing of the novel method. The proposed method provides reduction of curing cycle times for different adhesive materials and improvement of the overall process efficiency.

ISBN 978-3-8396-1333-7



FRAUNHOFER VERLAG